

2008

Voltage-activated currents and their modulation in somatic muscle cells of the nematode *Ascaris suum*

Saurabh Verma
Iowa State University

Follow this and additional works at: <https://lib.dr.iastate.edu/rtd>

 Part of the [Neuroscience and Neurobiology Commons](#), [Neurosciences Commons](#), [Parasitology Commons](#), and the [Physiology Commons](#)

Recommended Citation

Verma, Saurabh, "Voltage-activated currents and their modulation in somatic muscle cells of the nematode *Ascaris suum*" (2008).
Retrospective Theses and Dissertations. 15815.
<https://lib.dr.iastate.edu/rtd/15815>

This Dissertation is brought to you for free and open access by the Iowa State University Capstones, Theses and Dissertations at Iowa State University Digital Repository. It has been accepted for inclusion in Retrospective Theses and Dissertations by an authorized administrator of Iowa State University Digital Repository. For more information, please contact digirep@iastate.edu.

Voltage-activated currents and their modulation in somatic muscle cells
of the nematode *Ascaris suum*

By

Saurabh Verma

A dissertation submitted to the graduate faculty
in partial fulfillment of the requirements for the degree of
DOCTOR OF PHILOSOPHY

Major: Physiology (Pharmacology)

Program of Study Committee:
Richard J. Martin, Major Professor
Jeffery Beetham
Timothy A. Day
Mary Heather W. Greenlee
Edward yu
Alan P. Robertson

Iowa State University

Ames, Iowa

2008

Copyright © Saurabh Verma, 2008. All rights reserved.

UMI Number: 3316171

INFORMATION TO USERS

The quality of this reproduction is dependent upon the quality of the copy submitted. Broken or indistinct print, colored or poor quality illustrations and photographs, print bleed-through, substandard margins, and improper alignment can adversely affect reproduction.

In the unlikely event that the author did not send a complete manuscript and there are missing pages, these will be noted. Also, if unauthorized copyright material had to be removed, a note will indicate the deletion.



UMI Microform 3316171
Copyright 2008 by ProQuest LLC
All rights reserved. This microform edition is protected against
unauthorized copying under Title 17, United States Code.

ProQuest LLC
789 East Eisenhower Parkway
P.O. Box 1346
Ann Arbor, MI 48106-1346

TABLE OF CONTENTS

Chapter 1. Introduction	1
1.1. Introduction	1
1.2. Thesis Organization	3
Chapter 2. Literature review	4
2.1. Nematode parasites and the model nematode	4
2.1.1. <i>Ascaris</i> and ascariasis	6
2.2. Body wall muscle cell and neuromuscular junction in nematodes	7
2.2.1. Belly	9
2.2.2. Arm	10
2.2.3. Spindle	11
2.3. Nervous system in <i>Ascaris suum</i>	11
2.3.1. Anatomy of <i>Ascaris</i> nervous system	12
2.3.2. Nervous commissures in nematodes	13
2.4. Physiology of the body-wall muscle cell in nematodes	15
2.4.1. Membrane potential of the muscle cell	16
2.4.2. Spontaneous activity of the muscle cell	17
2.5 Nematode neuropeptides and neurotransmitters	19
2.5.1 FMFRamide like peptides (FLPs)	19
2.5.2 FLP distribution in <i>Ascaris suum</i>	20
2.5.3 FLP distribution in other nematodes	22
2.5.4 <i>Ascaris</i> FLPs	23
2.5.5 Other nematode FLPs	25

2.5.6 Effects of nematode FLPs	30
2.5.7 Nematode FLP receptors	38
2.5.8 Nematode neurotransmitters	40
2.6 Voltage-activated currents	43
2.6.1 Voltage-activated calcium currents	43
2.6.2 Voltage-activated potassium currents	49
2.7 Anthelmintics	55
2.7.1 Nicotinic agonists	55
2.7.2 Glutamate-gated chloride channel modulators	56
2.7.3 Benzimidazoles	58
2.7.4 Cyclo-octadepsipeptides	58
2.7.5 Others anthelmintics	60
2.8 Hypothesis	61
2.9 References	63
Chapter 3. The nematode neuropeptide, AF2 (KHEYLRF-NH ₂), increases voltage-activated calcium currents in <i>Ascaris suum</i> muscle	80
3.1 Abstract	80
3.2 Introduction	81
3.3 Materials and Methods	83
3.4 Results	87
3.5 Discussion	95
3.6 Acknowledgements	102
3.7 References	102

3.8 Figures and legends	106
Chapter 4. Effects of SDPNLRF-amide (PF1) on voltage-activated currents in <i>Ascaris suum</i> muscle	116
4.1 Abstract	116
4.2 Introduction	117
4.3 Materials and Methods	119
4.4 Results	122
4.5 Discussion	129
4.6 Acknowledgements	134
4.7 References	134
4.8 Legends to figures	138
4.9 Figures	141
Chapter 5. Effects of the muscarinic agonist, 5-methylfurmethiodide, on contraction and electrophysiology of <i>Ascaris suum</i> muscle	152
5.1 Abstract	152
5.2 Introduction	153
5.3 Materials and Methods	155
5.4 Results	161
5.5 Discussion	171
5.6 Acknowledgements	175
5.7 References	175
5.8 Legends to figures	179
5.9 Figures	183

Chapter 6. General Discussion	193
Appendix	197
Acknowledgements	208

Chapter 1. Introduction

Voltage-activated ion channels are a class of transmembrane proteins found in excitable cells. These channels are key to the rapid and accurate transmission of information among cells in vertebrates and invertebrates alike. They play a very important role in electrically excitable cells, allowing influx or efflux of ions in response to membrane potential change. There are three major types of voltage-activated ion channels which are responsible for maintaining cell viability and physiological functions; calcium, potassium and sodium. Voltage-activated currents have been isolated in nematodes and are associated with depolarization (calcium channels) or recovery of the cell after the depolarization (potassium channels). Voltage-activated potassium channels play an important role in recovery of cells after depolarization. While the entry of extracellular calcium into muscle cells after ACh induced depolarization is essential to the contractile process. Entry of calcium is facilitated by voltage-activated calcium channels. Different subtypes of voltage-activated calcium channels have been identified in vertebrates. In nematodes, advances in *C. elegans* genomics led to the identification of voltage-activated calcium channel subtypes. These subtypes show some homology to vertebrate calcium channels but are pharmacologically and physiologically different. The understanding of the physiology of these different voltage-activated channels is becoming increasingly important as we try to attenuate the development of resistance to present anthelmintics. Major classes of anthelmintics produce their effect by modulating neuromuscular system either indirectly or directly. Therefore, it is important for us to understand the physiology of these channels in the worms to

either identify novel drug target sites or understand the mechanism of the development of resistance. Recently a new class of anthelmintic compounds, cyclo-octadepsipeptides, has been approved for animal use. Their modes of action include latrophillin receptors activation, PF1 like neuropeptide release and more recently demonstrated activation of voltage-activated calcium dependent potassium channels. It is known from previous work done in *A. suum* and *C. elegans* that there are voltage-activated channels on the muscle membrane. Electrophysiological recordings in *A. suum* and other nematodes have shown that these currents may be modulated by different anthelmintics. We used voltage-clamp and current-clamp techniques to study voltage-activated currents in the pig parasitic nematode *A. suum* somatic muscle cells. We were able to isolate two types of voltage-activated calcium currents and a type of outward potassium current. We have characterized these currents pharmacologically and kinetically. We also observed that these currents, if modulated, could potentiate the response of cholinergic anthelmintics. Further, we used different endogenous nematode neuropeptides to modulate these currents. Neuropeptides and their receptors offer novel drug targets, not only for the development of new anthelmintics, but also to increase the potency of existing drugs. We anticipate that our observations will increase the understanding of worm physiology and validate the potential for exploring neuropeptide receptors for anthelmintic chemotherapy.

1.1 Thesis Organization

Within this thesis, an introduction is presented describing some of the reasons for studying voltage-activated currents and nematode neuropeptides. In chapter 2, I reviewed the work of researchers in related fields of nematode physiology and FMFRamide related peptides (FLPs). The following three chapters (Chapters 3,4, & 5) are each manuscripts which are either published or submitted for publication explaining in detail the work done by the author and collaborators on the subject of this dissertation. The papers represent the majority of the work done by the author towards the characterization of voltage-activated currents in *Ascaris suum*. In chapter 3, I describe the isolation of voltage-activated currents and their modulation by the endogenous neuropeptide, AF2. Chapter 4 explains the effects of PF1 and AF3 on the voltage-activated currents. In chapter 5, I describe the effects of a muscarinic agonist (5-methylfurmethiodide) on contraction and electrophysiology. I appear as first author in all the three papers. Chapter 5 is for the final paper (Trailovic et al., 2007), where I conducted the voltage-clamp and many of the current-clamp experiments. In chapter 6, the general discussion, I summarize the observations of my PhD studies and discuss the significance of the observations and future courses of action.

Chapter 2. Literature review

2.1 Nematode parasites and model nematode

Parasitism is a relationship between organisms of different species in which one organism (parasite) benefits from the association while the other (host) is harmed. Parasites are classified broadly as ectoparasites and endoparasites depending upon their location. Parasites are smaller than their host and usually show a high degree of species specificity. Most parasitic infections are not deadly but cause a tremendous burden on animals and humans due to high morbidity. These infections lead to poor growth, decreased immune functions, weight loss, anemia and impairment of cognitive skills in humans. In animals they cause serious loss in production due to poor growth, decreased immunity and poor weight gain beside chronic debilitation. Ectoparasites, as their name suggests, are associated with infections to the outer surface of the body. Whereas, endoparasites are the ones which live inside the host, in different tissues and organs. Ectoparasites include blood sucking arthropods, ticks, fleas, mites and lice. The ectoparasites attach or burrow into skin leading to different skin conditions. Endoparasites broadly include helminths and protozoa. Protozoa are microscopic, unicellular organisms which can be parasitic or free living. Helminths are large, segmented multi-cellular organisms. The mature worms reside in the GI tract, circulatory system (blood & lymph) or subcutaneous tissues. The larval stages travel through different body systems inducing disease symptoms. The word helminth is derived from the Greek word for worms. Helminths fall under three main groups: flatworms (platyhelminths); thorny-headed worms (acanthocephalans); roundworms (nematodes). Parasitic nematodes

include: roundworms (*Ascaris lumbricoides*, *Ascaris suum*, and *Trichuris vulpis*), hookworms (*Ancylostoma caninum*, *Necator americanus*), heartworms (*Dirofilaria immitis*), pinworms (*Enterobius vermicularis*), strongyles (*Strongyloids spp.*) and filarial worms (*Wuchereria bancrofti*, *Brugia malayi*). Nematodes have life cycles which include adult males and females, they reproduce sexually and eggs are laid by the female. Larvae develop in these eggs, hatch and progress through a series of developing larval stages until they reach adulthood as sexually mature males and females and the cycle begins again. Most nematodes follow this basic life cycle pattern, although some may also include variations and additional complexities. Figure 2.1 shows the phylogenetic tree representing evolutionary associations between vertebrates, nematodes and other animals (Dunn *et al.*, 2008).

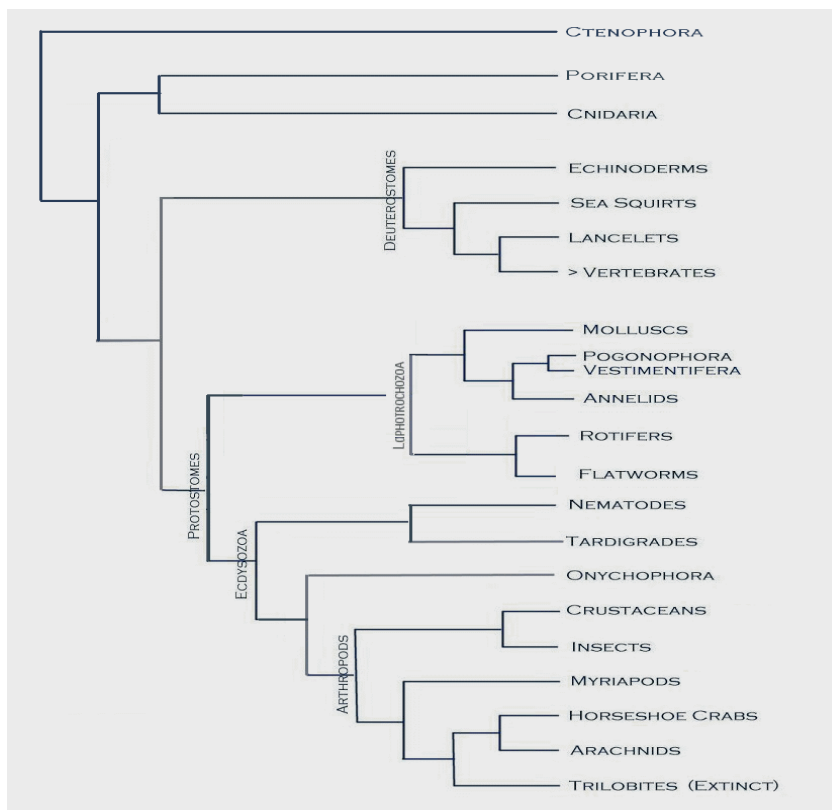


Figure 2.1 Phylogram of the 77-taxon RaxML maximum likelihood analyses conducted under the WAG model. Modified from Dunn *et al.*, 2008.

2.1.1 *Ascaris* and ascariasis

The Millennium Declaration of the World Health Organization included a group of 13 parasitic and bacterial infectious diseases listed as neglected tropical diseases (Hotez *et al.*, 2007). Ascariasis is the most common parasitic infection in the list, with an estimated 807 million people infected and 4.2 billion people at risk. Helminths are of economic and welfare concern in animals. Ascariasis in man is caused by *Ascaris lumbricoides* and a related species *Ascaris suum* causes infection in swine. Adult females (20-40 cm) are bigger than the male in size (15-30 cm). Females are identified by the presence of large ovaries occupying the posterior $\sim 2/3^{\text{rd}}$ of the worm. A row of small teeth on the lips of *Ascaris suum* separates the two species anatomically (Sen *et al.*, 1963). Even though the two species are very similar and closely related, cross species infections are rare (Urquhart *et al.*, 1987). *Ascaris spp.* has a worldwide presence but is more common in temperate climates. Adult *A. lumbricoides* and *A. suum* normally reside in the small intestine. The nematode life cycle involves six stages which includes the egg, four larval stages (L1, L2, L3, L4), and an adult stage. The female *A. suum/A. lumbricoides* lays more than 200,000 eggs in a day which are passed in the feces of the infected host. Ascariasis follows the ingestion of infective fertile eggs contaminating food or soil. Eggs, upon reaching the small intestine hatch to release the larvae. These larvae then migrate through the intestinal wall reaching the lungs. In humans, larvae in the lungs induce host sensitization and lung inflammation. L3 larvae molt to the L4 stage in the lungs and migrate up the trachea and are swallowed. These L4 develop into adult worms in the small intestine. Serious complications arise in cases where larvae

migrate into sensitive tissues like the brain or other vital organs forming abscesses. The most common symptoms of ascariasis include abdominal pain, nausea and disturbed gastrointestinal tract functions.

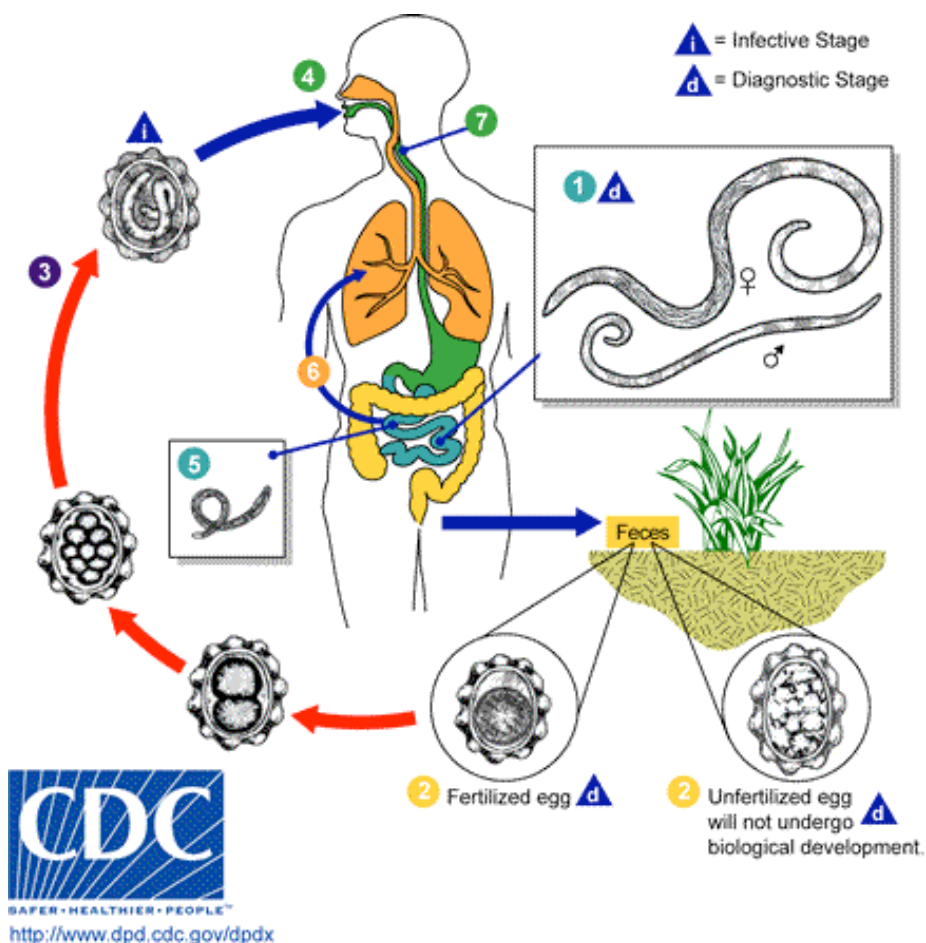


Figure 2.2 The lifecycle of *A. lumbricoides*. Adult worms live in the intestinal lumen. Eggs laid by the female are passed with feces. Eggs embryonate and become infective. Following ingestion of contaminated food and water, larvae hatch in the host intestine. Larvae migrate through the intestinal wall to reach the lungs. L4 larvae migrate to the trachea and are swallowed. Upon reaching small intestine L4 larvae develop into adult worms. (<http://www.dpd.cdc.gov/dpdx> date: 05/31/08)

2.2 Body wall muscle cell and neuromuscular junction in nematodes

Figure 2.3 shows a cross section of an adult *Ascaris*. From outside to inside it includes cuticle, hypodermis and muscle layer. The musculature of *Ascaris* consists almost entirely of longitudinal muscles and these muscles are classified as obliquely

striated (Rosenbluth, 1965a; Rosenbluth, 1965b; Stretton, 1976). Body wall muscles are divided by two lateral lines into ventral and dorsal layers (del Castillo *et al.*, 1989). Each half is innervated by individual nerve cords. Somatic muscle cells of *Ascaris* have three parts (Figure 2.4, 2.5) : spindle region, which is the contractile region and anchors the muscle to hypodermis, cell body which is formed by a balloon like structure called the muscle belly, which contains the nucleus, and muscle arms arising from the base of the belly and extending finger like projections to the nerve cord. The different components of *Ascaris* muscles are described in detail here.

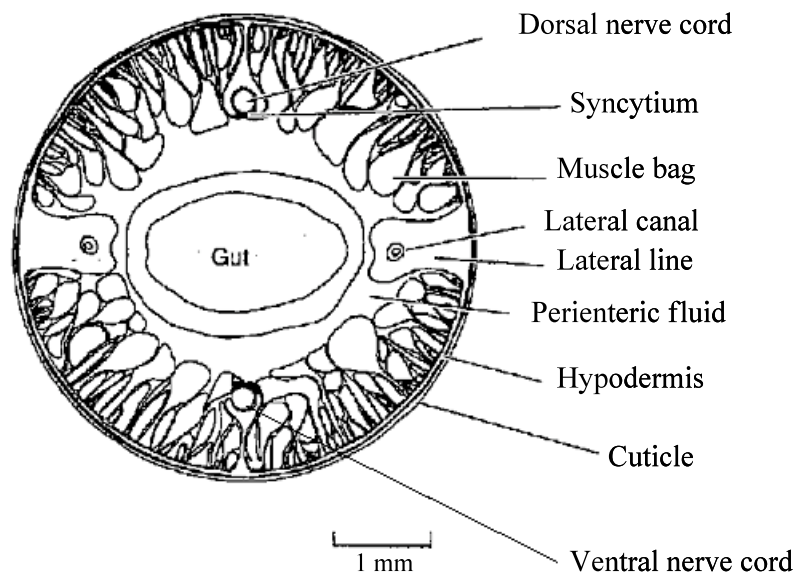


Figure 2.3 (Thorn *et al.*, 1987) Transverse section of *Ascaris*. The dorsal and ventral nerve cords are indicated as well as the two small lateral nerve cords. The two lateral lines separate somatic muscles into ventral and dorsal layers.

2.2.1 Belly

The belly or bag region of the *Ascaris* muscle is in the body cavity or pseudocoel. The belly contains nucleus, fibrillar bundles of cytoskeleton and mitochondria (Debell *et al.*, 1963). The belly serves as an endoskeleton and has only

basic internal structures. The belly is filled with glycogen granules which are depleted during starvation or exercise (Rosenbluth, 1965b). The main function of the belly is assumed to be as a store providing glycogen when the animal faces scarcity of food.

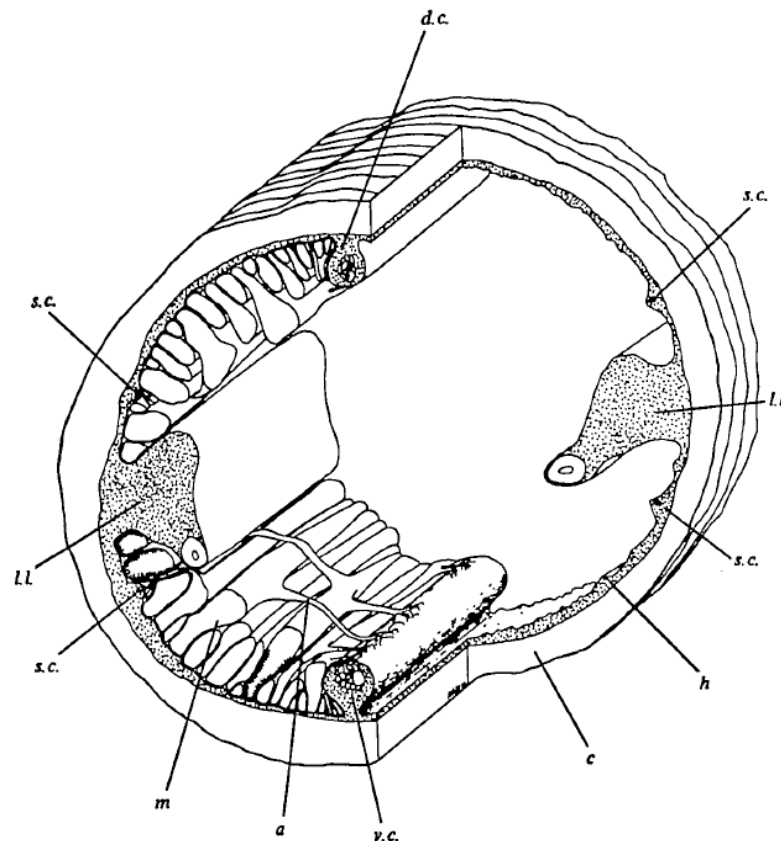


Figure 2.4 (Stretton, 1976) Diagram of short length of the body of *Ascaris* showing relationship of the muscle cells to nerve cord. *a*, muscle arm; *c*, cuticle; *d.c.*, dorsal cord; *h*, hypodermis, *l.l.*, lateral line; *m*, muscle cell; *s.c.*, sublateral cord; *v.c.*, ventral cord.

2.2.2 Arm

The muscle belly gives rise to the arm, an innervation process which can originate from any part of the belly (Rosenbluth, 1965b). Some bellies give rise to more than one arm. The arm in proximity to the nerve cord becomes thinner and divides into several finger like processes, and forms a syncytium (del Castillo *et al.*,

1989). The processes from an arm interdigitate with processes from other arms and form a cap of muscle fingers. The arms reach the nerve cord in bundles separated by ~400-500 μm gaps. The syncytium (cap of processes) forms synapses with the nerve cord for impulse conduction (Figure 2.5).

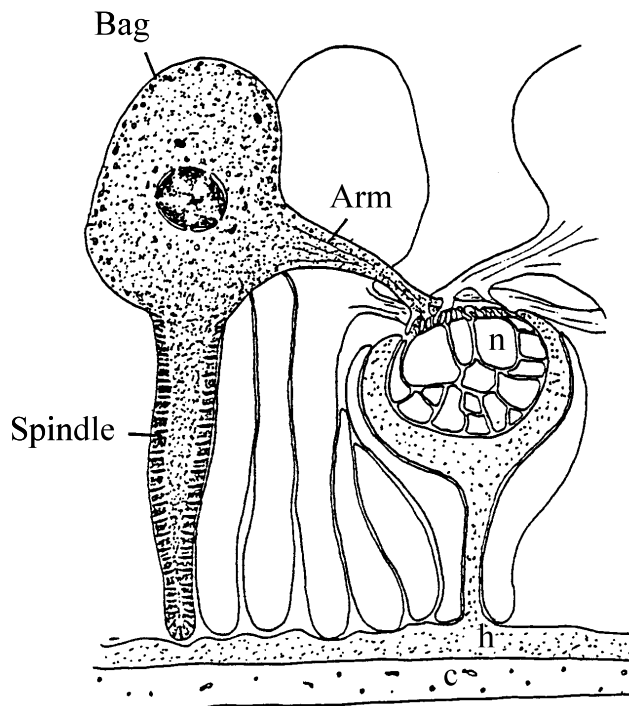


Figure 2.5 (Rosenbluth, 1965b) Schematic diagram of the muscle cell and the neuromuscular junction. The muscle cell includes a spindle, a belly (or bag) and arms. The neuromuscular junction is formed between the end of the arms (which forms a syncytium) and the nerve cord. n: nerve cord; h: hypodermis; c: cuticle.

There are two types of junctions in *Ascaris* for communication – neuromuscular junctions (between nerve and muscle arm) and tight junctions (between the muscle arms). The tight junction between two muscle cells presumably have two functions: synchronization of electrical activity in group of muscle cells by forming a functional syncytium; and have better control over muscle cells which are not able to make direct contact with nerve cells (del Castillo *et al.*, 1989).

2.2.3 The spindle

The contractile apparatus of the muscle cell is obliquely striated and is limited to the spindle region of the cell. The spindle is made up of U shaped fibers forming tube shaped structure which is attached to hypodermis. Fibers has two sections : the sarcoplasmic core which is continuous with the belly; and the cortex which contains the contractile apparatus (Rosenbluth, 1965a). The double array of thick and thin filaments interdigitate to form A, H and I bands. However unlike vertebrates their is no Z line but Z bundles and dense bodies (Rosenbluth, 1965a). Sarcoplasmic reticulum is virtually absent in *Ascaris* somatic muscle cells which is probably the reason for slow speed of contraction (Rosenbluth, 1967).

2.3. Nervous system in *Ascaris suum*

The nervous system in *Ascaris* is simple with 298 neurons (Stretton *et al.*, 1992). The neurons are classified broadly as sensory, interneuron and motor neuron. The neurons are also classified according to the neurotransmitter released by them: cholinergic, GABAergic *etc.* The motor nervous system in *Ascaris* is simple with each fiber sending a straight fiber with none to two branch points. The neurons have short spines (1-2 μm) where they make synapse to muscle (Stretton *et al.*, 1978). Neuromuscular contacts are made by muscle arms branching out to form synapse at the neuronal spines.

2.3.1 Anatomy of *Ascaris* nervous system

The nervous system of *Ascaris* is composed of three major structural regions: (i) nerve ring and associated ganglia at the anterior end, (ii) major dorsal and ventral nerve cords and the smaller subventral and subdorsal cords which runs along the

animal to tail, and (iii) smaller caudal ganglia in the posterior region (del Castillo *et al.*, 1989; Stretton *et al.*, 1978). The anterior nerve ring is the primary target of sensory neurons and produces cephalic motor output. Dorsal and ventral nerve cords also arise from the nerve ring (Fig.2.6).

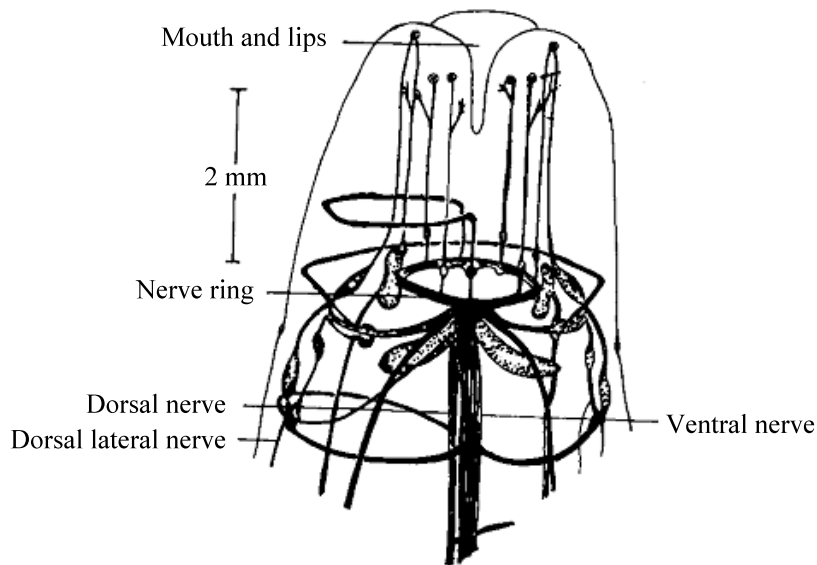


Figure 2.6 (Crompton *et al.*, 1979) The anterior part of the nervous system in *Ascaris*. The nerve ring receives the primary sensory input and gives rise to the cephalic muscle motor output. The two major nerve cords, dorsal and ventral, originate from the nerve ring.

The connection commissures form a pattern along the length of the nematode body leading to the formation of five segments. Thus the motor nervous system is composed of five repeating subunits or segments and each unit is composed of eleven motor neurons. The morphological differences divide the eleven segmental motor neurons into seven types: one of DI, DE2 and DE3, two of DE1, VI, V1 and V2 (Stretton *et al.*, 1978) Table 2.1. The cell bodies of all the motor neurons are located in the ventral nerve cord and three form synapses with ventral muscle cells while the other four form synapses with dorsal muscles. There are six non-segmental interneurons with their cell bodies either in the anterior or posterior region. All the

segmental neurons are motor neurons as they form synapses either in the dorsal or ventral cord but not in both (del Castillo *et al.*, 1989; Stretton *et al.*, 1978).

Ascaris neuron type	Neuro-muscular region	output	function in Ascaris
DE3	Dorsal		Excitatory
DE2	Dorsal		Excitatory
DE1	Dorsal		Excitatory
DI	Dorsal		Inhibitory
VI	Ventral		Inhibitory
V-1	Ventral		
V-2	Ventral		Excitatory*

Table 2.1 (Stretton *et al.*, 1978) *Ascaris* neuronal types and distribution.

*Function of V-1 and V- 2 neurons has not yet been fully elucidated.

2.3.2. Nervous commissures in nematodes

As mentioned previously the nervous system of *Ascaris* is characterized by a repeating pattern of neurons, called segments (Stretton *et al.*, 1978). The ventral cord sends out branches which travel across the body and form connections with the dorsal cord, Fig. 2.9. These connecting branches between dorsal and ventral cords are called “commissures”. The commissures are located in the hypodermis underneath the cuticle. There is bilateral symmetry in distribution of commissures in that for every left handed commissure there are six right handed commissures, Fig. 2.7. Neuromuscular synapses are formed by four of the seven neuronal types in the dorsal cord, Fig. 2.7. In *Ascaris* females five copies of repeating segments are found with three pairs of left handed commissures anterior to the first segment. In males the difference is the presence of four extra left handed commissures at the caudal end (Stretton, 1976).

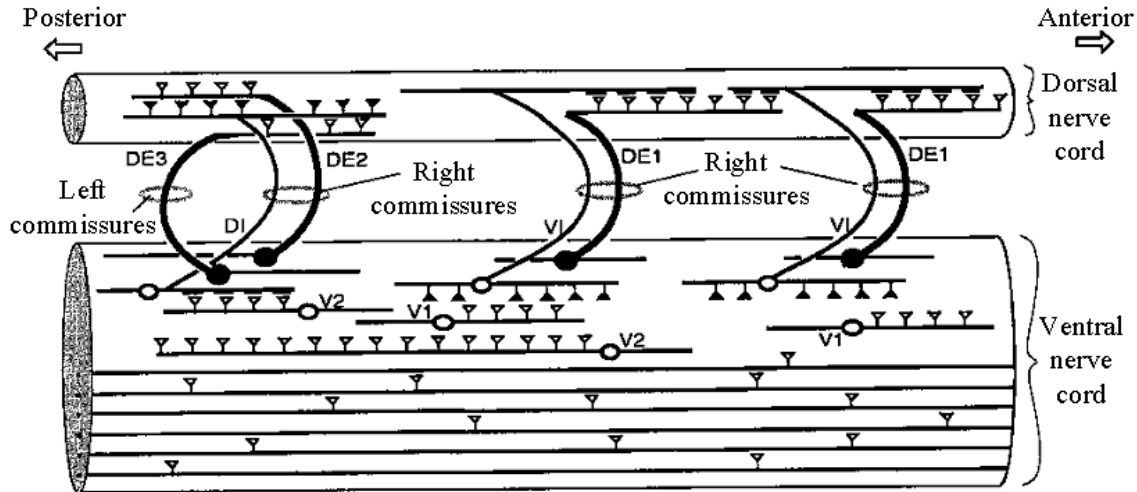


Figure 2.7 (Martin *et al.*, 1996) Diagram of the dorsal and ventral nerve cord in one segment of *Ascaris*. Seven anatomical types of motoneurons are present: dorsal excitatory (DE1, DE2 and DE3), dorsal inhibitory (DI), ventral inhibitory (VI), ventral excitatory (V1 and V2).

- Inhibitory motor neuron
- Excitatory motor neuron
- △ Inhibitory output
- ▲ Excitatory output

As observed in the model nematode *C.elegans*, there are two pairs of commissures in the head region, called right and left amphid and deirid commissures. There are three pairs of right and left commissures in the tail: lumbar, dorsorectal and dorsolateral. The pharyngeal ring is formed by an enlarged commissure with ~200 processes surrounding the bulb region of pharynx. The pharynx has two commissures: nerve ring and terminal bulb commissures. There are more than 40 commissures which grow out of ventral nerve cord and connect to the dorsal nerve cord across the length of the worm (Hedgecock *et al.*, 1987; White *et al.*, 1986).

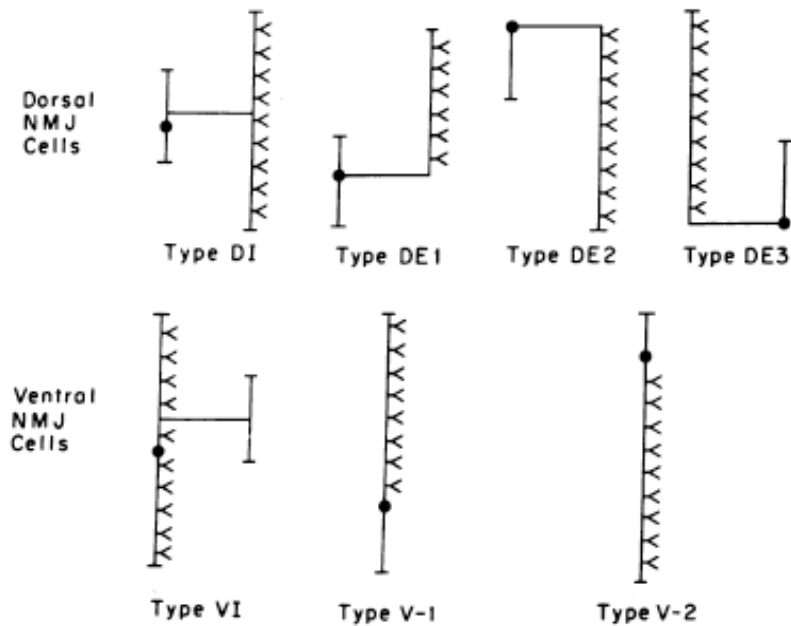


Figure 2.8 (Stretton *et al.*, 1978) The seven types of segmental neurons and their commissures.

2.4. Physiology of the body-wall muscle cell in nematodes

Nerves form synapses with fingers at the end of muscle arms to conduct impulses. Apart from the neuromuscular junction, the muscles also form connections between muscle cells through gap junctions. These connections are important to synchronize the activity of muscle cells in a region as all the muscle cells do not make contact with nerve cord. The action potential is induced in the muscle arms or near the nerve cord. Gap-junctions are the major means of initiating recruitment of neighboring muscle cells, which do not form direct connections with nerve (Debell *et al.*, 1963; del Castillo *et al.*, 1967). Close to half of the muscle cells make contacts with more than one nerve (Rosenbluth, 1965b).

2.4.1. Membrane potential of the muscle cell

The ionic mechanisms involved in the maintenance of the resting membrane potential in *Ascaris* are very different from vertebrate muscles. The striking difference is the relative insensitivity of the *Ascaris* muscle to changes in concentration of the extracellular ions, potassium and sodium (Brading *et al.*, 1971; del Castillo *et al.*, 1964a). The resting membrane potential of *Ascaris* somatic muscle is ~ -30 mV (Debell *et al.*, 1963). The resting membrane potential decreased by only 1.5 mV with a 10 fold increase in the bath potassium concentrations. Similar results were obtained with sodium but the *Ascaris* muscles cell was found to be sensitive to changes in extracellular chloride although not as much as in vertebrates (Brading *et al.*, 1964; del Castillo *et al.*, 1964a). del Castillo *et al.*, (1964) proposed the presence of a high resistance potassium and low resistance chloride battery in the cell membrane to explain the results. The hypothesis was later countered by Brading and Caldwell (1971). The insensitive nature of the resting membrane potential to sodium, potassium and chloride cannot be explained by the Goldman-Hodgkin-Katz equation. It has been suggested that other ions are involved in maintaining the insensitive nature of the cell membrane. The results can be explained by a modified Goldman-Hodgkin-Katz equation:

$$E = \frac{RT}{F} \ln \frac{P_K [K]_o + P_{Na} [Na]_o + P_{Cl} [Cl]_i + x}{P_K [K]_i + P_{Na} [Na]_i + P_{Cl} [Cl]_o + y}$$

Where $p_k[Na]$ etc. are product permeability constants and ionic concentrations and x & y represents the contribution of other ions. The contribution of the other ions (x and y) is much larger than the contribution of sodium, potassium or chloride (Brading *et al.*, 1971). Brading and Caldwell (1971) proposed that the insensitivity of the

muscle membrane was due to the effects of an electrogenic pump. The sodium, potassium and chloride fluxes are smaller when compared with large fluxes of carboxylic acids across the *Ascaris* muscle membrane (Brading *et al.*, 1971). It was proposed that the abnormal behavior is linked to electrogenic sodium pump in which outward movement of sodium ions is independent of another ion (Caldwell, 1973; Caldwell, 1972). The muscle belly has been found to possess ACh, GABA receptors (Martin, 1980; Martin, 1982). Thorn and Martin (1987) have also shown the presence of large calcium-activated chloride channel on the belly region. We have yet to come up with a satisfactory mechanism to explain the distinct membrane potential responses of *Ascaris*. The possible role of ACh, GABA and calcium-activated chloride channels in maintaining the membrane potential has not been elucidated, although it seems that the calcium channels have an important function.

2.4.2 Spontaneous activity of muscle cell

The resting membrane potential in *Ascaris* is regularly superimposed upon by spontaneous depolarizations at 1.5-7 per second. Each spontaneous depolarization is composed of a slow wave with spikes superimposed (Debell *et al.*, 1963). *Ascaris* muscles demonstrate three types of spontaneous activity: graded spike potentials (10-50 ms), slow waves (100-1000 ms) and long lasting modulatory waves (3-20 ms), Fig. 2.11 (Weisblat *et al.*, 1976). The spike potentials are affected by the concentration of calcium in the bath solution, the lower the concentration, smaller the spikes. These observations coupled with the absence of effect of sodium suggest that spikes are in fact mediated by calcium ions. Also the spikes are blocked by lanthanum and cobalt (Weisblat *et al.*, 1976). The slow waves on the other hand

are more complex and the involvement of both sodium and calcium has been proposed. Ion substitution experiments confirmed that both sodium and calcium can carry currents during slow waves (Weisblat *et al.*, 1976). del Castillo *et al.*, (1989) concluded that spontaneous electrical activity of the *Ascaris* somatic muscle cells is myogenic in nature, originating from the syncytium. The syncytial membrane generates pacemaker potentials which give rise to spikes that traverse from arm and belly to the spindle region to activate contraction. The slow waves and spikes generated from the syncytium are modulated by the interaction of neurotransmitters including GABA and ACh (del Castillo *et al.*, 1989). The voltage-dependent channel density is low in motor nerves and the somatic muscle cell membrane which is compensated by the increased excitability of the syncytial membrane. The syncytial membrane boosts the signals generated by the nervous system ensuring that there is no loss of signal strength at the spindle (del Castillo *et al.*, 1989).

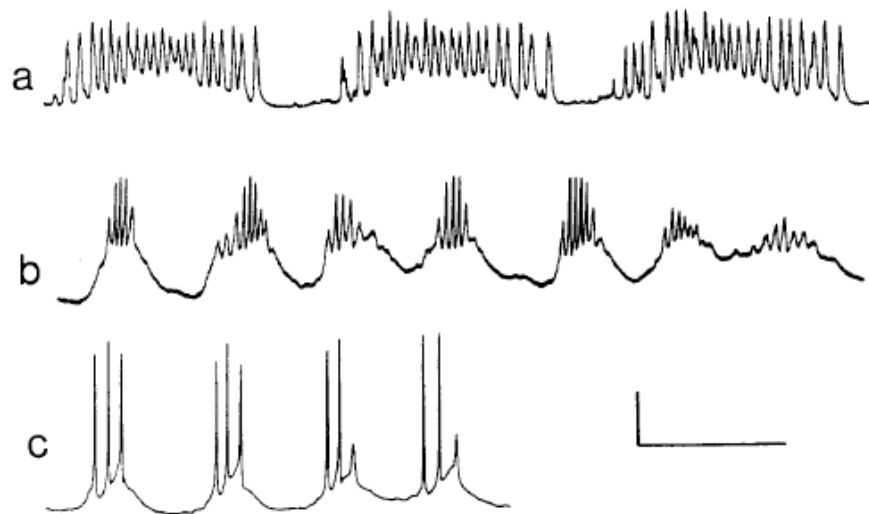


Figure 2.9 (Weisblat *et al.*, 1976) Spontaneous activity of the *Ascaris* somatic muscle cells. a) Modulated spontaneous activity. b) Previous recording on expanded scale to show slow waves and super imposed spikes. c) Slow waves and spikes. Scale, 10 mV x 12 s in a, 10 mV x 1 s in b and c.

2.5 Nematode neuropeptides and neurotransmitters

The metazoan nervous system possesses a significant peptidergic signaling system. Peptidergic neurotransmitters and peptidergic parasitic neurons are of early evolutionary origin as they are found in the major branches of metazoans, cnidarians and helminths and also in other invertebrates (Halton *et al.*, 1994; Shaw, 1996), Table 2.2. The mode of synthesis is the biggest difference between the peptidergic transmitters and classical neurotransmitters. Classical neurotransmitters are synthesized and metabolized in nerve terminals. Peptides are genetically encoded and are synthesized in the cell bodies of neurons as peptide precursors that are then processed within vesicles, mature vesicles then are transported to nerve terminals along the axon (Shaw, 1996).

2.5.1 FMFRamide like peptides

Nematode neuropeptides are endogenous intercellular signaling molecules. Most of the neuropeptides interact with G-protein coupled receptors on the cell surface and initiate intracellular transduction or cytosolic signaling cascades (Maule *et al.*, 2001), some neuropeptides also evoke fast responses by directly acting on ion channels (Purcell *et al.*, 2002). Peptidergic signaling molecules are very diverse in nature and have been isolated from helminths, arthropods and other invertebrates (Taussig *et al.*, 1986), Table 2.2. FMFRamide-like peptides (FLPs) or FMFRamide-related peptides (FaRPs) are the largest known family of invertebrate regulatory neuropeptides. The first neuropeptide of the FMFRamide (Phe-Met-Arg-pheNH₂) family was isolated from the molluscan brain (Price *et al.*, 1977). Later antibodies were used for immunohistochemical staining which revealed immunoreactivity to this

peptide in various nematode species. Most are small peptides (≤ 20 amino acids) which are not members of the neuropeptide Y family and possess a C-terminal RFamide motif, an aromatic residue a hydrophobic residue and are classified as FLPs. The FLP system in nematodes is very complex with 42 *flp* encoding genes identified in both free living and parasitic nematodes with each *flp* gene coding for at least one distinct peptide (Cowden *et al.*, 1993a; Cowden *et al.*, 1995; Keating *et al.*, 1995; McVeigh *et al.*, 2005; Rosoff *et al.*, 1992; Rosoff *et al.*, 1993). More than 20 FLPs have been structurally characterized in *A. suum* so far (Cowden *et al.*, 1993a; Cowden *et al.*, 1995; Cowden *et al.*, 1989; Davis *et al.*, 1996). Some FLPs are active across species in invertebrates, arthropods and insects. Some neuropeptides isolated from *Ascaris* affect other nematodes (Maule *et al.*, 2002; Mousley *et al.*, 2005a). PCR-based cDNA analysis of expressed sequence tag database of parasitic nematodes have led to identification of approximately 290 distinct FLPs in the nematodes (Mousley *et al.*, 2005a). More than 200 peptidergic signaling molecules have been identified in arthropods (Mousley *et al.*, 2004; Mousley *et al.*, 2005b).

2.5.2 FLP distribution in *Ascaris*

Immunocytochemistry and confocal scanning laser microscopy have led to the identification of many structurally distinct FLPs. Their abundance of immunoreactivity to FMRFamide peptides in nematodes, in fact more than 75% of neurons in *Ascaris suum* are immunopositive to FLP antiserum (Brownlee *et al.*, 1996; Cowden *et al.*, 1993a; Cowden *et al.*, 1995; Davenport *et al.*, 1988). Table 2.3 shows in detail the immunopositive components of the *A. suum* nervous system.

FLP immunoreactivity has been identified in all neuronal components (central, peripheral and enteric) and subtypes including motor-, sensory-, and interneurons (Brownlee *et al.*, 1993a; Brownlee *et al.*, 1993b; Cowden *et al.*, 1993a; Fellowes *et al.*, 1999). FLP immunostaining is also widespread in all the nerve cords and more than half the ganglia of circumpharyngeal ring are FLP positive. FaRP immunopositive nerves have been identified in association with pharyngeal and vagina-vera muscles. Varicose nerve fibers with FLP immunoreactive dense core vesicles (120-160 nm) were identified around ovijector muscles. The peptidergic nerves are varicose in nature as they accumulate secretory vesicles (Fellowes *et al.*, 1999). *Ascaris* pharyngeal innervation is complex and involves cholinergic, serotonergic and peptidergic vesicles (120-160 nm)

Species	Localization of immunostaining	Reference
<i>Ascaris suum</i>	CNS, PNS and ENS	Davenport <i>et al.</i> , 1988; Sithigorngul <i>et al.</i> , 1990; Cowden <i>et al.</i> , 1993; Brownlee <i>et al.</i> , 1993a,b, 1994; Fellowes <i>et al.</i> , 1999
<i>Brugia pahangi</i>	CNS	Warbrick <i>et al.</i> , 1992
<i>Dirofilaria immitis</i>	CNS	Warbrick <i>et al.</i> , 1992
<i>Haemonchus contortus</i>	CNS, PNS and ENS	Geary <i>et al.</i> , unpublished observations
<i>Onchocerca volvulus</i>	CNS	Geary <i>et al.</i> , 1995
<i>Trichostrongylus colubriformis</i>	CNS	Geary <i>et al.</i> , 1995
<i>Caenorhabditis elegans</i>	CNS, PNS and ENS	Li and Chalfie, 1986; Atkinson <i>et al.</i> , 1988; Schinkmann and Li, unpublished observations
<i>Caenorhabditis vulgaris</i>	CNS	Schinkmann and Li, 1994
<i>Cystidicola faronis</i>	CNS	Wigren and Fagerholm, 1993
<i>Goodeyus ulmi</i>	CNS	Leach <i>et al.</i> , 1987
<i>Heterodera glycines</i>	CNS and PNS	Atkinson <i>et al.</i> , 1988
<i>Panagrellus redivivus</i>	CNS, PNS and ENS	Geary <i>et al.</i> , unpublished observations
<i>Romanomeris culicivorax</i>	CNS and PNS	Jagdale and Gordon, 1994

CNS, central nervous system; PNS, peripheral nervous system; ENS, enteric nervous system.

Table 2.2 (Maule *et al.*, 2001) Localization of FMRFamide- like peptides in helminths.

Component of nervous system	FaRP-immunoreactive neurones (%)
Circumpharyngeal nerve ring	> 50
Lateral ganglia cells	> 30
Retrovesicular ganglion	> 20
Ventral ganglion	> 50
Dorsal ganglion	100
Subdorsal and subventral ganglia	> 80
Subdorsal sensory cells	80
Tail ganglia cells (females)	> 75
Pharyngeal neurones	90
Ovijector neurones	100

Table 2.3 (Maule *et al.*, 2001) FLP immunoreactivity in *Ascaris suum* nervous system.

2.5.3 FLP distribution in other helminths

The molecular characterization of nematode FLPs was pioneered by Rosoff *et al.* (1992). Completion of *C. elegans* genome sequence has led to detailed study of FLPs in its neuromuscular system, which can be applicable to other nematodes (White *et al.*, 1986). FLP immunoreactivity in *C. elegans* was found to be only 10% with 30 neurons being immunopositive for FLPs in contrast to widespread reactivity demonstrated in *Ascaris* (Schinkmann *et al.*, 1992). *flp-1lacZ* reporter constructs and *in situ* hybridization techniques have led to the identification of 23 *flp* genes encoding 60 different FLPs in *C. elegans* (Li *et al.*, 1999; Nelson *et al.*, 1998b; Rosoff *et al.*, 1992). Other than immunohistochemistry, expressed sequence tag (EST) analysis coupled with PCR-based cDNA analysis have led to identification of novel *flp*-encoding gene homologues in four nematode clades (McVeigh *et al.*, 2005; Mousley *et al.*, 2005a). Interestingly neuropeptide sequences are found to be conserved across free living and parasitic nematodes. So far 290 distinct FLPs have been identified across parasitic nematode ESTs.

Helminth FLPs also share similar motifs with FLPs found in organisms from some other phyla. FLPs have been identified by immunostaining in platyhelminths; cestodes, digeneans, monogeneans and turbellarians. Immunoreactivity has been seen in both peripheral and central nervous systems as well as in the reproductive system (Halton *et al.*, 1994). FLP immunoreactivity has been identified throughout the nervous system in trematodes *e.g. Fasciola hepatica* and *Schistosoma mansoni*. Immunoreactivity was also seen in the somatic musculature and the muscles associated with egg laying flat worms (Day *et al.*, 1999; Marks *et al.*, 1995a). A role for RFamides and FLPs has also been proposed in egg formation in platyhelminths (Shaw *et al.*, 1996). The platyhelminth FLPs share the RFamide motif at the C-terminal but they contain different N-terminal amino acid sequences.

All the studies done so far have revealed that FLPs occur in all neuronal subtypes and the number and position of FLP positive neurons is very well conserved between diverse species not only in helminths but also in insects and arthropods.

2.5.4 *Ascaris* FLPs

The first nematode neuropeptide isolated from *Ascaris suum* was AF1. It is a heptapeptide (Lys-Asn-Glu-Phe-Ile-Arg-Phe-NH₂) which was isolated from methanol extracts of *Ascaris* head (Cowden *et al.*, 1989). This was the first endogenous neuropeptide shown to have physiological role in *Ascaris* neuromuscular system. So far 20 endogenous FLPs with different physiological actions have been isolated and characterized from *Ascaris suum*, Table 2.4. Since all these neuropeptides were isolated from *Ascaris* they were designated as *Ascaris* FMRFamide-like peptides

(AF) and they were numbered in chronological order of their discovery. One of the peptides, AF17, included in the list of FLPs differs in C-terminal sequence, it possesses a HFamide sequence instead of RFamide. Multiple-copy neuropeptide genes identified in invertebrates is a feature of *Ascaris* FLP encoding genes. It has been shown that six FLPs isolated from *A. suum* are encoded on single gene *afp-1* (Edison *et al.*, 1997). Three of the four transcripts of *afp-1* differed only in the untranslated region but had similar protein coding sequence. It is assumed that single nematode neuropeptide gene can code for a range of related, but structurally unique neuropeptides. So far six *afp* genes has been identified in *Ascaris suum* (Edison *et al.*, 1997; Mousley *et al.*, 2005a). The most abundant of all FLPs is AF2 which differs from AF1 by three amino acid substitutions (Cowden *et al.*, 1993b). AF2 has also been isolated from *Heamonchus contortus*, *C. elegans* and *Panagrellus redivivus* (Marks *et al.*, 1995b; Maule *et al.*, 1996).

Neuropeptide code	Neuropeptide sequence	Identified molecule(s)
AF1	KNEFIRF . NH ₂	Peptide
AF2	KHEYLRF . NH ₂	Peptide
AF3	AVPGVLR . NH ₂	Peptide; cDNA
AF4	GDVPGVLR . NH ₂	Peptide; cDNA
AF5	SGKPTFIRF . NH ₂	Peptide
AF6	FIRF . NH ₂	Peptide
AF7	AGPRFIRF . NH ₂	Peptide
AF8	KSAYMRF . NH ₂	Peptide
AF9	GLGPRPLRF . NH ₂	Peptide
AF10	GFGDEMSPGVLR . NH ₂	Peptide; cDNA
AF11	SDIGISEPNFLRF . NH ₂	Peptide
AF12	FGDEMSPGVLR . NH ₂	Peptide
AF13	SDMPGVLR . NH ₂	Peptide; cDNA
AF14	SMPGVLR . NH ₂	Peptide; cDNA
AF15	AQTFVRF . NH ₂	Peptide
AF16	ILMRF . NH ₂	Peptide
AF17	FDRDFMHF . NH ₂	Peptide
AF18	XXXXPNFLRF . NH ₂	Peptide
AF19	AEGLSSPLIRF . NH ₂	Peptide
AF20	GMPGVLR . NH ₂	Peptide; cDNA

Table 2.4 (Maule *et al.*, 2001) Primary sequences of *A. suum* FLPs.

2.5.5 Other nematode FLPs

Completion of the *C. elegans* genome sequencing project has led to the identification of various *flp* genes. Table 2.5 shows the complete list of *flp* genes and their corresponding peptides identified to date. 29 *flp* genes are identified so far and expression of at least 15 genes is confirmed by PCR and other techniques (Li, 2005; Maule *et al.*, 1997; Nelson *et al.*, 1998a). 68 different peptides are encoded on different *flp* genes identified in *C. elegans*, there are 60 known *C. elegans* FLPs (McVeigh *et al.*, 2005). Similar to *Ascaris* AF17, *C. elegans* also has two peptides, KPNFMRYG (*flp-1*) and EDGNAPFGTMKFG (*flp-3*), which do not have the characteristic RFamide motif at the C-terminal end. *flp* genes have also been identified in the related species *C. vulgaris* (Schinkmann *et al.*, 1992). The gene *Cv-*

flp-1 shares a strong sequence homology in the coding region with *C. elegans flp-1*. The neuropeptide precursor protein differs by four conservative amino acid changes and the RFAntisera stained a similar subset of cells in both the species, suggesting that the function and regulation of these peptides is conserved between these two species (Schinkmann *et al.*, 1994). Several other peptide encoding genes like *flp-1*, *flp-6*, *flp-8*, *flp-11* and *flp-14* have also been identified in other nematode species which suggest conservation of structures but the conservation of function of these peptides between different species has yet to be completely determined.

FLPs have been structurally and functionally characterized in other nematode species as well. Five FLPs have been identified in the free living nematode *P. redivivus* and three FLPs have been identified in *Haemonchus contortus*. Work done by Geary *et al.* (1992) lead to the identification of two novel FLPs from nematode *P. redivivus*: SDPNLRFamide (*P. redivivus* FLP-1, PF1) and SADPNFLRFamide (PF2). Since then more peptides: KSAYMRFamide (PF3/AF8) (Maule *et al.*, 1994b); KPNFIRFamide (PF4) (Maule *et al.*, 1995a); KHEYLRFamide (AF2) (Maule *et al.*, 1994a) ; and AMRNALVRFamide and NGAPQPFVRFamide (Maule *et al.*, 2001) have been identified in *P. redivivus*. It was noted that except for PF4 all the PF peptides showed complete identity with *C. elegans* peptides. These observations again confirm the evolutionary conservation of neuropeptide sequences and possibly functions in nematodes. Two peptides isolated from *H. contortus*: KSAYMRFamide (PF3/AF8) and KHEYLRFamide (AF2) are found in all four nematode species studied extensively for FLPs (Keating *et al.*, 1995; Marks *et al.*, 1999). As in *Ascaris*,

AF2 is the most abundant neuropeptide in *P. redivivus*, *C.elegans* and *H. contortus* making it the most abundant FLP in the nematode phyla identified so far.

In platyhelminths FMRFamide immunoreactivity has been seen but the immunocytochemical staining pattern is virtually identical to another peptide family NPF (Neuropeptide-F). So far only three flatworm FLPs have been isolated from turbellaria, and the cestode family: *Dugesia tigrina* – GYIRFNH₂ (Johnston *et al.*, 1996); *Artiposthia triangulata* – RYIRFNH₂ (Maule *et al.*, 1994c); and *Moniezia expansa* – GNFRFNH₂ (Maule *et al.*, 1993). The isolation of FLPs from trematodes has been unsuccessful so far. However, functional FLP receptors have been identified in *Schistosoma mansoni* muscles, where RYIRFamide isolated from flatworms demonstrated the highest potency compared to other FLPs (Day *et al.*, 1999; Day *et al.*, 1994). The high degree of potency of the turbellarian FLP in inducing contractions in digenean muscles (*S. mansoni*) suggests that it is the most closely related endogenous ligand for the receptor. Interestingly turbellarians are the proposed evolutionary ancestors of parasitic digeneans (Shaw *et al.*, 1996). Table 7.1 (Appendix) shows the complete list of *flp* genes so far identified from different clades of the phylum *Nematoda*. Some of the genes as mentioned in the Table were characterized from EST's due to unavailability of complete genome sequences for all the nematodes in different clades.

<i>flp-1</i>	<i>flp-7</i>	<i>flp-14</i>
KPNFMRYG	TPMQRSSMVRFG	*KHEYLRFG
AGSDPNFLRFG	SPMQRSSMVRFG	*KHEYLRFG
*SQPNFLRFG	SPMQRSSMVRFG	*KHEYLRFG
*ASGDPNFLRFG	SPMQRSSMVRFG	*KHEYLRFG
*SDPNFLRFG	SPMERSAMVRFG	
*AAADPNFLRFG	SPMDRSKMVRFG	<i>flp-15</i>
*SADPNFLRFG	TPMQRSSMVRFG	GGPQGPLRFG
KPNFLRFG		GPSGPLRFG
<i>flp-2</i>	<i>flp-8</i>	<i>flp-16</i>
LRGEPIRFG	**KNEFIRFG	**AQTFVRFG
SPREPIRFG	**KNEFIRFG	**AQTFVRFG
	**KNEFIRFG	GQTFVRFG
<i>flp-3</i>	<i>flp-9</i>	<i>flp-17</i>
SPLGTMRFG	*KPSFVRFG	KSAFVRFG
TPLGTMRFG	*KPSFVRFG	KSAFVRFG
SAEPFGTMRFG		KSQYIRFG
NPENDTPFGTMRFG	<i>flp-10</i>	
ASEDALFGTMRFG	QPKARSGYIRFG	<i>flp-18</i>
EDGNAPFGTMKFG		DFDGAMPGVLRFG
EAEELGTMRFG	<i>flp-11</i>	EMPGVLRFG
SADDSAPFGTMRFG	**AMRNALVRFG	KSVPGVLRFG
NPLGTMRFG	ASGGMRNALVRFG	SVPGVLRFG
	**NGAPQPFVRFG	EIPGVLRFG
<i>flp-4</i>	<i>flp-12</i>	SEVPGVLRFG
PTFIRFG	*RNKFEFIRFG	DVPGVLRFG
ASPSFIRFG		*SVPGVLRFG
<i>flp-5</i>	<i>flp-13</i>	Peptides from other putative <i>flp</i> genes
APKPKFIRFG	SDRPTRAMDSPLIRFG	TKFQDFLRFG
AGAKFIRFG	**AADGAPLIRFG	AMRNSLVRFG
GAKFIRFG	*APEASPFIRFG	DYDFVRFG
	**AADGAPLIRFG	DGFVRFG
<i>flp-6</i>	APEASPFIRFG	AFFKNVLRFG
*KSAYMRFG	ASPSAPLIRFG	
*KSAYMRFG	SPSAVPLIRFG	
*KSAYMRFG	SAAAPLIRFG	
*KSAYMRFG	ASSAPLIRFG	
*KSAYMRFG		
*KSAYMRFG		

*Peptides that have been isolated and sequenced from *C. elegans*.

**Peptides that have been isolated from nematode species other than *C. elegans*.

Other putative *flp* genes were identified using search strings comprising C-terminal tetrapeptides of known FaRPs plus a C-terminal G (amide donor) residue in searches of the *C. elegans* BLAST server, wormpep 17.

Table 2.5 (Maule *et al.*, 2001) *C. elegans flp* genes and FLP sequences.

2.5.6 Effects of nematode FLPs

We know of a large number of FLPs and *flp* genes in nematodes but the physiology of each of them has not been fully elucidated. There is a big gap between structural identification and physiological function of these peptides. *A. suum* is the most commonly used nematode for investigating the effects of these neuropeptides on the nematode neuromuscular system. Due to conservation of FLP sequence across nematode species, the information could be used for a foundation applicable across the phylum (Mousley *et al.*, 2005a). Here we have to keep in mind that although FLP immunoreactivity has been demonstrated across the nematode phylum, we still don't have the distribution pattern of individual FLPs. The functional studies in *Ascaris* have been done in most detail using somatic body wall muscles (Cowden *et al.*, 1993b), neurons, the ovijector (Brownlee *et al.*, 1993a), and the pharynx (Brownlee *et al.*, 1999).

Table 2.7 and 2.8 describes in detail the different *flp* genes, FLP peptides synthesized and effects of different peptides on the pharynx, somatic body wall muscles and nervous system of *Ascaris suum*. I will discuss here representative neuropeptides of different classes from *Ascaris* and other nematodes.

KNEFIRFamide (AF1) and KHEYLRamide (AF2)

These are hepta peptides isolated from *A. suum*. The two peptides have very similar pharmacology (Cowden *et al.*, 1993b; Cowden *et al.*, 1989). AF1 and AF2 abolish locomotory waves at the injection site when injected in whole worms. On muscle strip preparations AF1 and AF2 induced a biphasic response, on initial

inhibitory phase followed by an extended period of excitatory contractions (Cowden *et al.*, 1989; Maule *et al.*, 1995a; Pang *et al.*, 1995). AF2 was more potent than AF1 in inducing muscle contraction, the threshold concentration of AF1 was 1 nM (Bowman *et al.*, 1996) compared to 10 pM for AF2 (Cowden *et al.*, 1993b). The effects of AF1 and AF2 were found to be dose-dependent, the inhibitory phase decreasing with increasing concentration of AF1 and at concentrations higher than 1 μ m the inhibitory phase was abolished. However, at concentrations <100 nM, the inhibitory phase was extended (Bowman *et al.*, 1996; Pang *et al.*, 1995). Experiments with denervated muscle strips showed that the excitatory and inhibitory responses were mediated by different receptors. The excitatory phase was abolished in denervated muscle strips, suggesting the excitatory receptors are neuronal while inhibitory receptors are muscular in location. Electrophysiological studies demonstrated the inhibition of dorsal and ventral inhibitory neurons with no effect on excitatory motor neurons. It also reversibly abolished the oscillatory responses. AF2 also increased the ACh induced excitatory junction potential. Structure-activity studies with AF1 and AF2 also demonstrated the probable presence of two different receptors for the two responses (Pang *et al.*, 1995). Chimera studies with AF1 and AF2 have also shown that the two peptides act on different receptors, AF1 antagonist didn't block the effects of AF2. It has also been postulated that AF2 acts both pre- and post-synaptically at the neuromuscular junction to elicit muscle responses. AF2 increased the excitatory junction potential in *A. suum* muscles treated with nicotinic antagonist. AF2 not only potentiated the ACh induced muscle contraction (Pang *et al.*, 1995) but also it potentiated the ACh

induced depolarization of the *A. suum* muscles (Trailovic *et al.*, 2005). AF2 has also been found to stimulate cAMP levels in *A. suum* body wall muscles (Thompson *et al.*, 2003) but the cAMP does not seem to play a role in the AF2 induced excitability of muscle cells (Trailovic *et al.*, 2005).

Effects of AF1 and AF2 have also been shown on the vagina vera of the *A. suum*. The vagina vera, unlike body wall muscles, is circular in structure. Both peptides inhibit the spontaneous contraction but only AF1 induced the biphasic response seen in somatic muscle cells (Fellowes *et al.*, 1998). In sheep nematode *H. contortus* AF2 inhibited the ACh induced muscle contractions (Marks *et al.*, 1999). *AVPGVLRFamide (AF3) and GDVPGVLRFamide (AF4)*

Six C-terminal PGVLRFamide peptides (AF3, AF4, AF10, AF13, AF14 and AF20, Table. 2.7) have been isolated from *A. suum* and have been shown to increase muscle tension, they are excitatory in nature (Davis *et al.*, 1996). Both AF3 and AF4 induced muscle contractions and like AF2 they increased the muscle cAMP levels. However, electrophysiological recording showed that the AF3 and AF4 induced muscle depolarization was independent of ACh receptor activation or inhibition (Trim *et al.*, 1997). Also cobalt was more effective at blocking the AF3 and AF4 induced depolarization of muscle membrane than those of ACh. These results confirm that AF3 and AF4 produce their effect without an effect on muscle nAChR's (Trim *et al.*, 1997), the effect on second messengers is yet to be completely understood. AF3 and AF4 had complex multiphasic effects on ovijector, initial contraction followed by relaxation and a period of inactivity. The effects of AF3 & AF4 are different from AF1 & AF2 suggesting that there are different receptors for

different peptides (Fellowes *et al.*, 2000; Fellowes *et al.*, 1998). AF3 and AF4 produced similar responses in the related species, *Ascaridia galli* suggesting that the effects of these peptides are not limited to *A. suum* in nematodes (Trim *et al.*, 1998).

SDPNFLRFamide (PF1), SADPNFLRFamide (PF2)

PF1 and PF2 both have been isolated from the free living nematode *P. redivivus* (Geary *et al.*, 1992) and *C. elegans* (Rosoff *et al.*, 1993). Although they have not been identified in *A. suum*, both produce profound inhibitory effects in *A. suum* muscle (Maule *et al.*, 1994b). Both PF1 and PF2 produced similar inhibitory effects on muscle cells: prolonged dose-dependent flaccid paralysis and slow hyperpolarization. PF1 relaxes ACh and levamisole contracted muscles and inhibits the excitatory peptides AF1 and AF2. The effects of PF1 and PF2 on muscle cells were nerve cord independent and Ca^{2+} -dependent (Franks *et al.*, 1994; Maule *et al.*, 1995a). It has been hypothesized that a NO (nitric oxide) pathway is responsible for the effects of PF1 and PF2 on muscles. Inhibitors of NOS (NO synthase), the enzyme responsible for NO generation, has been found to block the effects PF1 & PF2 on muscle cells. Also, the NO donor nitroprusside mimicked the PF1 induced muscle relaxation in *A. suum* muscle (Bowman *et al.*, 1995). Interestingly, NOS activity was highest and NOS binding was most pronounced in the *Ascaris* hypodermal layer associated with muscles.

On the vagina vera preparation PF1 and PF2 produced circular muscle relaxation (shortening) and flaccid paralysis at high concentrations. But lower concentrations caused transient cessation of contractions which resumed after

addition of peptides, PF1 and PF2. PF2 produced measurably greater response compared to PF1 (Fellowes *et al.*, 2000).

Other PF peptides also have effects on the *Ascaris* musculature (Table 2.7). KSAYMRFamide (PF3) was the first peptide demonstrated to have different effects on dorsal and ventral musculature; PF3 contracts ventral but relaxes dorsal muscles (Maule *et al.*, 1995a). PF4 (KPFIRFamide) is the only neuropeptides shown to have a direct effect on ion channels (Purcell *et al.*, 2002). PF4 has inhibitory effects on *Ascaris* body wall muscles, inducing nerve cord independent and Cl⁻ dependent reversible relaxation. Electrophysiologically it also produced hyperpolarization of muscle cells (Maule *et al.*, 1995a; Maule *et al.*, 1995b). Table 2.7 and 2.8 gives a detailed summary of different peptides and their effects on nematode systems.

Nematode peptide (and abbreviation)	Effects on neuromuscular system of <i>Ascaris suum</i>	Effects on vagina <i>vera</i>
KN6yEFIRFamide (AF1)	Biphasic effects \geq (1 nM) on muscle strips. Relaxation followed by increased muscle contractility. Small (1-2 mV) depolarization of muscle cells. Abolishes slow membrane potentials and increases input conductance's of VI and DI inhibitory neurons.	Biphasic effects (\geq 10 nM) – profound contraction followed by period of relaxation.
KHEYLRFamide (AF2)	Qualitatively similar biphasic effects on muscle strips to those of AF 1 but much more potent (\geq 1 pM). Potentiates ACh-induced contraction, and increases the amplitude of EJPs; Stimulates cAMP levels.	Reduces contraction frequency (0.1 μ M)
AVPGVLRFamide (AF3)	Contraction of dorsal muscle strips (0.1 μ M). Increases sensitivity of muscle to ACh but action is independent of ACh receptor; decreases cAMP levels.	Multi-phasic effects (\geq 1 mM) – transient contraction than relaxation and return of contractile activity
GDVPGVLRFamide (AF4)	Contraction of dorsal muscle strips (0.1 μ M).	Similar effects to AF3 but less potent (3 nM)
SDPNFLRFamide (PFI)	Slow Ca^{2+} -dependent and nerve cord-independent relaxation (\geq 1 nM) and flaccid paralysis of muscle strips. Decreases amplitude of EJPs. Effects may involve NO. Dose-dependent hyperpolarization (\leq 12 mV) of muscle cells.	Induces a transient flaccid paralysis (\geq 3 nM)
SADPNFLRFamide (PF2)	Similar effects to PFI (see above).	Transient flaccid paralysis (\geq 1 nM)
KSAYHRFamide [AF8 (PF3)]	Nerve cord-dependent contraction of ventral (\geq 0.1 μ M) and relaxation of dorsal (\geq 1 μ M) muscle strips. Concentration-dependent inhibition of 5-HT-stimulated pharyngeal pumping.	Reduces contraction frequency and amplitude (\geq 0.1 μ M)
KPNFIRFamide (PF4)	Rapid Cl^- dependent and nerve cord-independent relaxation of muscle strips (\geq 1 nM). Concentration-dependent hyperpolarization (4-6 mV) and increase in input conductance of muscle cells.	Induces flaccid paralysis (\geq 10 nM)

Table 2.7 (Day *et al.*, 1999; Maule *et al.*, 1996) Effects of nematode FLPs on *Ascaris suum* neuromuscular and reproductive system.

Gene	Peptide	Peptide title	Behavioral effects	<i>Ascaris suum</i> body wall muscle response type (bwRT)	Pharynx	Electrophysiology
<i>flp-1</i>	KPNFIRFa	PF4	<i>C. elegans</i> flp-1 KO: uncoordinated movement, hyperactivity, defective nose touch response, osmotic avoidance and egg laying	bwRT2	NE As PP	
	SADPNFLRFa	PF2			↓ Ce APF; As PP	
	SDPNFLRFa	PF1		bwRT1	↓ Ce APF; As PP	
	SDIGISEPNFLRFa	AF11	As PI: ma	bwRT1		DE2↑Rin↓EPSP↑; DI↑Rin↓
<i>flp-2</i>	LRGEPiRFa					
	SPREPIRFa				↑ Ce APF	
<i>flp-3</i>	SPLGTMRFa					
	SAEPFGTMRFa				↓ Ce APF	
<i>flp-4</i>	ASPSFIRFa					
	SGKPTFIRFa	AF5	As PI: ↓ movement	bwRT3		DE2↑Rin↓EPSP↑; DI↓Rin↓
	AGPRFIRFa	AF7	As PI: ↓ movement			DE2↓EPSP↑; DI↓Rin↓
	PTFIRFa				↑ Ce APF	
<i>flp-5</i>	AGAKFIRFa					
	GAKFIRFa				↑ Ce APF	
	APKPKFIRFa					
	FIRFa	AF6	As PI: negligible		NE As PP	DE2↑EPSP↑; DI↓Rin↓
<i>flp-6</i>	KSAYMRFa	AF8/PF3	As PI: ma, ventral coiling	Ventral: bwRT3 Dorsal bwRT1	↑ Ce APF; ↓ As PP	DE2↓Rin↓EPSP↓; DI↑↓Rin↓
<i>flp-7</i>	SPMERSAMVRFa					
	SPMQRSSMVRFa				NE Ce APF	
<i>flp-8</i>	KNEFIRFa	AF1	As PI: ↓	bwRT4	↑ Ce APF; ↓ As PP	DE2↑Rin↓EPSP↑; DI↓Rin↓
<i>flp-9</i>	KPSFVRFa		<i>C. elegans</i> flp-9 KO: Reduced locomotion	No effect	↓ Ce APF	
<i>flp-10</i>	QPKARSGYIRFa				NE Ce APF	
<i>flp-11</i>	AMRNALVRFa				↓ Ce APF	
	NGAPQPFRFa					
<i>flp-12</i>	RNKFEFIRFa				NE Ce APF	

Gene	Peptide	Peptide title	Behavioral effects	<i>Ascaris suum</i> body wall muscle response type (bwRT)	Pharynx	Electrophysiology
<i>flp-13</i>	AADGAPLIRFa			bwRT1		
	AEGLSSPLIRFa	AF19	As PI: ma			DE2↓Rin↓EPSPa↓; DI↓Rin↓
					↓ Ce APF	
	APEASPFIRFa			bwRT1		
	ASSAPLIRFa					
<i>flp-14</i>	KHEYLRFa	AF2/PF5	As PI: ↑	bwRT4	↑ Ce APF; NE As PP	DE2↑Rin↑↓; DI- Rin↓
<i>flp-15</i>	GPSGPLRFa					
	GGPQGPLRFa				↓ Ce APF	
<i>flp-16</i>	AQTFVRFa	AF15	As PI: ma		↓ Ce APF	DE2↑Rin↓EPSP↑; DI↑Rin↓
	GQTFVRFa					
<i>flp-17</i>	KSQYIRFa				↑ Ce APF	
	KSAFVRFa				↑ Ce APF	
<i>flp-18</i>	AVPGVLRFa	AF3	As PI: ↑	bwRT3	NE As PP	DE2↑Rin↑EPSP↑; DI- Rin↓
	GDVPGVLRFa	AF4		bwRT3	NE As PP	DE2↑Rin↑EPSP↓; DI↓Rin↓
	GFGDEMSPGVLRFa	AF10		bwRT3		DE2↑Rin↑; DI- Rin↓
				bwRT3		DE2↑Rin↑EPSP↑; DI↓Rin↓
	GMPGVLRFa	AF20				
				bwRT3		DE2↑Rin↑; DI-
	SDMPGVLRFa	AF13				
				bwRT3		DE2↑Rin↑EPSP↑; DI↓Rin↓
	SMPGVLRFa	AF14				
	SVPGVLRFa			bwRT3		
	EMPGVLRFa				↓ Ce APF	
<i>flp-19</i>	ASWASSVRFa					
	WANQVRFa				↓ Ce APF	
<i>flp-20</i>	AMMRFa				NE Ce APF	
<i>flp-21</i>	GLGPRPLRFa	AF9	<i>C. elegans</i> flp-21 KO enhances social feeding, overexpression suppresses social feeding; As PI: ↓	bwRT3	↓ Ce APF	DE2↑EPSP↑; DI↓Rin↓
<i>flp-22</i>	SPSAKWMRFa				↑ Ce APF	
<i>flp-23</i>	TKFQDFLRFa				NE Ce APF	
<i>flp-24</i>	VPSAADMMIRFa			No effect		
<i>flp-29</i>	ILMRFa	AF16	As PI: negligible		NE As PP	DE2- EPSP↓; DI-
	FDRDFMHFa	AF17	As PI: ma	bwRT3		

Table 2.8 Functional classes of nematode FLPs (McVeigh *et al.*, 2006).

^a In peptide sequences, a indicates amide.

^b Peptide titles indicate the species from which peptides have been biochemically isolated: AF, *A. suum* FLP; PF, *P. redivivus* FLP.

^c 'As PI' denotes analysis of worm behavior following pseudocoelomic injection into adult *A. suum*; ↑, increased movement; ↓, decreased movement; ma, movement abolished; negligible, negligible effect. Only gross descriptions of effects, based on qualitative descriptions of Ref. Nelson *et al.*, (1998b), are given; for more detailed descriptions of behavioral effects, see Refs. Davis *et al.*, (2001) and Reinitz *et al.*, (2000)

^d bwRT denotes *A. suum* dorsal body wall muscle response types 1–4: 1, slow inhibitory; 2, fast inhibitory; 3, excitatory; 4, biphasic;

^e ovRT denotes *A. suum* ovijector response types 1–5: 1, inhibitory; 2, excitatory; 3, transient contraction; 4, transient contraction followed by spastic paralysis; 5, relaxation followed by increased activity.

^f 'As PP' denotes effects on *A. suum* 5-HT stimulated pharyngeal pumping; Ce APF denotes effects on *C. elegans* pharyngeal action potential frequency; NE, no effect.

^g DE2 denotes a hyperpolarizing (↓), depolarizing (↑) or negligible (–) effect on *A. suum* DE2 motoneurons; R_{in} details an increase (↑), decrease (↓) or biphasic effect (↑↓) on neuronal input resistance; EPSP denotes an increase (↑) or decrease (↓) on excitatory postsynaptic potential frequency; EPSPa denotes changes in excitatory postsynaptic potential amplitude; DI denotes a hyperpolarizing (↓), depolarizing (↑), biphasic (↑↓) or negligible (–) effect on *A. suum* DI motoneurons;

^h McVeigh, P., Marks, N.J., Maule, A.G., unpublished. Cited by McVeigh *et al.*, 2006

^a In peptide sequences, a indicates amide.

^b Peptide titles indicate the species from which peptides have been biochemically isolated: AF, *A. suum* FLP; PF, *P. redivivus* FLP.

^c 'As PI' denotes analysis of worm behavior following pseudocoelomic injection into adult *A. suum*; ↑, increased movement; ↓, decreased movement; ma, movement abolished; negligible, negligible effect. Only gross descriptions of

2.5.7 Nematode FLP receptors

Most nematode neuropeptides activate seven-transmembrane G-protein coupled receptors (GPCR's) to induce their effects. Indirect data obtained from worm physiology, heterologous expression and reverse genetics has identified GPCR's as potential target receptors of FLPs (Kubiak *et al.*, 2007; Kubiak *et al.*, 2003a; Kubiak *et al.*, 2003b; Li *et al.*, 1999; Reinitz *et al.*, 2000; Thompson *et al.*, 2003). Completion of the *C. elegans* genome sequence and preliminary data has lead to the identification of ~ 54 candidate for neuropeptide GPCR's. There are close to ~ 60 neuropeptide genes in *C. elegans*. Different spliced forms of *C. elegans* GPCR's have also been cloned, sequenced and expressed in variety of systems but

functional consequences of this variation have yet to be determined (Komuniecki *et al.*, 2004; Lowery *et al.*, 2003). More recently deorphanization and cloning of *C. elegans* GPCR's as FLP receptors (Kubiak *et al.*, 2007; Kubiak *et al.*, 2003b) and their functional expression has also confirmed the GPCR mediated effects of FLPs (Greenwood *et al.*, 2005; Mertens *et al.*, 2006; Mertens *et al.*, 2005). Unlike the apparent promiscuous expression of FLPs in different tissues the cloned receptors are found to be relatively selective towards their ligand. The studies so far have provided data for potential ligand-receptor pairs but all the activating ligands have not been tested as yet. Also, most of the results obtained are in *in-vitro* experiments and *in-vivo* receptor ligand expression has yet to confirm the same. Unlike nematodes, no FLP receptors have been identified so far in flatworms. Although based on functional studies GPCR signaling systems have been implicated in the FLP responses, (McVeigh *et al.*, 2005).

Conclusion

From the identification of more than 60 nematode FLPs, it is apparent that the nematode signaling system is highly developed and plays an important role in worm physiology. It is also possible that FLPs, like neuropeptides, interact with other signaling pathways, not only modulating the different physiological systems, but also playing a role in the development of worms. Therefore they offer a potential target for the development of anthelmintic drugs. With the availability of different tools for investigation it is the right time to seriously consider them and their receptors as candidates for novel anthelmintics.

2.5.8 Nematode neurotransmitters

Acetylcholine (ACh) was the first molecule to be classified as a neurotransmitter in vertebrates. ACh and γ -aminobutyric acid (GABA) were the two neurotransmitters identified to modulate electrical activity in somatic muscles of *A. suum* (del Castillo *et al.*, 1964a; Stretton *et al.*, 1978). We now have evidence to prove that serotonin, histamine, dopamine along with neuropeptides play important roles in the nematode neuromuscular system (<http://wormbook.com>). ACh is the major excitatory and GABA is the major inhibitory neurotransmitter in the *A. suum* nervous system (del Castillo *et al.*, 1964a; del Castillo *et al.*, 1964b; Stretton *et al.*, 1978). Originally, it was hypothesized that ACh and GABA were receptors located exclusively at the synaptic junction (del Castillo *et al.*, 1964a; Norton *et al.*, 1957) but this was proven otherwise with advances in the understanding of the electrophysiology of muscles. Now we know that apart from neuromuscular synapses, AChR's and GABAR's are present extra-synaptically on the muscle bag region (Brading *et al.*, 1971; Martin, 1982).

Acetylcholine (ACh)

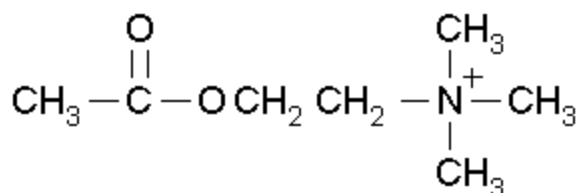


Figure 2.10 The chemical structure of acetylcholine.

ACh is one of the major neurotransmitter with more than a third of neurons in *C. elegans* releasing ACh. The stimulating action of ACh on *A. suum* muscle was first demonstrated by Baldwin and Moyle (1949) and later the excitatory nature of the

AChR was confirmed by Colquhoun *et al.*, (1991). In vertebrates there are two distinct AChR's; nicotinic (activated by nicotine) and muscarinic (activated by muscarine). Nicotinic receptors (nAChR's) are ionotropic in nature have five subunits, each unit is composed of four transmembrane domains, and belong to the group of ligand gated ion channels. Where as, muscarinic receptors (mAChR's) have seven transmembrane domains and belonged to group of GPCR's (Katzung, 2003). Muscle contraction assays (Robertson *et al.*, 2002) and single channel recordings (Qian *et al.*, 2006) in *Ascaris* have lead to the identification of three pharmacologically distinct nAChR's; L-, N-, and B-type. As the name indicates they respond to ACh and nicotinic agonists such as levamisole, nicotine and buprenorphine. More recently ACh-gated chloride channels have been identified in *C. elegans* (ACC-1,-2, -3 and -4). The expression and function of these ion channels is not understood.

Muscarinic agonists were found to be weak or ineffective in modulating muscle contraction in *A. suum* (Natoff, 1969; Rozhkova *et al.*, 1978) leading to the hypothesis that AChR's in *Ascaris* are only the nicotinic type. However later, ligand binding studies in nematode *C. elegans* confirmed the presence of muscarinic receptors in nematodes (Culotti *et al.*, 1983). Three genes coding mAChR's have been identified in *C. elegans*; *gar-1*, *gar-2* and *gar-3* (Lee *et al.*, 2000; Park *et al.*, 2003; Park *et al.*, 2000). Among the three mAChR's (GAR-1,-2 and -3) GAR-3 isoform appears most similar to mammalian mAChR's. Interestingly, mAChR's (GAR's) can undergo alternative splicing which plays a significant role in maintaining molecular diversity in ACh GPCR's in *C. elegans*. In *A. suum*, like *C. elegans* genes

coding for *gar-1*, *gar-2* and *gar-3* have been identified in genomic sequences. GAR-1 mAChR in *A. suum* have been cloned, it has two isoforms 1A and 1B. These isoforms are similar to GAR-1 isoforms found in *C. elegans* (M. Kimber and T. Day, pers. comm.).

γ-amino butyric acid (GABA)

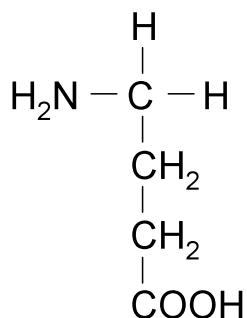


Figure 2.11 The chemical structure of GABA.

GABA is an amino-acid neurotransmitter and is synthesized from glutamate (Bazemore *et al.*, 1956). GABA is an inhibitory neurotransmitter in *Ascaris* (Martin *et al.*, 1991). Although the pharmacology of GABA receptors in *C. elegans* differs from vertebrates, two types of GABA receptors are identified in *C. elegans* based on sequence similarity, GABA_A and GABA_B. GABA_A receptors are associated with chloride channels and are inhibitory in nature (Parri *et al.*, 1991). GABA_B is a G_{i/o} coupled receptor and its activation inhibits either voltage-gated calcium channels or activates potassium channels in vertebrates (Campbell *et al.*, 1993). Most of the vertebrate GABA_A agonists are active on the *A. suum* receptor (Holden-Dye *et al.*, 1989; Holden-Dye *et al.*, 1988). The GABA neurons are well conserved in different nematodes. In *C. elegans* 26 neurons use GABA as a neurotransmitter (Guastella *et*

al., 1991; Johnson *et al.*, 1987). GABA inhibits foraging and muscle contractions but contracts enteric muscles during defecation in *C. elegans* (McIntire *et al.*, 1993).

Glutamate

A glutamatergic pathway has been shown to play a significant role in *Ascaris* locomotion and pharyngeal functions (Davis, 1998). The DE2 motor neuron is the primary target in the *A. suum* nervous system. Ionotropic ligand-gated GluR's have been found to mediate excitatory and inhibitory neurotransmission in *C. elegans* (Brockie *et al.*, 2003). Out of 10 excitatory GluR subunits identified in *C. elegans*, GLR-1 – GLR-8 are similar to vertebrate non-NMDA receptors. NMR-1 and NMR-2 have similarity with NMDA receptors. GluCl receptors are also identified in *C. elegans*, *Ascaris* and *H. contortus* (Cully *et al.*, 1996; Forrester *et al.*, 1999; Jagannathan *et al.*, 1999; Portillo *et al.*, 2003) these receptors are the target site of ivermectin (Cully *et al.*, 1994; Martin, 1996). GluCl channels are expressed in pharyngeal muscles and neurons (Dent *et al.*, 2000; Laughton *et al.*, 1997; Vassilatis *et al.*, 1997b).

Serotonin

Serotonin (5-HT) receptors have been identified in *Ascaris* pharynx and ventral cord motor neurons in the tail region of males (Johnson *et al.*, 1996). Eight type of neurons are found to be immunopositive for 5-HT in *C. elegans*. Application of serotonin (Horvitz *et al.*, 1982; Waggoner *et al.*, 1998) or serotonin knockout worms (Loer *et al.*, 1993; Waggoner *et al.*, 1998) show locomotory defects with increased rate of egg laying. G-protein coupled serotonin receptors (SER-1, SER-4 and SER-7) have been identified in *C. elegans*. These receptors are expressed in

pharyngeal neurons and muscles (Hamdan *et al.*, 1999; Hobson *et al.*, 2003; Hobson *et al.*, 2006; Olde *et al.*, 1997).

Dopamine

Some evidence of dopaminergic signaling has been shown in *A. suum* (Sulston *et al.*, 1975). In *C. elegans* there are eight neurons which use dopamine as neurotransmitter. Dopamine signaling is linked to environmentally based behavior in *C. elegans*. It has been shown that dopamine signaling helps in learning and memory in worms (Bettinger *et al.*, 2004; Colbert *et al.*, 1995). DOP-1 –DOP-4 are four dopaminergic receptors identified in *C. elegans* (Suo *et al.*, 2002)

2.6 Voltage-activated currents

2.6.1 Voltage-activated calcium currents

Ca²⁺ channels mediate Ca²⁺ influx in response to membrane depolarization in many different cell types and especially in excitable cells. Ca²⁺ entry in to cells through voltage-gated calcium channels (VGCC's) acts as second messenger of electrical signaling and initiates intracellular events such as, muscle contraction, neurotransmitter release secretion, gene expression and cellular differentiation. Their activity is essential to couple electrical signals on the cell surface to physiological events inside cells. High levels of Ca²⁺ entry can lead to toxicity as these events are based on a balanced entry of Ca²⁺ into the system. The importance of regulation of Ca²⁺ entry in cells is reflected by the presence of several subtypes of Ca²⁺ channels in vertebrate system, Table 2.14. Each of these channels is distinct in their location, kinetics, pharmacology and distribution. The first evidence of different channel types was found in starfish eggs (Hagiwara *et al.*, 1975) and then in

mammalian neurons (Carbone *et al.*, 1984; Fedulova *et al.*, 1985) These channels are protein complexes with four or five distinct subunits. The biggest subunit α_1 is the most common site of channel regulation as it contains the conduction pore, voltage sensor and gating apparatus of the channel thus, α_1 determines the pharmacological and electrophysiological diversity of the channel. The α_1 subunit is composed of four homologous domains (I-IV), with six transmembrane segments in each. The S4 segment serves as the voltage sensor and the pore loop between S5 & S6 determines ion conductance and selectivity (Catterall *et al.*, 2005). There are ten α_1 channel types associated with six different classes of calcium channels. In addition to the α subunit there are three auxiliary subunits: α_2 - δ , β and γ , which are also responsible for modulation of the channel complex, Figure 2.14.

L-type calcium currents are high-voltage-activated (strong depolarization), long lasting currents which are blocked by calcium channel antagonists, like dihydropyridines (DHP), phenylalkylamines, and benzothiazepines. They are the major calcium carrying currents in muscles and endocrine cells. L-type low-voltage-activated calcium currents are also identified in neurons and pacemaker cells.

The dihydropyridine insensitive high voltage-activated currents are of three types, N-, P/Q-, and R-type. These currents are blocked by different peptide toxins but not by L-type calcium channel blockers, Table 2.9. N-types are neuronal channel types (Nowycky *et al.*, 1985), whereas P-type were first isolated from purkinje cells (Hillman *et al.*, 1991), Q-type arise from the same molecular entity as P-types so are combined together (Randall *et al.*, 1995). N-and P/Q-type calcium channels are the main subtypes responsible for synaptic transmission and are located at

neuromuscular junctions. The residual calcium currents which are resistant to dihydropyridines and the N and P/Q channel toxins are classified as R-type calcium currents (Randall *et al.*, 1995).

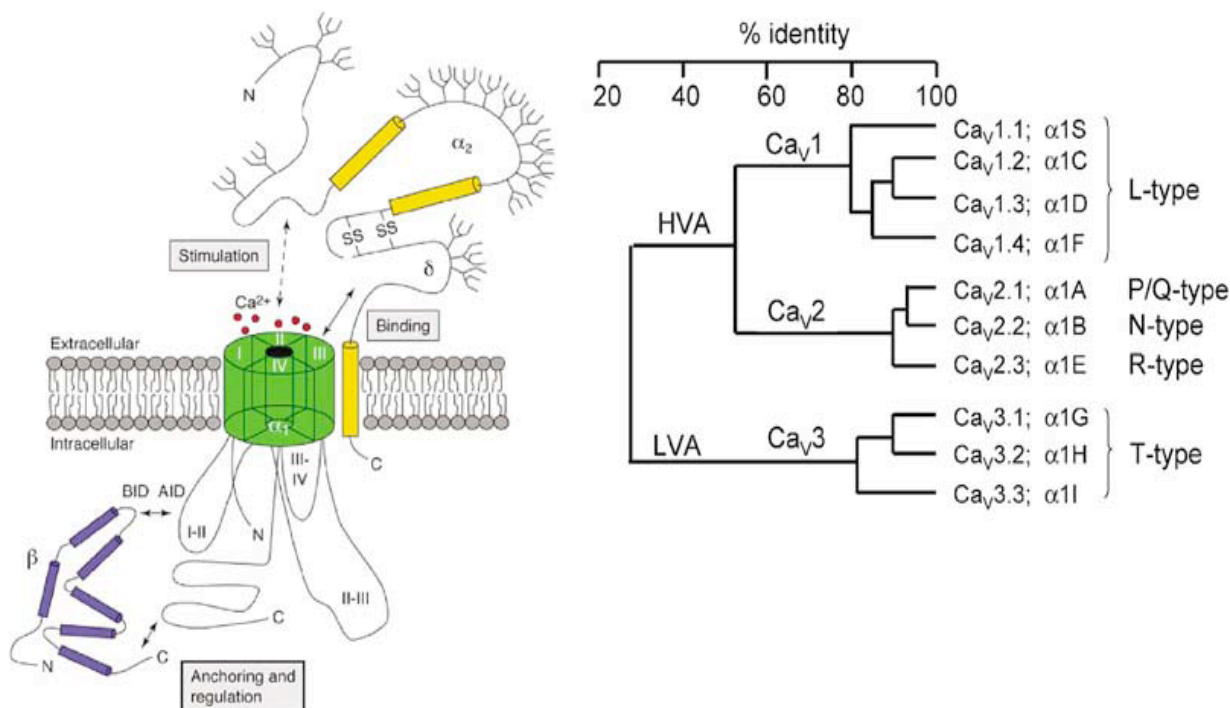


Figure 2.12 (Dolphin, 2006) Structure of voltage-gated calcium channels, there are five components (α_1 , α_2 , β , δ and γ). Calcium channel dendrogram, showing the percent identity between different calcium channel types.

The low-voltage-activated calcium channel currents which can be activated by small depolarizations of cell membrane are grouped as T-type channels. These channels are responsible for low threshold spikes which in turn modulate sodium channels. Three T-type channels have been cloned recently (Perez-Reyes, 2003). T-type channels are activated at lower voltages, inactivate quickly and are poor conductors of barium. Different T-type calcium channels are pharmacologically separated on the basis of their response to nickel and selective block by lower concentration of mibefradil (Perez-Reyes *et al.*, 2006).

Channel	Current	Localization	Specific Antagonists	Cellular Functions
CaV1.1	L	Skeletal muscle; transverse tubules	Dihydropyridines; phenylalkylamines; benzothiazepines	Excitation-contraction coupling
CaV1.2	L	Cardiac myocytes; smooth muscle myocytes; endocrine cells; neuronal cell bodies; proximal dendrites	Dihydropyridines; phenylalkylamines; benzothiazepines	Excitation-contraction coupling; hormone release; regulation of transcription; synaptic integration
CaV1.3	L	Endocrine cells; neuronal cell bodies and dendrites; cardiac atrial myocytes and pacemaker cells; cochlear hair cells	Dihydropyridines; phenylalkylamines; benzothiazepines	Hormone release; regulation of transcription; synaptic regulation; cardiac pacemaking; hearing; neurotransmitter release from sensory cells
CaV1.4	L	Retinal rod and bipolar cells; spinal cord; adrenal gland; mast cells	Dihydropyridines; phenylalkylamines; benzothiazepines	Neurotransmitter release from photoreceptors
CaV2.1	P/Q	Nerve terminals and dendrites; neuroendocrine cells	ω -Agatoxin IVA	Neurotransmitter release; dendritic Ca ²⁺ transients; hormone release
CaV2.2	N	Nerve terminals and dendrites; neuroendocrine cells	ω -Conotoxin-GVIA	Neurotransmitter release; dendritic Ca ²⁺ transients; hormone release
CaV2.3	R	Neuronal cell bodies and dendrites	SNX-482	Repetitive firing; dendritic calcium transients
CaV3.1	T	Neuronal cell bodies and dendrites; cardiac and smooth muscle myocytes	None	Pacemaking; repetitive firing
CaV3.2	T	Neuronal cell bodies and dendrites; cardiac and smooth muscle myocytes	None	Pacemaking; repetitive firing
CaV3.3	T	Neuronal cell bodies and dendrites	None	Pacemaking; repetitive firing

Table 2.9 (Catterall, 2000) Different classes of vertebrate calcium channels.

In the parasitic nematode *A. suum*, modulation of the spike potential has been attributed to voltage-activated calcium currents (Martin *et al.*, 1992; Weisblat *et al.*, 1976). Voltage-activated currents were isolated from somatic muscle cells of *A. suum* which are pharmacologically and kinetically similar to vertebrate P/Q-type currents (Verma *et al.*, 2007). In the absence of a complete genome sequence for *A. suum* the isolation of calcium currents is based mainly on pharmacology and kinetics. Completion of the genome sequence of *C.elegans* has paved the way for

identification of calcium channel homologues, functionally and genetically. All the major types of calcium channel have been identified in *C. elegans*: EGL-19 (L-type); UNC-2 (N-, P/Q- & R-type) and CCA-1 (T-type).

egl-19 encodes for α_1 subunit L-type voltage-activated calcium channel which is expressed in body wall muscles and pharyngeal muscles (Lee *et al.*, 1997). Patch-clamp studies and *egl-19* mutants of *C. elegans* confirmed that this channel is dihydropyridine sensitive and exhibit calcium dependent inactivation, characteristics of vertebrate L-type calcium currents. EGL-19 in *C. elegans* controls body wall muscle functions and also modulates pharyngeal action potentials (Jospin *et al.*, 2002; Shtonda *et al.*, 2005) .

The *C. elegans unc-2* gene encodes for a α_1 subunit structurally related to mammalian dihydropyridine insensitive- high-voltage-activated channels. The *unc-2* gene has greatest similarity to vertebrate $Ca_v2.3$ subunits (R-type current), but is also similar to $Ca_v2.1$ and $Ca_v2.2$ subunits (N- and P/Q-type currents) (Mathews *et al.*, 2003; Schafer *et al.*, 1995). In *C. elegans* the *cca-1* gene is expressed in pharyngeal muscles and encodes protein CCA-1 which has around a 70% similarity to mammalian Ca_v3 subunits (T-type current) (Steger *et al.*, 2005). CCA-1 T-type currents improve excitatory effect of synaptic inputs and modulate pharyngeal contraction (Shtonda *et al.*, 2005). Two more channels identified in *C. elegans*, *nca-1* and *nca-2*, are not similar to any mammalian calcium channels. NCA-1 and NCA-2 are similar to one another and to a channel in yeast *Schizosaccharomyces pombe* (Bargmann, 1998). These channels are found in the nervous system and ventral cord and are recently associated with neuronal transmission in *C. elegans* (Yeh *et*

al., 2008). Figure 2.15 shows the different calcium channels identified in *C. elegans* and its percent homology with vertebrate calcium channels.

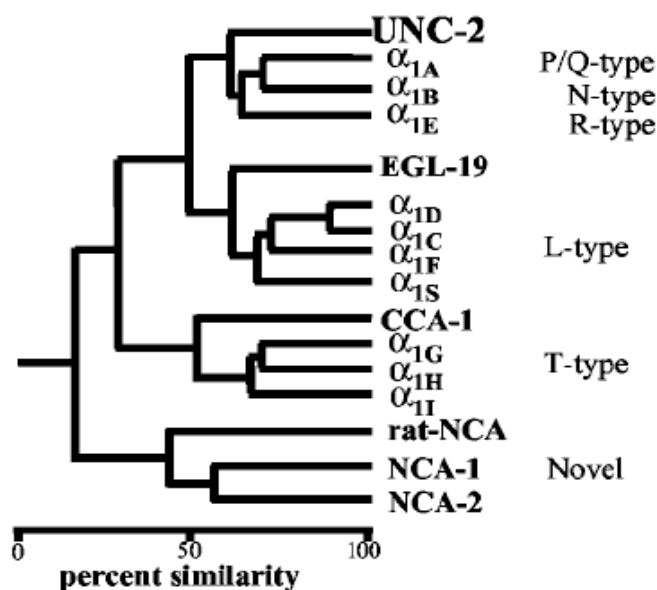


Figure 2.13 (Mathews *et al.*, 2003) Phylogenetic comparison of *C. elegans* and vertebrate calcium channel α_1 subunits.

Functional voltage-gated calcium channels have also been identified in platyhelminths. The first indication of voltage-activated currents was reported by Blair and Anderson (1994) in muscle fibers of a parasitic flatworm, *B. candida*. Later on calcium currents were also recorded from *Dugesia tigrina* (Cobbett *et al.*, 2003) and *S. mansoni* (Day *et al.*, 2000; Day *et al.*, 1993). Currents from *S. mansoni* were pharmacologically characterized and found to be associated with body wall muscle contraction (Mendonca-Silva *et al.*, 2006). Interestingly, in schistosomes three high voltage-activated α_1 calcium channel subunits have been identified. Based on sequence similarity to mammalian calcium channels two α units loosely resemble non-L-type α_1 subunits and one is related to L-type α_1 (Kohn *et al.*, 2001b). Along with α subunits two $\text{Ca}_v\beta$ s subunits also have been cloned from *S. mansoni* and *S.*

japonicum (Kohn *et al.*, 2001a). β subunits in *Schistosoma* are functionally and structurally different from mammalian β subunits. Unlike in mammals, β subunits modulate sensitivity of α subunits in schistosomes (Jeziorski *et al.*, 2006). Voltage-gated calcium channels are assumed to be the target site of anthelmintic praziquantel in schistosomes (Greenberg, 2005).

2.6.2 Voltage-activated potassium currents

Voltage-gated potassium channels comprise the largest and most diverse group of transmembrane ion channels in mammals. These channels are crucial for bringing the cell to resting phase after depolarization. There are 40 known genes in mammalian genome representing them. They maintain the potassium ion dependent component of the membrane potential and are critical to many physiological processes. The first potassium channel gene was the *Drosophila* voltage-gated *shaker* channel. α subunits form the ion conducting pore as is the case in voltage-gated calcium channels. The voltage-activated potassium channels are divided into twelve families based on the α subunit, K_v1-12 (Gutman *et al.*, 2005). Voltage-gated potassium channel group also include calcium-activated (K_{Ca}), inward-rectifying (K_{IR}), and two pore (K_{2P}) families; these families are classified separately and numbered according to their discovery. All the voltage-activated potassium channels are composed of six/seven segments with S4 being the segment conferring voltage sensitivity (Gutman *et al.*, 2003).

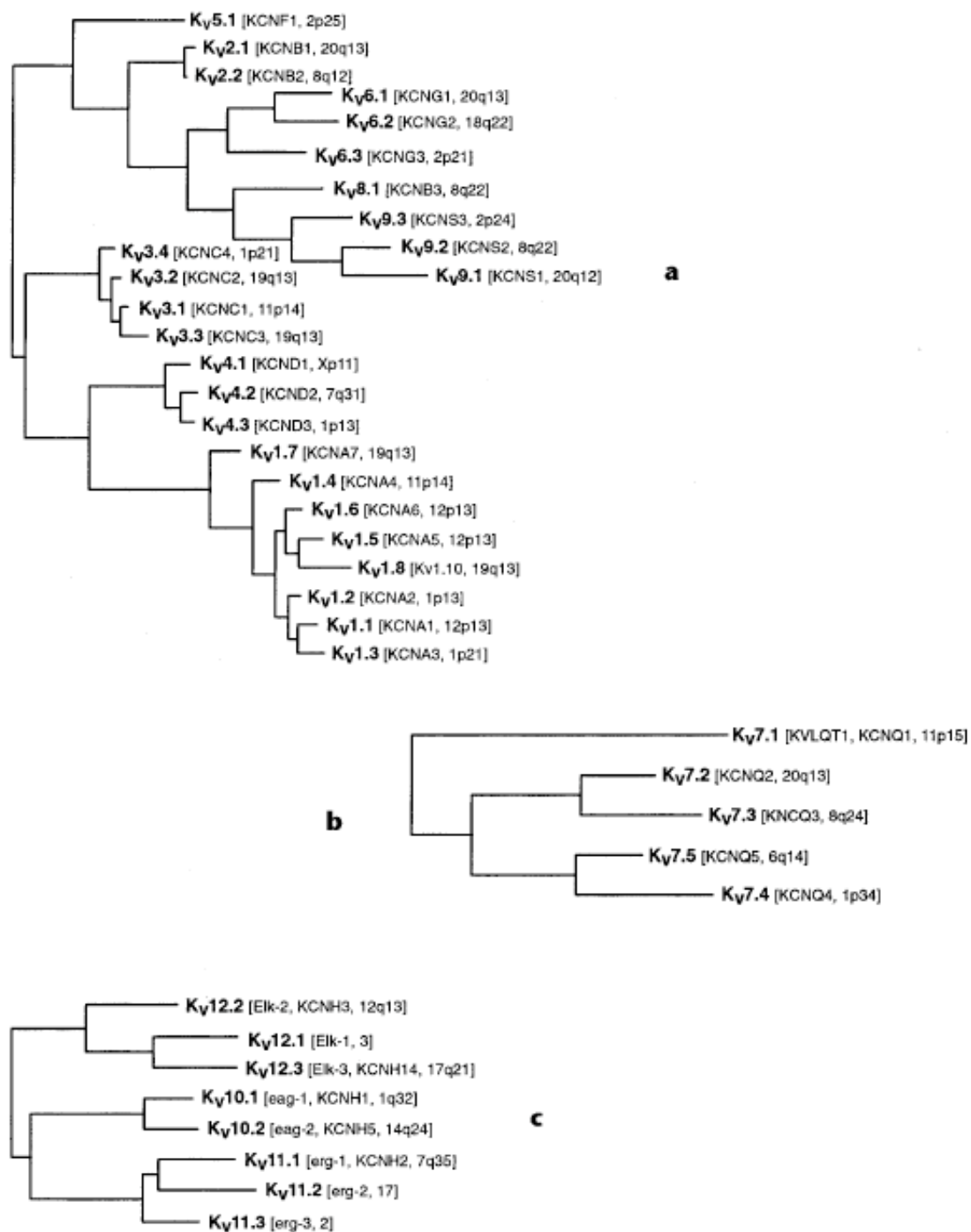


Figure 2.14 (Gutman *et al.*, 2005) Phylogenetic trees of the K_v Channels

Neuronal activity in mammals is maintained by different K_v channels. K_v channels are involved in action potential threshold frequency and the burst duration

of action potentials. *Drosophila* mutants of K_V channels demonstrate abnormal hyper excitability.

K_{IR} has a long cytoplasmic pore and negatively charged amino acids on the wall for inward rectification. These channels play an important physiological role in function of many organs, including brain, kidney, ears, retina and endocrine cells. Changes in channel proteins have been described in different disease conditions in humans (Kubo *et al.*, 2005).

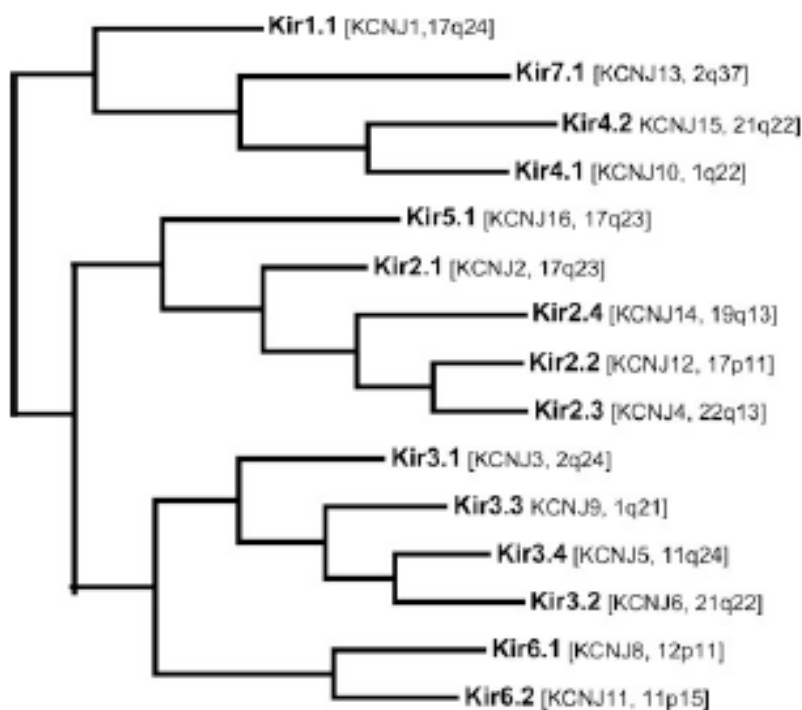


Figure 2.15 (Kubo *et al.*, 2005) Phylogenetic trees of the K_{IR} Channels

K_{Ca} channels are the second major group of the voltage-gated potassium channels. These channels are modulated by entry of calcium and changes in the membrane potential of the cell. They include three small conductance K_{Ca} channels (K_{Ca} 2.1, 2.2 and 2.3); intermediate conductance channels K_{Ca} 3.1 and K_{Ca} Slo (1.1, 4.1, 4.2 and 5.1) channels, Fig. 2.16. The first

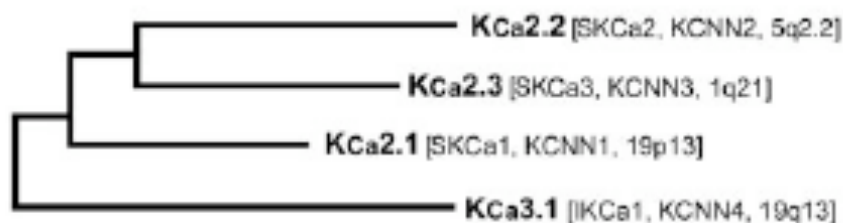
two groups are voltage insensitive and are activated by low concentration of calcium while the K_{Ca} 1.1 channel is activated by both membrane depolarization and internal calcium. Both small and intermediate conductance channels play important role in calcium dependent signaling in excitable and non excitable cells. They do not bind calcium but detect calcium by calmodulin binding and the resulting conformational changes (Rang, 2003; Wei *et al.*, 2005). SLO-1 channels of this group are the most studied channels and were first identified in *Drosophila* “slowpoke” mutants. SLO-1 channels are calcium dependent very high conductance potassium channels, “Big K” or “Maxi K channels” (Ghatta *et al.*, 2006).

IUPHAR names of the members of the K_{Ca} group of potassium channels are shown, together with their HGNC designations and other commonly used names.

IUPHAR	HGNC	Other
$K_{Ca}1.1$	<i>KCNMA1</i>	Slo, Slo1, BK
$K_{Ca}2.1$	<i>KCNN1</i>	$SK_{Ca}1$
$K_{Ca}2.2$	<i>KCNN2</i>	$SK_{Ca}2$
$K_{Ca}2.3$	<i>KCNN3</i>	$SK_{Ca}3$
$K_{Ca}3.1$	<i>KCNN4</i>	$IK_{Ca}1$
$K_{Ca}4.1$	<i>KCNT1</i>	Slack, Slo2.2
$K_{Ca}4.2$	<i>KCNT2</i>	Slick, Slo2.1
$K_{Ca}5.1$	<i>KCNU1</i>	Slo3

BK, big-conductance K^+ channel; SK, small-conductance K^+ channel; IK, intermediate-conductance K^+ channel.

A



B

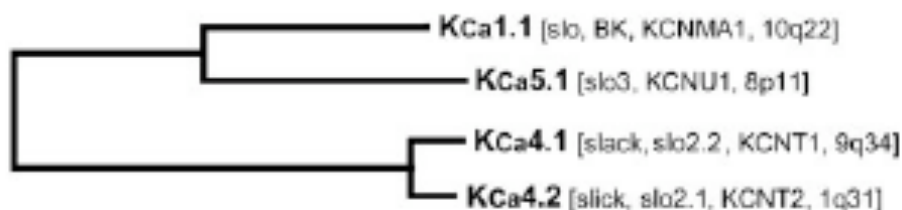


Figure 2.16 (Wei *et al.*, 2005) Phylogenetic trees of the K_{Ca} Channels

Figure 2.17 represents the structure of a SLO-1 channel as first identified in *C. elegans*: S9 and S10 segments determine the calcium sensitivity of the channels and a series of highly conserved negatively charged residues on the S10 domain forms the “calcium bowl” responsible for calcium binding (Wei *et al.*, 1994). Coupling between calcium binding and channel activation as well as molecular characterization of other domains has not been completely resolved in *C. elegans*. There are two *slo* (1 & 2) genes in *C. elegans* (Wang *et al.*, 2001). *slo-1* is

expressed in both motor neurons and body wall muscle, but transgenic animal studies have shown that SLO-1 produces its effect by neural signaling. In the pharynx *slo-1* is expressed in neurons and regulates feeding. More recently forward genetic screens in *C. elegans* have also demonstrated that *slo-1* mutants are resistant to the novel anthelmintic emodepside (Guest *et al.*, 2007). SLO-1 offers an exciting target for the development of novel anthelmintics.

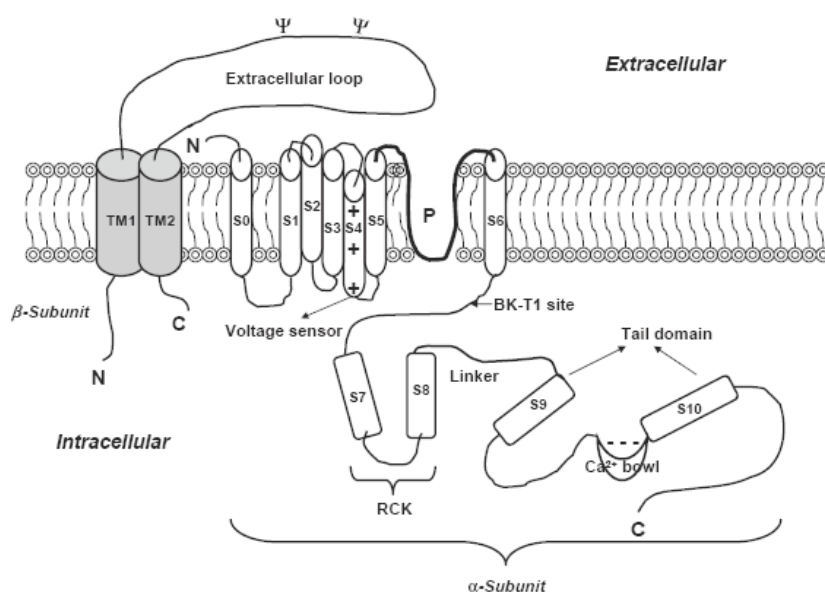


Figure 2.17 (Ghatta *et al.*, 2006) Structure of the BK (SLO-1) Channel.

Outward potassium currents have been described in the parasitic nematode *A. suum* (Martin *et al.*, 1992). These currents are sensitive to potassium channel blockers; 4-AP, and TEA. It has been assumed that potassium currents contribute to slow waves and modulation waves in electrophysiological recordings in *A. suum* (Weisblat *et al.*, 1976). Recently Trailovic *et al.*, (2007) have shown that depolarizing effect of cholinergic agents can be potentiated by potassium channel blockers.

2.7 Anthelmintics

The drugs used to control helminth parasitic infections are called anthelmintics. Anthelmintics offer a very important and successful method to control and treat parasitic helminth infections in animals and humans. Antinematodal drugs currently available in market are very helminth specific and have little effect on vertebrate physiology at recommended doses. The Following section discusses the major anthelmintics classes and their mode of action.

2.7.1 Nicotinic agonists

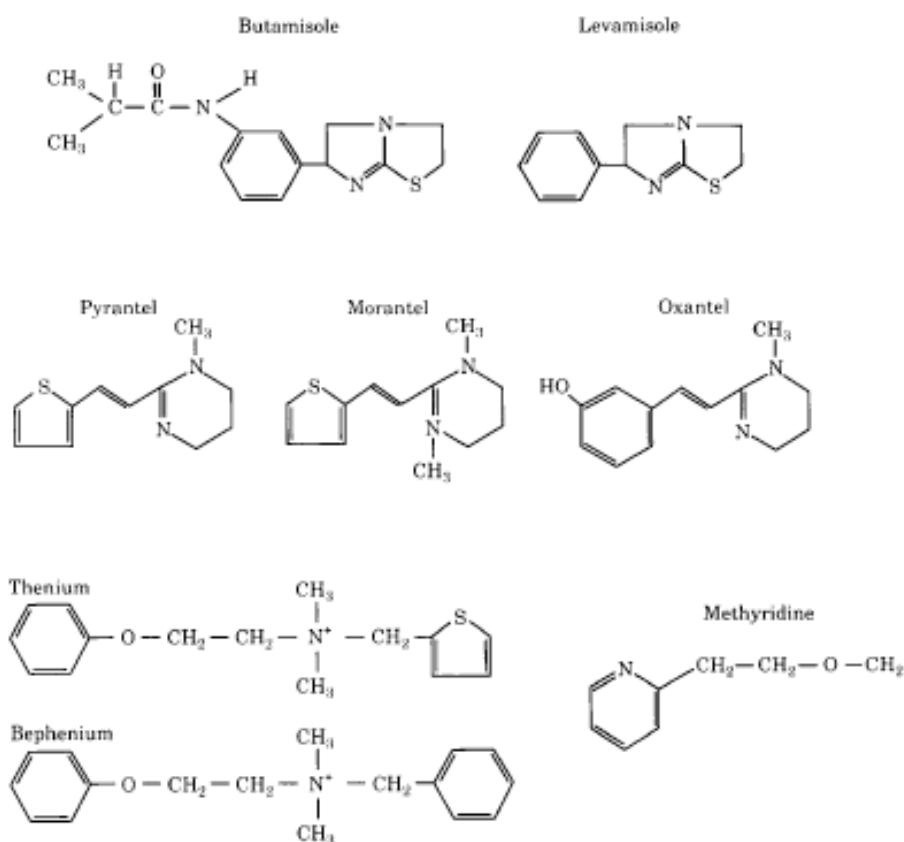


Figure 2.18 Nicotinic agonists

There are four different groups of drugs which acts as nicotinic receptor agonists to produce their effects. These are the imidazolethiazoles (levamisole,

tetramisole); the tetrahydropyrimidines (pyrantel, morantel and oxantel); the quaternary ammonium salts (bephenium and thenium) and the pyrimidines (methyridine) (Robertson *et al.*, 1993). These compounds are selective agonist of nematode nAChR's (Janssen, 1976; Martin *et al.*, 2007). They produce contraction and spastic paralysis and subsequent expulsion of worms from the host animal. The AChR's are present on somatic muscles cells and depolarization leads to entry of calcium and contraction. Electrophysiological recordings in nematode parasites *A. suum* and *O. dentatum* using *levamisole* and its analogues induces depolarization, contraction and increase in spike frequency (Aceves *et al.*, 1970; Martin *et al.*, 1997; Robertson *et al.*, 1993). The levamisole sensitive nAChR has been identified at the single channel level in, *A. suum*, *O. dentatum* and *C. elegans* (Richmond *et al.*, 1999; Robertson *et al.*, 2002; Robertson *et al.*, 1993). Levamisole induced contraction was found to be irreversible which could not be inhibited by atropine, tubocurarine, hexamethonium or piperazine (Coles *et al.*, 1975; Coles *et al.*, 1974).

Amino-acetonitrile derivatives (AAD's) are a novel class of anthelmintics which act on nAChR's. AAD's response is mediated by ACR-23, which belongs to nematode specific DEG-3 group of nAChR's (Kaminsky *et al.*, 2008).

2.7.2 Glutamate gated-chloride channel modulators

This group includes group of complex 16-membered macrocyclic lactones, avermectins, isolated from the fermented mixture of *Streptomyces avermitilis* (Chabala *et al.*, 1980). This group includes ivermectin, abamectin, doramectin, milbemycin D and moxidectin. These compounds are structurally similar to macrolide antibiotics but they don't have any antibiotic or antifungal properties.

Avermectins are highly efficacious against ectoparasites as well as endoparasites in man and animals (Campbell, 1985). The target site for ivermectins is glutamate-gated chloride channels in nerve and muscles. The ivermectins interact selectively with parasitic GluCl channels preventing their closure, increasing chloride permeability. Chloride influx leads to hyperpolarization, decreasing or inhibiting neuronal transmission and this leads to paralysis of somatic muscles, inhibition of pharyngeal pumping and death of worms (Geary *et al.*, 1993; Ōmura, 2002; Omura *et al.*, 2004). Glutamate-gated chloride channels are found only in nematodes, insects and ticks. Glutamate gated receptors in mammals are located in CNS whereas in arthropods and nematodes they are located in peripheral nervous system making avermectins very safe and effective anthelmintics (Duce *et al.*, 1985). GluCl channels have been identified in *C. elegans* and *Xenopus* oocytes (Cully *et al.*, 1994; Cully *et al.*, 1996; Vassilatis *et al.*, 1997a). Also the location of avermectin sensitive GluCl channel has been identified in pharyngeal muscles of the parasitic nematode *A. suum* (Martin, 1996)

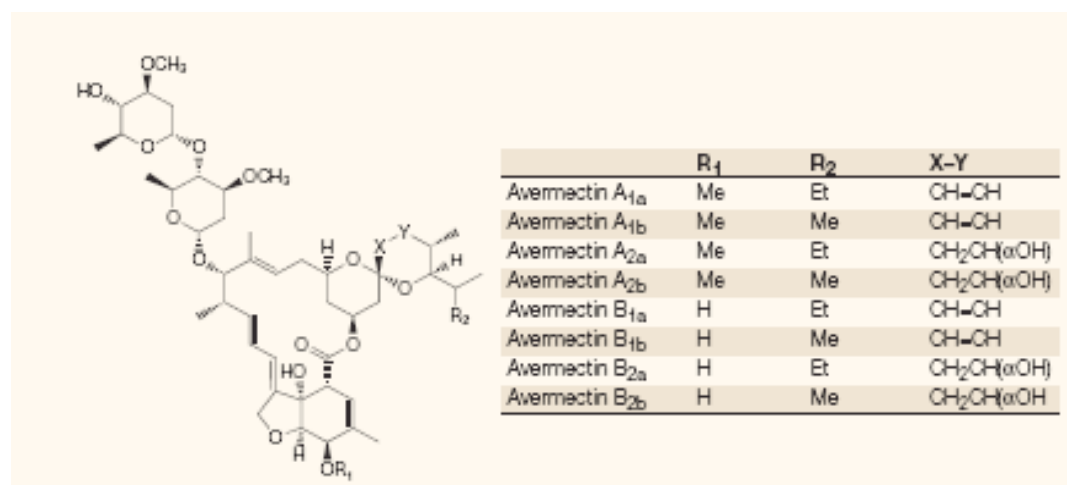


Figure 2.19 (Omura *et al.*, 2004) Avermectin. Structure of eight different compounds isolated from fermentation.

2.7.3 Benzimidazoles

This class of drugs falls under category of drugs which interact selectively with nematode β -tubulin (Borgers *et al.*, 1975). The list of compounds includes thiabendazole, fenbendazole, mebendazole, albendazole and prodrugs: febantel, thiophanate and netobimin. Benzimidazoles interaction with β -tubulin compromises the worm cytoskeleton. In *A. suum* pronounced degenerative changes were seen in cell cytoplasm with loss of glycogen, formation of autophagic vacuoles and decrease in number of microvilli (Borgers *et al.*, 1975). In *C. elegans* benzimidazoles impairs locomotion, reproduction and inhibit oocyte development. In *C. elegans* the sensitivity is mediated by single gene *ben-1* (Driscoll *et al.*, 1989), the isolation of this gene is being exploited to understand benzimidazole resistance in *H. contortus* (Kwa *et al.*, 1994).

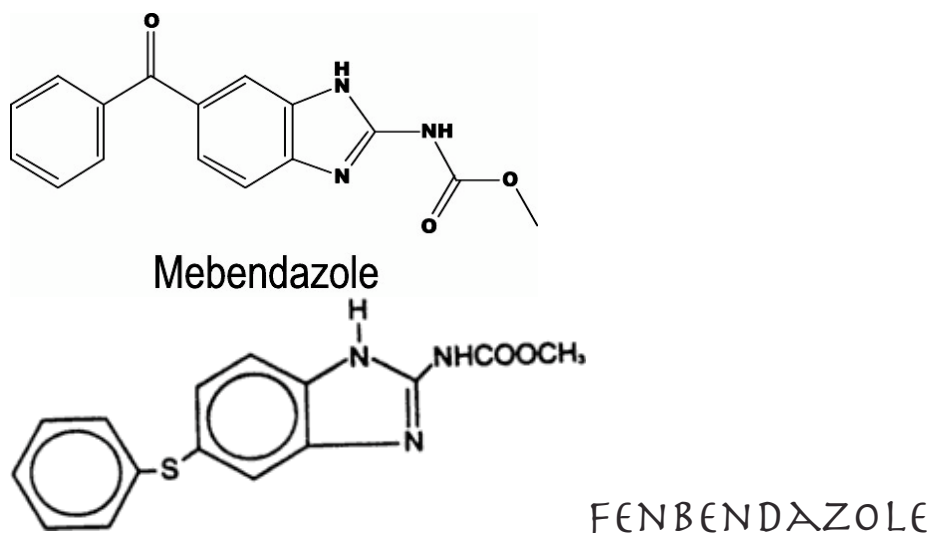


Figure 2.20 Chemical structures of benzimidazole derivatives.

2.7.4 Cyclo-octadepsipeptides

This group includes emodepside a semi-synthetic derivative of PF1022A, a fermentation product isolated from the fungus *Mycelia sterilia*. It is a broad spectrum

anthelmintic effective against worms resistant to all the other groups of drugs due to its novel mode of action (Harder *et al.*, 2002). In *A. suum* emodepside caused muscle relaxation and inhibition of ACh or neuropeptide induced muscle contraction. The response was found to be dependent on calcium and potassium, mimicking the effects of the neuropeptides PF1 and PF2 (Willson *et al.*, 2003). RNAi knockouts of latrophillin genes, *lat-1* and *lat-2*, in *C. elegans* showed involvement of latrophillin in mode of action emodepside (Bull *et al.*, 2007; Willson *et al.*, 2004). But studies later demonstrated that *lat-2* mutants are insensitive to emodepside suggesting that latrophillin receptors are not the primary targets (Guest *et al.*, 2007). Forward genetic screens have very recently identified mutants of the *slo-1* gene which are resistant to emodepside (Guest *et al.*, 2007). SLO-1 is a calcium-activated potassium channel; it is expressed in the *C.elegans* nervous and muscular system but not in pharyngeal muscles (Holden-Dye *et al.*, 2007). A SLO-1 mediated mode of action also supports the calcium and potassium dependent effects of emodepside.

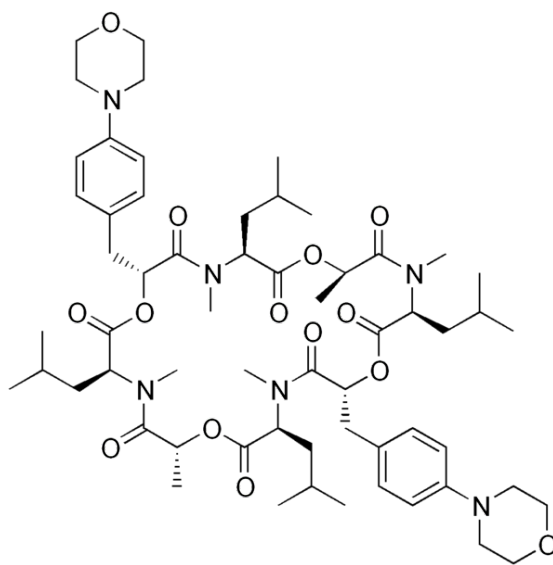


Figure 2.21 Chemical structure of emodepside.

2.7.5 Other anthelmintics

This group includes important anthelmintics which have different mode of action than as any of the previous classes; piperazine and praziquantel. Piperazine is a GABA agonist and acts on ligand-gated chloride channel on synaptic or extra synaptic membrane (Martin, 1980; Martin, 1982). Piperazine exposure increases the opening of chloride channel on muscle membrane causing hyperpolarization, increased conductance and leading to spastic paralysis. Electrophysiologically piperazine activated single channel chloride channel currents have been recorded in *A. suum* (Martin, 1985; Martin, 1987).

Praziquantel is a selective anthelmintic for schistosomes (Andrews *et al.*, 1983). Anthelmintic effects of praziquantel are mediated by increase in calcium permeability of parasitic muscle and / or tegument (Blair *et al.*, 1994; Mehlhorn *et al.*, 1983). Increased calcium influxes across calcium induce calcium release (CICR) channels in tegument membrane have been implicated in the effects of praziquantel on schistosomes (Bennett *et al.*, 1997; Day *et al.*, 1992).

2.8 Hypothesis

It is clear from the review preceding that there are a number of interesting and unanswered questions. In this thesis I investigated the following hypotheses:

1. Entry of calcium from extracellular sources is responsible for muscle contraction in *A. suum* somatic muscle cells. It is assumed that spikes and slow waves induced under current clamp in *A. suum* muscles are calcium dependent. These spikes are potentiated by the excitatory neuropeptide, AF2. Our first hypothesis was that spiking is due to the opening of voltage-activated calcium channels. AF2 increased the spiking and therefore the hypothesis was that AF2 will positively modulate the voltage-activated calcium currents.

2. There are two distinct calcium currents in *A. suum* somatic muscle cells. The two currents are pharmacologically different. The second hypothesis was that both of the two currents can be modulated, negatively and positively, by FLPs. We investigated the effects of excitatory (AF3) and inhibitory (PF1) neuropeptide FLPs on the two calcium currents.

3. The third hypothesis was aimed at investigating the role of muscarinic receptors in muscle contraction. Our hypothesis was that muscarinic receptors play some role in somatic muscle contraction and muscarinic AChR's in nematodes modulate voltage-activated currents in the somatic muscle cells of *A. suum*. Colquhoun *et al*, (1991) tested effects of different mammalian cholinergic agonists including furtrethonium, muscarine, pilocarpine, arecoline, McN A343, bethanecol and

oxtremerine, on *A. suum* somatic muscle cells. They found that furtrethonium was the most potent. We therefore selected 5-methylfurmethiodide (MFI), which is a potent muscarinic agonist for further study on muscle contraction in *A. suum*. We studied the effect of the muscarinic agonist, MFI along with levamisole and acetylcholine on contraction and electrophysiology of the somatic muscle cells in *A. suum*.

References

- Aceves, J, Erlij, D, Martinez-Maranon, R (1970) The mechanism of the paralyzing action of tetramisole on *Ascaris* somatic muscle. *Br J Pharmacol* **38**(3): 602-607.
- Andrews, P, Thomas, H, Pohlke, R, Seubert, J (1983) Praziquantel. *Med Res Rev* **3**(2): 147-200.
- Bargmann, CI (1998) Neurobiology of the *Caenorhabditis elegans* genome. *Science* **282**(5396): 2028-2033.
- Bazemore, A, Elliott, KA, Florey, E (1956) Factor I and gamma-aminobutyric acid. *Nature* **178**(4541): 1052-1053.
- Bennett, JL, Day, T, Liang, FT, Ismail, M, Farghaly, A (1997) The development of resistance to anthelmintics: a perspective with an emphasis on the antischistosomal drug praziquantel. *Exp Parasitol* **87**(3): 260-267.
- Bettinger, JC, McIntire, SL (2004) State-dependency in *C. elegans*. *Genes Brain Behav* **3**(5): 266-272.
- Blair, KL, Bennett, JL, Pax, RA (1994) *Schistosoma mansoni*: myogenic characteristics of phorbol ester-induced muscle contraction. *Exp Parasitol* **78**(3): 302-316.
- Borgers, M, De Nollin, S (1975) Ultrastructural changes in *Ascaris suum* intestine after mebendazole treatment in vivo. *J Parasitol* **61**(1): 110-122.
- Bowman, JW, Friedman, AR, Thompson, DP, Ichhpurani, AK, Kellman, MF, Marks, N, Maule, AG, Geary, TG (1996) Structure-activity relationships of KNEFIRFamide (AF1), a nematode FMRFamide-related peptide, on *Ascaris suum* muscle. *Peptides* **17**(3): 381-387.
- Bowman, JW, Winterrowd, CA, Friedman, AR, Thompson, DP, Klein, RD, Davis, JP, Maule, AG, Blair, KL, Geary, TG (1995) Nitric oxide mediates the inhibitory effects of SDPNFLRFamide, a nematode FMRFamide-related neuropeptide, in *Ascaris suum*. *J Neurophysiol* **74**(5): 1880-1888.
- Brading, AF, Caldwell, PC (1964) The effect of ions on the resting potentials of muscle cells in *Ascaris lumbricoides*. *J Physiol* **173**.
- Brading, AF, Caldwell, PC (1971) The resting membrane potential of the somatic muscle cells of *Ascaris lumbricoides*. *J Physiol* **217**(3): 605-624.
- Brockie, PJ, Maricq, AV (2003) Ionotropic glutamate receptors in *Caenorhabditis elegans*. *Neurosignals* **12**(3): 108-125.

Brownlee, DJ, Fairweather, I, Holden-Dye, L, Walker, RJ (1996) Nematode neuropeptides: Localization, isolation and functions. *Parasitol Today* **12**(9): 343-351.

Brownlee, DJ, Fairweather, I, Johnston, CF (1993a) Immunocytochemical demonstration of neuropeptides in the peripheral nervous system of the roundworm *Ascaris suum* (Nematoda, Ascaroidea). *Parasitol Res* **79**(4): 302-308.

Brownlee, DJ, Fairweather, I, Johnston, CF, Smart, D, Shaw, C, Halton, DW (1993b) Immunocytochemical demonstration of neuropeptides in the central nervous system of the roundworm, *Ascaris suum* (Nematoda: Ascaroidea). *Parasitology* **106** (Pt 3): 305-316.

Brownlee, DJ, Walker, RJ (1999) Actions of nematode FMRFamide-related peptides on the pharyngeal muscle of the parasitic nematode, *Ascaris suum*. *Ann N Y Acad Sci* **897**: 228-238.

Bull, K, Cook, A, Hopper, NA, Harder, A, Holden-Dye, L, Walker, RJ (2007) Effects of the novel anthelmintic emodepside on the locomotion, egg-laying behaviour and development of *Caenorhabditis elegans*. *Int J Parasitol* **37**(6): 627-636.

Caldwell, PC (1973) Possible mechanisms for the linkage of membrane potentials to metabolism by electrogenic transport processes with special reference to *Ascaris* muscle. *J Bioenerg* **4**(1): 201-209.

Caldwell, PC (1972) Sodium ion and potassium ion transport and permeability: a comparison between squid giant axons and ascaris muscle fibres. *Biochem J* **127**(3): 54P.

Campbell, V, Berrow, N, Dolphin, AC (1993) GABAB receptor modulation of Ca²⁺ currents in rat sensory neurones by the G protein G(0): antisense oligonucleotide studies. *J Physiol* **470**: 1-11.

Campbell, WC (1985) Ivermectin: an update. *Parasitol Today* **1**(1): 10-16.

Carbone, E, Lux, HD (1984) A low voltage-activated calcium conductance in embryonic chick sensory neurons. *Biophys J* **46**(3): 413-418.

Catterall, WA (2000) Structure and regulation of voltage-gated Ca²⁺ channels. *Annu Rev Cell Dev Biol* **16**: 521-555.

Catterall, WA, Perez-Reyes, E, Snutch, TP, Striessnig, J (2005) International Union of Pharmacology. XLVIII. Nomenclature and structure-function relationships of voltage-gated calcium channels. *Pharmacol Rev* **57**(4): 411-425.

Chabala, JC, Mrozik, H, Tolman, RL, Eskola, P, Lusi, A, Peterson, LH, Woods, MF, Fisher, MH, Campbell, WC, Egerton, JR, Ostlind, DA (1980) Ivermectin, a new broad-spectrum antiparasitic agent. *J Med Chem* **23**(10): 1134-1136.

Cobbett, P, Day, TA (2003) Functional voltage-gated Ca²⁺ channels in muscle fibers of the platyhelminth *Dugesia tigrina*. *Comp Biochem Physiol A Mol Integr Physiol* **134**(3): 593-605.

Colbert, HA, Bargmann, CI (1995) Odorant-specific adaptation pathways generate olfactory plasticity in *C. elegans*. *Neuron* **14**(4): 803-812.

Coles, GC, East, JM, Jenkins, SN (1975) Mechanism of Action of Anthelmintic Levamisole. *General Pharmacology* **6**(4): 309-313.

Coles, GC, Jenkins, S (1974) Reversible Invitro Paralysis of Nematodes by Levamisole. *Parasitology* **69**(Oct): R22-R22.

Cowden, C, Sithigorngul, P, Brackley, P, Guastella, J, Stretton, AO (1993a) Localization and differential expression of FMRFamide-like immunoreactivity in the nematode *Ascaris suum*. *J Comp Neurol* **333**(3): 455-468.

Cowden, C, Stretton, AO (1993b) AF2, an *Ascaris* neuropeptide: isolation, sequence, and bioactivity. *Peptides* **14**(3): 423-430.

Cowden, C, Stretton, AO (1995) Eight novel FMRFamide-like neuropeptides isolated from the nematode *Ascaris suum*. *Peptides* **16**(3): 491-500.

Cowden, C, Stretton, AO, Davis, RE (1989) AF1, a sequenced bioactive neuropeptide isolated from the nematode *Ascaris suum*. *Neuron* **2**(5): 1465-1473.

Crompton, DWT, Joyner, SM (1979) Parasitic worms
x, 207 p.

Cully, DF, Vassilatis, DK, Liu, KK, Paress, PS, Van der Ploeg, LH, Schaeffer, JM, Arena, JP (1994) Cloning of an avermectin-sensitive glutamate-gated chloride channel from *Caenorhabditis elegans*. *Nature* **371**(6499): 707-711.

Cully, DF, Wilkinson, H, Vassilatis, DK, Etter, A, Arena, JP (1996) Molecular biology and electrophysiology of glutamate-gated chloride channels of invertebrates. *Parasitology* **113** **Suppl**: S191-200.

Culotti, JG, Klein, WL (1983) Occurrence of muscarinic acetylcholine receptors in wild type and cholinergic mutants of *Caenorhabditis elegans*. *J Neurosci* **3**(2): 359-368.

Davenport, TR, Lee, DL, Isaac, RE (1988) Immunocytochemical demonstration of a neuropeptide in *Ascaris suum* (Nematoda) using an antiserum to FMRFamide. *Parasitology* **97** (Pt 1): 81-88.

- Davis, RE (1998) Neurophysiology of glutamatergic signalling and anthelmintic action in *Ascaris suum*: pharmacological evidence for a kainate receptor. *Parasitology* **116 (Pt 5)**: 471-486.
- Davis, RE, Stretton, AO (1996) The motornervous system of *Ascaris*: electrophysiology and anatomy of the neurons and their control by neuromodulators. *Parasitology* **113 Suppl**: S97-117.
- Day, TA, Bennett, JL, Pax, RA (1992) Praziquantel: The enigmatic antiparasitic. *Parasitol Today* **8(10)**: 342-344.
- Day, TA, Haithcock, J, Kimber, M, Maule, AG (2000) Functional ryanodine receptor channels in flatworm muscle fibres. *Parasitology* **120 (Pt 4)**: 417-422.
- Day, TA, Maule, AG (1999) Parasitic peptides! The structure and function of neuropeptides in parasitic worms. *Peptides* **20(8)**: 999-1019.
- Day, TA, Maule, AG, Shaw, C, Halton, DW, Moore, S, Bennett, JL, Pax, RA (1994) Platyhelminth FMRFamide-related peptides (FaRPs) contract *Schistosoma mansoni* (Trematoda: Digenea) muscle fibres in vitro. *Parasitology* **109 (Pt 4)**: 455-459.
- Day, TA, Orr, N, Bennett, JL, Pax, RA (1993) Voltage-gated currents in muscle cells of *Schistosoma mansoni*. *Parasitology* **106 (Pt 5)**: 471-477.
- Debell, JT, Delcastillo, J, Sanchez, V (1963) Electrophysiology of the Somatic Muscle Cells of *Ascaris Lumbricoides*. *J Cell Physiol* **62**: 159-177.
- del Castillo, J, De Mello, WC, Morales, T (1964a) Inhibitory action of gamma-aminobutyric acid (GABA) on *Ascaris* muscle. *Experientia* **20(3)**: 141-143.
- del Castillo, J, De Mello, WC, Morales, T (1967) The initiation of action potentials in the somatic musculature of *Ascaris lumbricoides*. *J Exp Biol* **46(2)**: 263-279.
- del Castillo, J, Demello, WC, Morales, T (1964b) Mechanism of the Paralyzing Action of Piperazine on *Ascaris* Muscle. *Br J Pharmacol Chemother* **22**: 463-477.
- del Castillo, J, Rivera, A, Solorzano, S, Serrato, J (1989) Some aspects of the neuromuscular system of *Ascaris*. *Q J Exp Physiol* **74(7)**: 1071-1087.
- Dent, JA, Smith, MM, Vassilatis, DK, Avery, L (2000) The genetics of ivermectin resistance in *Caenorhabditis elegans*. *Proc Natl Acad Sci U S A* **97(6)**: 2674-2679.
- Dolphin, AC (2006) A short history of voltage-gated calcium channels. *Br J Pharmacol* **147 Suppl 1**: S56-62.

Driscoll, M, Dean, E, Reilly, E, Bergholz, E, Chalfie, M (1989) Genetic and molecular analysis of a *Caenorhabditis elegans* beta-tubulin that conveys benzimidazole sensitivity. *J Cell Biol* **109**(6 Pt 1): 2993-3003.

Duce, IR, Scott, RH (1985) Actions of dihydroavermectin B1a on insect muscle. *Br J Pharmacol* **85**(2): 395-401.

Dunn, CW, Hejnol, A, Matus, DQ, Pang, K, Browne, WE, Smith, SA, Seaver, E, Rouse, GW, Obst, M, Edgecombe, GD, Sorensen, MV, Haddock, SH, Schmidt-Rhaesa, A, Okusu, A, Kristensen, RM, Wheeler, WC, Martindale, MQ, Giribet, G (2008) Broad phylogenomic sampling improves resolution of the animal tree of life. *Nature* **452**(7188): 745-749.

Edison, AS, Messinger, LA, Stretton, AO (1997) *afp-1*: a gene encoding multiple transcripts of a new class of FMRFamide-like neuropeptides in the nematode *Ascaris suum*. *Peptides* **18**(7): 929-935.

Fedulova, SA, Kostyuk, PG, Veselovsky, NS (1985) Two types of calcium channels in the somatic membrane of new-born rat dorsal root ganglion neurones. *J Physiol* **359**: 431-446.

Fellowes, RA, Dougan, PM, Maule, AG, Marks, NJ, Halton, DW (1999) Neuromusculature of the ovijector of *Ascaris suum* (Ascaroidea, nematoda): an ultrastructural and immunocytochemical study. *J Comp Neurol* **415**(4): 518-528.

Fellowes, RA, Maule, AG, Marks, NJ, Geary, TG, Thompson, DP, Halton, DW (2000) Nematode neuropeptide modulation of the vagina vera of *Ascaris suum*: in vitro effects of PF1, PF2, PF4, AF3 and AF4. *Parasitology* **120** (Pt 1): 79-89.

Fellowes, RA, Maule, AG, Marks, NJ, Geary, TG, Thompson, DP, Shaw, C, Halton, DW (1998) Modulation of the motility of the vagina vera of *Ascaris suum* in vitro by FMRF amide-related peptides. *Parasitology* **116** (Pt 3): 277-287.

Forrester, SG, Hamdan, FF, Prichard, RK, Beech, RN (1999) Cloning, sequencing, and developmental expression levels of a novel glutamate-gated chloride channel homologue in the parasitic nematode *Haemonchus contortus*. *Biochem Biophys Res Commun* **254**(3): 529-534.

Franks, CJ, Holden-Dye, L, Williams, RG, Pang, FY, Walker, RJ (1994) A nematode FMRFamide-like peptide, SDPNFLRFamide (PF1), relaxes the dorsal muscle strip preparation of *Ascaris suum*. *Parasitology* **108** (Pt 2): 229-236.

Geary, TG, Price, DA, Bowman, JW, Winterrowd, CA, Mackenzie, CD, Garrison, RD, Williams, JF, Friedman, AR (1992) Two FMRFamide-like peptides from the free-living nematode *Panagrellus redivivus*. *Peptides* **13**(2): 209-214.

Geary, TG, Sims, SM, Thomas, EM, Vanover, L, Davis, JP, Winterrowd, CA, Klein, RD, Ho, NF, Thompson, DP (1993) *Haemonchus contortus*: ivermectin-induced paralysis of the pharynx. *Exp Parasitol* **77**(1): 88-96.

Ghatta, S, Nimmagadda, D, Xu, X, O'Rourke, ST (2006) Large-conductance, calcium-activated potassium channels: structural and functional implications. *Pharmacol Ther* **110**(1): 103-116.

Greenberg, RM (2005) Ca²⁺ signalling, voltage-gated Ca²⁺ channels and praziquantel in flatworm neuromusculature. *Parasitology* **131 Suppl**: S97-108.

Greenwood, K, Williams, T, Geary, T (2005) Nematode neuropeptide receptors and their development as anthelmintic screens. *Parasitology* **131 Suppl**: S169-177.

Guastella, J, Johnson, CD, Stretton, AO (1991) GABA-immunoreactive neurons in the nematode *Ascaris*. *J Comp Neurol* **307**(4): 584-597.

Guest, M, Bull, K, Walker, RJ, Amliwala, K, O'Connor, V, Harder, A, Holden-Dye, L, Hopper, NA (2007) The calcium-activated potassium channel, SLO-1, is required for the action of the novel cyclo-octadepsipeptide anthelmintic, emodepside, in *Caenorhabditis elegans*. *Int J Parasitol* **37**(14): 1577-1588.

Gutman, GA, Chandy, KG, Adelman, JP, Aiyar, J, Bayliss, DA, Clapham, DE, Covarrubias, M, Desir, GV, Furuichi, K, Ganetzky, B, Garcia, ML, Grissmer, S, Jan, LY, Karschin, A, Kim, D, Kuperschmidt, S, Kurachi, Y, Lazdunski, M, Lesage, F, Lester, HA, McKinnon, D, Nichols, CG, O'Kelly, I, Robbins, J, Robertson, GA, Rudy, B, Sanguinetti, M, Seino, S, Stuehmer, W, Tamkun, MM, Vandenberg, CA, Wei, A, Wulff, H, Wymore, RS (2003) International Union of Pharmacology. XLI. Compendium of voltage-gated ion channels: potassium channels. *Pharmacol Rev* **55**(4): 583-586.

Gutman, GA, Chandy, KG, Grissmer, S, Lazdunski, M, McKinnon, D, Pardo, LA, Robertson, GA, Rudy, B, Sanguinetti, MC, Stuehmer, W, Wang, X (2005) International Union of Pharmacology. LIII. Nomenclature and molecular relationships of voltage-gated potassium channels. *Pharmacol Rev* **57**(4): 473-508.

Hagiwara, S, Ozawa, S, Sand, O (1975) Voltage clamp analysis of two inward current mechanisms in the egg cell membrane of a starfish. *J Gen Physiol* **65**(5): 617-644.

Halton, DW, Shaw, C, Maule, AG, Smart, D (1994) Regulatory peptides in helminth parasites. *Adv Parasitol* **34**: 163-227.

Hamdan, FF, Ungrin, MD, Abramovitz, M, Ribeiro, P (1999) Characterization of a novel serotonin receptor from *Caenorhabditis elegans*: cloning and expression of two splice variants. *J Neurochem* **72**(4): 1372-1383.

Harder, A, von Samson-Himmelstjerna, G (2002) Cyclooctadepsipeptides--a new class of anthelmintically active compounds. *Parasitol Res* **88**(6): 481-488.

Hedgecock, EM, Culotti, JG, Hall, DH, Stern, BD (1987) Genetics of cell and axon migrations in *Caenorhabditis elegans*. *Development* **100**(3): 365-382.

Hillman, D, Chen, S, Aung, TT, Cherksey, B, Sugimori, M, Llinas, RR (1991) Localization of P-type calcium channels in the central nervous system. *Proc Natl Acad Sci U S A* **88**(16): 7076-7080.

Hobson, RJ, Geng, J, Gray, AD, Komuniecki, RW (2003) SER-7b, a constitutively active Galphas coupled 5-HT7-like receptor expressed in the *Caenorhabditis elegans* M4 pharyngeal motorneuron. *J Neurochem* **87**(1): 22-29.

Hobson, RJ, Hapiak, VM, Xiao, H, Buehrer, KL, Komuniecki, PR, Komuniecki, RW (2006) SER-7, a *Caenorhabditis elegans* 5-HT7-like receptor, is essential for the 5-HT stimulation of pharyngeal pumping and egg laying. *Genetics* **172**(1): 159-169.

Holden-Dye, L, Krogsgaard-Larsen, P, Nielsen, L, Walker, RJ (1989) GABA receptors on the somatic muscle cells of the parasitic nematode, *Ascaris suum*: stereoselectivity indicates similarity to a GABAA-type agonist recognition site. *Br J Pharmacol* **98**(3): 841-850.

Holden-Dye, L, O'Connor, V, Hopper, NA, Walker, RJ, Harder, A, Bull, K, Guest, M (2007) SLO, SLO, quick, quick, slow: calcium-activated potassium channels as regulators of *Caenorhabditis elegans* behaviour and targets for anthelmintics. *Invert Neurosci* **7**(4): 199-208.

Holden-Dye, L, Walker, RJ (1988) ZAPA, (Z)-3-[(aminoiminomethyl)thio]-2-propenoic acid hydrochloride, a potent agonist at GABA-receptors on the *Ascaris* muscle cell. *Br J Pharmacol* **95**(1): 3-5.

Horvitz, HR, Chalfie, M, Trent, C, Sulston, JE, Evans, PD (1982) Serotonin and octopamine in the nematode *Caenorhabditis elegans*. *Science* **216**(4549): 1012-1014.

Hotez, PJ, Molyneux, DH, Fenwick, A, Kumaresan, J, Sachs, SE, Sachs, JD, Savioli, L (2007) Control of neglected tropical diseases. *N Engl J Med* **357**(10): 1018-1027.

Jagannathan, S, Laughton, DL, Critten, CL, Skinner, TM, Horoszok, L, Wolstenholme, AJ (1999) Ligand-gated chloride channel subunits encoded by the *Haemonchus contortus* and *Ascaris suum* orthologues of the *Caenorhabditis elegans* gbr-2 (avr-14) gene. *Mol Biochem Parasitol* **103**(2): 129-140.

Janssen, PA (1976) The levamisole story. *Prog Drug Res* **20**: 347-383.

Jeziorski, MC, Greenberg, RM (2006) Voltage-gated calcium channel subunits from platyhelminths: potential role in praziquantel action. *Int J Parasitol* **36**(6): 625-632.

Johnson, CD, Reinitz, CA, Sithigorngul, P, Stretton, AO (1996) Neuronal localization of serotonin in the nematode *Ascaris suum*. *J Comp Neurol* **367**(3): 352-360.

Johnson, CD, Stretton, AO (1987) GABA-immunoreactivity in inhibitory motor neurons of the nematode *Ascaris*. *J Neurosci* **7**(1): 223-235.

Johnston, RN, Shaw, C, Halton, DW, Verhaert, P, Blair, KL, Brennan, GP, Price, DA, Anderson, PA (1996) Isolation, localization, and bioactivity of the FMRFamide-related neuropeptides GYIRFamide and YIRFamide from the marine turbellarian *Bdelloura candida*. *J Neurochem* **67**(2): 814-821.

Jospin, M, Jacquemond, V, Mariol, MC, Segalat, L, Allard, B (2002) The L-type voltage-dependent Ca²⁺ channel EGL-19 controls body wall muscle function in *Caenorhabditis elegans*. *J Cell Biol* **159**(2): 337-348.

Kaminsky, R, Ducray, P, Jung, M, Clover, R, Rufener, L, Bouvier, J, Weber, SS, Wenger, A, Wieland-Berghausen, S, Goebel, T, Gauvry, N, Pautrat, F, Skripsky, T, Froelich, O, Komoin-Oka, C, Westlund, B, Sluder, A, Maser, P (2008) A new class of anthelmintics effective against drug-resistant nematodes. *Nature* **452**(7184): 176-180.

Katzung, BG (2003) Basic and Clinical Pharmacology (9th ed.). *McGraw-Hill Medical Publication*.

Keating, CD, Holden-Dye, L, Thorndyke, MC, Williams, RG, Mallett, A, Walker, RJ (1995) The FMRFamide-like neuropeptide AF2 is present in the parasitic nematode *Haemonchus contortus*. *Parasitology* **111** (Pt 4): 515-521.

Kohn, AB, Anderson, PA, Roberts-Misterly, JM, Greenberg, RM (2001a) Schistosome calcium channel beta subunits. Unusual modulatory effects and potential role in the action of the antischistosomal drug praziquantel. *J Biol Chem* **276**(40): 36873-36876.

Kohn, AB, Lea, J, Roberts-Misterly, JM, Anderson, PA, Greenberg, RM (2001b) Structure of three high voltage-activated calcium channel alpha1 subunits from *Schistosoma mansoni*. *Parasitology* **123**(Pt 5): 489-497.

Komuniecki, RW, Hobson, RJ, Rex, EB, Hapiak, VM, Komuniecki, PR (2004) Biogenic amine receptors in parasitic nematodes: what can be learned from *Caenorhabditis elegans*? *Mol Biochem Parasitol* **137**(1): 1-11.

Kubiak, TM, Larsen, MJ, Bowman, JW, Geary, TG, Lowery, DE (2007) FMRFamide-like peptides (FLPs) encoded on the flp-18 precursor gene activate two isoforms of the orphan *Caenorhabditis elegans* G-protein-coupled receptor Y58G8A.4 heterologously expressed in mammalian cells. *Biopolymers*.

Kubiak, TM, Larsen, MJ, Davis, JP, Zantello, MR, Bowman, JW (2003a) AF2 interaction with *Ascaris suum* body wall muscle membranes involves G-protein activation. *Biochem Biophys Res Commun* **301**(2): 456-459.

Kubiak, TM, Larsen, MJ, Zantello, MR, Bowman, JW, Nulf, SC, Lowery, DE (2003b) Functional annotation of the putative orphan *Caenorhabditis elegans* G-protein-coupled receptor C10C6.2 as a FLP15 peptide receptor. *J Biol Chem* **278**(43): 42115-42120.

Kubo, Y, Adelman, JP, Clapham, DE, Jan, LY, Karschin, A, Kurachi, Y, Lazdunski, M, Nichols, CG, Seino, S, Vandenberg, CA (2005) International Union of Pharmacology. LIV. Nomenclature and molecular relationships of inwardly rectifying potassium channels. *Pharmacol Rev* **57**(4): 509-526.

Kwa, MS, Veenstra, JG, Roos, MH (1994) Benzimidazole resistance in *Haemonchus contortus* is correlated with a conserved mutation at amino acid 200 in beta-tubulin isotype 1. *Mol Biochem Parasitol* **63**(2): 299-303.

Laughton, DL, Lunt, GG, Wolstenholme, AJ (1997) Alternative splicing of a *Caenorhabditis elegans* gene produces two novel inhibitory amino acid receptor subunits with identical ligand binding domains but different ion channels. *Gene* **201**(1-2): 119-125.

Lee, RY, Lobel, L, Hengartner, M, Horvitz, HR, Avery, L (1997) Mutations in the alpha1 subunit of an L-type voltage-activated Ca²⁺ channel cause myotonia in *Caenorhabditis elegans*. *Embo J* **16**(20): 6066-6076.

Lee, YS, Park, YS, Nam, S, Suh, SJ, Lee, J, Kaang, BK, Cho, NJ (2000) Characterization of GAR-2, a novel G protein-linked acetylcholine receptor from *Caenorhabditis elegans*. *J Neurochem* **75**(5): 1800-1809.

Li, C (2005) The ever-expanding neuropeptide gene families in the nematode *Caenorhabditis elegans*. *Parasitology* **131 Suppl**: S109-127.

Li, C, Nelson, LS, Kim, K, Nathoo, A, Hart, AC (1999) Neuropeptide gene families in the nematode *Caenorhabditis elegans*. *Ann N Y Acad Sci* **897**: 239-252.

Loer, CM, Kenyon, CJ (1993) Serotonin-deficient mutants and male mating behavior in the nematode *Caenorhabditis elegans*. *J Neurosci* **13**(12): 5407-5417.

Lowery, DE, Geary, TG, Kubiak, TM, Larsen, MJ (2003) G protein-coupled receptors and modulators thereof. *US Patent No. 6,632,621*.

Marks, NJ, Halton, DW, Maule, AG, Brennan, GP, Shaw, C, Southgate, VR, Johnston, CF (1995a) Comparative analyses of the neuropeptide F (NPF)- and FMRFamide-related peptide (FaRP)-immunoreactivities in *Fasciola hepatica* and *Schistosoma* spp. *Parasitology* **110** (Pt 4): 371-381.

Marks, NJ, Sangster, NC, Maule, AG, Halton, DW, Thompson, DP, Geary, TG, Shaw, C (1999) Structural characterisation and pharmacology of KHEYLRFamide (AF2) and KSAYMRFamide (PF3/AF8) from *Haemonchus contortus*. *Mol Biochem Parasitol* **100**(2): 185-194.

Marks, NJ, Shaw, C, Maule, AG, Davis, JP, Halton, DW, Verhaert, P, Geary, TG, Thompson, DP (1995b) Isolation of AF2 (KHEYLRFamide) from *Caenorhabditis elegans*: evidence for the presence of more than one FMRFamide-related peptide-encoding gene. *Biochem Biophys Res Commun* **217**(3): 845-851.

Martin, RJ (1980) The effect of gamma-aminobutyric acid on the input conductance and membrane potential of *Ascaris* muscle. *Br J Pharmacol* **71**(1): 99-106.

Martin, RJ (1982) Electrophysiological effects of piperazine and diethylcarbamazine on *Ascaris suum* somatic muscle. *Br J Pharmacol* **77**(2): 255-265.

Martin, RJ (1996) An electrophysiological preparation of *Ascaris suum* pharyngeal muscle reveals a glutamate-gated chloride channel sensitive to the avermectin analogue, milbemycin D. *Parasitology* **112** (Pt 2): 247-252.

Martin, RJ (1985) gamma-Aminobutyric acid- and piperazine-activated single-channel currents from *Ascaris suum* body muscle. *Br J Pharmacol* **84**(2): 445-461.

Martin, RJ (1987) The gamma-aminobutyric acid receptor of *Ascaris* as a target for anthelmintics. *Biochem Soc Trans* **15**(1): 61-65.

Martin, RJ, Pennington, AJ, Duittoz, AH, Robertson, S, Kusel, JR (1991) The physiology and pharmacology of neuromuscular transmission in the nematode parasite, *Ascaris suum*. *Parasitology* **102** Suppl: S41-58.

Martin, RJ, Robertson, AP (2007) Mode of action of levamisole and pyrantel, anthelmintic resistance, E153 and Q57. *Parasitology* **134**(Pt 8): 1093-1104.

Martin, RJ, Robertson, AP, Bjorn, H, Sangster, NC (1997) Heterogeneous levamisole receptors: a single-channel study of nicotinic acetylcholine receptors from *Oesophagostomum dentatum*. *Eur J Pharmacol* **322**(2-3): 249-257.

Martin, RJ, Thorn, P, Gration, KA, Harrow, ID (1992) Voltage-activated currents in somatic muscle of the nematode parasite *Ascaris suum*. *J Exp Biol* **173**: 75-90.

Martin, RJ, Valkanov, MA, Dale, VM, Robertson, AP, Murray, I (1996) Electrophysiology of *Ascaris* muscle and anti-nematodal drug action. *Parasitology* **113** Suppl: S137-156.

Mathews, EA, Garcia, E, Santi, CM, Mullen, GP, Thacker, C, Moerman, DG, Snutch, TP (2003) Critical residues of the *Caenorhabditis elegans* unc-2 voltage-gated calcium channel that affect behavioral and physiological properties. *J Neurosci* **23**(16): 6537-6545.

Maule, A, Shaw, C, Halton, D, Thim, L (1993) GNFFRFamide: a novel FMRFamide-immunoreactive peptide isolated from the sheep tapeworm, *Moniezia expansa*. *Biochem Biophys Res Commun* **193**(3): 1054-1060.

Maule, AG, Geary, TG (1997) Neuropeptide gene identification using the polymerase chain reaction. *Methods Mol Biol* **73**: 27-40.

Maule, AG, Geary, TG, Bowman, JW, Marks, NJ, Blair, KL, Halton, DW, Shaw, C, Thompson, DP (1995a) Inhibitory effects of nematode FMRFamide-related peptides (FaRPs) on muscle strips from *Ascaris suum*. *Invert Neurosci* **1**(3): 255-265.

Maule, AG, Geary, TG, Bowman, JW, Shaw, C, Falton, DW, Thompson, DP (1996) The Pharmacology of Nematode FMRFamide-related Peptides. *Parasitol Today* **12**(9): 351-357.

Maule, AG, Marks, NJ, Halton, DW (2001) Parasitic Nematodes: Molecular biology, Biochemistry and Immunology (Ed. M.W. Kennedy and W. Harnett). *CABI International*: 415-440.

Maule, AG, Mousley, A, Marks, NJ, Day, TA, Thompson, DP, Geary, TG, Halton, DW (2002) Neuropeptide signaling systems - potential drug targets for parasite and pest control. *Curr Top Med Chem* **2**(7): 733-758.

Maule, AG, Shaw, C, Bowman, JW, Halton, DW, Thompson, DP, Geary, TG, Thim, L (1994a) The FMRFamide-like neuropeptide AF2 (*Ascaris suum*) is present in the free-living nematode, *Panagrellus redivivus* (Nematoda, Rhabditida). *Parasitology* **109** (Pt 3): 351-356.

Maule, AG, Shaw, C, Bowman, JW, Halton, DW, Thompson, DP, Geary, TG, Thim, L (1994b) KSAYMRFamide: a novel FMRFamide-related heptapeptide from the free-living nematode, *Panagrellus redivivus*, which is myoactive in the parasitic nematode, *Ascaris suum*. *Biochem Biophys Res Commun* **200**(2): 973-980.

Maule, AG, Shaw, C, Bowman, JW, Halton, DW, Thompson, DP, Thim, L, Kubiak, TM, Martin, RA, Geary, TG (1995b) Isolation and preliminary biological characterization of KPNFIRFamide, a novel FMRFamide-related peptide from the free-living nematode, *Panagrellus redivivus*. *Peptides* **16**(1): 87-93.

Maule, AG, Shaw, C, Halton, DW, Curry, WJ, Thim, L (1994c) RYIRFamide: a turbellarian FMRFamide-related peptide (FaRP). *Regul Pept* **50**(1): 37-43.

McIntire, SL, Jorgensen, E, Horvitz, HR (1993) Genes required for GABA function in *Caenorhabditis elegans*. *Nature* **364**(6435): 334-337.

McVeigh, P, Geary, TG, Marks, NJ, Maule, AG (2006) The FLP-side of nematodes. *Trends Parasitol* **22**(8): 385-396.

McVeigh, P, Leech, S, Mair, GR, Marks, NJ, Geary, TG, Maule, AG (2005) Analysis of FMRFamide-like peptide (FLP) diversity in phylum Nematoda. *Int J Parasitol* **35**(10): 1043-1060.

Mehlhorn, H, Kojima, S, Rim, HJ, Ruenwongsa, P, Andrews, P, Thomas, H, Bunnag, B (1983) Ultrastructural investigations on the effects of praziquantel on human trematodes from Asia: *Clonorchis sinensis*, *Metagonimus yokogawai*, *Opisthorchis viverrini*, *Paragonimus westermani* and *Schistosoma japonicum*. *Arzneimittelforschung* **33**(1): 91-98.

Mendonca-Silva, DL, Novozhilova, E, Cobbett, PJ, Silva, CL, Noel, F, Totten, MI, Maule, AG, Day, TA (2006) Role of calcium influx through voltage-operated calcium channels and of calcium mobilization in the physiology of *Schistosoma mansoni* muscle contractions. *Parasitology* **133**(Pt 1): 67-74.

Mertens, I, Clinckspoor, I, Janssen, T, Nachman, R, Schoofs, L (2006) FMRFamide related peptide ligands activate the *Caenorhabditis elegans* orphan GPCR Y59H11AL.1. *Peptides* **27**(6): 1291-1296.

Mertens, I, Vandingenen, A, Clynen, E, Nachman, RJ, De Loof, A, Schoofs, L (2005) Characterization of an RFamide-related peptide orphan GPCR in *C. elegans*. *Ann N Y Acad Sci* **1040**: 410-412.

Mousley, A, Marks, NJ, Halton, DW, Geary, TG, Thompson, DP, Maule, AG (2004) Arthropod FMRFamide-related peptides modulate muscle activity in helminths. *Int J Parasitol* **34**(6): 755-768.

Mousley, A, Maule, AG, Halton, DW, Marks, NJ (2005a) Inter-phyla studies on neuropeptides: the potential for broad-spectrum anthelmintic and/or endectocide discovery. *Parasitology* **131 Suppl**: S143-167.

Mousley, A, Moffett, CL, Duve, H, Thorpe, A, Halton, DW, Geary, TG, Thompson, DP, Maule, AG, Marks, NJ (2005b) Expression and bioactivity of allatostatin-like neuropeptides in helminths. *Int J Parasitol* **35**(14): 1557-1567.

Natoff, IL (1969) The pharmacology of the cholinceptor in muscle preparations of *Ascaris lumbricoides* var. suum. *Br J Pharmacol* **37**(1): 251-257.

Nelson, LS, Kim, K, Memmott, JE, Li, C (1998a) FMRFamide-related gene family in the nematode, *Caenorhabditis elegans*. *Brain Res Mol Brain Res* **58**(1-2): 103-111.

Nelson, LS, Rosoff, ML, Li, C (1998b) Disruption of a neuropeptide gene, *flp-1*, causes multiple behavioral defects in *Caenorhabditis elegans*. *Science* **281**(5383): 1686-1690.

Norton, S, De Beer, EJ (1957) Investigations on the action of piperazine on *Ascaris lumbricoides*. *Am J Trop Med Hyg* **6**(5): 898-905.

Nowycky, MC, Fox, AP, Tsien, RW (1985) Three types of neuronal calcium channel with different calcium agonist sensitivity. *Nature* **316**(6027): 440-443.

Olde, B, McCombie, WR (1997) Molecular cloning and functional expression of a serotonin receptor from *Caenorhabditis elegans*. *J Mol Neurosci* **8**(1): 53-62.

Ōmura, S (2002) in *Macrolide Antibiotics — Chemistry, Biology and Practice* 2nd edn (ed. Omura, S.). (*Academic Press, 2002*). 571-576.

Omura, S, Crump, A (2004) The life and times of ivermectin - a success story. *Nat Rev Microbiol* **2**(12): 984-989.

Pang, FY, Mason, J, Holden-Dye, L, Franks, CJ, Williams, RG, Walker, RJ (1995) The effects of the nematode peptide, KHEYLRFamide (AF2), on the somatic musculature of the parasitic nematode *Ascaris suum*. *Parasitology* **110** (Pt 3): 353-362.

Park, YS, Kim, S, Shin, Y, Choi, B, Cho, NJ (2003) Alternative splicing of the muscarinic acetylcholine receptor GAR-3 in *Caenorhabditis elegans*. *Biochem Biophys Res Commun* **308**(4): 961-965.

Park, YS, Lee, YS, Cho, NJ, Kaang, BK (2000) Alternative splicing of gar-1, a *Caenorhabditis elegans* G-protein-linked acetylcholine receptor gene. *Biochem Biophys Res Commun* **268**(2): 354-358.

Parri, HR, Holden-Dye, L, Walker, RJ (1991) Studies on the ionic selectivity of the GABA-operated chloride channel on the somatic muscle bag cells of the parasitic nematode *Ascaris suum*. *Exp Physiol* **76**(4): 597-606.

Perez-Reyes, E (2003) Molecular physiology of low-voltage-activated t-type calcium channels. *Physiol Rev* **83**(1): 117-161.

Perez-Reyes, E, Lory, P (2006) Molecular biology of T-type calcium channels. *CNS Neurol Disord Drug Targets* **5**(6): 605-609.

Portillo, V, Jagannathan, S, Wolstenholme, AJ (2003) Distribution of glutamate-gated chloride channel subunits in the parasitic nematode *Haemonchus contortus*. *J Comp Neurol* **462**(2): 213-222.

Price, DA, Greenberg, MJ (1977) Structure of a molluscan cardioexcitatory neuropeptide. *Science* **197**(4304): 670-671.

Purcell, J, Robertson, AP, Thompson, DP, Martin, RJ (2002) The time-course of the response to the FMRFamide-related peptide PF4 in *Ascaris suum* muscle cells indicates direct gating of a chloride ion-channel. *Parasitology* **124**(Pt 6): 649-656.

Qian, H, Martin, RJ, Robertson, AP (2006) Pharmacology of N-, L-, and B-subtypes of nematode nAChR resolved at the single-channel level in *Ascaris suum*. *FASEB J* **20**(14): 2606-2608.

Randall, A, Tsien, RW (1995) Pharmacological dissection of multiple types of Ca²⁺ channel currents in rat cerebellar granule neurons. *J Neurosci* **15**(4): 2995-3012.

Rang, HP (2003) *Pharmacology*. Edinburgh: Churchill Livingstone: page 60.

Reinitz, CA, Herfel, HG, Messinger, LA, Stretton, AO (2000) Changes in locomotory behavior and cAMP produced in *Ascaris suum* by neuropeptides from *Ascaris suum* or *Caenorhabditis elegans*. *Mol Biochem Parasitol* **111**(1): 185-197.

Richmond, JE, Jorgensen, EM (1999) One GABA and two acetylcholine receptors function at the *C. elegans* neuromuscular junction. *Nat Neurosci* **2**(9): 791-797.

Robertson, AP, Clark, CL, Burns, TA, Thompson, DP, Geary, TG, Trailovic, SM, Martin, RJ (2002) Paraherquamide and 2-deoxy-paraherquamide distinguish cholinergic receptor subtypes in *Ascaris* muscle. *J Pharmacol Exp Ther* **302**(3): 853-860.

Robertson, SJ, Martin, RJ (1993) Levamisole-activated single-channel currents from muscle of the nematode parasite *Ascaris suum*. *Br J Pharmacol* **108**(1): 170-178.

Rosenbluth, J (1967) Obliquely striated muscle. 3. Contraction mechanism of *Ascaris* body muscle. *J Cell Biol* **34**(1): 15-33.

Rosenbluth, J (1965a) Ultrastructural organization of obliquely striated muscle fibers in *Ascaris lumbricoides*. *J Cell Biol* **25**(3): 495-515.

Rosenbluth, J (1965b) Ultrastructure of somatic muscle cells in *Ascaris lumbricoides*. II. Intermuscular junctions, neuromuscular junctions, and glycogen stores. *J Cell Biol* **26**(2): 579-591.

Rosoff, ML, Burglin, TR, Li, C (1992) Alternatively spliced transcripts of the *flp-1* gene encode distinct FMRFamide-like peptides in *Caenorhabditis elegans*. *J Neurosci* **12**(6): 2356-2361.

Rosoff, ML, Doble, KE, Price, DA, Li, C (1993) The *flp-1* propeptide is processed into multiple, highly similar FMRFamide-like peptides in *Caenorhabditis elegans*. *Peptides* **14**(2): 331-338.

Rozhkova, EK, Maliutina, TA, Shishov, BA (1978) [Effect of several cholinomimetic and anticholinesterase substances on the somatic musculature of the nematode *Ascaris suum*]. *Zh Evol Biokhim Fiziol* **14**(6): 597-599.

Schafer, WR, Kenyon, CJ (1995) A calcium-channel homologue required for adaptation to dopamine and serotonin in *Caenorhabditis elegans*. *Nature* **375**(6526): 73-78.

Schinkmann, K, Li, C (1994) Comparison of two *Caenorhabditis* genes encoding FMRFamide(Phe-Met-Arg-Phe-NH₂)-like peptides. *Brain Res Mol Brain Res* **24**(1-4): 238-246.

Schinkmann, K, Li, C (1992) Localization of FMRFamide-like peptides in *Caenorhabditis elegans*. *J Comp Neurol* **316**(2): 251-260.

Sen, R, Lapage, S, and Glassett, M (1963) The aetiology of diarrhoeal diseases in children at Ibadan, Nigeria. *J Trop Pediatr*(9): 25-32.

Shaw, C (1996) Neuropeptides and their evolution. *Parasitology* **113 Suppl**: S35-45.

Shaw, C, Maule, AG, Halton, DW (1996) Platyhelminth FMRFamide-related peptides. *Int J Parasitol* **26**(4): 335-345.

Shtonda, B, Avery, L (2005) CCA-1, EGL-19 and EXP-2 currents shape action potentials in the *Caenorhabditis elegans* pharynx. *J Exp Biol* **208**(Pt 11): 2177-2190.

Steger, KA, Shtonda, BB, Thacker, C, Snutch, TP, Avery, L (2005) The *C. elegans* T-type calcium channel CCA-1 boosts neuromuscular transmission. *J Exp Biol* **208**(Pt 11): 2191-2203.

Stretton, A, Donmoyer, J, Davis, R, Meade, J, Cowden, C, Sithigorngul, P (1992) Motor behavior and motor nervous system function in the nematode *Ascaris suum*. *J Parasitol* **78**(2): 206-214.

Stretton, AO (1976) Anatomy and development of the somatic musculature of the nematode *Ascaris*. *J Exp Biol* **64**(3): 773-788.

Stretton, AO, Fishpool, RM, Southgate, E, Donmoyer, JE, Walrond, JP, Moses, JE, Kass, IS (1978) Structure and physiological activity of the motoneurons of the nematode *Ascaris*. *Proc Natl Acad Sci U S A* **75**(7): 3493-3497.

Sulston, J, Dew, M, Brenner, S (1975) Dopaminergic neurons in the nematode *Caenorhabditis elegans*. *J Comp Neurol* **163**(2): 215-226.

Suo, S, Sasagawa, N, Ishiura, S (2002) Identification of a dopamine receptor from *Caenorhabditis elegans*. *Neurosci Lett* **319**(1): 13-16.

Taussig, R, Scheller, RH (1986) The *Aplysia* FMRFamide gene encodes sequences related to mammalian brain peptides. *DNA* **5**(6): 453-461.

Thompson, DP, Davis, JP, Larsen, MJ, Coscarelli, EM, Zinser, EW, Bowman, JW, Alexander-Bowman, SJ, Marks, NJ, Geary, TG (2003) Effects of KHEYLRFamide and KNEFIRFamide on cyclic adenosine monophosphate levels in *Ascaris suum* somatic muscle. *Int J Parasitol* **33**(2): 199-208.

Thorn, P, Martin, RJ (1987) A high-conductance calcium-dependent chloride channel in *Ascaris suum* muscle. *Q J Exp Physiol* **72**(1): 31-49.

Trailovic, SM, Clark, CL, Robertson, AP, Martin, RJ (2005) Brief application of AF2 produces long lasting potentiation of nAChR responses in *Ascaris suum*. *Mol Biochem Parasitol* **139**(1): 51-64.

Trailovic, SM, Verma, S, Clark, CL, Robertson, AP, Martin, RJ (2007) Effects of the muscarinic agonist, 5-methylfurmethiodide, on contraction and electrophysiology of *Ascaris suum* muscle. *Int J Parasitol*.

Trim, N, Brooman, JE, Holden-Dye, L, Walker, RJ (1998) The role of cAMP in the actions of the peptide AF3 in the parasitic nematodes *Ascaris suum* and *Ascaridia galli*. *Mol Biochem Parasitol* **93**(2): 263-271.

Trim, N, Holden-Dye, L, Ruddell, R, Walker, RJ (1997) The effects of the peptides AF3 (AVPGVLRamide) and AF4 (GDVPGVLRamide) on the somatic muscle of the parasitic nematodes *Ascaris suum* and *Ascaridia galli*. *Parasitology* **115** (Pt 2): 213-222.

Urquhart, GM, Armour, J, Duncan, JL, Dunn, AM, Jennings, FW (1987) In Vet Parasitology. *Longman Publications*.

Vassilatis, DK, Arena, JP, Plasterk, RH, Wilkinson, HA, Schaeffer, JM, Cully, DF, Van der Ploeg, LH (1997a) Genetic and biochemical evidence for a novel avermectin-sensitive chloride channel in *Caenorhabditis elegans*. Isolation and characterization. *J Biol Chem* **272**(52): 33167-33174.

Vassilatis, DK, Elliston, KO, Paress, PS, Hamelin, M, Arena, JP, Schaeffer, JM, Van der Ploeg, LH, Cully, DF (1997b) Evolutionary relationship of the ligand-gated ion channels and the avermectin-sensitive, glutamate-gated chloride channels. *J Mol Evol* **44**(5): 501-508.

Verma, S, Robertson, AP, Martin, RJ (2007) The nematode neuropeptide, AF2 (KHEYLRF-NH₂), increases voltage-activated calcium currents in *Ascaris suum* muscle. *Br J Pharmacol* **151**(6): 888-899.

Waggoner, LE, Zhou, GT, Schafer, RW, Schafer, WR (1998) Control of alternative behavioral states by serotonin in *Caenorhabditis elegans*. *Neuron* **21**(1): 203-214.

Wang, ZW, Saifee, O, Nonet, ML, Salkoff, L (2001) SLO-1 potassium channels control quantal content of neurotransmitter release at the *C. elegans* neuromuscular junction. *Neuron* **32**(5): 867-881.

Wei, A, Solaro, C, Lingle, C, Salkoff, L (1994) Calcium sensitivity of BK-type KCa channels determined by a separable domain. *Neuron* **13**(3): 671-681.

Wei, AD, Gutman, GA, Aldrich, R, Chandy, KG, Grissmer, S, Wulff, H (2005) International Union of Pharmacology. LII. Nomenclature and molecular relationships of calcium-activated potassium channels. *Pharmacol Rev* **57**(4): 463-472.

Weisblat, DA, Byerly, L, Russell, RL (1976) Ionic mechanisms of electrical activity in somatic muscles of the nematode *Ascaris lumbricoides*. *J Comp Physiol [A]* **111**: 93-113.

White, JG, Southgate, E, Thomson, JN, Brenner, S (1986) The structure of the nervous system of the nematode *Caenorhabditis elegans*. *Philos. Trans. R. Soc. Lond., B, Biol. Sci.* **314**(1165): 1-340.

Willson, J, Amliwala, K, Davis, A, Cook, A, Cuttle, MF, Kriek, N, Hopper, NA, O'Connor, V, Harder, A, Walker, RJ, Holden-Dye, L (2004) Latrotoxin receptor signaling engages the UNC-13-dependent vesicle-priming pathway in *C. elegans*. *Curr Biol* **14**(15): 1374-1379.

Willson, J, Amliwala, K, Harder, A, Holden-Dye, L, Walker, RJ (2003) The effect of the anthelmintic emodepside at the neuromuscular junction of the parasitic nematode *Ascaris suum*. *Parasitology* **126**(Pt 1): 79-86.

Yeh, E, Ng, S, Zhang, M, Bouhours, M, Wang, Y, Wang, M, Hung, W, Aoyagi, K, Melnik-Martinez, K, Li, M, Liu, F, Schafer, WR, Zhen, M (2008) A putative cation channel, NCA-1, and a novel protein, UNC-80, transmit neuronal activity in *C. elegans*. *PLoS Biol* **6**(3): e55.

Chapter 3. The nematode neuropeptide, AF2 (KHEYLRF-NH₂), increases voltage-activated calcium currents in *Ascaris suum* muscle.

British Journal of Pharmacology 2007 Jul; 151(6):888-99. Epub 2007 May 21.

S Verma, AP Robertson and RJ Martin

Department of Biomedical Science, Iowa State University, Ames, IA, 50010, USA

3.1 Abstract

Background and purpose: Resistance to all the classes of anti-nematodal drugs like the benzimidazoles, cholinergic agonists and avermectins, has now been recorded in animals and/or humans. The development of novel anthelmintics is an urgent and imperative need. Receptors of nematode neuropeptides have been suggested to be suitable target sites for novel anthelmintic drugs.

Experimental approach: To investigate the effect of AF2 on calcium-currents in *Ascaris suum* somatic muscle cells we employed the two-micropipette current-clamp and voltage-clamp techniques.

Key Results: Here we report the isolation of voltage-activated transient inward calcium currents. These currents are similar in characteristics to *C. elegans* UNC-2 type currents, non-L-type calcium currents. Following a 2-minute application of 1 μ M AF2, there was a significant long-lasting increase in the transient inward calcium current; AF2 increased the maximum current (from -84 nA to -158 nA) by shifting the threshold in the hyperpolarizing direction (V_{50} changed from -7.2 to -12.8 mV) and increasing the maximum conductance change from 1.91 to 2.94 μ S.

Conclusion and Implications: These studies demonstrate a mechanism by which AF2 increases the excitability of the neuromuscular system by modulating calcium currents in nematodes. A selective small molecule ligand agonist of the AF2 receptor is predicted to increase the contraction and act synergistically with cholinergic anthelmintics and could counter resistance to these compounds.

3.2 Introduction

Nematode parasites have a diverse biology and infect plants, insects, animals and humans. In most cases, they cause significant damage to their host. Chemical agents (anthelmintics) that have a selective toxic effect on the parasites have been developed to control and treat these infections. In most cases, these drugs were produced for domestic animal use, before they were developed for human use. This can be explained by the fact that the market for antiparasitic drugs in animals (\$ 11 billion U.S. world sales) is bigger than the market for human treatment (\$ 0.5 billion U.S. world sales). Regrettably, resistance to all the classes of anti-nematodal drugs like the benzimidazoles, cholinergic agonists and avermectins, has now been recorded in animals and/or humans (Dent et al., 2000; Geerts and Gryseels, 2001; Wolstenholme et al., 2004; Geary 2005; Martin et al., 2005). The development of novel anthelmintics is an urgent and imperative need.

Beginning with AF1 and AF2, a series of more than 20 novel neuropeptides have been isolated from the parasitic nematode *Ascaris suum* (Stretton et al., 1991). Receptors of nematode neuropeptides have been suggested to be suitable target sites for novel anthelmintic drugs (Greenwood et al., 2005; Mousley et al., 2005). Neuropeptides, known as FMRFamide-like peptides or FLPs, possess a C-terminal

motif usually comprising of an aromatic residue, a hydrophobic residue and an Arg-Phe-amide (Maule et al., 2002). These neuropeptides modulate neuromuscular function. The neuromuscular system is a recognized target for the nicotinic and avermectin anthelmintics. Evidence has also been gathered (Mousley et al., 2005) that shows that FLPs have activities in an extensive range of nematode parasites and even activities in arthropods. Although initially, it was considered that FLP receptors were not present in vertebrate hosts (Geary et al., 1999), it has now been recognized that a number of FLPs have physiological effects in vertebrates, including modulation of food intake (Dockray, 2004), anti-nociception (Pittaway, et al., 1987) and increased blood pressure (Thiemermann et al., 1991). Despite the possibility that there are FLP receptors in vertebrates, there is still optimism that selective small ligands may be found and developed for antiparasitic use (Mousley et al., 2005, Greenwood et al., 2005).

AF2 is the FLP that has been recovered in the greatest quantities from *Ascaris suum* (Cowden and Stretton, 1993), *C. elegans* (Marks et al., 1995), *Haemonchus contortus* (Marks et al., 1999), and *Panagrellus redivivus* (Maule et al., 1994). AF2 has pronounced effects on muscle contraction of nematodes. At concentrations $> 1 \mu\text{M}$, AF2 produces excitatory responses in nematodes (Cowden and Stretton, 1993). The abundance of AF2 in very diverse nematodes and the effects on the nematode neuromuscular system suggest that AF2 receptors should be suitable targets for novel broad-spectrum anthelmintics. Consequently, we have continued the exploration of the effects of AF2 and found that it potentiates the contractile effects of acetylcholine on *Ascaris suum* muscle strips (Trailovic et al.,

2005). We have also observed that it increased spike frequency in electrophysiological experiments suggesting effects on voltage-activated currents.

We have now tested this hypothesis using voltage-clamp to examine these currents in muscle cells of the parasitic nematode *Ascaris suum*. Here we report effects of AF2 on voltage-activated currents in *Ascaris suum* muscle. We found that following application of AF2 there was a long-lasting increase in the transient inward calcium current. These studies are important because they demonstrate a mechanism by which AF2 increases the excitability of the neuromuscular system of nematodes. A selective small molecule ligand of the AF2 receptor is predicted to increase contraction and act synergistically with cholinergic anthelmintics and could counter development of resistance to these compounds.

3.3 Materials and Methods

Collection of worms

Adult *Ascaris suum* were obtained weekly from the IBP pork packing plant at Storm Lake City, Iowa. Worms were maintained in Locke's solution [NaCl (155mM), KCl (5 mM), CaCl₂ (2 mM), NaHCO₃ (1.5 mM) and glucose (5 mM)] at a temperature of 32°C. The Locke's solution was changed daily and the worms were used within 4 days of collection.

Muscle preparation

1 cm muscle tissue flaps were prepared by dissecting the anterior part of the worm, 2-3 cm caudal to the head. A body muscle flap preparation was then pinned onto a Sylgard™-lined 3 ml Petri-dish. The intestine was removed to expose the muscle cells. The preparation was continuously perfused, unless otherwise stated,

with a calcium-Ringer containing 4-aminopyridine to reduce potassium currents with the following composition (mM) : NaCl 23, Na-acetate 110, KCl 24, CaCl₂ 6, MgCl₂ 5 , glucose 11 , HEPES 5 and 4-aminopyridine 5; NaOH was used to adjust the pH to 7.6. The preparation was maintained in the experimental chamber at 34°C using a Warner heating collar [DH 35] and heating the incoming perfusate with a Warner instruments (TC 324B) in line heating system (Hamden, CT, USA). The perfusate was applied at 4-6 ml/min through a 19- gauge needle placed directly over the muscle bag recorded from. Calcium substitution experiments were performed using a magnesium-Ringer (composition in mM: NaCl 23, Na-acetate 110, KCl 24, MgCl₂ 11, glucose 11, HEPES 5, 4-aminopyridine 5mM, and EGTA 0.5; NaOH was used to adjust the pH to 7.6). The sodium and calcium substitution experiments were conducted using NMDG-Ringer (composition in mM : NMDG Cl 23, NMDG-acetate 110, KCl 24, MgCl₂ 11, glucose 11, HEPES 5 and 4-aminopyridine 5; CsOH was used to adjust the pH to 7.6). AF2 (1µM), verapamil (100 µM), nickel (30 µM) and cobalt (10 mM) were applied in calcium-Ringer as described in results.

Electrophysiology

Two-micropipette voltage-clamp and current-clamp techniques were employed to examine the electrophysiological effects in the *Ascaris* muscle bag region (Fig.1). Borosilicate capillary glass (Harvard Apparatus, Holliston, MA, USA) micropipettes were pulled on a Flaming Brown Micropipette puller (Sutter Instrument Co., Novato, CA, USA) and filled with 3 M potassium acetate or mixture of 1.5 M potassium acetate and 1.5 M cesium acetate. The cesium acetate was included in pipette solution to block outward potassium currents. Current-clamp micropipettes

and the voltage-sensing micropipettes for voltage-clamp had a resistance of 20-30 M Ω ; the current-injecting micropipette for voltage-clamp had a resistance of around 4 M Ω . The recordings were obtained by impaling the bag region of the *Ascaris* muscle with both micropipettes. All experiments were performed using an Axoclamp 2B amplifier, a 1320A Digidata interface and pClamp 8.2 software (Axon Instruments, CA). All data were displayed and analyzed on a Pentium IV based desktop computer.

Current-clamp experiments were performed by injecting a hyperpolarizing pulse of 40 nA for 500 ms at 0.28 Hz frequency through the current-injecting micropipette and the other micropipette recorded the change in membrane potential. Cells with stable resting membrane potentials over a period of 30 minutes and input conductance of less than 2.5 μ S were used for analysis.

For voltage-clamp, the amplifier gain was set to more than 100 for all recordings. We also took extra care to keep the resistance of the current-injecting micropipette low (4 M Ω) and keeping the amplifier gain high. The phase lag was set to 1.5 ms in all the experiments to limit oscillation. In addition, muscles closer to the nerve cord were impaled for experimental study, as they were rounder muscle cells with short arms to keep the space-clamp effective. Muscle cells close to the nerve cord were also found to possess larger calcium currents.

For activation of calcium currents, muscle cells were held at -35mV during the voltage-clamp experiments and stepped through a series of voltage-steps that increased by 5mV and lasted 130 ms. The protocol had step potentials of -25 mV, -20 mV, -15 mV, -10 mV, -5 mV, 0 mV, +5 mV, +10 mV, +15 mV, and +20 mV. In

separate experiments, we studied the steady state inactivation kinetics of the calcium current. We used conditioning prepulses of 130 ms that were applied before the step potential 0 mV. To investigate outward-currents, step potentials of: -25 mV, -15 mV, -5 mV, +5 mV, +15 mV, and +25 mV were used lasting 200 ms. The holding potential again was -35 mV. The currents displayed were leak-subtracted using five 1 mV depolarizing steps that were scaled by the pClamp 8.2 software. Drugs were applied initially under current-clamp before effects on voltage-activated currents were tested under voltage-clamp. Cells with uniform membrane potentials more negative than -25 mV over a period of 40 minutes and resting conductance of less than $3\mu\text{S}$ over the course of experiment were selected for the voltage-clamp studies.

Drugs

An AF2 (Sigma, Genosys) 3mM stock solution was prepared every week and kept in Ependorf tubes at $-12\text{ }^{\circ}\text{C}$. The AF2 stock solution was thawed just before use to make up the $1\text{ }\mu\text{M}$ AF2 for the experiments. A $100\text{ }\mu\text{M}$ verapamil solution was prepared fresh for each experiment. 100 mM cobalt chloride stock was prepared every week. Fresh $30\text{ }\mu\text{M}$ nickel and $1\text{ }\mu\text{M}$ acetylcholine solution was prepared for every experiment. All drugs were obtained from Sigma-Aldrich, St. Louis, MO. All the stock solutions were made using double distilled water.

Statistical Analysis

Currents were plotted against the function of step potential to determine current-voltage relationships. For the inactivation curve, peak-current values were plotted against the prepulse potentials. All the statistical analysis was done using Graph Pad Prism software (version 4.0, San Diego, CA, USA). Paired *t*-test was

used to test significant difference in peak current response in control and test recordings; significance levels were set at $p < 0.05$.

3.4 Results

AF2 increases the frequency of small-waves and large-spikes

In a sample of 18 muscle cells from different preparations 12 cells were active and showed depolarizing small-spikes and large-spikes (Weisblat et.al., 1976). In the other 6 quiet cells, the membrane potential showed no depolarization. The effect of a 2-minute application of $1\mu\text{M}$ AF2 on the resting membrane potential and input conductance of the 12 active muscle cells was a small but statistically significant ($p=0.03$) depolarization without a noticeable effect on input conductance. In these 12 experiments, before the application of AF2, the resting membrane potential was 31.6 ± 2.1 mV and the input conductance was 2.66 ± 0.14 μS (means \pm S.E.); after application of AF2, the membrane potential was 29.5 ± 1.6 mV with an input conductance of 2.68 ± 0.12 μS (mean \pm S.E.). In the other 6 quiet preparations, AF2 had no detectable effect on membrane potential or input conductance.

In 5 of the 12 active preparations, AF2 produced an increase in the frequency of small-spikes and large-spikes that returned towards control levels following AF2 washout; in 7 of the 12 active preparations, the increased spiking was maintained even after washout, Fig 2A. The large-spike frequency increased from 0.03 spikes per second before AF2 to 0.1 spikes per second after AF2; and the small-spikes frequency increased from 0.08 spikes per second to 0.15 spikes per second after AF2, Fig. 2B. In 5 of the 12 active preparations, there was no noticeable effect of AF2 on small-spikes or large-spikes. AF2 also produced an increase in the rate of

rise of the potential of the small-spikes and the large-spikes, suggesting that AF2 can increase the inward current producing these depolarizations. In Fig. 2C, the rate of rise of the large-spikes ranged between 1.2 to 1.4 Vs⁻¹ before AF2: after AF2, the rate of rise increased to 1.3 to 1.7 Vs⁻¹. In the experiment illustrated in Fig 2, the small-spike rate of rise was 0.05 to 0.06 Vs⁻¹ before AF2 and 0.08 to 0.09 Vs⁻¹ after AF2. The amplitudes of the large-spikes and small-spike were also increased after AF2 application. The large-spikes increased from 28.6 ± 0.4 mV before AF2, to 31.5 ± 0.14 mV after AF2 application, Fig 2C; the amplitude of small-spikes increased from 3.7 ± 0.2 mV before AF2 to 6.9 ± 1.8 mV after AF2 application, Fig 2B. These effects on small-spikes and large-spikes together with their increased rate of rise, suggested that AF2 increases voltage-activated inward currents. Consequently, we explored the effects of AF2 under voltage-clamp as described in the experiments below.

Effects of AF2 on voltage-activated currents

we investigated effects on voltage-activated currents by switching the recording system to the voltage-clamp mode. Fig. 3A shows initial records of total voltage-activated currents. These currents possessed: 1) an initial transient inward current, more visible at a step potential of 0mV; and 2) a larger sustained outward potassium current, more visible at a step potential of +25mV (Thorn et al., 1987).

Effects of AF2 on voltage-activated currents were not observed during application of AF2 but increased in a time dependent manner after AF2 application. Fig. 3 shows effects of a 2-minute application of 1μM AF2 after a delay of 4 minutes.

AF2 produced a small reduction in the peak outward current but a larger increase in the transient inward current, Fig. 3A & B. The outward peak current at the +25 mV voltage-step was 315 ± 81 nA, mean \pm S.E., in 5 preparations: this decreased significantly to 304 ± 77.2 nA, mean \pm S.E., ($p = 0.04$ paired *t-test*). The small effect of AF2 on the current-voltage plot of the outward peak currents is shown in Fig 3C. When we examined the peak transient inward current at 0mV, we found that it increased significantly from -224 ± 24 nA to -260 ± 26 nA, mean \pm S.E. in 5 preparations ($p = 0.016$, paired *t-test*). Thus, we observed the effects of AF2 on the two currents and that the effect on the transient inward current was proportionately bigger than on the outward current.

Our next step was to separate the transient inward current from the outward current. We did this by using cesium in the recording electrodes and adding 5 mM 4-AP to the bathing solution to block potassium currents. Also, we changed the voltage protocol to examine the activation of the inward current, in more detail: we increased the number of depolarizing voltage-steps to every 5 mV and shortened the length of the voltage-steps from 200 ms to 120 ms.

Activation of the transient inward currents

The muscle cells were held at -35 mV. Fig. 4A is a representative recording of the voltage-activated inward currents where the outward potassium currents were blocked by 5mM 4-AP applied in the bath and cesium in the recording micropipettes. The currents were characterized by a large transient inward current and a small-sustained inward current that was $< 10\%$ of the peak.

Fig 4B shows that the peak inward current was induced by a step potential to 0 mV. A similar observation was made in 16 preparations. The peak current-voltage relationship was extrapolated to predict the reversal potential (E_{rev}) for each experiment. In the experiment shown in Fig. 4C, we used linear regression and extrapolation to estimate the reversal potential (+42 mV) and then the calculated conductance changes from the peak inward currents and driving forces ($E_{rev} - V$) to obtain the activation curve, Fig 4C. The activation curve was then fitted by the Boltzmann equation:

$$G = G_{max} / \{1 + \exp [(V_{50} - V)/K_{slope}]\};$$

Where G is the conductance change, G_{max} is the maximum conductance change, V_{50} is the half-maximum step-voltage, V is the step-voltage and K_{slope} is the slope factor. For the experiment in Fig 4C, V_{50} was -11.3 ± 0.8 mV (mean \pm S.E.), G_{max} was $4.5 \pm 0.1 \mu\text{S}$ (mean \pm S.E.) and the slope factor was 5.5 ± 0.7 mV. In 8 similar experiments, V_{50} ranged between -13.3 mV to -7 mV, G_{max} ranged between $1.7 \mu\text{S}$ to $4.5 \mu\text{S}$ and the slope factor ranged between 4.5 to 7.5 mV. We discuss the characteristics of different calcium currents later.

Effect of AF2 on transient inward currents

Fig 5A shows a representative experiment of effects following a 2-minute application of $1 \mu\text{M}$ AF2 on the peak transient inward current. We followed the same analytical approach as before to prepare the activation curves and to test the effect of AF2 on the transient inward currents. Fig. 5A, B, C & D show that AF2 increased the current by shifting the activation curve to the left and increasing the maximum

conductance change. The peak current at the 0 mV step increased from -84 nA in the control to -158 nA after AF2 application, Fig. 5 A & B. The control activation curve had a V_{50} of -7.2 ± 0.4 mV and a G_{max} of 1.91 ± 0.02 μ S. After AF2, V_{50} was -12.8 ± 0.4 mV and the G_{max} was 2.94 ± 0.03 μ S, Fig 5C. Thus, there was an hyperpolarizing shift of 5.4 mV in V_{50} and a 52% increase in G_{max} in this experiment. The slope factor for the curve changed from the control 7.0 ± 0.4 mV to 4.4 ± 0.3 mV after application of AF2.

It was clear from the experiment described in Fig. 5 A-C and from similar observations in 10 other experiments that AF2 increased the transient inward current. We were interested in determining the time-dependent nature and duration of this effect. To do this we measured the % increase in the inward peak current at the 0 mV step-potential and followed this every 4 minutes. We found that the potentiation took at least 8 minutes to reach a maximum and lasted for more than twenty minutes after washing the AF2. Fig. 5 D shows the mean \pm S.E. % increases from 11 experiments. The average potentiation for the 11 recordings after 17 minutes was $29 \pm 8\%$. There was wide variation ranging between 15 % - 89%. In addition, we also examined the effect of the AF2 on the small sustained inward current and found it to be without significant effect (9 preparations) illustrating the fact that AF2 had its major effect on the transient inward current.

AF2 did not affect inactivation of transient inward currents

The inactivation of the transient inward currents (Figure 6) was tested by using a pre-pulse protocol. The muscle cells were held at -35 mV, then taken to

different pre-pulses for 130 ms to allow inactivation, and then finally stepped to a test-voltage of 0 mV. The pre-pulses were from -45 to 0 mV. The inactivation curves, produced by plotting the peak inward currents against the pre-pulse potentials, were fitted by the Boltzmann's equation; example pre-AF2 treatment and post-AF2 treatment inactivation curves are shown in Figure 6b. Overall, I_{max} had a value of -81.0 ± 18.8 nA, before AF2 application and was -97.3 ± 21.3 nA, after AF2 application (no significant change, $P > 0.05$, $n=6$). V_{50} before AF2 application was -21.1 ± 1.3 mV, and after AF2 application was -22.3 ± 1.6 mV; no significant change, ($P > 0.05$, $n=6$). In addition, the slope factor was not significantly different in the control, 6.4 ± 0.7 mV, as compared to after AF2 application, 8.0 ± 0.9 mV ($P > 0.05$, $n=6$). These experiments showed that the exposure to AF2 did not affect the inactivation characteristics of the inward current.

The transient inward current is calcium dependent

We performed calcium substitution experiments to test effects on the transient inward current. Fig. 7A shows representative recordings, where the amplitude of the transient inward current was reduced, reversibly, by removing calcium and bathing the preparation in a magnesium-Ringer solution for 10 mins. The current returned towards normal on wash.

Fig. 7B shows the current-voltage plots for this particular experiment. In 6 experiments, the peak current at 0 mV in the absence of calcium was significantly reduced from -123.3 ± 11.7 nA, mean \pm S.E., to -21.7 ± 13.7 nA mean \pm S.E., in the

magnesium-Ringer solution. The inward current recovered to -80.8 ± 13.4 nA mean \pm S.E., after perfusion with the control, calcium-Ringer solution for 10 min.

Fig.7C shows a bar chart (mean \pm S.E., n = 6) of the peak currents at the step potential of 0 mV as a % of the control. These experiments showed that removal of the calcium reduced the inward current by 83% and suggested that most of the transient current is carried by calcium. In these experiments, we were not able to reversibly abolish all of the transient inward current despite bathing the preparations in calcium-free Ringer for more than 20 minutes. The remaining current suggests that a small proportion of the inward current is carried by other ions.

Effects of sodium and calcium substitution on the transient inward current

To examine the effect of sodium substitution on the transient inward current we substituted both sodium and calcium with N-methyl D-glucamine (NMDG), as a non-permeant cation. In the NMDG-Ringer we found that there was only a small residual inward current and found that the addition of sodium could produce a modest increase in the amplitude of the inward current. However, only addition of calcium produced a large and significant increase in the transient inward current.

The Fig. 8A₁ is a representative trace of the current in NMDG-Ringer; Fig. 8A₂ is a representative trace of the current trace following the addition of magnesium-Ringer (sodium present); and Fig. 8A₃ is the current trace following the addition of sodium and calcium when the muscle cell was in normal calcium-Ringer solution. The current-voltage relationship for this experiment is shown in Fig. 8B. The peak inward current at 0 mV in NMDG-Ringer was -26 nA; it increased to -39 nA following

the addition of sodium; and increased to -73 nA when sodium and calcium were present (calcium-Ringer).

In 6 experiments, the peak transient inward current in NMDG-Ringer at 0 mV was -13.8 ± 5.3 nA (mean \pm S.E.). This current was -23.8 ± 3.1 nA (mean \pm S.E.) in magnesium-Ringer (sodium present) and it increased to -37.2 ± 2.4 nA (mean \pm S.E., $n = 6$) in calcium-Ringer. Fig. 8C shows a bar chart of the currents expressed as a % of the control (NMDG-Ringer). The increase in the transient inward currents in calcium-Ringer was 260 ± 69 % and was significant ($p < 0.01$, *paired t-test*, $n = 6$). These experiments demonstrated that in the absence of sodium and calcium there was a small voltage-activated inward current. However, only the addition of calcium produced a large voltage-activated current. Sodium did not substitute for calcium. Subsequently we refer to this inward current as the voltage-activated calcium current.

Effect of some calcium channel antagonists on the transient voltage-activated calcium current

We have seen that most of the transient inward current is carried by calcium and that it is increased following AF2 treatment. We were interested to determine effects of some calcium channel antagonists, to see if the current had pharmacological properties that resembled mammalian calcium currents.

We tested effects of 10 mM cobalt on the voltage-activated calcium current, Fig. 9. Fig 9A shows representative traces of the reversible inhibition of the calcium current. In this particular experiment, the current at 0 mV decreased from -78.3 nA

(control) to -6.2 nA in the presence of 10 mM cobalt; the current recovered to -78.0 nA after 25 minutes wash. Fig 9B shows the current-voltage plots from this experiment. Fig 9C shows a bar chart of normalized currents obtained from 7 preparations before, during and at different times following wash. All of these experiments showed that 10 mM cobalt was effective at inhibiting the calcium current.

We also tested effects of 30 μ M nickel, a T-type calcium channel antagonist, and 100 μ M verapamil, a non-selective calcium channel antagonist, Fig 10. Both of these agents were without effect. These observations suggested that the pharmacology of the calcium current is different to that of vertebrates.

Effect of acetylcholine on the transient calcium current

There is evidence of muscarinic receptors present on *Ascaris* muscle (Colquhoun et al., 1991). We tested for the effects of 1 μ M acetylcholine in 6 preparations and found no effects suggesting that muscarinic receptors do not modulate calcium currents in *Ascaris* muscle.

3.5 Discussion

Spikes in Ascaris

Ascaris muscle is capable of producing full action potentials as well as partial spikes (DeBell et al., 1963). The spikes are suggested to start at the neuromuscular-junction (syncytium) and then to travel to the bag region of the muscle via the arms of the muscle cell. We can see here that the bag region, from where we recorded, is capable of conducting voltage-activated currents to support

spikes. The electrical activity and modulation of the spikes seen in *Ascaris* has been modeled by Turner (2001) who has shown that a combination of voltage-activated calcium currents, voltage activated potassium currents (Martin et al., 1992) and a calcium-activated chloride currents (Thorn and Martin, 1987) can produce repeating bursts of spikes in an oscillatory mode that is observed in fresh preparations (Weisblat et al., 1976). An increase in the calcium entry is predicted to change the pattern of this oscillation (Turner, 2001). In this manuscript, we have explored the effects of the neuropeptide, AF2, on the calcium currents.

AF2

Cowden and Stretton, (1993); Pang et al., (1995); Reinitz et al., (2000); Maule et al., (2002) and Trailovic et al., (2005) have described how brief application of AF2 to *Ascaris suum* muscle strips produces a long-lasting increase in the contractility and electrical excitability. Trailovic et al., (2005), have also observed that brief application of AF2 results in a long-lasting potentiation of depolarizing responses to acetylcholine applied to *Ascaris suum* muscle cells. This latter observation showed that AF2 has direct excitatory effects on *Ascaris suum* muscle and contrasts with earlier observations involving cut-nerve-cord experiments (Maule et al., 1995) that suggested that AF2 has post-synaptic inhibitory effects on *Ascaris* muscle. We have described, here, how AF2 increases the amplitude and frequency of small-spikes and large-spikes. When we applied AF2 for a 2-minute period to the muscle cells, we found that there was an increase in the transient inward current that lasted for more than 20 minutes after washout. AF2 produced an increase in the maximum

and the threshold shifted in the hyperpolarizing direction. The increase in this inward current suggests it was responsible for the change in spontaneous depolarizations observed under current-clamp. The small effect of AF2, Fig. 3, on the total outward current suggests that the decreased outward current is not the primary cause of the increased excitability of the muscle cells.

The transient inward current is carried by calcium

We can say that the current producing the muscle spikes is mediated by voltage-activated calcium channels for the following reasons: the amplitude of *Ascaris* muscle spikes are reduced in low-Ca Ringer solutions (Weisblat et al., 1976); the transient inward current is blocked by 1mM lanthanum (Martin et al., 1992); removal of calcium reduces the amplitude of the transient inward current, Fig. 7; removal of sodium and calcium in the NMDG-Ringer abolishes the transient inward current; addition of calcium, but not sodium, allowed the transient current to reappear, Fig. 8; and addition of cobalt, Fig. 9 abolished the transient current. All of these observations are consistent with calcium being the major, but not necessarily the exclusive charge carrier of the current. The reversal potential of the current in this series of experiment was estimated by extrapolation and was around +45 mV. The predicted Nernst calcium potential with 6 mM extracellular calcium and 1 μ M intracellular calcium is +110 mV, some 65 mV more positive than we observed. Despite the prediction of a more positive reversal potential for calcium, others have made similar observations for the *C. elegans* L-type EGL-19, calcium channels (Jospin et al., 2002); and for the calcium channels in vertebrate preparations (Nowcyky et al., 1985). Collectively, these observations suggest that the calcium

channel in nematode and mammalian preparations is not exclusively permeable to calcium, but may also be permeable to other monovalent ions including sodium and potassium. Although we replaced all cations with NMDG we found that a residual inward current remained in some preparations, Fig. 8. This remaining inward current is not likely to be carried by cations (no permeable cations in NMDG-Ringer) so it may be produced by closing of outward calcium-dependent chloride channel current (Thorn and Martin, 1987) which is present in *Ascaris* bag cells. We did not investigate this current in NMDG further.

Comparison of voltage-activated calcium currents in mammals and C. elegans

Voltage-gated calcium channel currents in vertebrates can be divided into three major groups (Catterall, 2000).

- 1) There is the T-type or transient calcium channel current that is activated at relatively negative potentials, positive to -70 mV (V_{50} -51 mV, K 7.0 mV; Fox et al, 1987). It inactivates with a time constant in the 20-50 ms range at potentials more positive than -60 mV. The different types of calcium channels are built around a transmembrane ion-channel protein that is known as the α_1 subunit. Ca_v3 protein subunits are the α_1 subunit for the T-type channels (Perez-Reyes et al., 1998). A similar current has been described in the nematode *C. elegans* pharyngeal muscle, coded for by the gene *cca-1* that has around 70% similarity to mammalian Ca_v3 subunits (Mathews et al., 2003; Shtonda et al., 2005).

- 2) There are the N-, P-, Q, and R-types of calcium currents that are activated at potentials positive to -30 mV (N- type: V_{50} -6.5 mV, K 6.5 mV; Fox et al, 1987) and that inactivate in the 50-80 ms range. The N-type current is resistant to block by nickel and nifedipine. Cloned $Ca_v2.2$ subunits conduct N-type currents (Dubel et al., 1992); cloned $Ca_v2.1$ subunits (Mori et al, 1991) conduct P-/Q-type currents; cloned $Ca_v2.3$ subunits conduct R-type currents (Randall and Tsien, 1995). The *unc-2* gene of the nematode *C.elegans* has the greatest similarity to the $Ca_v2.3$ subunits (R-type current) but is also similar to $Ca_v2.1$ & $Ca_v2.2$ α_1 subunits (N- & Q/P-type currents).
- 3) There is the L-type current that is activated by making bigger depolarizing steps to potentials positive to -10 mV (V_{50} +16.5 mV, K 5.5 mV; Fox et al, 1987). This current inactivates slowly with a time constant > 500 ms. The L-type calcium current is mediated by the Ca_v1 family of α_1 subunits, inhibited by nifedipine, verapamil and potentiated by Bay K 8644. In *C. elegans* body muscle and pharyngeal muscle a current similar to the L-type current is conducted through a channel formed by an α_1 subunit coded for by the *egl-19* gene (Shtonda and Avery, 2005).

In the nematode, *C. elegans*, genes coding for α_1 calcium channel subunits are: *cca-1*, *unc-2* and *egl-19* (see above) and *nca1* and *nca2*. *nca1* and *nca2* are outliers, similar to one another, and to a channel in the yeast *Schizosaccharomyces pombe* (Bargmann, 1998). They are found in the nervous system and ventral cord in *C. elegans* but their electrophysiological properties have not yet been described.

Membrane potential, activation of Ascaris and C. elegans calcium currents, and propagation distances

The *C. elegans* body muscle has a resting membrane potential averaging -19.7 mV so it is not surprising that there is only an L-type calcium (EGL-19) current present that requires potentials positive to -20 mV to activate it (V_{50} +0.95 mV, K 4.6 mV and E_{rev} +51mV) (Jospin et al., 2005). The *C. elegans* L-type current is only partially blocked by a high (1 μ M) concentration of nifedipine so it behaves differently to the mammalian L-type current. The *C. elegans* body wall muscle sometimes displays small-spikes or overshooting action potentials (Jospin et al., 2005). In *C. elegans*, the pharyngeal muscle has a more negative equilibrium membrane potential of -53.6 mV (Shtonda and Avery, 2005) and it has both T-type (CCA-1) and L-type (EGL-19) currents. These currents support the large overshooting action potential of the pharynx. The more negative resting membrane potential allows activation of the T-type current.

The resting membrane potential of *Ascaris* muscle cells is around -35 mV, and displays both small-spikes and overshooting action potentials along with slow waves. The voltage-activated current we observed has some but not all of the properties of the T-type and L-type currents: it inactivated but required a relatively depolarized potential for activation and was not inactivated at a holding potential of -35 mV. The *Ascaris* calcium current was not inhibited by 30 μ M nickel or 100 μ M verapamil and is therefore pharmacologically different to T- and L-types of current (Fox et al., 1987; Jospin et al., 2005; Shtonda and Avery, 2005). The *Ascaris* calcium current has properties similar to the N-, P/Q- and R-types and was unlike

currents carried by *C. elegans* EGL-19 and CCA-1. Sequence comparisons show that phenylalkylamine (verapamil) binding sites in *C. elegans* in the EGL-19 L-type homologue (Snutch et al., 1991; Frøkjær-Jensen et al., 2006) but not in other *C. elegans* non-L-type calcium channel homologues. The *Ascaris* calcium current was most like the currents expected to be carried by UNC-2. The need for propagated spike activity in body muscle cells may be more important in a large nematode like *Ascaris suum* where electrotonic conduction may not be sufficient to carry depolarizations over the larger distances as compared to much smaller *C.elegans*.

Significance of AF2 effects

A number of authors (Wolstenholme et al., 2004; Geary 2005; Martin et al., 2005) have raised concerns about the development of resistance to existing anthelmintics. Our approach has been to investigate the actions of cholinergic anthelmintics (levamisole), to understand better the mode of action of these drugs and to develop a pharmacological strategy for countering resistance to these compounds. AF2 is found in different nematode species and its potency on the nematode neuromuscular system makes AF2 (FLP) receptors an attractive target for the development of novel anthelmintic drugs. In muscle strips of *Ascaris suum*, AF2 potentiates the contractile responses to acetylcholine and levamisole (Marks et al., 1999; Kubiak et al., 2003) increases spiking, post-synaptic neuromuscular potentials (Pang et al., 1995; Brownlee and Walker, 1999) and depolarizing potentials in response to acetylcholine (Trailovic et al., 2005). These properties suggest that a synthetic AF2 ligand could be used to potentiate the effects of cholinergic

anthelmintics like levamisole and so counter effects of resistance to these compounds. In this paper, it is clear that AF2 could potentiate contractions induced by cholinergic anthelmintics, at least in part, by increasing the entry of calcium through voltage-activated channels. Other mechanisms by which AF2 may potentiate muscle contraction remain to be investigated.

3.6 Acknowledgement

We are pleased to acknowledge the support of the NIH to R.J.M.: RO1 A1047194.

3.7 References

Bargmann CI (1998). Neurobiology of the *Caenorhabditis elegans* genome. *Science* 282(5396):2028-33.

Carbone E and Lux HD (1984). A low voltage-activated, fully inactivating Ca channel in vertebrate sensory neurons. *Nature* 310:501-502.

Catterall WA (2000). Structure and regulation of voltage-gated Ca²⁺ channels. *Annu Rev Cell Dev Biol* 16:521-555.

Colquhoun L, Holden-Dye L, Walker RJ (1991). The pharmacology of cholinceptors on the somatic muscle cells of the parasitic nematode *Ascaris suum*. *J Exp Biol* 1991 Jul; 158:509-30.

Cowden C, Stretton AO (1993). AF2, an *Ascaris* neuropeptide: isolation, sequence, and bioactivity. *Peptides* 14(3):423-30.

DeBell JT, del Castillo J and Sanchez V (1963). Electrophysiology of the somatic muscle cells of *Ascaris lumbricoides*. *J Cell Physiol* 62:159-177.

Dent JA, Smith MM, Vassilatis DK, and Avery L (2000). The genetics of ivermectin resistance in *Caenorhabditis elegans*. *Proc Natl Acad Sci* 14; 97(6):2674-9.

Dockray GJ (2004). The expanding family of -RFamide peptides and their effects on feeding behaviour. *Exp Physiol*. 89(3):229-35.

Dubel SJ, Starr TV, Hell J, Ahlijanian MK, Enyeart JJ, Catterall WA, and Snutch TP (1992). Molecular cloning of the alpha-1 subunit of an omega-conotoxin-sensitive calcium channel. *Proc Natl Acad Sci* 89(11):5058-62.

Fox AP, Nowycky MC, Tsien RW (1987). Single-channel recordings of three types of calcium channels in chick sensory neurones. *J Physiol* 1987 Dec; 394:173-200.

Frøkjær-Jensen C, Kindt KS, Kerr RA, Suzuki H, Melnik-Martinez K, Gerstbreih B, Driscoll M, and Schafer WR (2006). Effects of Voltage-Gated Calcium Channel Subunit Genes on Calcium Influx in Cultured *C. elegans* Mechanosensory Neurons. *J Neurobiol* 66: 1125–1139.

Geary TG, Marks NJ, Maule AG, Bowman JW, Alexander-Bowman SJ, Day TA, Larsen MJ, Kubiak TM, Davis JP and Thompson DP (1999). Pharmacology of FMRFamide-related peptides in helminths. *Ann N Y Acad Sci* 897:212-227.

Geary, T G, Kubiak, T M (2005). Neuropeptide G-protein-coupled receptors, their cognate ligands and behavior in *Caenorhabditis elegans*. *Trends Pharmacol Sci* 26(2): 56-58.

Geerts S and Gryseels B (2001). Anthelmintic resistance in human helminths: a review *Trop Med Int Health* ;6(11) 915-921.

Greenwood K, Williams T, and Geary T (2005). Nematode neuropeptide receptors and their development as anthelmintic screens. *Parasitology* 131 Suppl: S169-77.

Jospin M, Jacquemond V, Mariol MC, Segalat L, and Allard B (2002). The L-type voltage-dependent Ca²⁺ channel EGL-19 controls body wall muscle function in *Caenorhabditis elegans*. *J Cell Biol* 159(2):337-48.

Kubiak TM, Larsen MJ, Davis JP, Zantello MR, Bowman JW (2003). AF2 interaction with *Ascaris suum* body wall muscle membranes involves G-protein activation. *Biochem Biophys Res Commun* 301(2):456-9.

Marks NJ, Maule AG, Geary TG, Thompson DP, Davis JP, Halton DW, Verhaert P and Shaw C (1997). APEASPFIRFamide, a novel FMRFamide-related decapeptide from *Caenorhabditis elegans*: structure and myoactivity. *Biochem Biophys Res Commun* 231:591-595.

Marks NJ, Sangster NC, Maule AG, Halton DW, Thompson DP, Geary TG, Shaw C (1999). Structural characterisation and pharmacology of KHEYLRFamide (AF2) and KSAYMRFamide (PF3/AF8) from *Haemonchus contortus*. *Mol Biochem Parasitol* 100(2):185-94.

Martin RJ, Thorn P, Gratton KA, Harrow ID (1992). Voltage-activated currents in somatic muscle of the nematode parasite *Ascaris suum*. *J Exp Biol* 173:75-90.

Martin RJ, Verma S, Levandoski M, Clark CL, Qian H, Stewart M and Robertson AP (2005). Drug resistance and neurotransmitter receptors of nematodes: recent studies on the mode of action of levamisole. *Parasitology* 131 Suppl: S71-S84.

Mathews EA, Garcia E, Santi CM, Mullen GP, Thacker C, Moerman DG and Snutch TP (2003). Critical residues of the *Caenorhabditis elegans unc-2* voltage-gated calcium channel that affect behavioral and physiological properties. *J Neurosci* 23:6537-6545.

Maule AG, Shaw C, Bowman JW, Halton DW, Thompson DP, Geary TG, Thim L (1994). The FMRFamide-like neuropeptide AF2 (*Ascaris suum*) is present in the free-living nematode, *Panagrellus redivivus* (Nematoda, Rhabditida). *Parasitology* 109 (Pt 3):351-6.

Maule AG, Geary TG, Bowman JW, Marks NJ, Blair KL, Halton DW, Shaw C and Thompson DP (1995). Inhibitory effects of nematode FMRFamide-related peptides (FaRPs) on muscle strips from *Ascaris suum*. *Invert Neurosci* 1:255-265.

Maule AG, Geary TG, Marks NJ, Bowman JW, Friedman AR and Thompson DP (1996). Nematode FMRFamide-related peptide (FaRP)-systems: occurrence, distribution and physiology. *Int J Parasitol* 26:927-936.

Maule AG, Mousley A, Marks NJ, Day TA, Thompson DP, Geary TG and Halton DW (2002). Neuropeptide signaling systems - potential drug targets for parasite and pest control. *Curr Top Med Chem* 2:733-758.

Mori Y, Friedrich T, Kim M-S, Mikami A, Nakai J, Ruth P, Bosse E, Hofmann E, Flockerzi V, Furuichi T, Mikoshiba K, Imoto K, Tanabe T, Numa S (1991). Primary structure and functional expression from complementary DNA of a brain calcium channel. *Nature* 350:398-402.

Mousley A, Maule AG, Halton DW and Marks NJ (2005). Inter-phyla studies on neuropeptides: the potential for broad-spectrum anthelmintic and/or endectocide discovery. *Parasitology* 131 Suppl:S143-S167.

Nowycky MC, Fox AP, and Tsien RW (1985). Three types of neuronal calcium channel with different calcium agonist sensitivity *Nature*. 316(6027):440-3.

Pang FY, Mason J, Holden-Dye L, Franks CJ, Williams RG, and Walker RJ (1995). The effects of the nematode peptide, KHEYLRFamide (AF2), on the somatic musculature of the parasitic nematode *Ascaris suum*. *Parasitology* 110 (Pt 3):353-62.

Perez-Reyes E, Cribbs LL, Daud A, Lacerda AE, Barclay J, Williamson MP, Fox M, Rees M and Lee JH (1998). Molecular characterization of a neuronal low-voltage-activated T-type calcium channel. *Nature* 391:896-900.

Pittaway KM, Rodriguez RE, Hughes J, Hill RG (1987). CCK 8 analgesia and hyperalgesia after intrathecal administration in the rat: comparison with CCK-related peptides. *Neuropeptides* 10(1):87-108.

Purcell J, Robertson AP, Thompson DP and Martin RJ (2002). The time-course of the response to the FMRFamide-related peptide PF4 in *Ascaris suum* muscle cells indicates direct gating of a chloride ion-channel. *Parasitology* 124:649-656.

Randall A and Tsien RW (1995). Pharmacological dissection of multiple types of Ca²⁺ channel currents in rat cerebellar granule neurons. *J Neurosci* 15(4):2995-3012.

Reinitz CA, Herfel HG, Messinger LA, Stretton AO (2000). Changes in locomotory behavior and cAMP produced in *Ascaris suum* by neuropeptides from *Ascaris suum* or *Caenorhabditis elegans*. *Mol Biochem Parasitol* 111(1):185-97.

Schafer WR and Kenyon CJ (1995). A calcium-channel homologue required for adaptation to dopamine and serotonin in *Caenorhabditis elegans*. *Nature* 375:73-78.

Shtonda B and Avery L (2005). CCA-1, EGL-19 and EXP-2 currents shape action potentials in the *Caenorhabditis elegans* pharynx. *J Exp Biol* 208:2177-2190.

Snutch TP, Tomlinson WJ, Leonard JP, Gilbert MM (1991). Distinct calcium channels are generated by alternative splicing and are differentially expressed in the mammalian CNS. *Neuron*. 7(1):45-57.

Stretton AOW, Cowden C, Sithigorngul P, and Davis RE (1991). Neuropeptides in the nematode *Ascaris suum*. *Parasitology* 102 Suppl: S107-16.

Thiemermann C, al-Damluji S, Hecker M, and Vane JR (1991). FMRF-amide and L-Arg-L-Phe increase blood pressure and heart rate in the anaesthetised rat by central stimulation of the sympathetic nervous system. *Biochem Biophys Res Commun* 28; 175(1):318-24.

Thorn P, Martin RJ (1987). A high-conductance calcium-dependent chloride channel in *Ascaris suum* muscle. *Q J Exp Physiol* 72(1):31-49.

Trailovic SM, Clark CL, Robertson AP and Martin RJ (2005). Brief application of AF2 produces long lasting potentiation of nAChR responses in *Ascaris suum*. *Mol Biochem Parasitol* 139:51-64.

Turner RE (2001). A model for an *Ascaris* muscle cell. *Exp Physiol* 86(5):551-9.

Weisblat DA, Byerly L and Russell RL (1976). Ionic mechanisms of electrical activity in somatic muscle of the nematode *Ascaris lumbricoides*. *J Comp Physiol* 111: 93-113.

Wolstenholme AJ, Fairweather I, Prichard R, von Samson-Himmelstjerna G, and Sangster NC (2004). Drug resistance in veterinary helminths. *Trends Parasitol* 20(10):469-76.

3.8 Figures and Legends

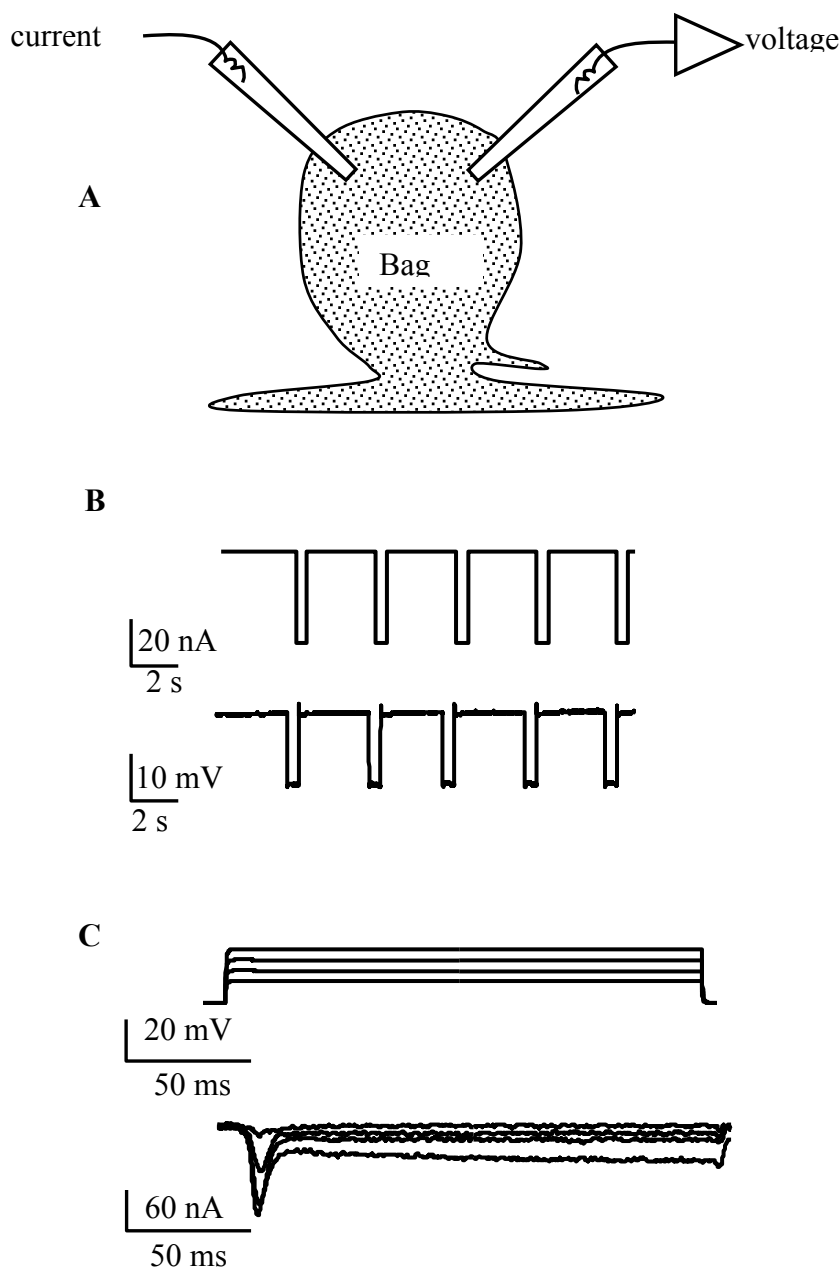


Figure 1. Electrophysiological techniques. **A:** Diagram of the location of two micropipettes for making current-clamp and voltage-clamp recordings from bag region of *Ascaris suum* somatic muscle. The current-injecting pipette and the voltage-sensing pipette are shown. **B:** Current-clamp recording showing membrane potential change (lower trace) in response to 0.5 sec, 40nA, current pulses (upper trace). Input conductance $3.7\mu\text{S}$. **C:** Voltage-clamp recording showing current responses (leak subtracted lower trace) in response to depolarizing potentials from a holding potential of -35mV . Note the presence of the voltage-activated transient inward current and a sustained current. Sustained currents were not prominent in all cells.

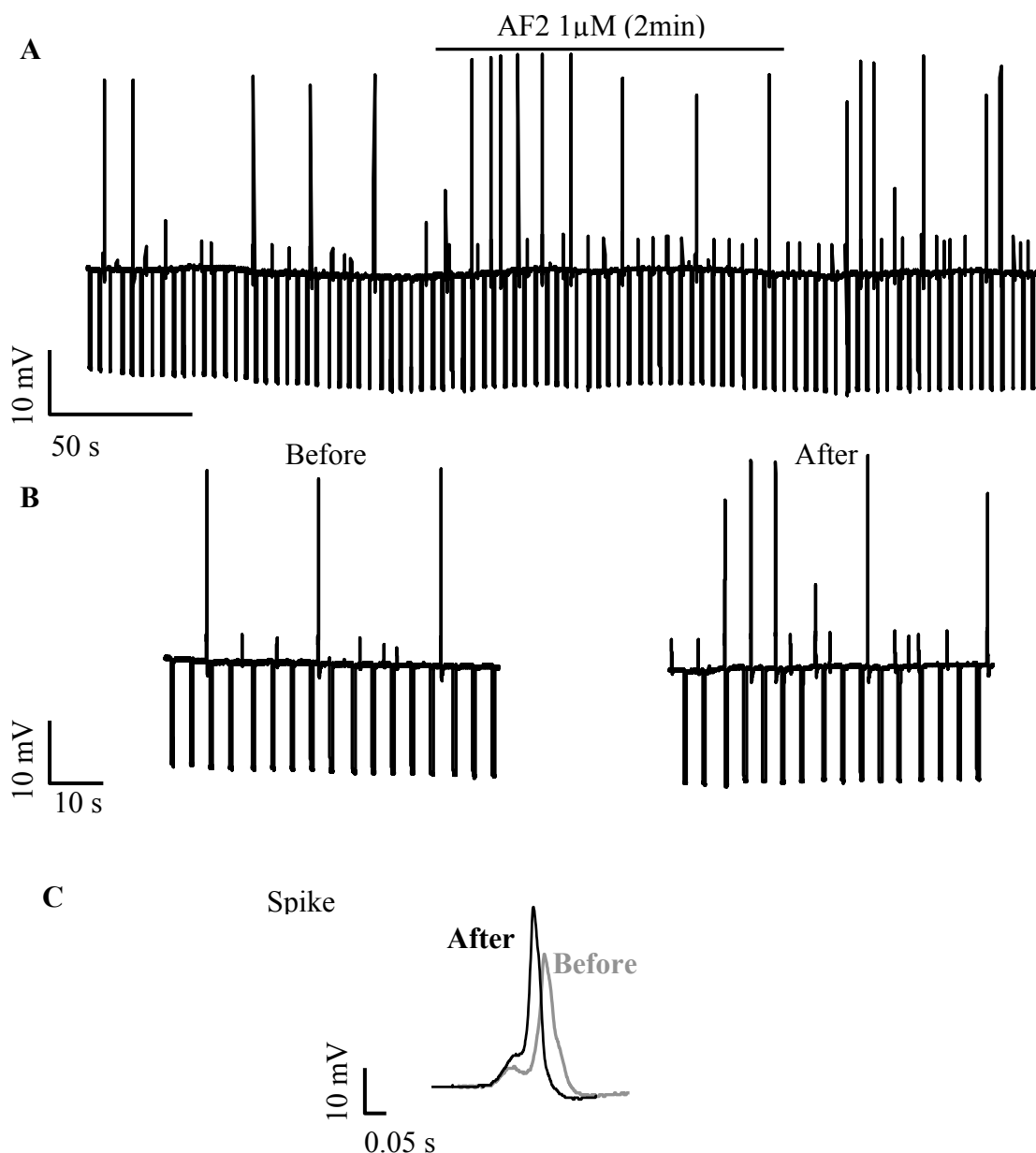


Figure 2. Effect of AF2 under current-clamp. Brief application of AF2 increases frequency of small and large spikes. **A:** Membrane potential record of somatic muscle in current clamp before, during and after application of $1\mu\text{M}$ AF2. **B:** The large spike frequency increased from 0.03 spikes per second before AF2 to 0.1 spikes per second after AF2; the small spike frequency increased from 0.08 spikes per second to 0.15 spikes per second. **C:** Represents the increase in the amplitude and rate of rise of large-spike before and after application of $1\mu\text{M}$ AF2.

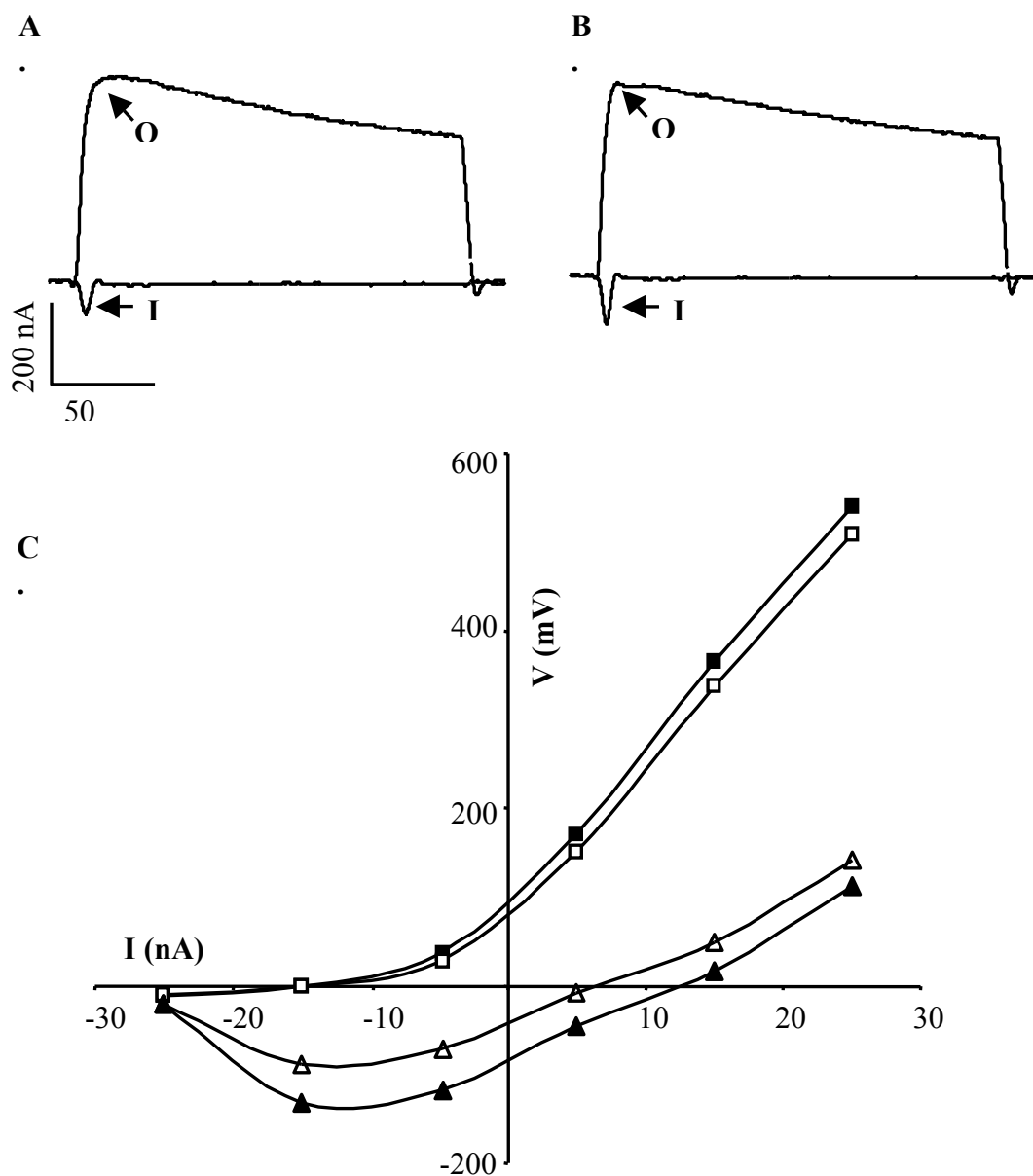


Figure 3. Effect of 2-minute application of $1\mu\text{M}$ AF2 on voltage-activated currents.

A: Control voltage-activated currents; peak total outward currents (O); peak inward currents (I) under K current block. **B:** Voltage-activated currents following AF2 treatment. Note the slight decrease in the peak outward current and the increase in the peak inward current. **C:** Current-voltage plot of the peak outward currents, the peak inward currents before, and following the 2-min application of $1\mu\text{M}$ AF2. ■: Control peak outward current. □: post AF2 peak outward current. Δ Control peak inward current. ▲: post AF2 peak inward current. Note that proportionately, the biggest effect was on the peak inward current

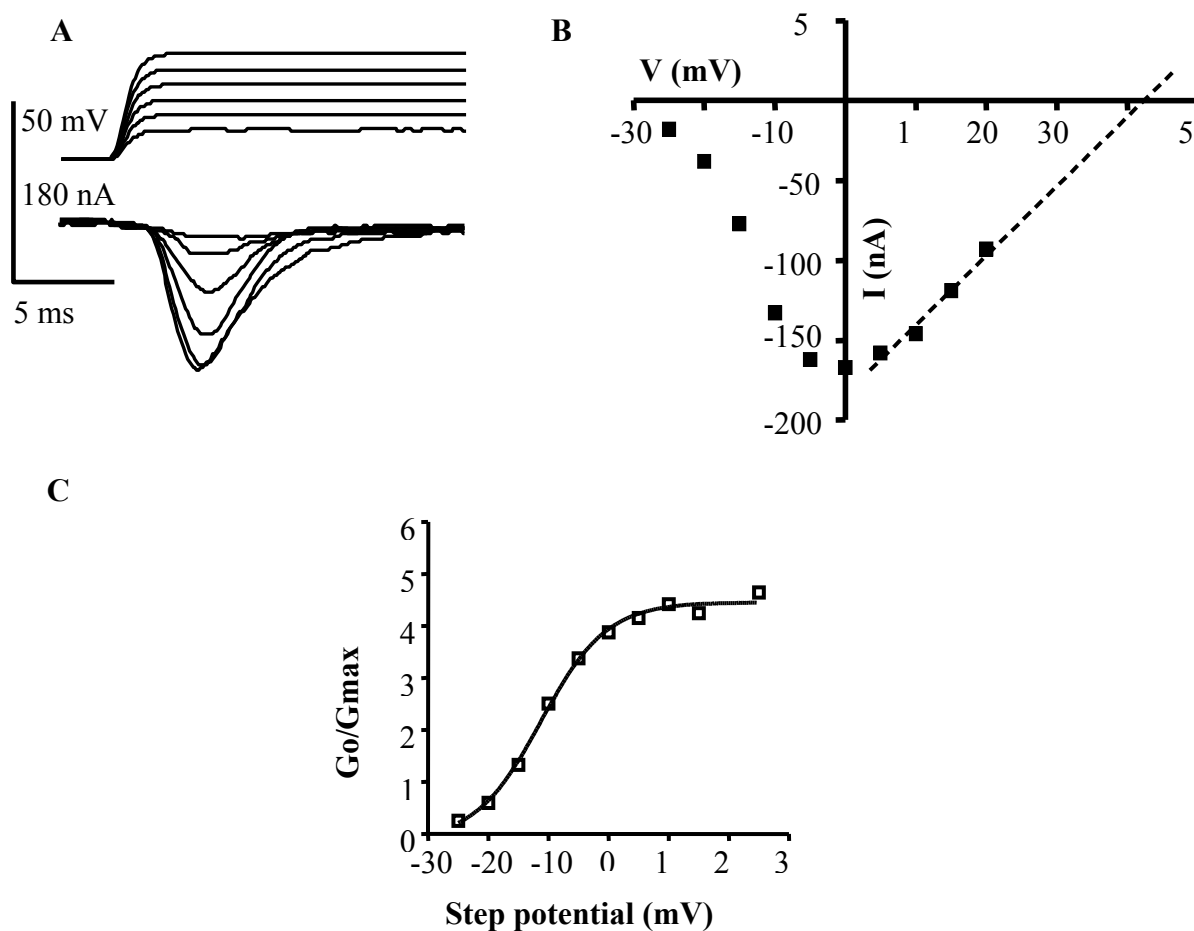


Figure 4. Activation curve of transient inward currents. **A:** Voltage-clamp records following depolarizing steps. Cell was held at -35 mV, and depolarizing steps from -35 mV to $+20$ mV were made. Top trace: voltage steps. Lower trace: leak subtracted current records. **B:** Peak-inward-current vs. step-potential plot from same cell as **A**. Step potentials: -25 mV, -20 mV, -15 mV, -10 mV, -5 mV, 0 mV, $+5$ mV, $+10$ mV, $+15$ mV, and $+20$ mV. The current-voltage relationship was extrapolated to predict reversal potential, $+42$ mV. **C:** Activation curve for experiment shown in **A** and **B**, fitted to Boltzmann equation ($V_{50} = 4.46$ mV, $G_{max} = -11.26$ μ S, $K_{slope} = 5.5$ mV).

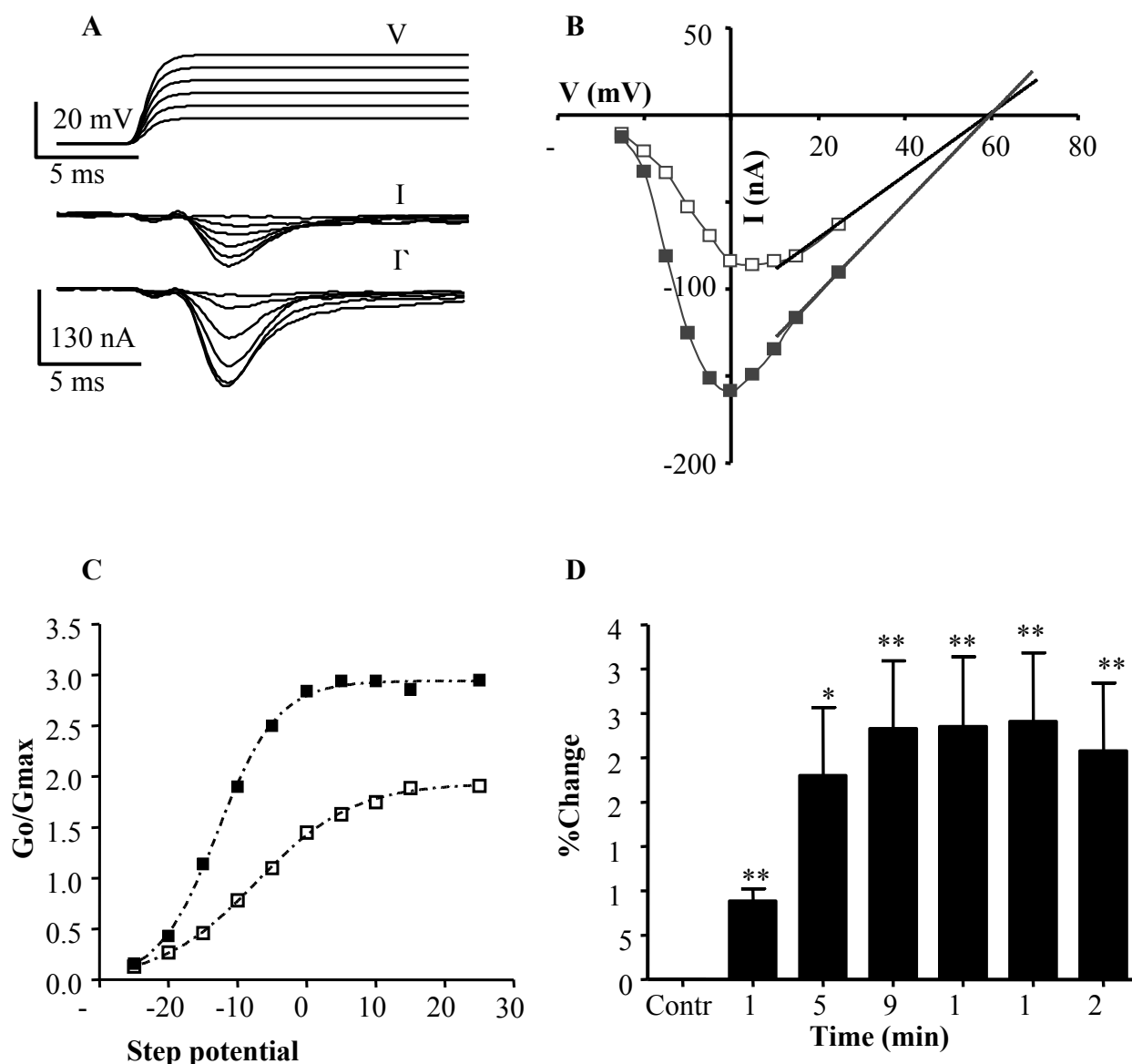


Figure 5. Transient inward currents show long-lasting potentiation after a 2-minute application of 1 μ M AF2. **A:** Voltage-gated transient-inward currents recorded before and 9 minutes after AF2 application. Note the increase in the amplitude of the peak inward currents. V: voltage steps; I: control currents; Γ : currents after AF2. **B:** Peak-current step-voltage relationship for experiment shown in A. Control (\square). 9 minutes after AF2 application (\blacksquare). Last three current points of each plot were extrapolated to obtain the reversal potential, 59mV. **C:** Activation curve showing decrease in G_{max} and hyperpolarizing shift in V_{50} after AF2. Control (\square). After AF2 application (\blacksquare). G_{max} increased from 1.91 μ S in control to 2.94 μ S after AF2. V_{50} shifted from -7.2 mV (control) to -12.8 mV after AF2, K_{slope} increased from 7.0 mV to 4.4 mV after AF2. **D:** Long-lasting potentiation of the % change of the peak transient inward current after AF2 application (paired t-test, n=12 preparations from separate worms, ** significance <0.01, * significance <0.05).

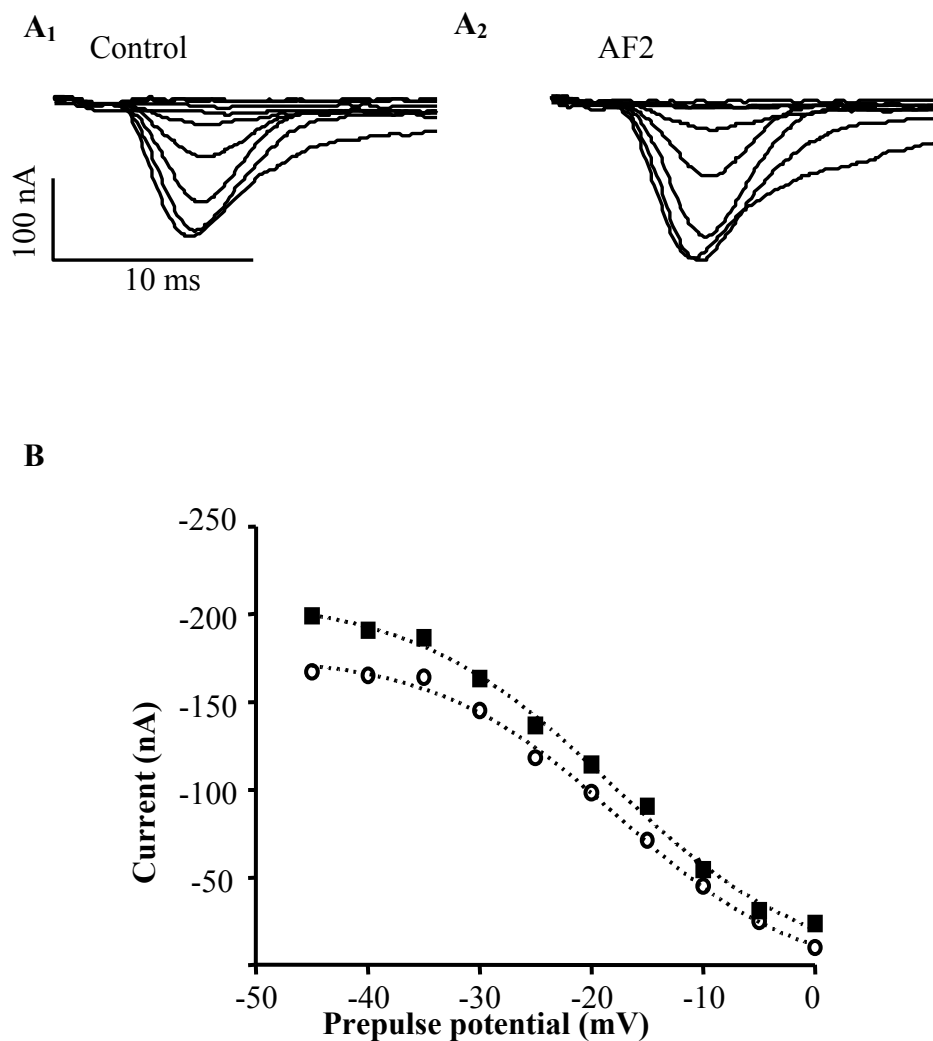


Figure 6. Effect of 1µM AF2 on the inactivation of the transient inward current. The transient inward currents were activated by a test pulse of 0 mV following 130 ms pre-pulses of 45 mV, -40 mV, -35 mV, -30 mV, -25 mV, -20 mV, -15 mV, -10 mV, -5 mV and 0 mV. **A1:** Shows the trace of control transient inward currents at 0 mV step potential after the pre-pulses. **A2:** Depicts the transient inward currents at 0mV step potential after the pre-pulses and following AF2 perfusion. **B:** Shows the plot of peak current against the pre-pulse potential the points were fitted to the inactivation curve as described by Boltzmann equation. (n = 6). ○: Control before AF2 I_{max} was -161.9 ± 3.4 nA; V_{50} was -16.8 ± 0.8 mV; K was 7.3 ± 0.7 mV; ■: After 1µM AF2. I_{max} was -189 ± 4 nA; V_{50} was -16 ± 1 mV; K_{slope} was 7.7 ± 0.8 mV. No significant changes

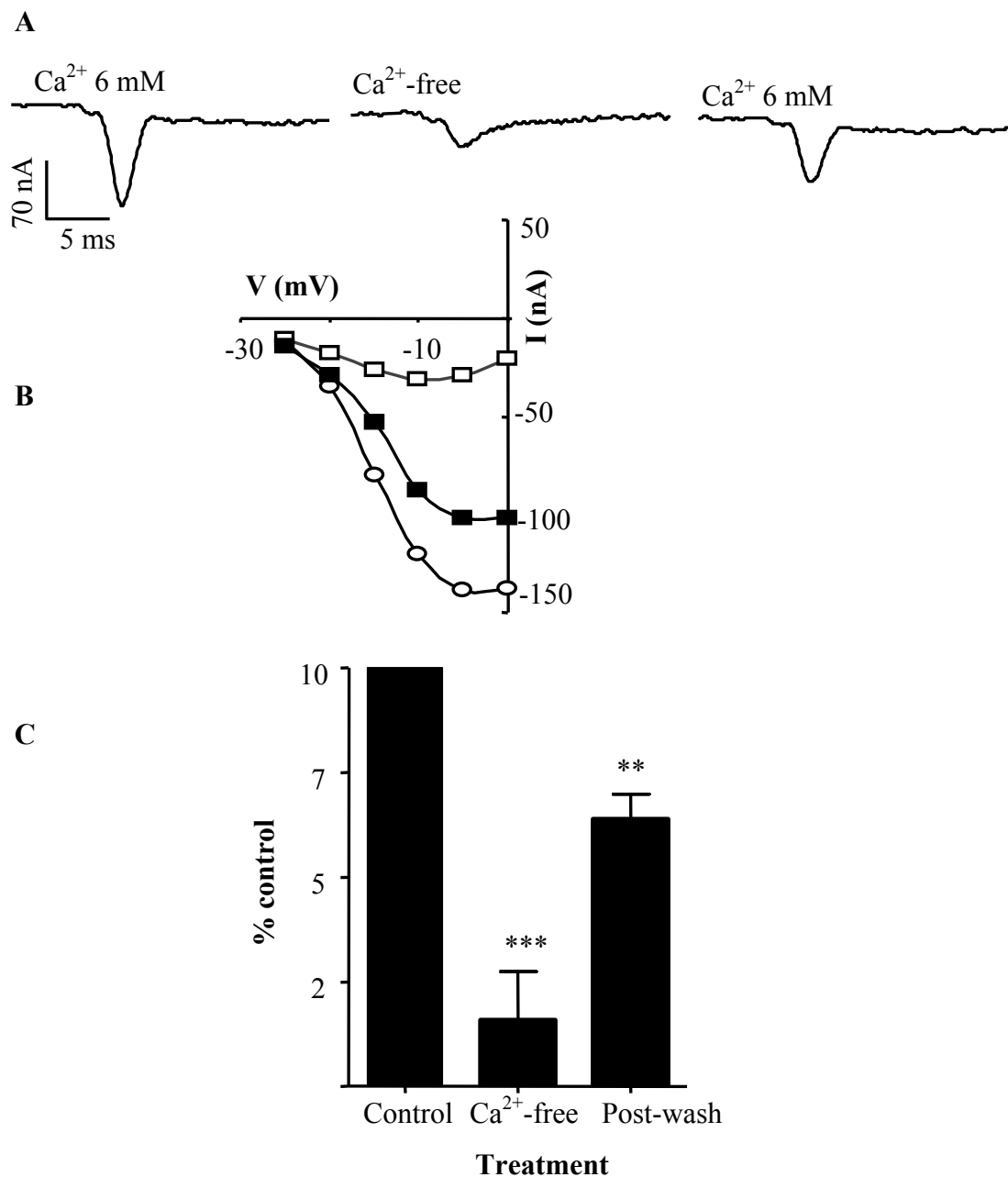


Figure 7. Calcium substitution decreases the amplitude of transient inward current.
A: Changes voltage-gated transient inward currents before and after calcium substitution.
B: current voltage relationship (I-V) plot from the same experiment. ○ Circles representing control (Calcium 6mM), □ Ca-free solution and ■ wash. **C:** Calcium substitution significantly suppressed the inward current and the effect was reversible (paired t-test, n = 6, p < 0.01).

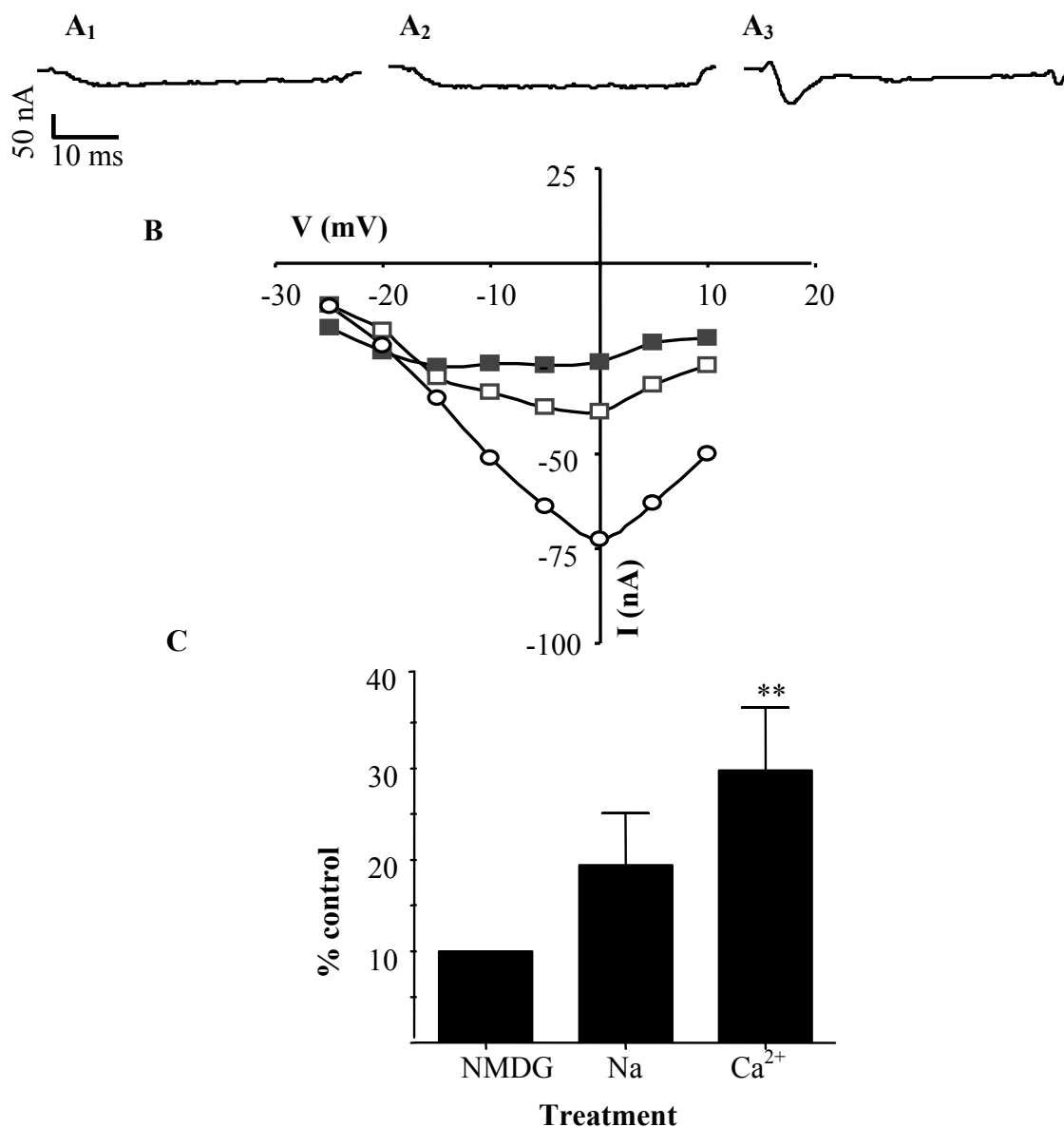


Figure 8. Effects of addition of sodium and calcium to NMDG bath solution. **A1:** Represent the trace of inward currents in the absence of sodium and calcium (NMDG Solution). **A2:** Represent the trace of inward currents in presence of sodium (sodium & calcium -free solution), same preparation. **A3:** Transient inward current in presence of calcium-Ringer, same preparation. Note that only calcium produced a transient inward current. All currents are at -5 mV voltage step. **B:** Current voltage relationships for the inward currents, ■ in absence of both sodium and calcium, □ in presence of Na, and ○ when both sodium and calcium present (APF). **C:** Percent change in the transient inward current with presence of calcium in the solution. The inward currents for NMDG were used for normalization for each preparation. Only the addition of Ca produced a significant increase in Normalized transient inward currents (paired t-test, $n=6$, $p<0.01$).

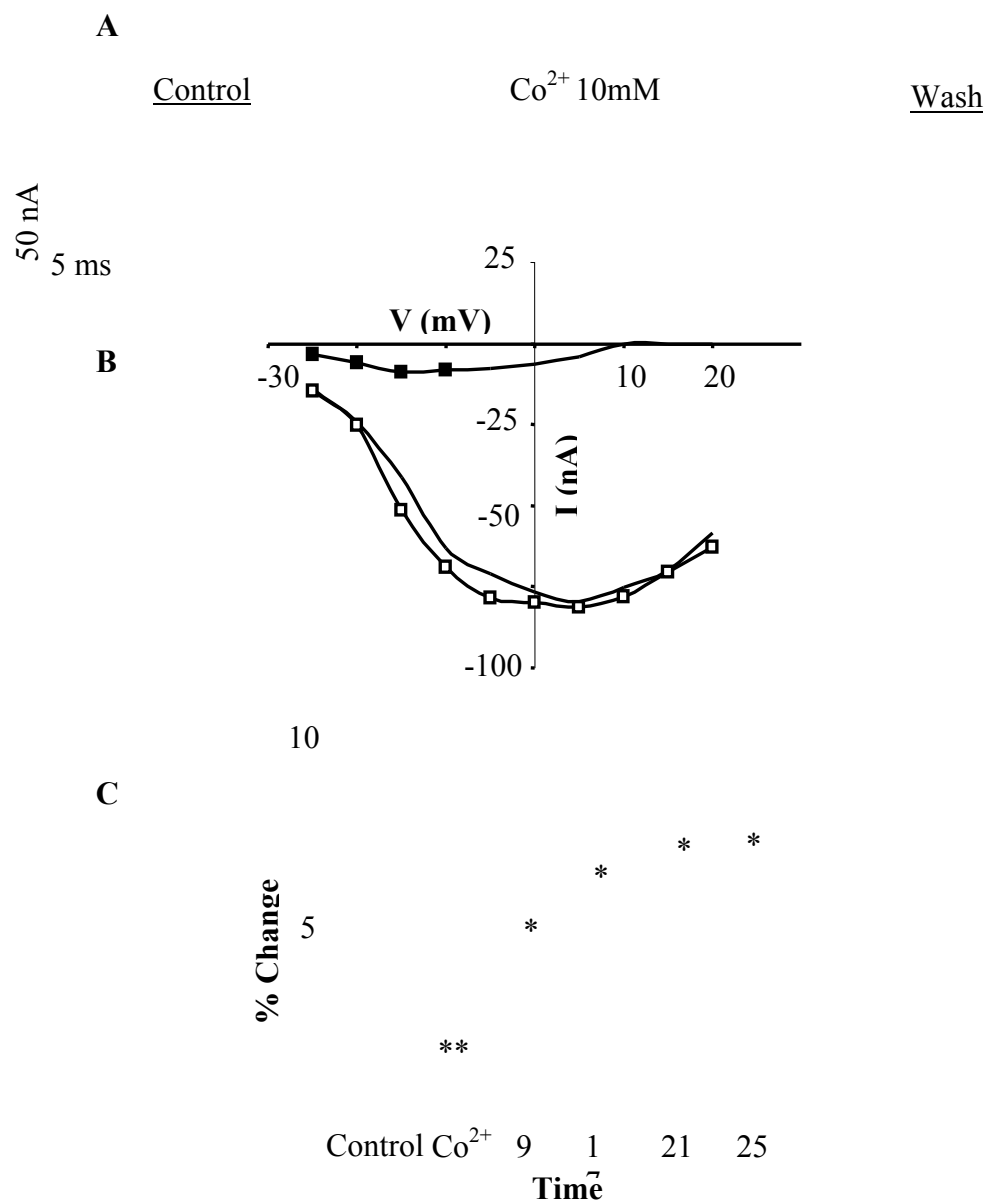


Figure 9. Cobalt blocked the transient inward currents. **A:** an experiment representing effect of cobalt on transient inward current at 0 mV. **B:** Current voltage relationships for the inward currents Control \square ; after 10 mM cobalt \blacksquare application and; \circ wash. **C:** Cobalt application significantly suppressed the peak transient inward currents (paired t-test, $n=7$, ** significance <0.01 , *** significance <0.001).

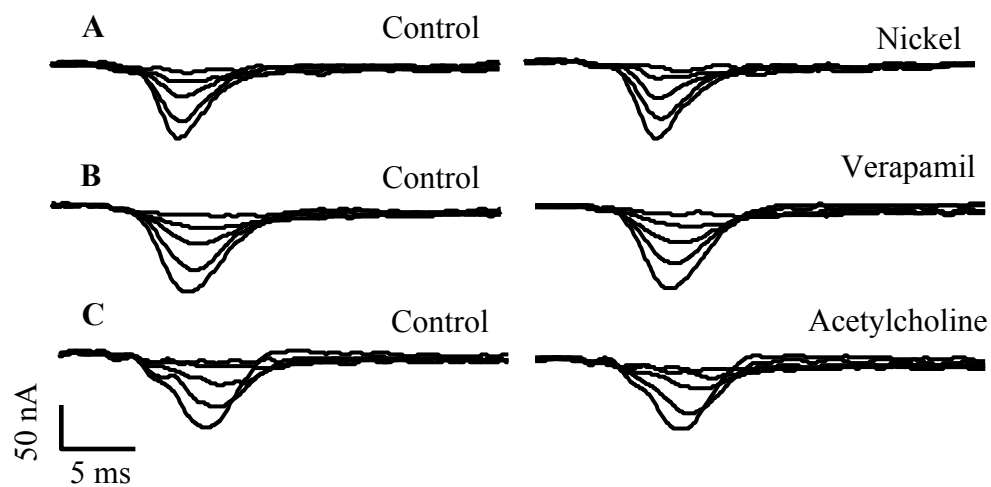


Figure 10. Lack of effect of nickel, verapamil and acetylcholine on transient inward current. Representative traces showing that application of **A:** Nickel ($30 \mu\text{M}$); **B:** Verapamil ($100 \mu\text{M}$), and; **C:** Acetylcholine (ACh $1 \mu\text{M}$) did not affect the transient inward current.

Chapter 4. Effects of SDPNLRF-amide (PF1) on voltage-activated currents in *Ascaris suum* muscle.

(Submitted for publication in *International Journal of Parasitology*)

S Verma, AP Robertson and RJ Martin

Department of Biomedical Science, Iowa State University, Ames, IA, 50010, USA

Key words: PF1; AF3; *Ascaris suum*; voltage-activated currents; calcium currents; potassium currents.

4.1 Abstract

Helminth infections are of significant concern in veterinary and human medicine. The drugs available for chemotherapy are limited in number and the extensive use of these drugs has led to the development of resistance in parasites of animals and humans (Geerts and Gryseels, 2000; Kaplan, 2004; Osei-Atweneboana et al., 2007). The cyclooctadepsipeptide, emodepside, belongs to a new class of anthelmintic that has been released for animal use in recent years. Emodepside has been proposed to mimic the effects of the neuropeptide PF1 on membrane hyperpolarization and membrane conductance (Willson et al., 2003). We investigated the effects of PF1 on voltage-activated currents in *A. suum* muscle cells. The whole cell voltage-clamp technique was employed to study these currents. Here we report two types of voltage-activated inward calcium currents: transient peak (I_{peak}) and a steady-state (I_{ss}). We found that 1 μ M PF1 inhibited the two calcium currents. The I_{peak} decreased from -146 nA to -99 nA ($p=0.0007$) and the I_{ss} decreased from -45 nA to -12 nA ($p=0.002$). We also found that PF1 in the presence of calcium increased the voltage-activated outward potassium current [from 521 nA to 628 nA ($p=0.004$)]. The effect

on the potassium current was abolished when calcium was removed and replaced with cobalt; it was also reduced at a higher concentration of PF1 (10 μ M). These studies demonstrate a mechanism by which PF1 decreases the excitability of the neuromuscular system by modulating calcium currents in nematodes. PF1 inhibits voltage-activated calcium currents and potentiates the voltage-activated calcium dependent potassium current. The effect on a calcium-activated-potassium channel appears to be common to both PF1 and emodepside (Guest et al., 2007). It will be of interest to investigate the actions of emodepside on calcium currents to further elucidate the mechanism of action.

4.2 Introduction

There is a group of 13 parasitic and bacterial infectious diseases listed as neglected tropical diseases in the Millennium Declaration of the United Nations (Hotez et al., 2007). Ascariasis is the most common parasitic infection in the list, with an estimated 807 million people infected and 4.2 billion people at risk (de Silva et al., 2003; Bethony et al., 2006). Helminth infections are also a welfare and economic concern in animals (Coles, 2001; Wolstenholme et al., 2004).

Chemotherapy is widely used to control these parasitic infections. The drugs available for chemotherapy are limited in number and the extensive use of these drugs has led to the development of resistance in parasites of animals and humans (Geerts and Gryseels, 2000; Kaplan, 2004; Osei-Atweneboana et al., 2007). The cyclooctadepsipeptide, emodepside, belongs to a new class of anthelmintic that has been released for animal use in recent years (Harder et al., 2003). Emodepside has

been proposed to mimic the effects of PF1 (Willson et al., 2003), an inhibitory FMRFamide like neuropeptide (FLP) in nematodes (McVeigh et al., 2006) .

FLP's have been isolated from both free living and parasitic nematodes (Geary et al., 1992; Geary et al., 1999; Husson et al., 2005; Li, 2005; McVeigh et al., 2006). There are more than 31 nematode *flp* genes that have been identified and found responsible for the synthesis of more than 90 FLP's (McVeigh et al., 2005). FLP's are associated with all the major neuronal systems in nematodes (Stretton et al., 1991; Brownlee et al., 1996; Brownlee and Walker, 1999; Geary and Kubiak, 2005). PF1 (SDPNFLRFamide) is a peptide that was originally isolated from an acetone extract of *Panagrellus redvivi* (Geary et al., 1992). PF1 has marked paralytic and hyperpolarizing effects on *A. suum* muscles (Franks et al., 1994; Bowman et al., 2002). Although PF1 has not been recovered from *A. suum*, Yew et al, (2005) have isolated related peptides with the C-terminal PNFLRFamide from *A. suum*. PF1 has been reported to antagonize the effects of acetylcholine and levamisole induced contractions (Franks et al., 1994; Geary et al., 1999). The effects of PF1 appear to be mediated by nitric oxide in *A. suum* (Bowman et al, 1995). The hyperpolarizing effect of PF1 is abolished by a combination of potassium channel antagonists and nitric oxide synthase (NOS) inhibitors. It has been shown that nematode NOS is partially dependent on calmodulin and completely dependent on calcium (Bowman et al., 1995; Bowman et al., 2002). These effects suggest a role for calcium for the mode of action of PF1.

Voltage-gated calcium channels play a major part in regulation of calcium entry from extracellular sources in nematodes (Jeziorski et al., 2000). Entry of

calcium through ion channels plays an important role in the physiological processes of contraction, secretion, synaptic transmission and signal transduction pathways (Catterall *et al.*, 2005). Voltage-gated calcium channels are modulated positively and negatively by G-protein coupled receptors in many species (Tedford and Zamponi, 2006) including neuropeptide receptors in *A. suum* (Verma *et al.*, 2007).

In this manuscript we investigate the effects of PF1 on voltage-activated calcium and potassium currents in *A. suum* muscle cells. We found that PF1 reduced peak and steady state inward calcium currents as well as increased voltage-activated potassium currents. These observations show that the inhibitory effects of PF1 also include effects on voltage-activated calcium currents. If PF1 does in fact mimic emodepside (Willson *et al.*, 2003), our observations suggest that emodepside will also affect voltage-activated calcium and potassium currents (Guest *et al.*, 2007).

4.3 Methods

Collection of worms

Adult *A. suum* were obtained weekly from the Tyson's pork packing plant at Storm Lake City, Iowa. Worms were maintained in Locke's solution [Composition (mM): NaCl 155, KCl 5, CaCl₂ 2, NaHCO₃ 1.5 and glucose 5] at a temperature of 32°C. The Locke's solution was changed daily and the worms were used within 4 days of collection.

Muscle preparation

1 cm muscle tissue flaps were prepared by dissecting the anterior part of the worm, 2-3 cm caudal to the head. A body muscle flap preparation was then pinned

onto a Sylgard™-lined 2 ml Petri-dish. The intestine was removed to expose the muscle cells (Trailovic, et al., 2005). The preparation was continuously perfused, unless otherwise stated, with APF-Ringer composition (mM): NaCl 23, Na-acetate 110, KCl 24, CaCl₂ 6, MgCl₂ 5, glucose 11, and HEPES 5; NaOH was used to adjust the pH to 7.6. To study inward currents calcium-Ringer solution was prepared by adding 4-aminopyridine (4-AP) (5mM) to APF-Ringer solution to reduce potassium currents and adjusting the pH to 7.6 by NaOH. The preparation was maintained in the experimental chamber at 34°C using a Warner heating collar [DH 35] and heating the incoming perfusate with a Warner instruments [SH 27B] in line heating system (Hamden, CT, USA). The perfusate was applied at 4-6 ml/min through a 19- gauge needle placed directly over the muscle bag recorded from. The calcium substitution experiments were conducted using cobalt-Ringer, composition (mM): NaCl 23, Na-acetate 110, KCl 24, CoCl₂ 6, MgCl₂ 5, glucose 11, HEPES 5 and 4-aminopyridine 5; NaOH was used to adjust the pH to 7.6. PF1 (1µM) and AF3 (1µM), were applied in APF-Ringer, calcium-Ringer or cobalt-Ringer as described in Results.

Electrophysiology

Two-micropipette voltage-clamp and current-clamp techniques were employed to examine the electrophysiological effects in the *A. suum* muscle bag region (Fig.1A). Borosilicate capillary glass (Harvard Apparatus, Holliston, MA, USA) micropipettes were pulled on a Flaming Brown Micropipette puller (Sutter Instrument Co., Novato, CA, USA) and filled with 3 M potassium acetate or a mixture of 1.5 M potassium acetate and 1.5 M cesium acetate. The cesium acetate was included in the pipette solution to block outward potassium currents when recording calcium

currents. Current-clamp micropipettes and the voltage-sensing micropipettes for voltage-clamp had a resistance of 20-30 M Ω ; the current-injecting micropipette for voltage-clamp had a resistance of 3-4 M Ω . The recordings were obtained by impaling the bag region of the *A. suum* muscle with both micropipettes. All experiments were performed using an Axoclamp 2B amplifier, a 1320A Digidata interface and pClamp 8.2 software (Molecular Devices, Sunnyvale, CA). All data were displayed and analyzed on a Pentium IV based desktop computer.

Current-clamp experiments were performed by injecting a hyperpolarizing pulse of 40 nA for 500 ms at 0.30 Hz through the current-injecting micropipette and the voltage sensing micropipette recorded the change in membrane potential (Fig.1B). Each set of experiments were repeated on preparations from separate worms to get the desired number of observations.

For voltage-clamp, we kept the resistance of the current-injecting micropipette low (3-4 M Ω) and the amplifier gain high (>100). The phase lag was set to 1.5 ms in all the experiments to limit oscillation. In addition, muscles closer to the nerve cord were selected for experimental study, as these were spherical cells with short arms which help to keep the space clamp effective. Muscle cells close to the nerve cord were also found to possess consistently bigger calcium currents.

For activation of calcium currents, muscle cells were held at -35mV during the voltage-clamp experiments and stepped through a series of voltage-steps of 5mV each: to -25 mV, -20 mV, -15 mV, -10 mV, -5 mV, 0 mV, +5 mV, +10 mV, +15 mV, and +20 mV (Fig. 1C) and lasted 40 ms. The currents displayed were leak-subtracted, by steps 1/10th of the test step with opposite polarity, using pClamp 8.2

software. The inward calcium currents were recorded at the peak (I_{peak}) of the currents and the steady state currents were recorded as an average at 25, 30 and 35 ms. Potassium currents were recorded as an average of the current values at 20, 35 and 40 ms for +20 mV voltage step in the plateau phase.

Drugs were applied initially under current-clamp before effects on voltage-activated currents were tested under voltage-clamp. Cells with uniform membrane potentials more negative than -25 mV over a period of 40 minutes and resting conductance of less than 2.5 μ S over the course of an experiment were selected for the voltage-clamp and current-clamp studies.

We used linear regression and extrapolation to estimate the reversal potential for different experiments. Then we calculated conductance changes from the inward currents and driving forces ($E_{rev} - V$) to obtain the activation curve (Verma, et al., 2007). The activation curve was then fitted by the Boltzmann equation.

Drugs

PF1 (SDPNFLRFamide) and AF3 (AVPGVLRamide) [98% purity, EZBiolab, Westfield, IN] 10 mM stock solutions were prepared in double distilled water every week and kept in Ependorf tubes at -12 °C. PF1 and AF3, stock solutions were thawed just before use to make up the 1 μ M or 10 μ M working solutions. All other chemicals were obtained from Sigma-Aldrich, St. Louis, MO.

Statistical Analysis

Currents were plotted against the step potential to determine current-voltage relationships. All the statistical analysis was done using Graph Pad Prism software (version 4.0, San Diego, CA, USA). Paired *t*-tests were employed to test the

statistical significance of the change in current responses in control and test recordings; significance levels were set at $p < 0.05$.

4.4 Results

Hyperpolarizing effect of PF1

Fig. 2A, shows a typical recording of the effects of PF1 on membrane potential and input conductance; in this cell the resting membrane potential was -32 mV and input conductance was 2.3 μS . Application of 1 μM PF1 produced a hyperpolarization of 5 mV and conductance increase of 0.1 μS . The effect did not wash off within 25 minutes.

Similar results were obtained in a total of 7 preparations. Fig. 2B summarizes the effects on membrane potential. The effect of 1 μM PF1 on membrane potential was statistically significant and the mean hyperpolarization was $5.0 \pm 0.8\text{mV}$ ($p = 0.004$). When we applied a higher concentration of PF1 (10 μM), the mean hyperpolarizing effect on membrane potential $6.2 \pm 0.7\text{ mV}$ ($n=6$).

Previous studies (Maule et al., 1995; Walker et al., 2000) have suggested that PF1 mediates its effects on membrane potential via a potassium conductance. We tested the effects of a high concentration of 4-AP. We found, Fig. 2B, that 5 mM 4-AP reduced but did not abolish the effects of 1 μM PF1 on membrane potential: $3.0 \pm 0.4\text{ mV}$ ($p= 0.01$, $n=11$). 4-aminopyridine however, does not block all types of potassium channels in *A. suum* (Martin et al, 1992). In order to further investigate the effects of PF1 we pursued our investigation of effects of PF1 on voltage-activated currents using voltage-clamp.

Effects of PF1 on voltage-activated potassium and calcium currents

Fig. 3A shows currents activated by voltage-steps from the holding potential of -35 mV to 0 mV and +20 mV. The step-potential of 0 mV (Fig. 3A) shows activation of the transient calcium current, I_{peak} (Verma et al., 2007). The step potential to +20 mV (Fig. 3A) shows activation of the outward potassium current, I_O (Thorn and Martin, 1987).

1 μ M PF1 produced an effect on the currents that increased slowly over a period of 10 minutes. In the representative recording, Fig. 3A, PF1 increased the potassium current from 241 nA to 310 nA and the calcium transient current decreased from -100 nA to -72 nA. Despite 20 minutes of continuous wash, the potassium current continued to increase to 445 nA but in contrast, the calcium transient current (I_{peak}) returned towards control values, -84 nA after 20 mins.

Fig 3B shows the effect of PF1 on the current-voltage plot of the potassium currents. Fig. 3C shows the effect of PF1 on the current-voltage plot of calcium transient currents. Notice again that the effect on the potassium currents is not reversed on washing but the effect on the calcium current is partially reversed on washing. This difference in wash-out suggests different regulation of the two currents. Fig. 3D & E summarizes the time-dependent effects on the potassium currents and the calcium currents in 6 different preparations. It can be seen by comparing Fig. 3D & E that the percentage increase in the potassium currents for the 6 recordings after 8 minutes application of PF1, $14 \pm 4 \%$ ($p=0.02$, $n=6$), was smaller than the percentage decrease of the calcium currents, $38 \pm 17 \%$ ($p=0.001$, $n=6$). We can also see that during the wash period the potassium current continues

to increase; but the decrease in the calcium currents is not maintained. Thus, we observed the effects of PF1 on the two currents and the effect on the calcium currents was proportionately bigger than on the potassium currents.

Effect of PF1 on transient inward and steady-state currents

Because there was a larger percentage effect on the calcium currents, we decided to investigate effects of PF1 on calcium currents in isolation. We did this by using cesium in the recording electrodes and 4-AP in the bath solution to block outward potassium currents (Verma *et al.*, 2007).

Fig. 4A is a representative recording showing the calcium current at -5 mV. The current is characterized by the presence of a transient peak (I_{peak}) and a steady-state component (I_{ss}). Fig 4A also shows effects of 1 μ M PF1 on these two components. The I_{peak} decreased from -132 nA to -112 nA and the I_{ss} decreased from -48 nA to -24 nA. Fig. 4B & C show effects of 1 μ M PF1 on the current voltage plots from the same experiment. Note that maximum I_{peak} is seen at 0 mV whereas the maximum I_{ss} is seen at +5 mV suggesting they are two distinct currents. Also notice in the I-V plot that proportionately, PF1 has a bigger effect on I_{ss} than on I_{peak} . Similar observations were made in 10 other experiments. Fig. 4D shows that the decrease for I_{peak} was $35 \pm 6\%$ ($p=0.001$, $n=10$). Fig. 4E shows that the decrease in the I_{ss} was $66 \pm 6\%$ ($p<0.001$, $n=10$). Despite a long period of washing for more than 20 minutes, we found that the effects of PF1 were not completely reversible.

Effect of PF1 in the presence of cobalt on the outward voltage-activated potassium current

We have seen effects of PF1 on isolated calcium currents. Our next step was to examine effects of PF1 on the potassium currents isolated from the calcium currents. To accomplish this we bathed the preparation in solutions where extracellular calcium was replaced by cobalt.

Fig 5A shows representative traces of the effect of PF1 on the potassium current. In this particular experiment, the current plateau slightly increased from 901 nA to 947 nA after PF1 application. Fig 5B shows the current-voltage plots from this experiment. Fig 5C shows a bar chart of peak outward currents obtained from 6 preparations before, during and at 20 min post-wash following PF1 application. It is evident that the increase produced by PF1 does not reach statistical significance in the absence of calcium. This is in contrast with the significant increase seen in the presence of calcium, Fig.3.

Effects of high concentrations of PF1 on calcium and potassium currents

We also investigated the effect of higher concentrations of PF1 on the calcium and potassium currents. In order to look at effects on these currents we again used APF-Ringer (calcium present but lacks 4-AP). Fig. 6A, shows a representative trace of the effects of 10 μ M PF1. PF1 produced an inhibitory effect on the I_{peak} calcium current: at -5 mV, the current decreased from -70 nA to -46 nA. The I_{peak} currents continued to decrease to -41 nA throughout the 20-minute post-wash period. The current voltage plot, Fig 6C shows the effect of PF1 on the I_{peak}

calcium currents. The calcium currents consistently failed to return towards control levels when this higher concentration of PF1 was used, Fig. 6E.

The effect of 10 μ M PF1 on the potassium current was small, Fig. 6B & D. The average increase in potassium currents for the 5 recordings after 9 minutes was 3 ± 2 % ($p=0.2$, $n=5$) this contrasts with the more dramatic decrease in the calcium current which averaged 40 ± 11 % ($p=0.003$, $n=5$), Fig. 6D & E. Thus 10 μ M PF1 compared to 1 μ M PF1 produced a smaller increase in the potassium current but a bigger decrease in calcium current (I_{peak}).

AF3 reverses the effects of PF1 on calcium currents

Fig. 7 shows a summary of the effects of 1 μ M AF3 on voltage-activated inward currents. Fig. 7A shows a representative trace of effects on currents activated at -5 mV. I_{peak} increased from -113 nA in the control to -158 nA after AF3 application. The I_{ss} increased from -22 nA to -39 nA. Fig. 7B & C shows current-voltage plots for I_{peak} and I_{ss} : notice that the peaks of these plots occur near ~ 0 mV for I_{peak} and $\sim +5$ mV for I_{ss} . When the percentage increases were averaged over 9 preparations, it was clear that the biggest effect was on the steady-state current. The average potentiation was 21 ± 7 % ($p=0.03$) for I_{peak} and the average potentiation for I_{ss} was 48 ± 8 % ($p=0.0003$). The effects of AF3 washed off gradually over a period of 20 minutes.

We described earlier the inhibitory effects of PF1 on calcium currents and how they failed to reverse on washing. In order to test the maintained viability of the preparation we followed application of PF1 with application of AF3, Fig. 8. We found

that AF3 reversed the inhibitory effects of PF1 on I_{peak} and I_{ss} . Fig 8A shows a representative recording, at -5 mV, of the effects of PF1 on the control calcium currents and its reversal by AF3. The effects on the current voltage plots of I_{peak} and I_{ss} are shown in Fig. 8B & C.

Fig. 8D & E summarizes the effects of PF1 and then AF3 application on I_{peak} and I_{ss} . The average decrease in I_{peak} from 5 experiments after application of PF1 was $26 \pm 7 \%$ ($p=0.02$) which recovered to $89 \pm 6\%$ ($p=0.0005$) after AF3 application. These effects were statistically significant. The average decrease in I_{ss} after PF1 application was $60 \pm 10 \%$ ($p=0.001$) which recovered to $104 \pm 28 \%$ ($p=0.04$) after AF3 application.

Fig. 9A & B shows the activation curves for the experiment shown in Fig. 8. The activation curve was obtained using the Boltzmann equation:

$$G = G_{max} / \{1 + \exp [(V_{50} - V) / K_{Slope}]\}$$

Where G is the conductance change, G_{max} is the maximum conductance change, V_{50} is the half maximum step-voltage, V is the step voltage and K_{Slope} is the slope factor. Fig. 9A represents the activation curve for I_{peak} currents. The control activation curve had a G_{max} of $3.6 \pm 0.04 \mu\text{S}$; V_{50} of $-20.8 \pm 1.5 \text{ mV}$ and K_{Slope} of 3.2 ± 0.6 . During PF1 application, G_{max} was $3.0 \pm 0.05 \mu\text{S}$; V_{50} was $-19 \pm 0.8 \text{ mV}$ and K_{Slope} was 3.04 ± 0.5 . Following AF3, G_{max} was $4.9 \pm 0.03 \mu\text{S}$; V_{50} was $-25.6 \pm 0.5 \text{ mV}$ and K_{Slope} was 4.7 ± 1.1 .

Fig. 9B is the activation curve for I_{ss} currents. The control activation curve had a G_{max} of $4.2 \pm 0.06 \mu\text{S}$; V_{50} was $-0.7 \pm 0.2 \text{ mV}$ and K_{Slope} was 3 ± 0.2 . During PF1 application, G_{max} was $2.9 \pm 0.1 \mu\text{S}$; V_{50} was $-0.9 \pm 0.4 \text{ mV}$ and K_{Slope} was 3.1 ± 0.3 .

Following AF3, G_{max} was $6.4 \pm 0.1 \mu\text{S}$; V_{50} was $-4.4 \pm 0.3 \text{ mV}$ and K_{Slope} was 3.8 ± 0.3 . For 4 averaged recordings the effect of PF1 and AF3 on G_{max} of I_{ss} was statistically significant, Table 1 & Fig. 9D. The effect of AF3 but not PF1 on G_{max} of I_{peak} was statistically significant, Table 1 & Fig. 9C. The effect of PF1 and AF3 on V_{50} of I_{peak} but not the V_{50} of I_{ss} was statistically significant, Table 1. The effect of PF1 on G_{max} of I_{ss} but the lack of effect on G_{max} of I_{peak} suggests that the two currents are separate with different kinetic properties.

4.5 Discussion

PF1 mechanism of action

PF1 was first recovered and identified from *P. redivivus* (Geary et al., 1992) and then from *C. elegans* (Rosoff et al., 1992). In *A. suum* four PNFLRFamides (AQDPNFL/IRFamide, ATDPNFL/IRFamide, APKPNFL/IRFamide and ENEKKAVPGVLTRFamide) have been proposed (Yew et al, 2005). 100 nM – 100 μM PF1 produces a long lasting flaccid paralysis of *A. suum* body-wall muscle strips and a 3 mV hyperpolarization (Franks et al., 1994; Bowman et al., 1995; Maule et al., 1995). The hyperpolarization is independent of extracellular chloride and is blocked by a combination of potassium channel antagonists and NOS inhibitors: 4-AP, tetra-ethyl-ammonium (TEA) and 7-nitroindazole (Bowman et al., 2002). During an investigation of the effects of PF1, Bowman et al., (1995) noted the complete dependence of *A. suum* NOS activity on calcium. Bowman et al., (2002) suggested that a possible explanation for the requirement for a combination of 4-AP, TEA and 7-nitroindazole to block PF1 hyperpolarizations is that PF1 opens a calcium channel in the nematode muscle membrane which activates the calcium sensitive NOS; the

NO produced gates a membrane potassium channel to cause the hyperpolarization and relaxation.

In our studies we examined the effects of PF1 on voltage-activated calcium currents. However, we found that the PF1 did not increase the calcium currents but actually inhibited them (Fig. 4). We also found that PF1, in the presence of calcium, increased the voltage-activated potassium current (Fig. 3). Interestingly, the effect on the voltage-activated potassium current was abolished when calcium was removed and replaced with cobalt and was reduced at a higher concentration of PF1 (Fig. 5 & 6). Our observations support the requirement for the presence of calcium for effects of PF1. Fig. 10 is a summary diagram of the effects of PF1 on the calcium and potassium currents.

Two type of calcium currents A. suum

The presence of voltage-activated calcium currents has been demonstrated in *A. suum* muscle cells (Martin et al., 1992; Verma et al., 2007). Here we have investigated the effects of the neuropeptides, PF1 and AF3, on transient (I_{peak}) and steady-state (I_{ss}) calcium currents. In *C. elegans*, several genes coding for calcium channels have been identified. There are low voltage-activated channels [CCA-1; T-type, Shtonda et al., (2005)] and high voltage-activated channels [UNC-2; R-type; Schafer et al., (1995) and EGL-19; L-type; Jospin et al., (2002)]. Different classes of calcium channels have not been genetically identified in *A. suum*.

I_{peak} in *A. suum* is most like (Verma et al., 2007) *C. elegans* UNC-2 type currents (Schafer et al., 1995); they are activated by potentials – 30 to + 30 mV and

inactivated in the 50-80 ms range. Verma et al., (2007) demonstrated that AF2, an excitatory neuropeptide, produces an increase in the I_{peak} current. Removal of calcium and addition of cobalt abolishes the I_{peak} in *A. suum* muscles, indicating that calcium is the major charge carrier of this current.

egl-19 encodes the L-type calcium channel in pharynx and body wall muscles in *C. elegans* (Lee et al., 1997). L-type calcium currents in *C. elegans* have a fast and a slow component but the components are not pharmacologically separate (Jospin et al., 2002). The I_{ss} current in *A. suum* is similar to the L-type calcium current as it has a high voltage threshold for activation (peaks $\sim +5$ mV) and is long lasting in nature (~ 30 ms). The I_{ss} current is abolished by cobalt and the absence of calcium, consistent with calcium being the major charge carrier.

Effects of AF3

The neuropeptide AF3 was first recovered from *A. suum* by Cowden et al., (1995) and found to stimulate contraction of *A. suum* muscle strips (Trim et al., 1997). We used AF3 to study voltage-activated currents and found that it increased I_{peak} and I_{ss} calcium currents. Previous investigations of the action of AF3 have demonstrated that it exerts a depolarizing effect which is blocked by cobalt (Trim et al., 1997; Brownlee and Walker, 1999), an action consistent with our observations on the voltage-activated calcium currents. We exploited the stimulatory effects of AF3 on the calcium currents to counter the actions of PF1 which are not otherwise easily reversed on washing (Franks et al., 1994). Our concern was to confirm that the calcium currents had not declined because of failing viability of the preparation. It

is interesting to note that AF3 had its biggest percentage effect on the I_{ss} but the neuropeptide AF2 has its biggest effect on the I_{peak} (Verma et al., 2007). The different actions by these two neuropeptides, on I_{peak} and I_{ss} , imply that they can be modulated separately and that the two currents have separate origins and physiological functions. It is possible that I_{ss} currents are similar to *C.elegans* EGL-19 L-type calcium currents that have been found in body wall, enteric, egg laying and pharyngeal muscles (Lee et al., 1997; Jospin et al., 2002). EGL-19 has been demonstrated to maintain the plateau phase of action potentials of pharyngeal muscles (Shtonda and Avery, 2005). The UNC-2 type calcium currents in *C. elegans* have similarities to the I_{peak} current and are associated with neurotransmitter release and calcium dependent action potentials in pharyngeal muscles (Schafer and Kenyon, 1995; Mathews et al., 2003). We do however caution, that we have not conclusively separated the I_{peak} and I_{ss} calcium currents in *A. suum* and there is a possibility that the two currents are due to the same channel with different levels of inactivation as described by Dick et al., (2008).

Emodepside and PF1

Emodepside, a semisynthetic derivative of PF1022A, is a novel cyclo-octadepsipeptide anthelmintic (Harder et al., 2003; von Samson-Himmelstjerna et al., 2005). Emodepside has potent paralytic effects on *A. suum* body wall muscles (Willson et al., 2003) and has a wide range of effects on *C. elegans* inhibiting development, locomotion, egg laying and feeding (Bull et al., 2007).

Martin et al., (1996) demonstrated that PF1022A does not produce its effect on *A. suum* muscles by mimicking the inhibitory neurotransmitter GABA or by antagonizing nicotinic receptors. It has been demonstrated that the parent compound PF1022A, interacts with latrophilin receptors (Saeger et al., 2001). The latrophilin receptors are G-protein coupled receptors involved in the regulation of transmitter release from dense core vesicles (Davletov et al., 1998). It has been suggested that emodepside induces latrophilin mediated release of transmitters by a pathway that involves UNC-13 dependent vesicle priming in *C. elegans* (Willson et al., 2004).

Another proposed mechanism of action of emodepside has been to mimic the effects of PF1 or to induce the release of PF1 (Willson et al., 2003). Both PF1 and emodepside produce relaxation, slow hyperpolarization and a small change in input conductance of *A. suum* muscle cells (Bowman et al., 2002; Willson et al., 2003). It has also been shown that the effects of PF1 in *A. suum* muscles are calcium dependent (Franks et al., 1994; Bowman et al., 1995) as are the effects of emodepside (Harder et al., 2003). Potassium channel blockers reduce hyperpolarization induced by both PF1 and emodepside (Harder et al., 2003).

We found that the PF1 did not increase the voltage-activated calcium currents but inhibited them. Our observations also demonstrated the importance of entry of calcium for an effect on voltage-activated potassium currents. Fig. 10 is a summary diagram showing the actions of PF1: PF1 cannot stimulate the potassium channel unless sufficient calcium is present in the cell. At high concentrations of PF1, calcium entry may be so reduced, preventing the effect of PF1 on the potassium currents. We have shown that PF1 inhibits voltage-activated calcium currents and

potentiates voltage-activated potassium currents. The action of emodepside in *C. elegans* has been shown to depend upon the SLO-1 pathway. SLO-1 is a calcium-activated-potassium channel (Guest et al., 2007). The effect on a calcium-activated-potassium channel appears to be common to both PF1 and emodepside. It will be of interest to investigate the actions of emodepside on calcium currents to further elucidate the mechanism of action of emodepside.

4.6 Acknowledgment

The project was supported by Grant Number R 01 AI 047194 from the national Institute of Allergy and Infectious Diseases. The content is solely the responsibility of the authors and does not necessarily represent the official views of the National Institute of Allergy and Infectious diseases of the National Institutes of Health.

4.7 Reference:

- Thorn, P., Martin, R.J., 1987. A high-conductance calcium-dependent chloride channel in *Ascaris suum* muscle. *Q J Exp Physiol* 72, 31-49.
- Bethony, J., Brooker, S., Albonico, M., Geiger, S.M., Loukas, A., Diemert, D., Hotez, P.J., 2006. Soil-transmitted helminth infections: ascariasis, trichuriasis, and hookworm. *Lancet* 367, 1521-1532.
- Bowman, J.W., Winterrowd, C.A., Friedman, A.R., Thompson, D.P., Klein, R.D., Davis, J.P., Maule, A.G., Blair, K.L., Geary, T.G., 1995. Nitric oxide mediates the inhibitory effects of SDPNFLRFamide, a nematode FMRFamide-related neuropeptide, in *Ascaris suum*. *J Neurophysiol* 74, 1880-1888.
- Bowman, J.W., Friedman, A.R., Thompson, D.P., Maule, A.G., Alexander-Bowman, S.J., Geary, T.G., 2002. Structure-activity relationships of an inhibitory nematode FMRFamide-related peptide, SDPNFLRFamide (PF1), on *Ascaris suum* muscle. *Int J Parasitol* 32, 1765-1771.
- Brownlee, D.J., Fairweather, I., Holden-Dye, L., Walker, R.J., 1996. Nematode neuropeptides: Localization, isolation and functions. *Parasitol Today* 12, 343-351.
- Brownlee, D.J., Walker, R.J., 1999. Actions of nematode FMRFamide-related peptides on the pharyngeal muscle of the parasitic nematode, *Ascaris suum*. *Ann N Y Acad Sci* 897, 228-238.

- Bull, K., Cook, A., Hopper, N.A., Harder, A., Holden-Dye, L., Walker, R.J., 2007. Effects of the novel anthelmintic emodepside on the locomotion, egg-laying behaviour and development of *Caenorhabditis elegans*. *Int J Parasitol* 37, 627-636.
- Catterall, W.A., Perez-Reyes, E., Snutch, T.P., Striessnig, J., 2005. International Union of Pharmacology. XLVIII. Nomenclature and structure-function relationships of voltage-gated calcium channels. *Pharmacol Rev* 57, 411-425.
- Coles, G.C., 2001. The future of veterinary parasitology. *Vet Parasitol* 98, 31-39.
- Davletov, B.A., Meunier, F.A., Ashton, A.C., Matsushita, H., Hirst, W.D., Lelianova, V.G., Wilkin, G.P., Dolly, J.O., Ushkaryov, Y.A., 1998. Vesicle exocytosis stimulated by alpha-latrotoxin is mediated by latrophilin and requires both external and stored Ca²⁺. *EMBO J* 17, 3909-3920.
- de Silva, N.R., Brooker, S., Hotez, P.J., Montresor, A., Engels, D., Savioli, L., 2003. Soil-transmitted helminth infections: updating the global picture. *Trends Parasitol* 19, 547-551.
- Dick, I.E., Tadross, M.R., Liang, H., Tay, L.H., Yang, W., Yue, D.T., 2008. A modular switch for spatial Ca²⁺ selectivity in the calmodulin regulation of CaV channels. *Nature* 451, 830-834.
- Franks, C.J., Holden-Dye, L., Williams, R.G., Pang, F.Y., Walker, R.J., 1994. A nematode FMRFamide-like peptide, SDPNFLRFamide (PF1), relaxes the dorsal muscle strip preparation of *Ascaris suum*. *Parasitology* 108 (Pt 2), 229-236.
- Geary, T.G., Price, D.A., Bowman, J.W., Winterrowd, C.A., Mackenzie, C.D., Garrison, R.D., Williams, J.F., Friedman, A.R., 1992. Two FMRFamide-like peptides from the free-living nematode *Panagrellus redivivus*. *Peptides* 13, 209-214.
- Geary, T.G., Marks, N.J., Maule, A.G., Bowman, J.W., Alexander-Bowman, S.J., Day, T.A., Larsen, M.J., Kubiak, T.M., Davis, J.P., Thompson, D.P., 1999. Pharmacology of FMRFamide-related peptides in helminths. *Ann N Y Acad Sci* 897, 212-227.
- Geary, T.G., Kubiak, T.M., 2005. Neuropeptide G-protein-coupled receptors, their cognate ligands and behavior in *Caenorhabditis elegans*. *Trends Pharmacol Sci* 26, 56-58.
- Geerts, S., Gryseels, B., 2000. Drug resistance in human helminths: current situation and lessons from livestock. *Clin Microbiol Rev* 13, 207-222.
- Guest, M., Bull, K., Walker, R.J., Amliwala, K., O'Connor, V., Harder, A., Holden-Dye, L., Hopper, N.A., 2007. The calcium-activated potassium channel, SLO-1, is required for the action of the novel cyclo-octadepsipeptide anthelmintic, emodepside, in *Caenorhabditis elegans*. *Int J Parasitol* 37, 1577-1588.
- Harder, A., Schmitt-Wrede, H.P., Krucken, J., Marinovski, P., Wunderlich, F., Willson, J., Amliwala, K., Holden-Dye, L., Walker, R., 2003. Cyclooctadepsipeptides--an anthelmintically active class of compounds exhibiting a novel mode of action. *Int J Antimicrob Agents* 22, 318-331.
- Hotez, P.J., Molyneux, D.H., Fenwick, A., Kumaresan, J., Sachs, S.E., Sachs, J.D., Savioli, L., 2007. Control of neglected tropical diseases. *N Engl J Med* 357, 1018-1027.

- Husson, S.J., Clynen, E., Baggerman, G., De Loof, A., Schoofs, L., 2005. Discovering neuropeptides in *Caenorhabditis elegans* by two dimensional liquid chromatography and mass spectrometry. *Biochem Biophys Res Commun* 335, 76-86.
- Jeziorski, M.C., Greenberg, R.M., Anderson, P.A., 2000. The molecular biology of invertebrate voltage-gated Ca(2+) channels. *J Exp Biol* 203, 841-856.
- Jospin, M., Jacquemond, V., Mariol, M.C., Segalat, L., Allard, B., 2002. The L-type voltage-dependent Ca²⁺ channel EGL-19 controls body wall muscle function in *Caenorhabditis elegans*. *J Cell Biol* 159, 337-348.
- Kaplan, R.M., 2004. Drug resistance in nematodes of veterinary importance: a status report. *Trends Parasitol* 20, 477-481.
- Lee, R.Y., Lobel, L., Hengartner, M., Horvitz, H.R., Avery, L., 1997. Mutations in the alpha1 subunit of an L-type voltage-activated Ca²⁺ channel cause myotonia in *Caenorhabditis elegans*. *Embo J* 16, 6066-6076.
- Li, C., 2005. The ever-expanding neuropeptide gene families in the nematode *Caenorhabditis elegans*. *Parasitology* 131 Suppl, S109-127.
- Martin, R.J., Thorn, P., Gratton, K.A., Harrow, I.D., 1992. Voltage-activated currents in somatic muscle of the nematode parasite *Ascaris suum*. *J Exp Biol* 173, 75-90.
- Mathews, E.A., Garcia, E., Santi, C.M., Mullen, G.P., Thacker, C., Moerman, D.G., Snutch, T.P., 2003. Critical residues of the *Caenorhabditis elegans* unc-2 voltage-gated calcium channel that affect behavioral and physiological properties. *J Neurosci* 23, 6537-6545.
- Maule, A.G., Geary, T.G., Bowman, J.W., Marks, N.J., Blair, K.L., Halton, D.W., Shaw, C., Thompson, D.P., 1995. Inhibitory effects of nematode FMRFamide-related peptides (FaRPs) on muscle strips from *Ascaris suum*. *Invert Neurosci* 1, 255-265.
- McVeigh, P., Leech, S., Mair, G.R., Marks, N.J., Geary, T.G., Maule, A.G., 2005. Analysis of FMRFamide-like peptide (FLP) diversity in phylum Nematoda. *Int J Parasitol* 35, 1043-1060.
- McVeigh, P., Geary, T.G., Marks, N.J., Maule, A.G., 2006. The FLP-side of nematodes. *Trends Parasitol* 22, 385-396.
- Osei-Atweneboana, M.Y., Eng, J.K., Boakye, D.A., Gyapong, J.O., Prichard, R.K., 2007. Prevalence and intensity of *Onchocerca volvulus* infection and efficacy of ivermectin in endemic communities in Ghana: a two-phase epidemiological study. *Lancet* 369, 2021-2029.
- Prasad, A.S., Sandstead, H.H., Schulert, A.R., El-Rooby, A.S., 1963. Urinary Excretion of Zinc in Patients with the Syndrome of Anemia, Hepatosplenomegaly, Dwarfism, and Hypogonadism. *J Lab Clin Med* 62, 591-599.
- Rosoff, M.L., Burglin, T.R., Li, C., 1992. Alternatively spliced transcripts of the flp-1 gene encode distinct FMRFamide-like peptides in *Caenorhabditis elegans*. *J Neurosci* 12, 2356-2361.
- Saeger, B., Schmitt-Wrede, H.P., Dehnhardt, M., Benten, W.P., Krucken, J., Harder, A., Von Samson-Himmelstjerna, G., Wiegand, H., Wunderlich, F., 2001. Latrophilin-like receptor from the parasitic nematode *Haemonchus contortus*

- as target for the anthelmintic depsipeptide PF1022A. *FASEB J* 15, 1332-1334.
- Schafer, W.R., Kenyon, C.J., 1995. A calcium-channel homologue required for adaptation to dopamine and serotonin in *Caenorhabditis elegans*. *Nature* 375, 73-78.
- Shtonda, B., Avery, L., 2005. CCA-1, EGL-19 and EXP-2 currents shape action potentials in the *Caenorhabditis elegans* pharynx. *J Exp Biol* 208, 2177-2190.
- Stretton, A.O., Cowden, C., Sithigorngul, P., Davis, R.E., 1991. Neuropeptides in the nematode *Ascaris suum*. *Parasitology* 102 Suppl, S107-116.
- Tedford, H.W., Zamponi, G.W., 2006. Direct G protein modulation of Cav2 calcium channels. *Pharmacol Rev* 58, 837-862.
- Trim, N., Holden-Dye, L., Ruddell, R., Walker, R.J., 1997. The effects of the peptides AF3 (AVPGVLRFamide) and AF4 (GDVPGVLRFamide) on the somatic muscle of the parasitic nematodes *Ascaris suum* and *Ascaridia galli*. *Parasitology* 115 (Pt 2), 213-222.
- Verma, S., Robertson, A.P., Martin, R.J., 2007. The nematode neuropeptide, AF2 (KHEYLRN-NH₂), increases voltage-activated calcium currents in *Ascaris suum* muscle. *Br J Pharmacol* 151, 888-899.
- von Samson-Himmelstjerna, G., Harder, A., Sangster, N.C., Coles, G.C., 2005. Efficacy of two cyclooctadepsipeptides, PF1022A and emodepside, against anthelmintic-resistant nematodes in sheep and cattle. *Parasitology* 130, 343-347.
- Walker, R.J., Franks, C.J., Pemberton, D., Rogers, C., Holden-Dye, L., 2000. Physiological and pharmacological studies on nematodes. *Acta Biol Hung* 51, 379-394.
- Willson, J., Amliwala, K., Harder, A., Holden-Dye, L., Walker, R.J., 2003. The effect of the anthelmintic emodepside at the neuromuscular junction of the parasitic nematode *Ascaris suum*. *Parasitology* 126, 79-86.
- Willson, J., Amliwala, K., Davis, A., Cook, A., Cuttle, M.F., Kriek, N., Hopper, N.A., O'Connor, V., Harder, A., Walker, R.J., Holden-Dye, L., 2004. Latrotoxin receptor signaling engages the UNC-13-dependent vesicle-priming pathway in *C. elegans*. *Curr Biol* 14, 1374-1379.
- Wolstenholme, A.J., Fairweather, I., Prichard, R., von Samson-Himmelstjerna, G., Sangster, N.C., 2004. Drug resistance in veterinary helminths. *Trends Parasitol* 20, 469-476.
- Yew, J.Y., Kutz, K.K., Dikler, S., Messinger, L., Li, L., Stretton, A.O., 2005. Mass spectrometric map of neuropeptide expression in *Ascaris suum*. *J Comp Neurol* 488, 396-413.

4.8 Legends

Figure 1. A: Diagram of the location of two micropipettes for making current-clamp and voltage-clamp recordings from bag region of *Ascaris suum* somatic muscle. The current-injecting pipette and the voltage-sensing pipette are shown

B: Current-clamp recording showing, 40nA, 0.5 sec, current pulses (upper trace) inducing change in membrane potential (lower trace).

C: Voltage-clamp recording showing depolarizing step-voltage from a holding potential of -35mV to 0 mV (upper trace) producing a current response (leak subtracted lower trace). Note the presence of the voltage-activated transient inward current (I_{peak}) and a sustained inward current (I_{ss}).

Figure 2. Effect of PF1 under current-clamp.

A: Representative trace showing change in membrane potential record of somatic muscle cells in current clamp before, during and after application of PF1 (1 μ M).

B: Shows a bar chart of the mean \pm S.E.M. membrane potential responses observed from different preparations. There was a significant hyperpolarization after PF1 application in all experimental conditions; the comparisons were made between the membrane potential before and after application of PF1 under different conditions. The comparison to responses between different conditions was not significant. PF1 (1 μ M, n=6) -5.0 ± 0.8 mV; PF1 (10 μ M, n=6) -6.25 ± 0.7 mV; PF1 (1 μ M, n=5) in the presence of cobalt (6mM) -6.4 ± 1.0 mV and PF1 (1 μ M, n=10) in presence of 4-AP (5mM) -3.2 ± 0.4 mV, respectively. (paired t-test, ** $p \leq 0.01$, * $p \leq 0.05$).

Figure 3. Effect of PF1 on voltage-activated currents.

A: Representative traces showing voltage-activated currents in control, during PF1 (1 μ M) application and post-wash. Two currents observed outward potassium currents (O) and transient inward calcium current (I_{peak}). Note the increase in the plateau of outward current and the decrease in the I_{peak} current. (APF-Ringer no calcium or potassium channel block).

B: Current-voltage plot of the mean potassium current before, during and after PF1 (1 μ M) application. Control: \square . PF1 (1 μ M): \bullet . Post-wash: \circ .

C: Current-voltage plot of the calcium transient inward current (I) before, during and after PF1 (1 μ M) application. Control: \square . PF1 (1 μ M): \bullet . Post-wash: \circ .

D: Long-lasting potentiation of the mean (O) potassium current before, during and after PF1 (1 μ M) application (paired t-test, n=6, ** $p \leq 0.01$, * $p \leq 0.05$).

E: Inhibition of the peak calcium transient inward current (I_{peak}) before, during and after PF1 (1 μ M) application (paired t-test, n=6, ** $p \leq 0.01$, * $p \leq 0.05$).

Figure 4. Effect of PF1 on voltage-activated calcium currents.

A: Voltage-activated inward currents, control and during the application of PF1 (1 μ M) (red); peak inward currents (I_{peak}) and steady state current (I_{ss}). Note decrease in the I_{peak} and the I_{ss} currents. Recordings were made in calcium-Ringer solution with cesium acetate in recording micropipettes.


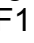

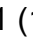
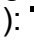

- B:** Current-voltage plot of the I_{peak} before, during and after PF1 (1 μ M) application. Control: . PF1 (1 μ M): . Post-wash: .
- C:** Current-voltage plot of I_{ss} before, during and after PF1 (1 μ M) application. Control: . PF1 (1 μ M): . Post-wash: .
- D:** Inhibition of the I_{peak} current during and after PF1 (1 μ M) application (paired t-test, $n=10$, ** $p \leq 0.01$, * $p \leq 0.05$).
- E:** Long-lasting inhibition of the mean I_{ss} current during and after PF1 (1 μ M) application (paired t-test, $n=9$, ** $p \leq 0.01$, * $p \leq 0.05$).

Figure 5. Lack of effect of PF1 (1 μ M) in presence of cobalt.

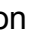


- A:** Representative traces showing the effect of PF1 (1 μ M) on voltage-activated outward currents in cobalt-APF. There was no change in the voltage-activated (outward) potassium currents during and after PF1 application. Recordings were made in cobalt-Ringer solution no potassium channel blockers.
- B:** Current-voltage plot of the mean (O) potassium currents before, during and after application of PF1 (1 μ M). Control: . PF1 (1 μ M): . Post-wash: .
- C:** There was no change in mean potassium current during and after PF1 (1 μ M) application in presence of cobalt (paired t-test, $n=6$, ** $p \leq 0.01$, * $p \leq 0.05$).

Figure 6. Effect of higher concentration of PF1.


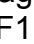



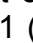






- A:** Representative traces showing voltage-activated currents; mean potassium currents (O); peak inward currents (I_{peak}). Voltage-activated currents: control, during PF1 (10 μ M) application and post-wash. Note the increase in the peak outward current and the decrease in the I_{peak} . Recordings were made in APF-Ringer.
- B:** Current-voltage plot of the mean potassium currents (O) during and after application of PF1 (10 μ M). Control: . PF1 (10 μ M): . Post-wash: .
- C:** Current-voltage plot of the I_{peak} currents during and after application of PF1 (10 μ M). Control: . PF1 (10 μ M): . Post-wash: . The biggest effect is on the I_{peak} current.
- D:** No significant potentiation of the mean (O) potassium current during and after PF1 (10 μ M) application
- E:** Significant inhibition of the I_{peak} current after PF1 (10 μ M) application (paired t-test, $n=5$, ** $p \leq 0.01$, * $p \leq 0.05$).





Figure 7. Effect of AF3 on voltage-activated inward currents.





- A:** Voltage-gated transient-inward currents recorded before and 9 minutes after AF3 application. Note the increase in the amplitude of the I_{peak} and the I_{ss} current. Recordings were made in calcium-Ringer solution with cesium acetate in recording micropipettes.
- B:** I_{peak} current-voltage relationship for the experiment shown in **A**. Control: . AF3 (1 μ M): . Post-wash: .
- C:** I_{ss} current-voltage relationship for the experiment shown in **A**. Control: . AF3 (1 μ M): . Post-wash: .
- D:** Potentiation of the I_{peak} current after AF3 (1 μ M) application (paired t-test, $n=9$, ** $p \leq 0.01$, * $p \leq 0.05$).

E: Long lasting potentiation of the I_{ss} current after AF3 application (paired t-test, n=9, ** $p \leq 0.01$, * $p \leq 0.05$).

Figure 8. AF3 triggers the recovery of PF1-inhibited currents.

A: Voltage-activated inward currents records: control; PF1 (1 μ M) (red) and; AF3 (1 μ M). Note the decrease in amplitude of the I_{peak} and the I_{ss} currents after PF1 application and recovery of currents after AF3 application. Recordings were made in calcium-Ringer solution with cesium acetate in recording micropipettes.


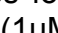
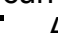
B: I_{peak} current step-voltage relationship for the experiment shown in **A**. Control: . PF1 (1 μ M): . AF3 (1 μ M): . Post-wash: .


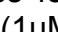
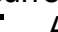
C: I_{ss} current step-voltage relationship for the experiment shown in **A**. Control: . PF1 (1 μ M): . AF3 (1 μ M): . Post-wash: .

D: Inhibition of the I_{peak} current after PF1 and recovery after AF3 application (paired t-test, n=5, ** $p \leq 0.01$, * $p \leq 0.05$).

E: Inhibition of the I_{ss} current after PF1 application and recovery after AF3 application. Note that AF3 potentiated the I_{ss} current (paired t-test, n=5, ** $p \leq 0.01$, * $p \leq 0.05$).

Figure 9. Activation curves for I_{peak} & I_{ss} .

A: Activation curves for I_{peak} currents before and during application of PF1 & AF3. Control: . PF1 (1 μ M): . AF3 (1 μ M): .

B: Activation curves for I_{ss} currents before and during application of PF1 & AF3. Control: . PF1 (1 μ M): . AF3 (1 μ M): .

C: Change in G_{max} of I_{peak} currents after AF3 application.

D: Change in G_{max} of I_{ss} currents after AF3 application.

Figure 10. Summary diagram of the effects of PF1 and AF3 on voltage-activated currents. PF1 inhibits the opening of voltage-activated calcium channels (I_{peak} & I_{ss}) and stimulates opening of potassium channels (K) but only in the presence of calcium. AF3 stimulates opening of voltage-activated calcium channels (I_{peak} & I_{ss}). Calcium is required to allow the inhibitory effect of PF1 on potassium currents. If sufficient calcium is not present (for example due to the presence of cobalt in the bathing solution or if a high concentration of PF1 is used inhibiting the voltage activated currents) the effect of PF1 on voltage-activated potassium current is prevented.

4.9 Figures

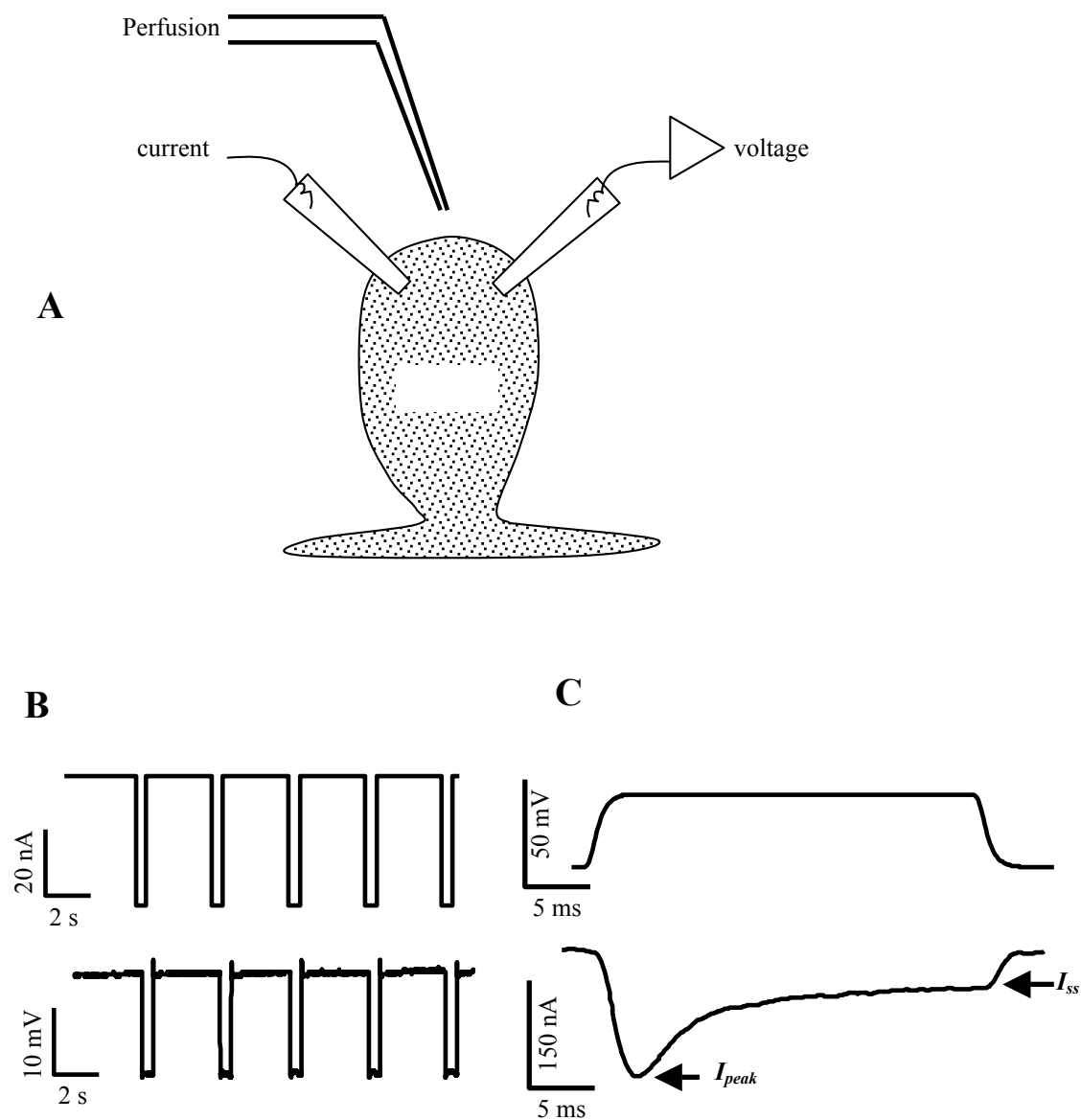


Figure 1. A: Diagram of the location of two micropipettes for making current-clamp and voltage-clamp recordings from bag region of *Ascaris suum* somatic muscle. The current-injecting pipette and the voltage-sensing pipette are shown

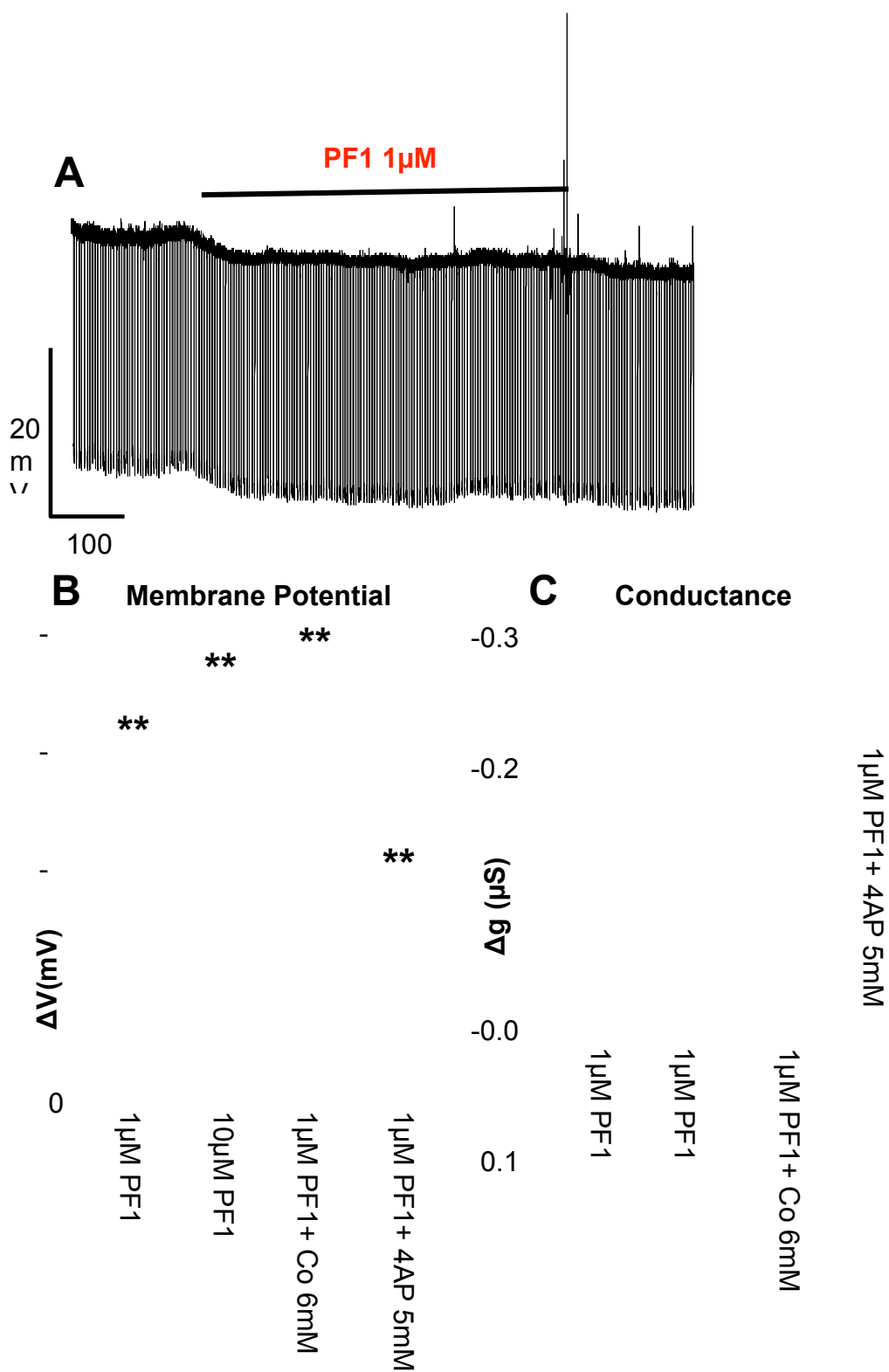


Figure 2. Effect of PF1 under current-clamp.

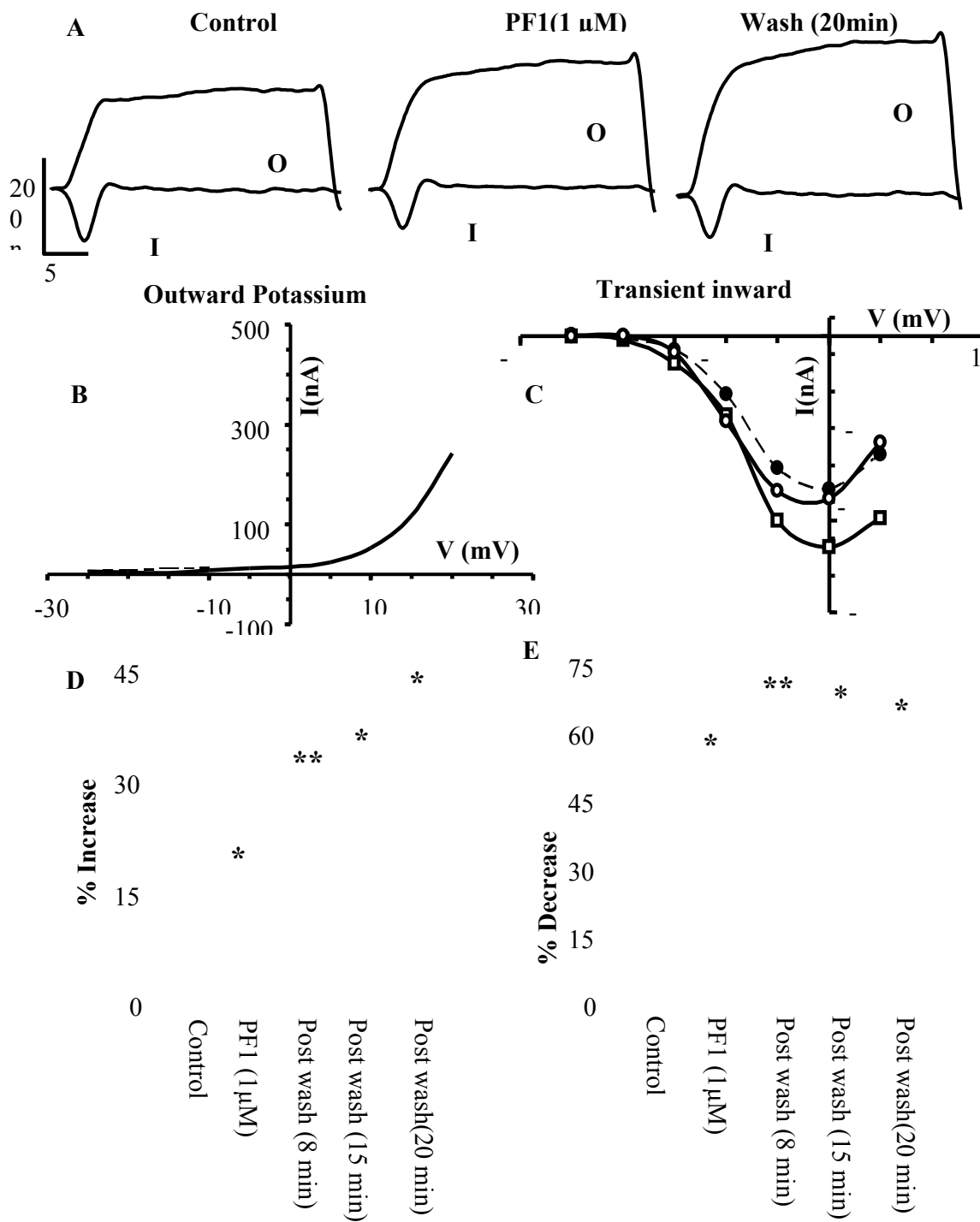


Figure 3. Effect of PF1 on voltage-activated currents.

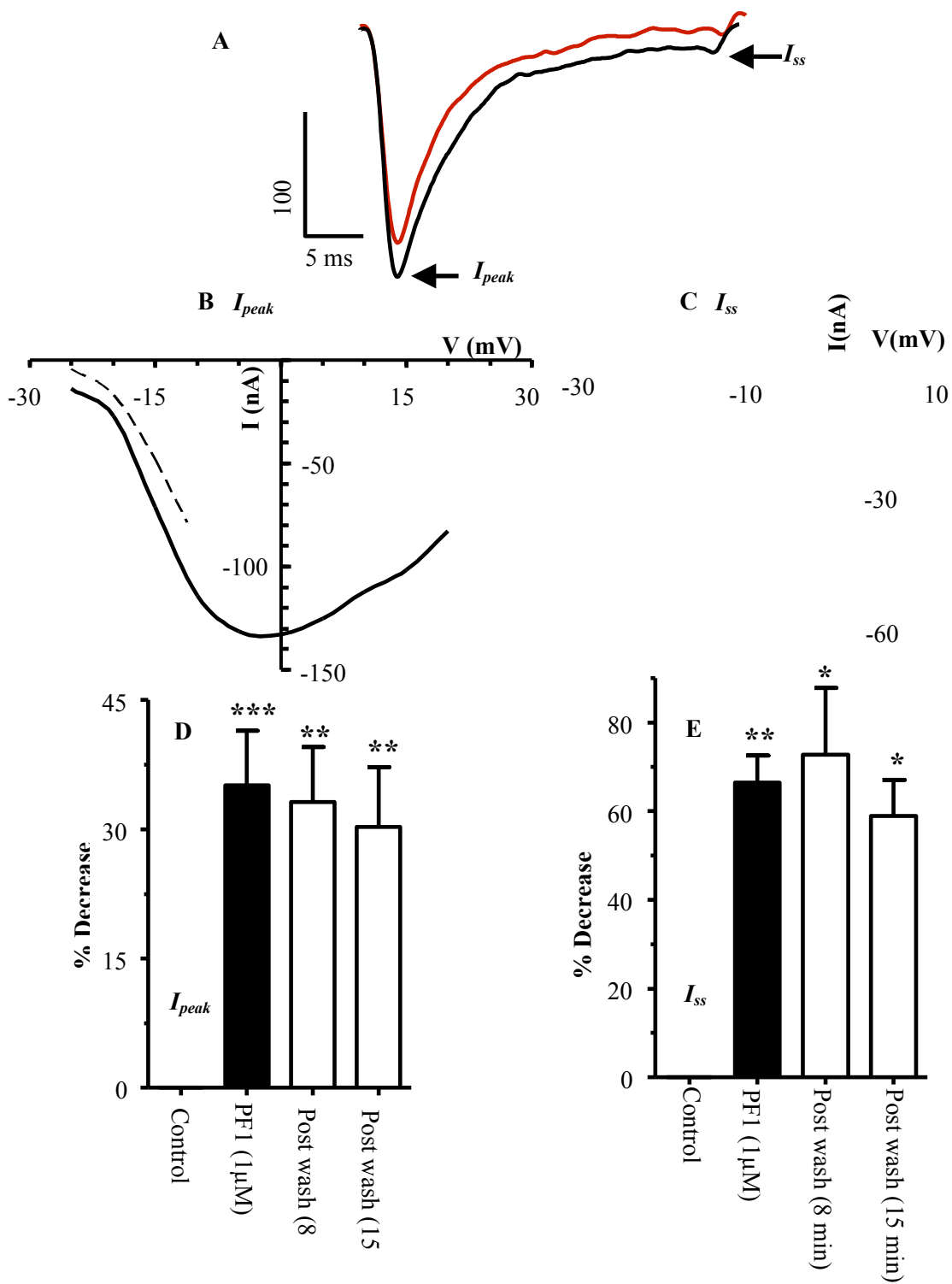


Figure 4. Effect of PF1 on voltage-activated calcium currents.

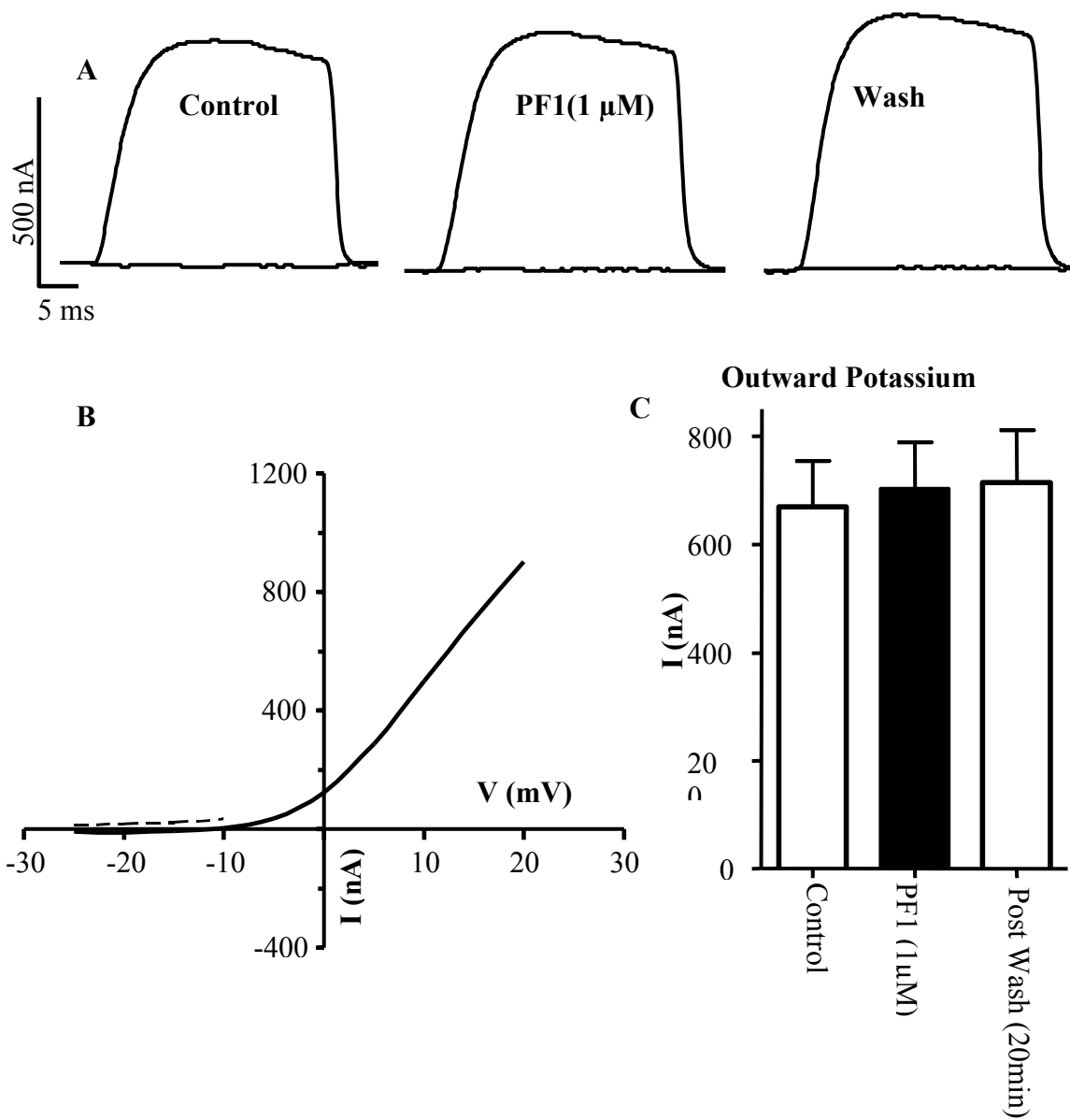


Figure 5. Lack of effect of PF1 (1 μ M) in presence of cobalt.

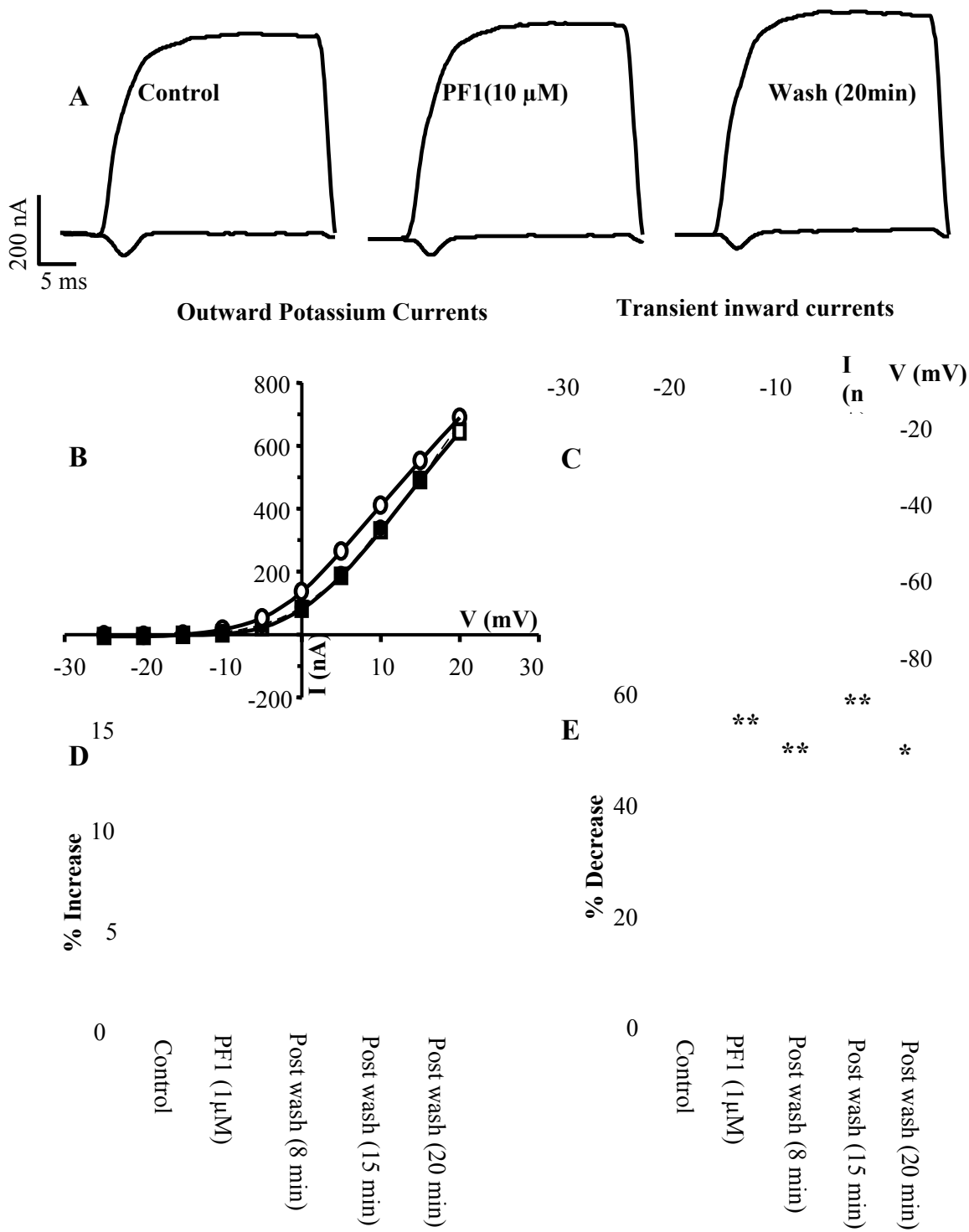


Figure 6. Effect of higher concentration of PF1.

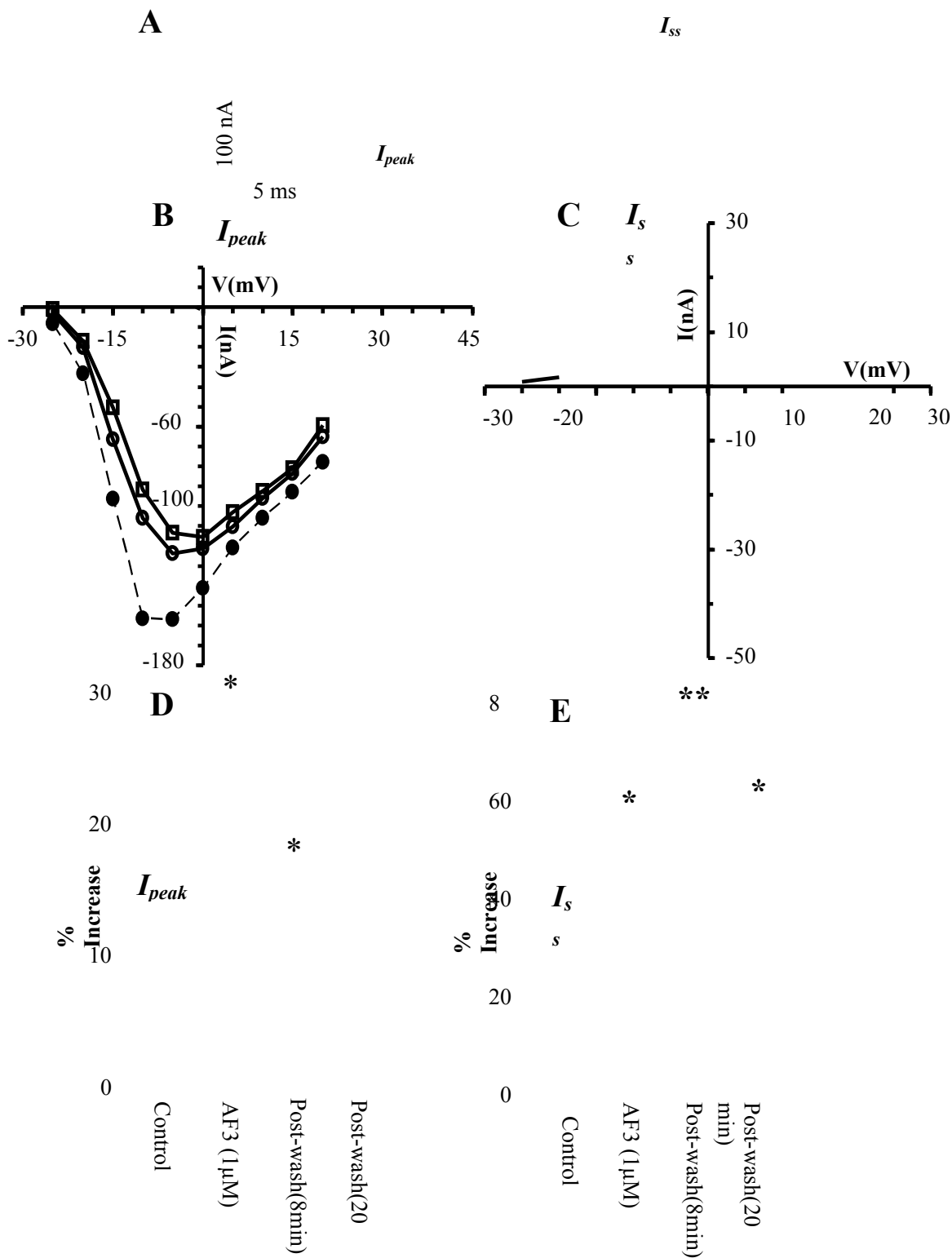


Figure 7. Effect of AF3 on voltage-activated inward currents.

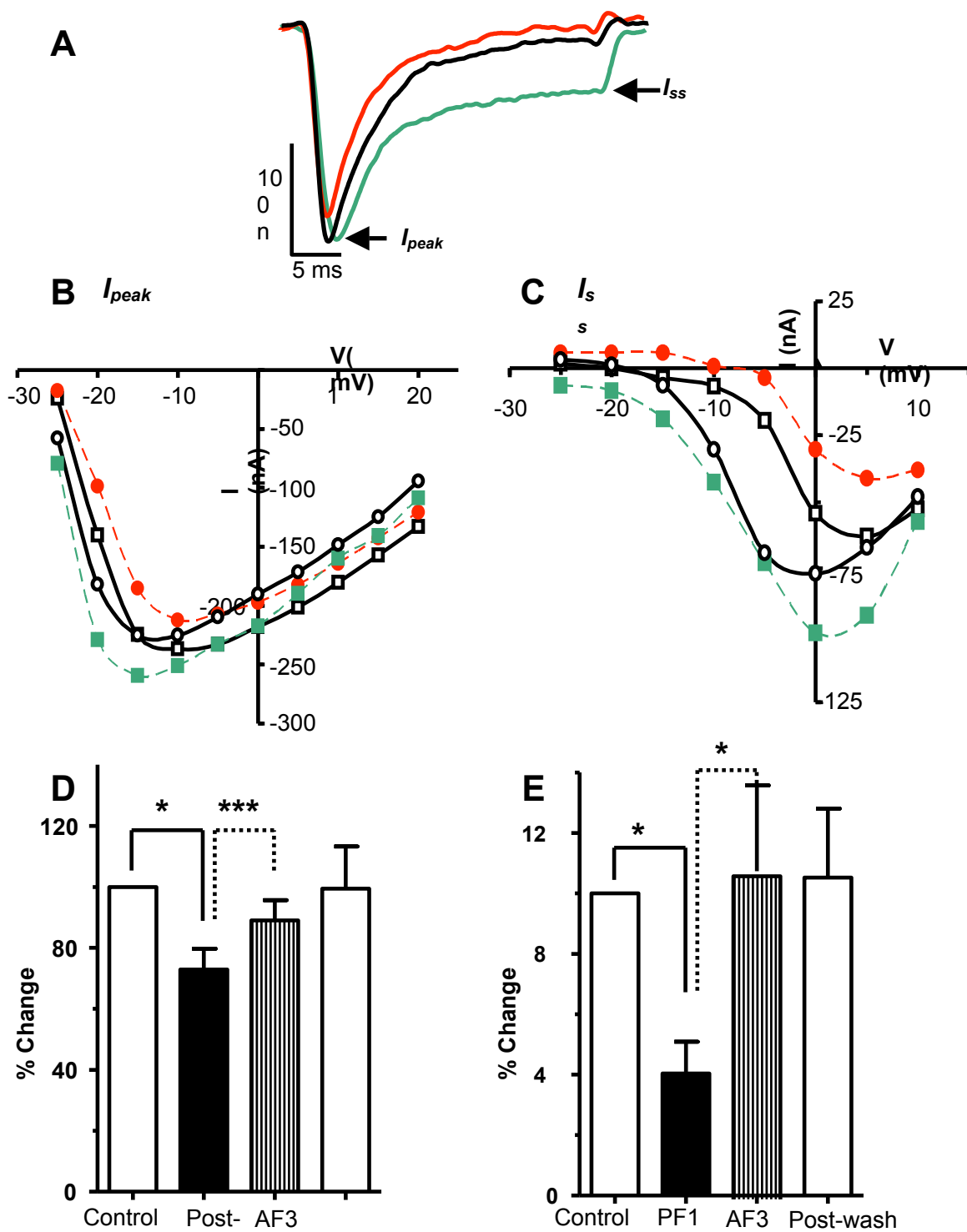


Figure 8. AF3 leads to recovery of currents inhibited by PF1.

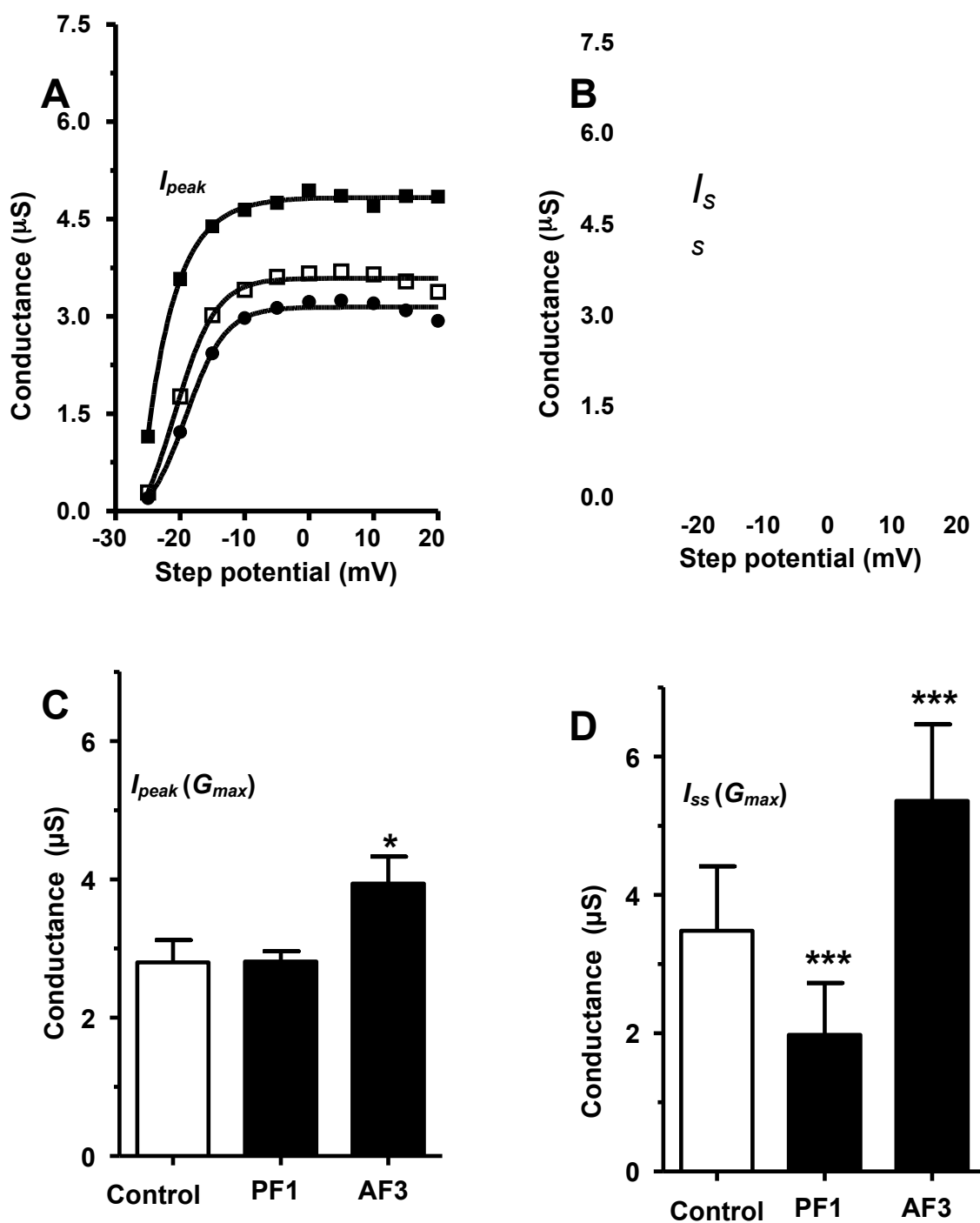


Figure 9. Activation curves for I_{peak} & I_{ss} .

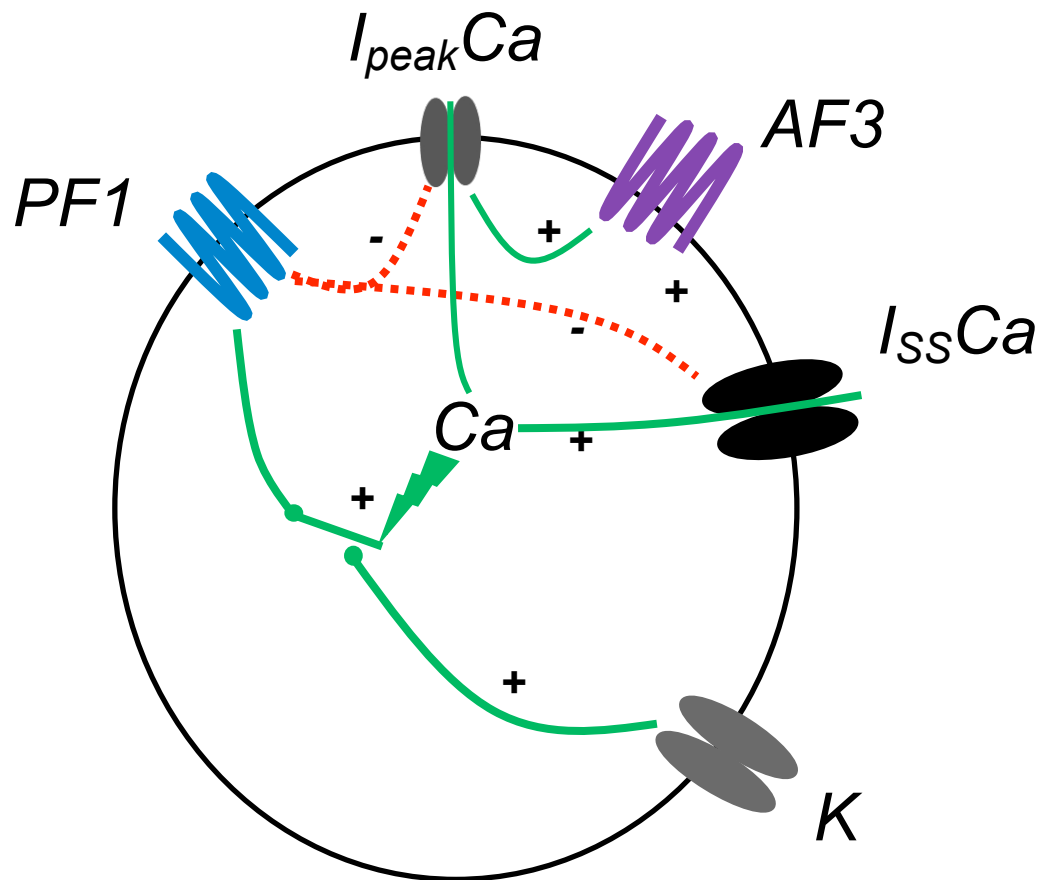


Figure 10. Summary of the effects of PF1 and AF3 on voltage-activated currents.

	Peak current			Steady-state current		
	Control	PF1	AF3	Control	PF1	AF3
<i>G</i>max (μS)	2.8 ± 0.3	2.8 ± 0.2	3.9 ± 0.4*	3.5 ± 0.9	2 ± 0.8***	5.4 ± 1.1***
<i>V</i>50 (mV)	-17 ± 1.7	-15 ± 1.9*	-21 ± 1.4*	-2.5 ± 2.6	-0.82 ± 1.9	-2.2 ± 2.7
<i>K</i>slope (mV)	3.5 ± 0.3	4.2 ± 0.5	4.3 ± 0.9	3.5 ± 0.7	2.4 ± 0.5*	4.4 ± 1.1*

Table. 1. Average values of the activation curves for *I* peak and *I*ss calcium currents fitted by Boltzmann equation (n=4 preparations from separate worms, *** p ≤ 0.005; ** p ≤ 0.01; * p ≤ 0.05). These averages are for the experiments where AF3 was used to trigger the recovery of PF1 inhibited calcium-currents (n=5).

**Chapter 5. Effects of the muscarinic agonist,
5-methylfurmethiodide, on contraction and electrophysiology of
Ascaris suum muscle.**

International J Parasitology (2008) Jul;38 (8-9):945-57. Epub 2007 Dec 8.

Sasa M. Trailovic*, Saurabh Verma*, Cheryl L. Clark, Alan P. Robertson,
and Richard J. Martin. (* Joint first authors.)

Department of Biomedical Sciences, Iowa State University, IA 50011, USA

5.1 Abstract

Contraction and electrophysiological effects of 5-methylfurmethiodide (MFI), a selective muscarinic agonist in mammals, were tested on *Ascaris suum* muscle strips. In a contraction assay, MFI produced weak contraction and was less potent than levamisole and acetylcholine. Atropine (3 μ M) a non-selective muscarinic antagonist in mammalian preparations, did not affect contractions produced by MFI. Mecamylamine (3 μ M) a nicotinic antagonist in *A. suum* preparations blocked the MFI contractions indicating that MFI had weak nicotinic agonist actions. In two-micropipette current-clamp experiments MFI, at concentrations greater than 10 μ M, produced concentration-dependent depolarizations and small increases in membrane conductance. The depolarizing effects were not abolished by perfusing the preparation in a calcium-free *Ascaris* Ringer solution to block synaptic transmission, suggesting that MFI effects were mediated by receptors on the muscle and were calcium-independent. A high concentration of mecamylamine, 30 μ M, only reduced the depolarizing responses by 42%, indicating that MFI also had effects on non-nicotinic receptors. Three non-nicotinic effects in the presence of 30 μ M

mecamylamine were identified using voltage-clamp: 1) MFI produced opening of mecamylamine-resistant non-selective-cation channel currents; 2) MFI inhibited opening of voltage-activated potassium currents; and 3) MFI increased the threshold of voltage-activated calcium currents. We suggest that a drug that is more selective for voltage-activated potassium currents, without effects on other channels like MIF, may be exploited pharmacologically as a novel anthelmintic or as an agent to potentiate the action of levamisole. In a larval migration assay we demonstrated that 4-aminopyridine (a potassium channel blocker) potentiated the effects of levamisole but MFI did not.

5.2 Introduction

The development of novel anthelmintics has been limited, so it is important to identify novel therapeutic lead compounds as well as methods for enhancing the potency of existing compounds that might counter drug resistance. The methods may include pharmacological agents that increase responses to the existing anthelmintics. Previously our studies have focused on levamisole and related drugs. Levamisole belongs to the ionotropic cholinergic agonist group of anthelmintics, that includes pyrantel, and that selectively produces muscle cell depolarization and spastic paralysis in parasitic nematodes (Aceves et al., 1970; Aubry et al., 1970). We have shown using current-clamp, voltage-clamp and patch-clamp, that electrophysiological responses to these anthelmintics can be observed in body muscle cells of the nematode parasites *A. suum* & *Oesophagostomum dentatum* (Martin, 1982; Pennington & Martin, 1990; Robertson & Martin, 1993; Robertson et al., 1994; Dale & Martin, 1995; Evans & Martin, 1996; Martin et al.,

2002; Robertson et al., 2002; Trailovic et al., 2002). These studies have identified nematode nicotinic acetylcholine gated receptor channels (nAChRs) over the nematode muscle cell surface that is selectively and directly gated by these anthelmintics. These studies have described down to the single-channel level, the agonist action and channel-blocking action of the anthelmintics.

If it were possible to find a drug that could stimulate nematode metabotropic cholinergic (G-protein coupled, muscarinic-like) receptors, it might be developed as a stand alone anthelmintic, or it might be used with ionotropic cholinergic anthelmintics to increase their potency. There is evidence in *A. suum* of metabotropic cholinergic receptors on muscle cells. Colquhoun et al. (1991) have tested a range of cholinergic agonists on the electrophysiology of *A. suum* muscle cells and found furtrethonium to be one of the more potent muscarinic agonists. Segerberg & Stretton (1993) have also found evidence of muscarinic-like receptors on *A. suum* muscle mediating depolarization and contraction; and Martin & Valkanov (1996) have described effects of acetylcholine potentiating the opening of mecamlamine-resistant non-selective cation channel currents (I_{bcac}) in isolated *A. suum* muscle bags. In *Caenorhabditis elegans* three G-protein coupled acetylcholine receptors (GAR-1, GAR-2 and GAR-3) have been reported (Hwang et al., 1999; Lee et al., 2000). GAR-3 is pharmacologically similar to the mammalian muscarinic receptor. GAR-1 and GAR-2 are pharmacologically unlike mammalian muscarinic receptors and are not antagonized by usual concentrations of muscarinic antagonists.

Colquhoun et al., (1991) tested effects on membrane potential of *A. suum* of a number of mammalian cholinergic agonists including furtrethonium, muscarine, arecoline, pilocarpine, McN A343, bethanocol and oxtremorine and furtrethonium was the most potent. We therefore selected 5-methylfurmethiodide (MFI, Fig.1 A) which is a potent mammalian muscarinic agonist (Newberry & Priestley, 1987) for further testing. In this paper we show that MFI in *A. suum* has four effects: 1) it is a weak nicotinic agonist; 2) it opens mecamlamine-resistant non-selective cation-channels; 3) it inhibits opening of voltage-activated potassium channels; and 4) it increases the threshold for activation of calcium channels. We discuss the significance of: mecamlamine-resistant channels and receptor operated channels (ROCs: TRPs). We also illustrate the use of inhibition of voltage-sensitive potassium channels as a method for potentiation of cholinergic anthelmintics.

5.3 Materials and Methods

Collection of worms

Adult *A. suum*, Fig. 1 B, were obtained weekly from the Tyson pork packing plant at Storm Lake, Iowa. Worms were maintained in Locke's solution [NaCl (155mM), KCl (5 mM), CaCl₂ (2 mM), NaHCO₃ (1.5 mM) and glucose (5 mM)] at 32 °C. The Locke's solution was changed daily.

Muscle contraction assay

A. suum were used for the contraction studies within 72 hours of collection, since the ability to contract vigorously to cholinergic agonists declined after this period. Two 1-cm body-flap preparations, one dorsal and one ventral, were made from each *A. suum* female from the region anterior to the genital pore, Fig. 1 B. Each

flap was monitored isometrically by attaching a force transducer in an experimental bath maintained at 37 °C containing 10 ml Ascaris Ringer (mM): NaCl, 23; Na-acetate, 110; KCl, 24; CaCl₂, 6; MgCl₂ 5; glucose, 11; HEPES, 5; pH 7.6 adjusted with NaOH and bubbled with nitrogen. Eight baths were used simultaneously. After dissection, the preparations were allowed to equilibrate for 15 min under an initial tension of 2.0 g. The antagonist was then added to the preparation 15 min before the application of the first concentration of the agonist. We ran two controls (no antagonist) and three replicate antagonist concentrations during each experiment (8 preparations). The dorsal and ventral flaps were assigned randomly in the experiments to reduce any potential error associated with differences in receptor populations. The agonists were added cumulatively with 2-3 minute intervals between applications and the responses were steady changes in tension. Results for individual flaps were rejected if the maximum change in tension, in response to agonist, did not exceed 0.5 g. The responses for each concentration were measured in grams and expressed in grams or as a % of the maximum tension produced by each individual flap preparation.

Changes in isometric muscle tension responses were monitored using a PowerLab System (AD Instruments) that consists of the PowerLab hardware unit and Chart for Windows software. The system allows for recording, displaying and analysis of experimental data. Sigmoid dose-response curves for each individual flap preparation at each concentration of antagonist were described by the Hill equation and fitted using Graph Pad Prism 4 software. The fits allowed estimation of *EC*₅₀s with 95% confidence intervals.

Electrophysiology

A 1cm long muscle tissue flap was prepared by dissecting the anterior part of the worm, 2-3 cm caudal to the head. The body muscle flap preparation was then pinned onto 3 ml Sylgard lined Petri-dish. The intestine was removed to expose the muscle bags. The preparation, Fig. 1 C, was continuously perfused, unless otherwise stated, with *Ascaris* Ringer solution. The preparation was maintained in the experimental chamber at 34 °C using a Warner Heating collar [DH 35] and heating the incoming perfusate with a Warner instruments (TC 324B) in-line heating system (Hamden, CT, USA). The perfusate was applied at 4-6 ml/min through a 19-gauge needle placed directly over the muscle bag that was being recorded from. Calcium-free experiments were performed using calcium-free *Ascaris* Ringer (Composition in mM: NaCl 23, Na-acetate 110, KCl 24, MgCl₂ 11, glucose 11, HEPES 5, and EGTA 0.5, NaOH was used to adjust the pH to 7.6). The sodium and calcium substitution experiments were conducted using n-methyl-d-glucamine Ringer (NMDG Ringer), composition in mM : NMDG Cl 23, NMDG-acetate 110, KCl 24, MgCl₂ 11 , glucose 11, HEPES 5 and 5 EGTA, CsOH was used to adjust the pH to 7.6. Calcium currents were recorded using modified *Ascaris* Ringer (calcium-Ringer) with added 5 mM 4-aminopyridine to reduce potassium currents.

Two-micropipette voltage-clamp and current-clamp techniques were employed to investigate whole cell currents in *A. suum*. Borosilicate capillary glass (Harvard Apparatus, Holliston, MA, USA) micropipettes were pulled on a P-97 Flaming Brown Micropipette puller (Sutter Instrument Co., Novato, CA, USA). The voltage-sensing and current-injecting micropipettes for the current-clamp and the

voltage-sensing micropipettes for voltage-clamp had resistances in the range 20-30 M Ω . The current-injecting micropipette for voltage-clamp had a resistance of 4-6 M Ω to keep the gain high and to facilitate clamp quality. The recordings were obtained by impaling both electrodes in the bag region of the *A. suum* muscle. All experiments were performed using an Axoclamp 2B amplifier, 1320A Digidata interface and Clampex 8.2 software (Axon Instruments, Sunnyvale, CA). All data were displayed and analyzed on a Pentium IV based desktop computer. The amplifier gain for voltage-clamp was more than 100 in all recordings. The phase lag was set to 1.5 ms in all experiments. In addition muscles closer to nerve cord were impaled for experimental study as they were rounder and with shorter arms to keep the membrane capacitance load low and to maintain the space-clamp. Only cells with stable membrane potentials more negative than -30 mV and of input conductance less than 2.5 μ S were selected for recording. To investigate the effects of MFI on currents at hyperpolarized and depolarized potentials at the same times, a ramped voltage protocol was used from a holding potential of -35mV. The voltage was stepped to -65 mV and over a period of 5 sec brought to -15 mV before stepping back to -35 mV. Leak subtraction was not used for the ramped-voltage experiments.

To investigate effects on inward and outward voltage-activated currents, voltage-steps of 5 mV each were used. The step potentials were: -25 mV, -20 mV, -15 mV, -10 mV, -5 mV, 0 mV, +5 mV, +10 mV, +15 mV and + 20 mV. Step potentials up to 150 ms were used for observing the outward potassium currents; step potential up to 50 ms were used for the inward calcium currents. The holding potential was -35 mV and leak subtraction was used to display the voltage-activated

currents (Verma et al., 2007). Outward potassium currents were observed using 3 M potassium acetate in the recording micropipettes. Calcium currents were observed using a combination of 1.5 M potassium acetate and 1.5 M cesium acetate in recording micropipettes; the cesium acetate was included in pipette solution to block outward potassium currents. For all voltage-clamp experiments, the drug applications were done in current-clamp for a minimum of 2 minutes before moving onto voltage-clamp. For current-clamp experiments a hyperpolarizing pulse of 40 nA was injected for 500 ms at 0.28 Hz frequency through the current-injecting micropipette and the other micropipette recorded the change in membrane potential.

Larval migration studies

Levamisole-sensitive *O. dentatum* were originally supplied by the Royal Veterinary and Agricultural School, Frederiksberg, Copenhagen and then reproduced at 6-9 month intervals by passage in pigs at Iowa State University, Ames, Iowa. The L_3 larvae isolates were maintained between passages in tap water refrigerated at 11 °C (changed every 2-4 months).

Between 1500-3000 L_3 's were ex-sheathed by 5-10 minute incubation in 1.5 % sodium hypochlorite solution. The larvae were then washed three times in migration buffer (composition: 0.85 % NaCl, 5 mM Tris-HCl, pH to 7.0 with 1 M NaOH) with the aid of centrifugation (5 min 1000 g). Approximately 150 larvae were collected with a pipette and placed in each of the drug concentrations to be tested for 2 hours at 37 °C. After this incubation, the larvae were re-suspended in fresh test solutions. A migration apparatus consisting of two tightly fitting plastic tubes (~10 mm length) that secured a 20 µm nylon filter (Small Parts Inc. Miami Lakes, FL.)

was placed in each test solution of a 24-well plate. The re-suspended larvae were added slowly to the top of each filter and allowed to migrate through the filters and into the wells during a 2 hr incubation at 37 °C. At the end of the incubation period, the number of larvae remaining within each of the filter tubes was counted and the number of larvae entering into the 24 well plates was counted. We then calculated the % not migrating for each of the concentrations. The relationship between the concentration of levamisole and the %-inhibited larvae was then examined by fitting sigmoidal dose-response curves.

Drugs

A 5-methylfurfurmethiodide (MFI), (Tocris Bioscience, Ellisville, Missouri) 3 mM stock solution was prepared every week and kept in 1.5 ml micro-tubes at -20 °C. The MFI stock solution was thawed just before use for experiments. All other drugs were obtained from Sigma-Aldrich, St. Louis, MO. All the stock solutions were made using double distilled water.

Statistical Analysis

Currents were plotted as a function of step potential to generate I-V curves. All the statistical analysis was done using Graph Pad Prism software (version 4.0, San Diego, CA, USA). Data were fitted with Boltzmann sigmoidal equation: $I = I_{max} / \{1 + \exp [(V_{50} - V)/K_{slope}]\}$. The EC_{50} concentrations for levamisole, acetylcholine and MFI were determined by fitting the standard sigmoidal dose-response relationship (slope =1) using the Graph Pad Prism software. Paired *t*-tests were used to test significant difference in responses with control and test recordings in the same preparation. Observations given are mean \pm standard error of the mean.

Minitab was used for analysis of variance using the general linear model to test the significance of effects of MFI and 4-AP in the larval migration studies.

5.4 Results

Contraction

MFI was less potent than levamisole and acetylcholine in the contraction assay. Fig. 2 A shows the contraction-concentration plots for levamisole, acetylcholine (with 3 μ M neostigmine to block cholinesterase) and MFI. The EC_{50} s (with 95% confidence intervals) were: levamisole: 0.7 (0.5 – 1.1, N= 18 preparations) μ M; acetylcholine 3.1 (1.9 – 4.9, N= 24 preparations) μ M; and MFI 221 (120- 410, N=18 preparations) μ M. MFI was not a full agonist and produced a maximum contraction that was around 30% of that produced by levamisole.

Atropine (3 μ M) did not inhibit (control: N = 4 preparations; atropine N=6 preparations) the contractile effects of MFI, Fig. 2 B, showing that the effects were not mediated by classic muscarinic receptors. However 3 μ M mecamylamine, Fig. 2 C, a nicotinic antagonist, completely blocked (N=4 preparations) contractions produced by MFI, showing that MFI has weak nicotinic effects sensitive to low concentrations of mecamylamine.

MFI depolarizations (current-clamp)

Fig. 3 A shows a representative recording of the effect of application, by rapid microperfusion, of 300 μ M MFI on the membrane potential and input conductance of an *A. suum* muscle cell. The dark central trace is the membrane potential which had a resting value of -35 mV; the downward deflection is the voltage response to the

injected current showing that the resting input conductance was 2.4 μS ; and the upward deflection is the anode break spike that followed the end of the 40 nA hyperpolarizing current pulse. The response, despite rapid MFI application, was a slow depolarization of 13 mV associated with a very small conductance increase of less than 0.1 μS ; the response took 75 sec from onset to reach its peak and was reversible on washing. The slow nature of the response to rapidly-applied MFI to *A. suum* muscle suggests that most of the response may not be mediated directly on ligand-gated channels (Purcell et al., 2002). The anode break spikes increased in amplitude during the application of the MFI as shown in Fig.3 A where there was an increase from 11 mV to 17 mV. Similar effects on anode break spikes were observed in the other preparations. One possible explanation for the effects on anode break spikes is an effect of MFI on voltage-sensitive currents associated with the spiking mechanism and this possibility is investigated subsequently in our manuscript.

Fig. 3 B shows a representative recording of the effect of different concentrations of MFI on the membrane potential and resting conductance of the muscle cell. There was little effect at 10 μM MFI but a more noticeable effect at 30 μM MFI; again notice the very slow onset and offset of the response. The depolarizations were concentration-dependent and reversible on washing. Fig. 3 C shows, for comparison, a recording from another preparation, the faster time-course (onset and offset) of the depolarizing response to 3 μM acetylcholine with the peak occurring in less than 9 sec; the MFI response was slower suggesting a different mechanism of action. The peak MFI concentration-depolarization relationships are

shown in Fig. 4; the relationships were determined in normal *Ascaris* Ringer and in Ca-free *Ascaris* Ringer solution and were not distinguishable. The concentration-conductance relationship, Fig 4 inset, in normal *Ascaris* and in Ca-free *Ascaris* Ringer solution however suggested that the presence of calcium could increase the MFI-induced conductance change, but we did not analyze this effect further. The fact that removal of calcium did not abolish the MFI response suggests that the effects of MFI are direct on muscle receptors and are not mediated trans-synaptically because calcium is required for synaptic transmission. The EC_{50} in the presence of calcium was 151 μM (95% confidence intervals 77– 262 μM , df 23, n= 6 preparations) which was not significantly different in calcium-free *Ascaris* Ringer, 191 μM (95% confidence intervals 76 – 540 μM , df 23, 6 preparations). We also determined the conductance-concentration plots in the presence and absence of calcium, Fig. 4 inset. The conductance changes associated with the depolarization responses were small, ranging up to 0.1 μS over the concentration range. The input conductance changes associated with nicotinic effects of acetylcholine are usually larger, up to 2.5 μS in *A. suum* muscle (Colquhoun *et al.*, 1991), suggesting again that the receptor population stimulated by MFI is not entirely nicotinic. The MFI conductance EC_{50} in the presence of calcium was 71 μM and in calcium-free Ringer, it was 58 μM . The lack of major effects of removing calcium on membrane potential suggests that calcium is not the major charge carrier mediating the depolarization.

Effect of atropine and mecamylamine on MFI depolarizations

Next, we tested effects of a high concentration of atropine, 30 μM , on the MFI depolarization response and found that it only had a small, but statistically significant inhibitory effect, Fig. 5 A. The mean response to 100 μM MFI was 9.8 ± 0.8 mV (N=4) and in the presence of 30 μM atropine it was 7.4 ± 0.8 mV (N=4, $p < 0.001$, paired *t-test*). These observations suggest that MFI did not mediate most of its effect on membrane potential by activating muscarinic (atropine sensitive) receptors.

When we tested the effects of a high concentration of mecamylamine (30 μM), it reduced but did not block depolarizing responses to 100 μM MFI, Fig. 5 B; the mean response before application of mecamylamine was 6.5 ± 1.0 mV (N=4), in the presence of mecamylamine the mean response was 3.3 ± 0.9 (N=4, $p < 0.01$, paired *t-test*). Since mecamylamine is a potent nicotinic antagonist in *A. suum* (Colquhoun et al., 1991), the modest antagonism of mecamylamine suggests that only part of the MFI response is mediated by nicotinic receptor channels; most of the response is mediated by other mecamylamine-resistant receptor ion-channel effects. In order to dissect out the ionic mechanisms involved we conducted voltage-clamp experiments to examine effects on specific voltage-activated currents.

Ramp voltage-clamp experiments

Initial voltage-clamp experiments showed that 100 μM MFI induced a steady inward current at a holding potential of -35 mV (mean 57 ± 9 nA) and that this was significantly reduced, but not blocked, (mean 42 ± 5 nA) in the presence of 30 μM mecamylamine ($p < 0.001$, paired *t-test*, N=7). We used 30 μM mecamylamine

subsequently in the voltage-clamp experiments to block nicotinic effects and isolate the non-nicotinic effects of MFI. Fig. 6 shows sections of a recording made during the ramp voltage-clamp experiments. The top trace (Fig. 6. A) shows the ramp protocol that was used: the potential was held at -35 mV between the ramp voltages, near to the normal resting membrane potential; there was then a step to -65 mV followed by a ramped depolarization over a 5 sec period to -15 mV; the membrane potential was then stepped back to -35 mV. These ramp pulses were repeated after 5 sec. The middle trace (Fig. 6 B) shows current traces: 1) Control, just before the application of MFI; and 2) during the plateau phase of the MFI response. Following washout of MFI, the currents returned towards control levels (data not shown).

MFI opens a mecamlamine-resistant non-selective cation channel

Fig. 6 B shows the ramp currents that were displayed without leakage correction. At -35 mV during the application of MFI, there was an increase in the inward holding current of 9 nA (follow the upper dashed line in Fig. 6 B). At -65 mV during the application of MFI, the inward current increased by 15 nA (follow the lower dashed line). The increases in current are plotted in Fig.6 C and extrapolated to estimate the reversal potential (E_{rev} : +10 mV) of the MFI current. The mean reversal potential in experiments on separate preparations was -6.0 ± 5.8 mV (N=5). Additionally, the current associated with the -35 mV to -65 mV voltage-step increased from -107 nA (control) to 113 nA in the presence of 100 μ M MFI and 30 μ M mecamlamine. In similar experiments on 5 different preparations, the mean

increase in the current step was 12.2 ± 3.6 nA and statistically significant (paired *t*-test, $p < 0.05$, $N=5$). For a 30 mV step, the increased current step seen in the ramp experiments corresponds to a mean membrane conductance increase of $0.4 \mu\text{S}$. The increased conductance and mean E_{rev} of -6 mV can be explained by MFI opening non-selective cation channels (Martin & Valkanov, 1996) which are mecamlamine-resistant. We also considered the possibility that the effect could be mediated by an increase in chloride channel conductance but this is unlikely since the estimated reversal potential would be more negative than -32 mV [based on an intracellular chloride concentration less than 20 mM (Brading and Caldwell, 1971), and an extracellular concentration of 69 mM as used in our experiments]. Thus one effect of MFI is to open mecamlamine-resistant, non-selective cation channels.

MFI also inhibits voltage-activated channel currents

Further inspection of the ramp currents, Fig. 7A, shows that the current step associated with the -15 mV to -35mV voltage-step decreased from 58 nA in the control to 46 nA in the presence of MFI. In experiments on 5 separate preparations, the mean reduction in the current step was 9.0 ± 1.1 nA and statistically significant (paired *t*-test, $p < 0.05$, $N=5$). For the 20 mV step, the reduction in current step corresponds to a reduction in membrane conductance of $0.45 \mu\text{S}$. Depolarization is known to activate voltage-sensitive potassium and voltage-sensitive calcium channels in *A. suum* muscle (Martin et al., 1992). The reduced current step (decreased membrane conductance) from -15 mV suggests that additional effects of

MFI are to inhibit opening of voltage-sensitive potassium and/or voltage-sensitive calcium channels. We investigated this possibility in the next series of experiments.

MFI inhibits opening of voltage-activated potassium currents

To isolate effects of MFI on voltage-activated potassium currents, we used a NMDG- Ringer to block voltage-activated inward currents (Martin et al., 1992; Verma et al., 2007) in the presence of 30 μM mecamylamine. Fig. 7 B shows the inhibitory effect of MFI on voltage-activated potassium currents activated by rectangular depolarizing step potential from a holding potential of -35 mV. Fig. 7 C plots peak outward currents against the step potential for the control and in the presence of 100 μM MFI. The plots were described by the Boltzmann equation (1):

$$I = I_{max} / \{1 + \exp [(V_{50} - V)/K_{slope}]\} \dots\dots\dots(1),$$

where I the peak current, I_{max} the maximum current V_{50} is the potential that produced the half-maximum effect, V is the step potential and K_{slope} is the slope of the plot. Table 1 shows the values estimated for the Boltzmann equation for the control and in the presence of MFI for the experiment shown if Fig 7 C. When the data from 5 different preparations were pooled we found that: (i) the V_{50} significantly increased ($p < 0.05$, *paired t-test* N=5) from a mean of 7.7 ± 0.9 mV to 11.1 ± 1.2 mV; (ii) the I_{max} significantly decreased ($p < 0.05$, *paired t-test* N=5) from a mean of 495 ± 138 to 311 ± 114 nA; and (iii) that *Slope* decreased significantly ($p < 0.05$, *paired t-test*, N=5) from 6.4 ± 0.4 nA.mV⁻¹ to 4.9 ± 0.6 nA.mV⁻¹. I_{max} , V_{50} and K_{slope} were all changed by MFI.

	Control	100 μ M MFI
<i>I</i>_{max}	745 nA.	427 nA
<i>V</i>₅₀	8.3 mV	11.3 mV
<i>K</i>_{slope}	5.6 nA. mV ⁻¹	4.9 nA.mV ⁻¹

Table 1. The constant values for equation (1), the Boltzmann equation, obtained by fitting the activation curve for the voltage-activated potassium currents. Note that 100 μ M MFI reduced the maximum activated current and raised the, V_{50} , threshold for activation of the current.

MFI also raises the threshold for activation of voltage-activated calcium currents

Fig. 8 A shows the reversible effect of 100 μ M MFI on the voltage-activated calcium currents. Fig. 8 B shows the current-voltage relationships of the calcium currents and that the effect of 100 μ M MFI was to increase the threshold for activation of the calcium current so that a greater depolarization was normally required to activate the same currents. Notice that between -20 mV and -5 mV that the calcium current is reduced by MFI but at 0 mV the current is the same. Similar increases in the threshold for activation of the calcium currents produced by MFI were observed in experiments on 4 separate preparations. The mean voltage-activated calcium current activated by a step from a holding potential of -35 mV to a step potential of -5 mV was -99.9 ± 10.6 nA; in the presence of 100 μ M MFI it was reduced significantly ($p < 0.05$, *paired t-test*, $N = 4$) to -75.1 ± 13.1 nA, Fig 8 C, and this returned to -97.6 ± 11.0 nA on washout.

Effects of MFI and 4-aminopyridine (4-AP) on levamisole inhibition of larval migration

One of our longer-term aims has been to identify pharmacological mechanisms that could be used to design novel therapeutic agents or to potentiate the effects of levamisole. However, MFI produced a number of effects on channel currents which were mutually antagonistic: the effect on inhibiting potassium channels would be excitatory, but the effects on calcium currents would be inhibitory. We were therefore interested to see if the anthelmintic effects of levamisole could be potentiated by addition of a selective potassium channel blocker and to compare effects of MFI. Fig. 9 shows the effects of 100 μ M MFI and 1 mM 4-AP (selective potassium channel blocker) on levamisole concentration-response plot in larval migration assays. The effect of MFI was statistically significant: it inhibited the effects of levamisole ($p < 0.001$, *f-test*, *df* 1, 62). The effects of 4-AP were also statistically significant and it potentiated the effect of levamisole ($p < 0.001$, *f-test*, *df* 1, 62). The levamisole control had an EC_{50} of 173 μ M (134 – 222 μ M: 95% confidence interval, N= 3 separate experiments); in the presence of MFI the levamisole EC_{50} was 1062 μ M (531 – 2124 μ M: 95% confidence interval N= 3 separate experiments); in the presence of 1 mM 4-aminopyridine, the levamisole EC_{50} was 47 μ M (29 – 75 μ M 95% confidence interval, N= 3 separate experiments). The EC_{50} s were significantly different, with non-overlapping confidence intervals. We found that 1 mM 4-AP was near threshold for inhibitory effects on migration. At low concentrations of levamisole, MFI had little effect but at higher levamisole concentrations it acted as a levamisole antagonist. The antagonism may be due to

MFI acting as partial (weak) nicotinic agonist or due to inhibition of calcium currents and these actions appear to limit the ability of MFI to potentiate the actions of levamisole. However, it was clear that 4-aminopyridine potentiated the effects of levamisole. Addition of 4-aminopyridine made levamisole 3.7 x s more potent, when comparing the *EC50s* due to antagonism of the potassium current.

5.5 Discussion

MFI effects in A. suum

We found evidence of effects of MFI in *A. suum* on four types of ion-channels, summarized in Fig. 10. In our muscle strip experiments we observed that MFI was a weak agonist producing contraction with a relative potency of 0.014 of acetylcholine. MFI did not produce a maximum contraction like acetylcholine or levamisole. The contraction appears to be mediated by nicotinic cholinergic receptors rather than muscarinic receptors because it was inhibited by a low concentration of mecamylamine (3 μ M), in *A. suum* (Colquhoun et al., 1991).

MFI also activated a mecamylamine-resistant non-selective cation channel current, inhibited voltage-activated potassium channel currents and raised the threshold of voltage-activated calcium channel currents, Fig. 10. The nicotinic channel currents, the non-selective cation channel currents and inhibition of the potassium current would contribute to depolarization and contraction, but the increase in the calcium current threshold would not. The calcium current effect probably limited the contractile effects of MFI in the muscle strip experiments.

Three subtypes of nicotinic acetylcholine receptor channels have been described in *A. suum* (Robertson et al., 2002; Qian et al., 2006). There is the *N*-

type, which is activated preferentially by nicotine; there is the *L*-type, which is activated preferentially by levamisole; and there is the *B*-type, which is activated preferentially by buphenium. It is possible that one nicotinic receptor subtype was not inhibited by mecamylamine. This is unlikely because of the potency of mecamylamine as a nicotinic antagonist in *Ascaris* (Colquhoun et al., 1991). We checked the potency of mecamylamine as antagonist of nicotine, levamisole and buphenium using our contraction assay to obtain contraction concentration plots in the absence of mecamylamine and then 0.03, 0.3 and 3.0 μM mecamylamine (at least 4 preparations for each agonist) were obtained. The pA_2 were calculated using standard methods (Robertson et al. 2002). Table 2 shows the pA_2 and IC_{50} (μM) values. The potency of mecamylamine against the three agonists makes it unlikely that the mecamylamine-resistant cation-channels are due to a nicotinic receptor subtype.

Agonist	pA_2	μM value of pA_2
nicotine	7.2	0.062
levamisole	6.6	0.235
buphenium	6.7	0.191

Table 2. The pA_2 and IC_{50} (μM) values obtained for mecamylamine with nicotine, levamisole or buphenium as agonist. Agonist contraction concentration plots in the absence of mecamylamine and then 0.03, 0.3 and 3.0 μM mecamylamine (4 or more preparations were used for each agonist) were obtained

Non-selective cation-channels and ROCs (TRP-channels)

The significance and function of the nicotinic cholinergic channels that mediate muscle contraction and the effects of ionotropic cholinergic anthelmintics

like levamisole have been described (Martin & Robertson, 2007), but the function of the MFI activated mecamlamine-resistant cation-channels is uncertain. Martin & Valkanov (1996) have described activation by acetylcholine of an atropine-resistant, mecamlamine-resistant non-selective cation channel current (I_{bcac}) which has slow kinetics and that this current may underlie the slow depolarization waves seen in *A. suum* muscle (Weisblat et al., 1976). Receptor operated channels (ROCs) which are non-selective cation channels are activated by a variety of ligands including muscarinic agonists and belong to the TRP group of channels (Albert and Large, 2006; Ramsey et al., 2006). The permeability properties of the mecamlamine-resistant non-selective cation channel, channels of the slow waves, I_{bcac} (Martin & Valkanov, 1996) and TRP-channels have some similarities. These similarities give rise to the possibility that the slow waves and I_{bcac} are conducted by a TRP-like channel (Zholos et al., 2004; Takai et al., 2004) that is activated by MFI. Interestingly, Arevalo & Saz (1992) have already demonstrated the activation of phospholipase C and production of diacylglycerol by acetylcholine in *A. suum* which activate ROCs (Beech et al., 2004).

Effects on potassium and calcium currents

We have examined, in *A. suum* muscle, the effects of MFI, which is known to activate M_1 receptors in rat cervical ganglion neurons. Mammalian muscarinic acetylcholine receptors are seven transmembrane receptors of the rhodopsin-like family where the natural agonist is acetylcholine (Caulfield et al., 1994). They are divided into five pharmacological subtypes, M_1 - M_5 . MFI produces depolarization in

rat cervical ganglion cells (Newberry and Priestley, 1987; Roberts and Newberry, 1990) by stimulation of receptors that produces closure of an inwardly rectifying potassium channel current known as the M-current (Caulfield et al., 1994). We have shown here that MFI also produces depolarization and inhibition of voltage-activated potassium currents in *A. suum*.

In other mammalian preparations stimulation of the M₁ receptor can also inhibit N- and R-type calcium currents (Melliti et al., 2001). We saw both inhibition of potassium currents and an increase in the threshold for calcium currents in *A. suum* muscle cells. It is not clear why MFI produces mutually opposing effects in *A. suum*. It is possible that the extrasynaptic location of MFI application is stimulating a mixture of cholinergic receptors that would not occur physiologically with synaptic release of acetylcholine. We also point out that we have not tested for any role of G-proteins in this study and it remains a possibility that the effect of MFI in *A. suum* may be via a direct action of MFI on the potassium or calcium channels. The slow speed of the MFI response however, suggests an indirect action on the ion-channels mediated by a second messenger (Purcell et al., 2002).

C. elegans muscarinic receptors (GARs)

In the model nematode *C. elegans*, three main categories of G-protein linked acetylcholine receptors have been described that are known as GARs (Hwang et al., 1999; Lee et al., 2000). GAR-1, GAR-2 and GAR-3 are molecular homologues of mammalian muscarinic acetylcholine receptors (Lee et al 2000). GAR-1 and GAR-2 are pharmacologically separable from mammalian muscarinic receptors: they are not

sensitive to all muscarinic antagonists. GAR-3 is molecularly and pharmacologically more like mammalian muscarinic receptors and is sensitive to atropine. In *C. elegans* the GAR-3 receptor is coupled to and inhibits opening of a potassium channel and enhances nicotinic receptor function via a $G_{\alpha q}$ protein in the male spicule muscle (Liu et al., 2007) but in the pharyngeal muscle GAR-3 stimulation enhances a calcium current (Steger & Avery, 2004).

Muscarinic-like receptors in Ascaris suum

There is much less molecular information available concerning *A. suum* GARs but homologues to GAR-1 are in EST data bases (BM281808 & BM 281722: NCBI) and their function and pharmacology remains to be characterized. At this stage we do not have enough information to determine which G-protein coupled acetylcholine receptors are coupled to potassium or other channels in *A. suum*.

There are a number of physiological and pharmacological reports indicating the presence of muscarinic-like receptors on *A. suum* body muscle. Colquhoun et al., (1999) have described the relative potency of a range of selective muscarinic agonists in *Ascaris suum*: furmethiodide (furethronium) had a relative potency of 0.007 (compared to acetylcholine); arecoline had a relative potency of 0.001 but oxremorine was without effect. In an isolated muscle bag preparation of *A. suum*, Martin & Valkanov (1996) observed evidence of a mecamylamine-resistant cholinergic receptor, stimulation of which increased the opening of a non-selective cation channel, an effect that was not blocked by atropine, mecamylamine or tubocurarine. In addition Segerberg & Stretton (1993) reported that pilocarpine, a

muscarinic agonist, produced a concentration-dependent depolarization in *A. suum* muscle that was not antagonized by a muscarinic antagonist (N-methyl-scopolamine) nor the nicotinic antagonist, tubocurarine. The lack of effect of oxtemorine and atropine in previous *A. suum* studies together with the modest effect of atropine in our studies suggests that a GAR-3-like receptor is not involved in mediating the effects of MFI.

5.6 Acknowledgments The project was supported by Grant Number R 01 AI 047194 from the national Institute of Allergy and Infectious Diseases. The content is solely the responsibility of the authors and does not necessarily represent the official views of the National Institute of Allergy and Infectious diseases of the National Institutes of Health.

5.7 References

- Aceves, J., Erlj, D., Martinez-Maranon, R., 1970. The mechanism of the paralyzing action of tetramisole on *Ascaris* somatic muscle. *Br J Pharmacol* 38, 602-607.
- Albert, A.P., Large, W.A., 2006. Signal transduction pathways and gating mechanisms of native TRP-like cation channels in vascular myocytes. *J Physiol* 570, 45-51.
- Arevalo, J.I., Saz, H.J., 1992. Effects of cholinergic agents on the metabolism of choline in muscle from *Ascaris suum*. *J Parasitol* 78, 387-392.
- Aubry, M.L., Cowell, P., Davey, M.J., Shevde, S., 1970. Aspects of the pharmacology of a new anthelmintic: pyrantel. *Br J Pharmacol* 38, 332-344.
- Brading, A.F., Caldwell, P.C. (1971). The resting membrane potential of the somatic muscle cells of *Ascaris lumbricoides*. *J. Physiol* . 217, 605- 624.
- Beech, D.J., Muraki, K., Flemming, R., 2004. Non-selective cationic channels of smooth muscle and the mammalian homologues of *Drosophila* TRP. *J Physiol* 559, 685-706.
- Caulfield, M.P., Jones, S., Vallis, Y., Buckley, N.J., Kim, G.D., Milligan, G., Brown, D.A., 1994. Muscarinic M-current inhibition via G alpha q/11 and alpha-

- adrenoceptor inhibition of Ca²⁺ current via G_{αo} in rat sympathetic neurones. *J Physiol* 477, 415-422.
- Colquhoun, L., Holden-Dye, L., Walker, R.J. The Pharmacology of cholinceptors on the somatic muscle cells of the parasitic nematode *Ascaris suum*. *J.Exp.Biol.* 158, 509-530. 1991.
- Dale, V.M., Martin, R.J., 1995. Oxantel-activated single channel currents in the muscle membrane of *Ascaris suum*. *Parasitology* 110 (Pt 4), 437-448.
- Evans, A.M., Martin, R.J., 1996. Activation and cooperative multi-ion block of single nicotinic-acetylcholine channel currents of *Ascaris* muscle by the tetrahydropyrimidine anthelmintic, morantel. *Br J Pharmacol* 118, 1127-1140.
- Hwang, J.M., Chang, D.J., Kim, U.S., Lee, Y.S., Park, Y.S., Kaang, B.K., Cho, N.J., 1999. Cloning and functional characterization of a *Caenorhabditis elegans* muscarinic acetylcholine receptor. *Receptors Channels* 6, 415-424.
- Lee, Y.S., Park, Y.S., Nam, S., Suh, S.J., Lee, J., Kaang, B.K., Cho, N.J., 2000. Characterization of GAR-2, a novel G protein-linked acetylcholine receptor from *Caenorhabditis elegans*. *J Neurochem* 75, 1800-1809.
- Liu, Y., LeBoeuf, B., Garcia, L.R., 2007. G_{α(q)}-coupled muscarinic acetylcholine receptors enhance nicotinic acetylcholine receptor signaling in *Caenorhabditis elegans* mating behavior. *J Neurosci* 27, 1411-1421.
- Martin, R.J., 1982. Electrophysiological effects of piperazine and diethylcarbamazine on *Ascaris suum* somatic muscle. *Br J Pharmacol* 77, 255-265.
- Martin, R.J., Robertson, A.P., 2007. Mode of action of levamisole and pyrantel, anthelmintic resistance, E153 and Q57. *Parasitology* 134, 1093-1104.
- Martin, R.J., Robertson, A.P., Wolstenholme, A.J., 2002. Mode of action of the macrocyclic lactones. In Vercruysse, J., Rew, R.S. (Eds.), CABI, Wallingford, pp. 125-140.
- Martin, R.J., Thorn, P., Gratton, K.A., Harrow, I.D., 1992. Voltage-activated currents in somatic muscle of the nematode parasite *Ascaris suum*. *J Exp Biol* 173, 75-90.
- Martin, R.J., Valkanov, M.A., 1996. Effects of acetylcholine on a slow voltage-activated non-selective cation current mediated by non-nicotinic receptors on isolated *Ascaris* muscle bags. *Exp Physiol* 81, 909-925.
- Melliti, K., Meza, U., Adams, B.A., 2001. RGS2 blocks slow muscarinic inhibition of N-type Ca(2+) channels reconstituted in a human cell line. *J Physiol* 532, 337-347.

- Newberry, N.R., Priestley, T., 1987. Pharmacological differences between two muscarinic responses of the rat superior cervical ganglion in vitro. *Br J Pharmacol* 92, 817-826.
- Pennington, A.J., Martin, R.J., 1990. A patch-clamp study of acetylcholine-activated ion channels in *Ascaris suum* muscle. *J Exp Biol* 154, 201-221.
- Purcell, J., Robertson, A.P., Thompson, D.P., Martin, R.J., 2002. The time-course of the response to the FMRFamide-related peptide PF4 in *Ascaris suum* muscle cells indicates direct gating of a chloride ion-channel. *Parasitology* 124, 649-656.
- Qian, H., Martin, R.J., Robertson, A.P., 2006. Pharmacology of N-, L-, and B-subtypes of nematode nAChR resolved at the single-channel level in *Ascaris suum*. *FASEB J*.
- Ramsey, I.S., Delling, M., Clapham, D.E., 2006. An introduction to TRP channels. *Annu Rev Physiol* 68, 619-647.
- Roberts, K.E., Newberry, N.R., 1990. A pharmacological study of the responses induced by muscarinic agonists on the isolated superior cervical ganglion of the guinea-pig. *Eur J Pharmacol* 186, 257-265.
- Robertson, A.P., Clark, C.L., Burns, T.A., Thompson, D.P., Geary, T.G., Trailovic, S.M., Martin, R.J., 2002. Paraherquamide and 2-deoxy-paraherquamide distinguish cholinergic receptor subtypes in *Ascaris* muscle. *J Pharmacol Exp Ther* 302, 853-860.
- Robertson, S.J., Martin, R.J., 1993. Levamisole-activated single-channel currents from muscle of the nematode parasite *Ascaris suum*. *Br J Pharmacol* 108, 170-178.
- Robertson, S.J., Pennington, A.J., Evans, A.M., Martin, R.J., 1994. The action of pyrantel as an agonist and an open channel blocker at acetylcholine receptors in isolated *Ascaris suum* muscle vesicles. *Eur J Pharmacol* 271, 273-282.
- Seegerberg, M.A., Stretton, A.O., 1993. Actions of cholinergic drugs in the nematode *Ascaris suum*. Complex pharmacology of muscle and motoneurons. *J Gen Physiol* 101, 271-296.
- Steger, K.A., Avery, L., 2004. The GAR-3 muscarinic receptor cooperates with calcium signals to regulate muscle contraction in the *Caenorhabditis elegans* pharynx. *Genetics* 167, 633-643.
- Takai, Y., Sugawara, R., Ohinata, H., Takai, A., 2004. Two types of non-selective cation channel opened by muscarinic stimulation with carbachol in bovine ciliary muscle cells. *J Physiol* 559, 899-922.

- Trailovic, S.M., Robertson, A.P., Clark, C.L., Martin, R.J., 2002. Levamisole receptor phosphorylation: effects of kinase antagonists on membrane potential responses in *Ascaris suum* suggest that CaM kinase and tyrosine kinase regulate sensitivity to levamisole. *J Exp Biol* 205, 3979-3988.
- Verma, S., Robertson, A.P., Martin, R.J., 2007. The nematode neuropeptide, AF2 (KHEYLRF-NH(2)), increases voltage-activated calcium currents in *Ascaris suum* muscle. *Br J Pharmacol* 151, 888-899.
- Weisblat.D.P., Byerly L., Russel, R.L. Ionic Mechanisms of electrical activity in the somatic muscle cell of the nematode *Ascaris lumbricoides*. *J Comp Physiol* 111, 93-113. 1976.
- Zholos, A.V., Tsytsyura, Y.D., Gordienko, D.V., Tsvilovskyy, V.V., Bolton, T.B., 2004. Phospholipase C, but not InsP3 or DAG, -dependent activation of the muscarinic receptor-operated cation current in guinea-pig ileal smooth muscle cells. *Br J Pharmacol* 141, 23-36.

5.8 Legends to figures

Fig 1. A: The chemical structure of 5-methylfurmethiodide.

B: *A. suum* muscle strip preparations are dissected from the anterior region of the worm and mounted in a water bath for the contraction assay.

C: Diagram of the two micro-pipette current-clamp and voltage-clamp recording from the bag region of the *A. suum* muscle cell and the application of solutions by microperfusion. The current-injecting micropipette (I) and voltage-sensing micropipette (V) are illustrated.

Fig. 2. A: Effect of MFI (■), acetylcholine with 3 μ M neostigmine to block cholinesterase (○) and levamisole (●) on contraction of *A. suum* muscle strips. EC_{50} s: MFI 221 μ M; acetylcholine, 3.1 μ M, levamisole, 0.7 μ M. Mean \pm S. E. maximum contractions are shown. MFI is not a full agonist and does not produce a maximum contraction.

B: Atropine (3 μ M applied 10 minutes before and maintained in the presence of the agonist) had no inhibitory effect on MFI muscle contractions. Control (■); 3 μ M atropine (□).

C: Mecamylamine (3 μ M) completely antagonizes the contractions of MFI. Control (●); 3 μ M atropine (○).

Fig 3. Effect of MFI on membrane potential and conductance.

A: Effect of 300 μ M MFI in the presence of 6 mM calcium. A 2-minute application of MFI produces a 10 mV depolarization and a small change in input conductance (downward pulses) but a clear increase in the anode break spikes produced at the end of each hyperpolarizing potential response to the injected current pulse. The central trace is the membrane potential, -35 mV; the downward deflection is the voltage response to injected current. The resting input conductance was 2.4 μ S; and the upward deflection is the anode break spike that followed the end of the 40 nA hyperpolarizing current pulse. There was a slow 13 mV depolarization associated with a very small conductance increase of 0.1 μ S; the response took 75 sec from onset to reach its peak. The anode break spikes increased in amplitude during MFI application from 11mV to 17 mV.

B: Lower time-resolution recording of a representative recording of applying increasing concentrations of MFI on the membrane potential and resting conductance of the muscle cell. There was little effect at 10 μ M MFI but a noticeable effect at 30 μ M MFI; again notice the very slow onset and offset of the response.

C: Representative recordings of the effect acetylcholine on membrane potential. Note that the time course is faster than that of MFI. The faster time-course (onset and offset) of the depolarizing response to 3 μ M acetylcholine with the peak occurring with our application method within 9 sec after onset.

Fig 4. Peak MFI depolarization-concentration relationships. The relationships were determined in normal *Ascaris* Ringer and in Ca-free *Ascaris* Ringer. The EC_{50} in the presence of calcium was 151 μ M and in calcium-free, it was 191 μ M. Number of preparations, N=6.

Inset: MFI-conductance-concentration plots in the presence and absence of calcium. The conductance change associated with the depolarization responses was small, up to 0.1 μ S

over the concentration range. The MFI EC_{50} in the presence of calcium was 71 μM and in calcium-free, it was 58 μM .

Fig 5. A: 30 μM atropine has a small but significant effect on the depolarizing responses to 100 μM MFI. Representative trace and bar chart (N=8). Control, 9.8 ± 0.8 mV; + atropine, 7.4 ± 0.8 mV.

B: 30 μM mecamylamine reduces, but does not completely block depolarizing responses to 100 μM MFI. Representative trace and bar chart (N=4). Control, 6.5 ± 1.0 mV; + mecamylamine, 3.3 ± 1.0 mV.

Fig. 6. A: Ramp-voltage protocol used to view effects of MFI on bag currents. The holding potential was -35 mV; the start of the ramp began at -65 mV and increased to -15 mV and then returned to -35 mV.

B: Effect of 100 μM MFI on voltage-ramp activated currents under voltage-clamp in the presence of 30 μM mecamylamine to block nicotinic effects. The holding current increased by -9nA at -35 mV and by -15 nA at -65 mV. The current record in B shows that the current-step associated with the voltage-step, -35mV to -65mV increased from 107 nA in the control to 113 nA in the presence of 100 μM MFI showing that MFI increased the membrane conductance at -35 mV. At -15 mV the current step associated with the -15 mV to -35mV voltage-step decreased from 58 nA in the control to 46 nA in the presence of MFI showing that MFI decreased the conductance of the membrane at -15 mV that could be associated with potassium channel block. The effect was reversible on washout (data not shown).

C: Estimation of the reversal potential (E_{rev}) of the MFI current induced at potential more negative than -35 mV. Extrapolation of the MFI induced currents at -35 and -65 mV gave +10mV as the reversal potential. Because of the composition of the intracellular and extracellular ions, the reversal potential is consistent with the current being due to opening of a non-selective cation channel. The high concentration of mecamylamine present suggests that this is not due to a nicotinic channel.

Fig. 7. Effect of MFI on depolarization-activated potassium currents in NMDG Ringer.

A: Ramp currents from experiment shown in Fig 6 B. Note that there is a reduction from 58 nA to 46 nA in the current step associated with the voltage step -15 to -35 mV indicating that 100 μM MFI limits opening of voltage-activated currents at depolarized potentials.

B: The muscle cell was held at -35 mV and rectangular depolarizing steps made to different potentials in 5 mV steps to activate the potential dependent potassium channels. The control currents are reduced in the presence of 100 μM MFI and increase again on wash.

C: Peak outward current-voltage plots, control (\bullet), in the presence of 100 μM MFI (\circ). The plots are fitted with the Boltzmann equation (equation-1) to obtain estimates of the constants (see Table 1). MFI inhibits the outward current by reducing the maximum current and decreasing the half-activation potential.

Fig 8. 100 μM MFI increases the threshold for activation of the voltage-activated calcium currents.

A: Control currents (left) activated by step potentials from a holding potential of -35 mV. Currents in the presence of 100 μM MFI (middle) and following washout (right).

B: Plot of the peak inward calcium current at different step potentials. Control (\bullet). 100 μM MFI (Δ). Wash (\square). Note that it takes a greater depolarization step to activate the current.

C: Bar chart of the peak calcium current at -5 mV in the control, presence of 100 μM MFI, and following washout. MFI had a significant ($P < 0.05$ *paired t-test* N=4) effect when compared to the control and wash.

Fig 9. Potentiation effect of 100 μM 4-aminopyridine (4-AP) and antagonistic effect of 100 μM MFI on levamisole inhibition of larval migration. *O. dentatum* ex-sheathed L3 larval migration assay. Control, levamisole response (\bullet). Levamisole with 1 mM 4-AP (\square). Levamisole with 100 μM MFI (Δ). MFI reduces the effect of levamisole at higher doses. N=3.

Fig 10. Summary diagram of the effects of MFI on the membrane ion-channels of *A. suum* muscle. MFI is a weak agonist of the nicotinic acetylcholine channels on the bag (up arrow: nAChR). MFI activates mecamylamine-resistant non-selective cation channels (up arrow: MRCAT: TRP?). MFI raises the threshold of voltage-activated calcium currents (down arrow: VACC). MFI inhibits opening of voltage-activated potassium currents (down arrow: K channels)

5.9 Figures

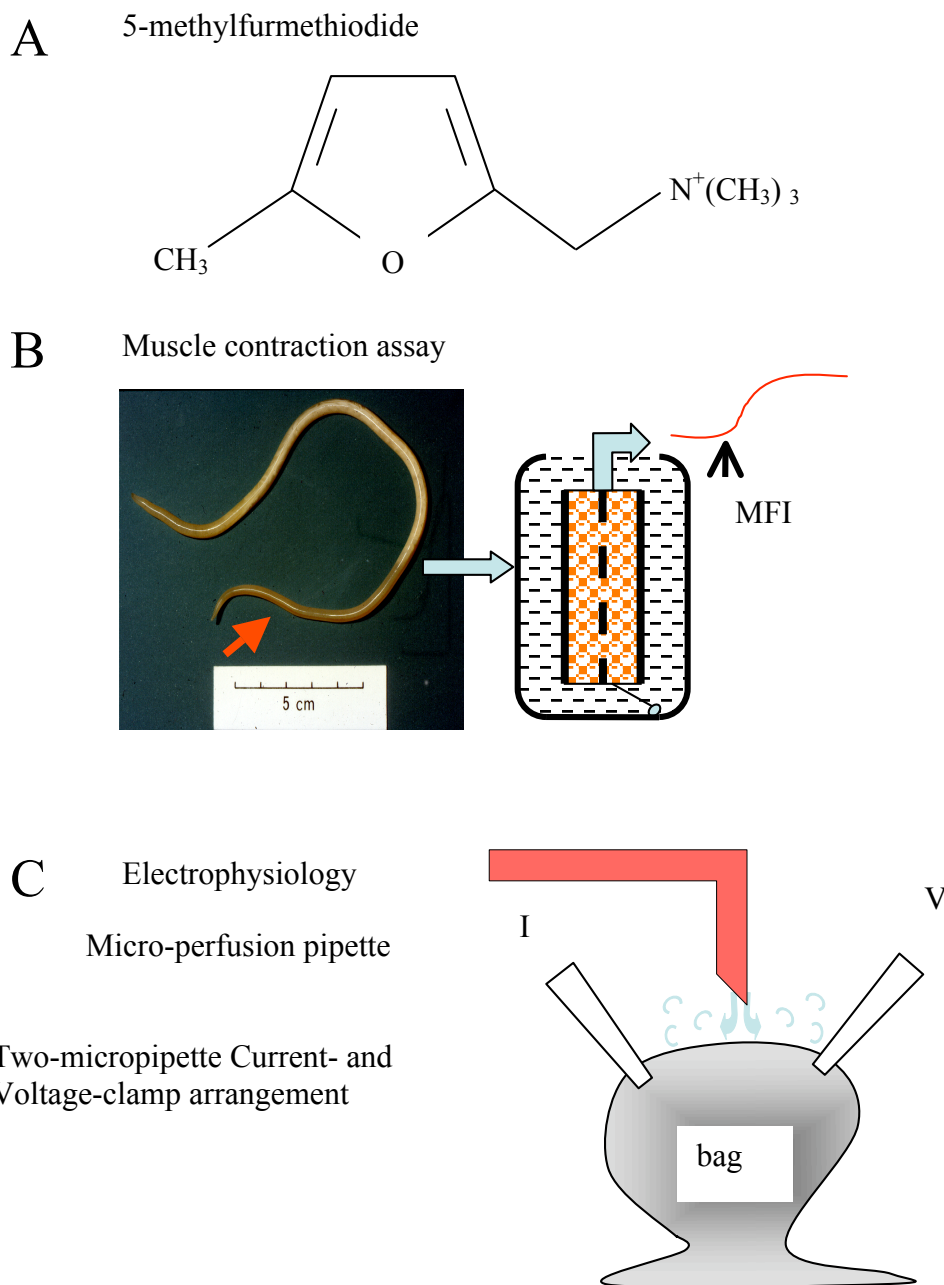


Fig 1. **A:** The chemical structure of 5-methylfurfmethiodide. **B:** *A. suum* muscle strip preparation for the contraction assay. **C:** Diagram of the two micro-pipette current-clamp and voltage-clamp recording from the bag region of the *A. suum* muscle cell.

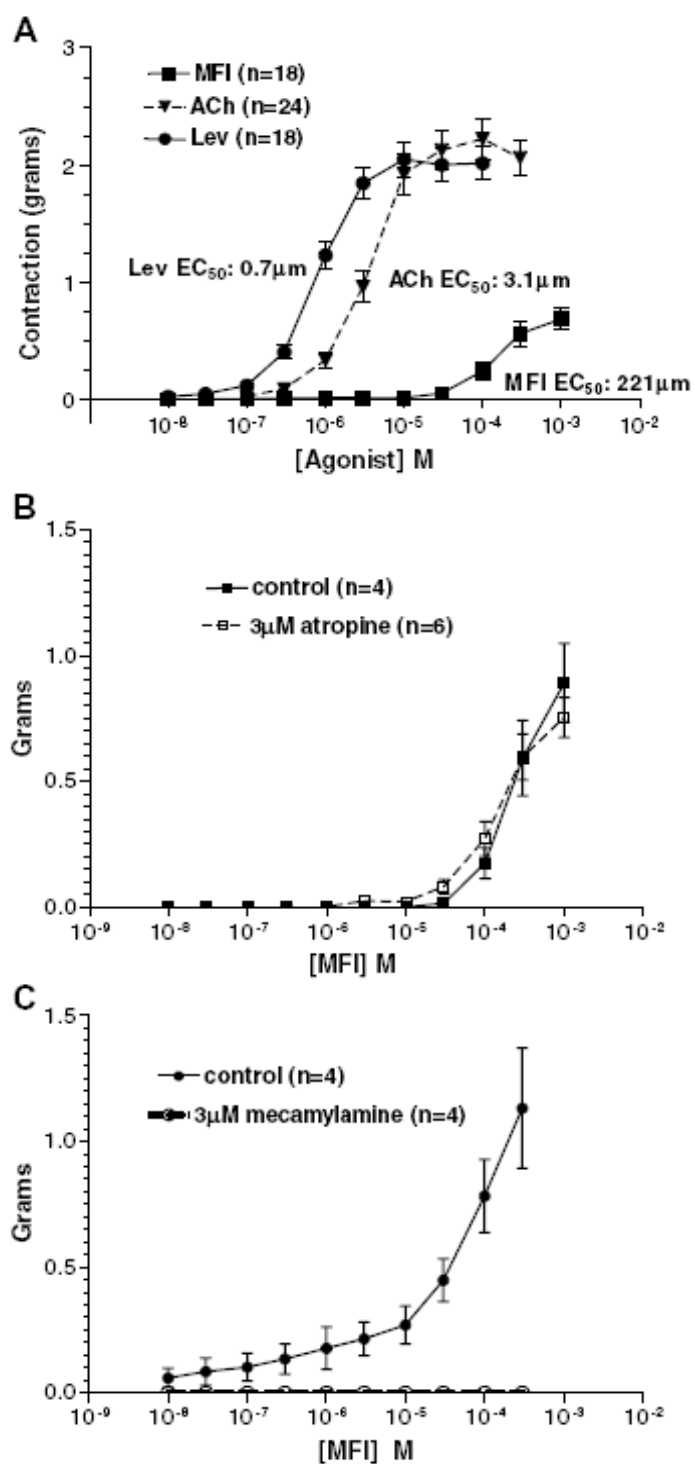


Fig. 2. A: Effect of MFI (■), acetylcholine (○) and levamisole (●) on contraction of *A. suum* muscle strips.

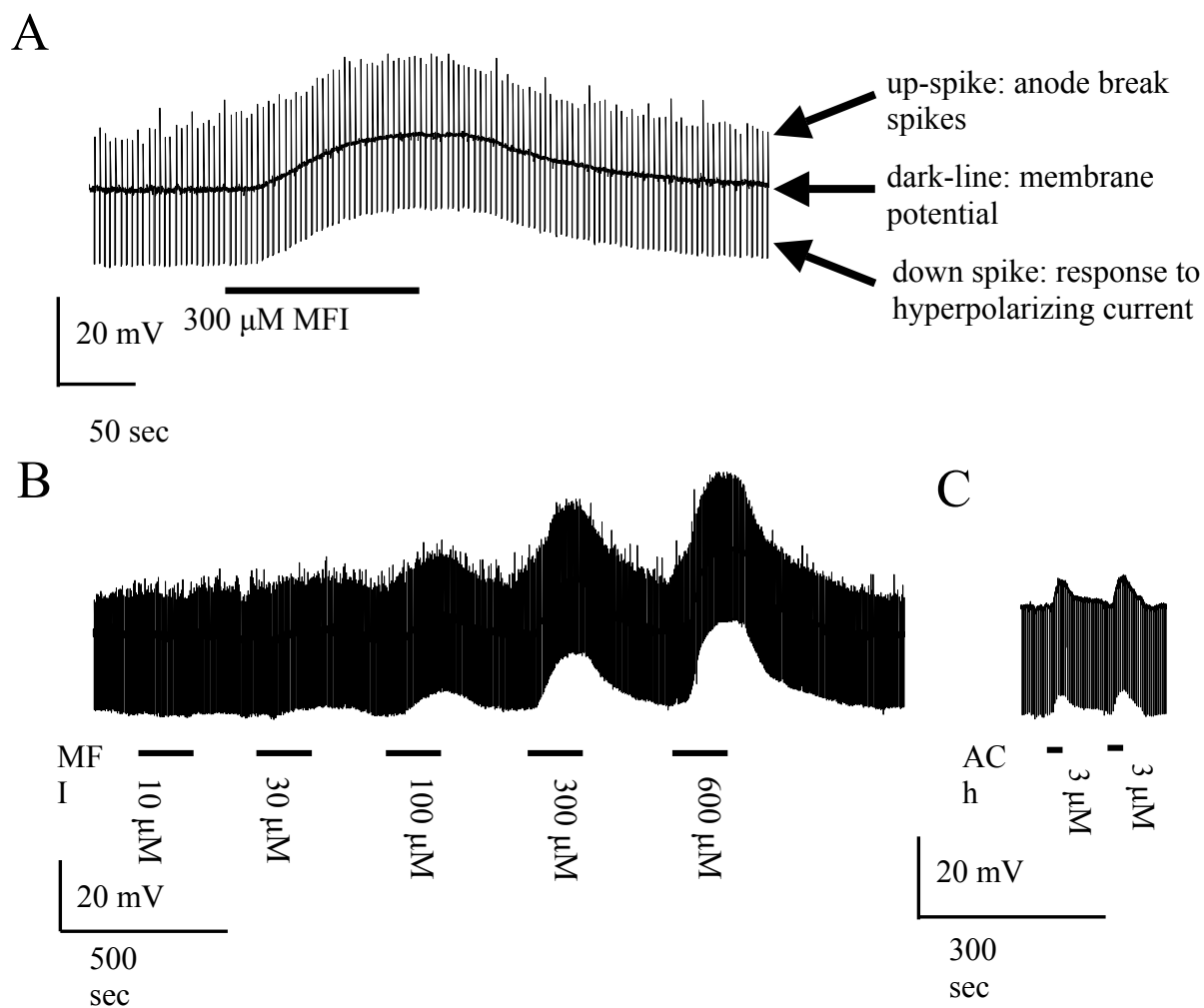


Fig 3. Effect of MFI on membrane potential and conductance.

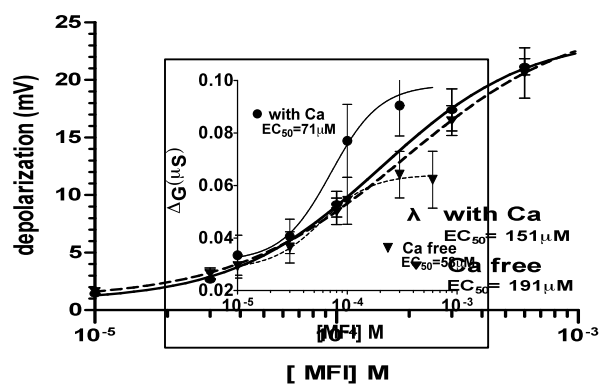


Fig 4. Peak MFI depolarization-concentration relationships.

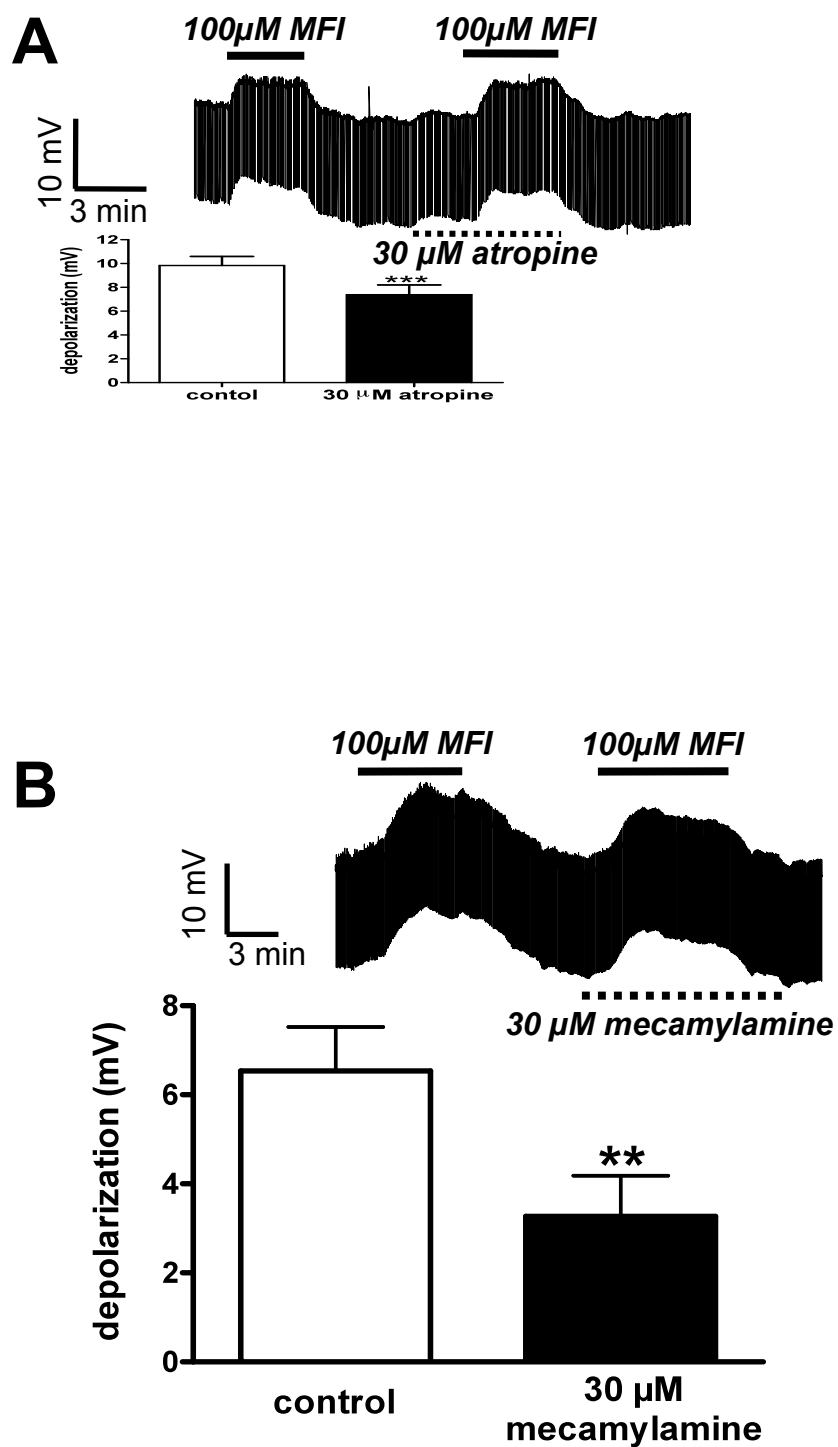
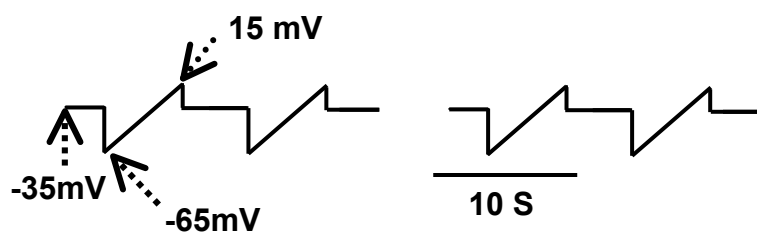
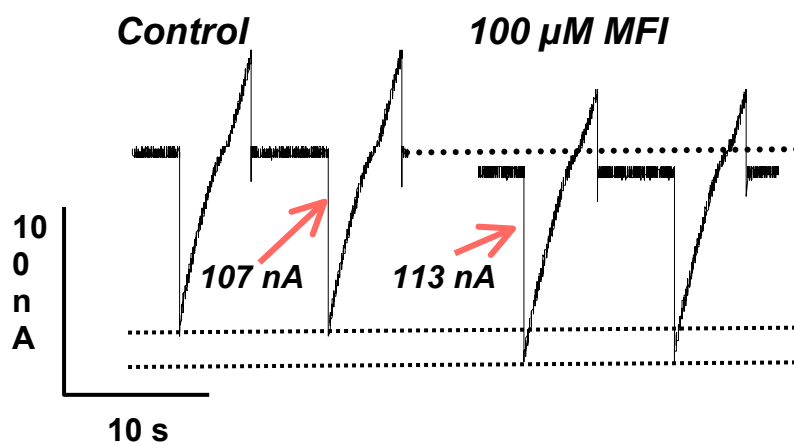


Fig.5 Effect of atropine on MFI response.

A Ramp voltage protocol



B Ramp currents



C MFI currents

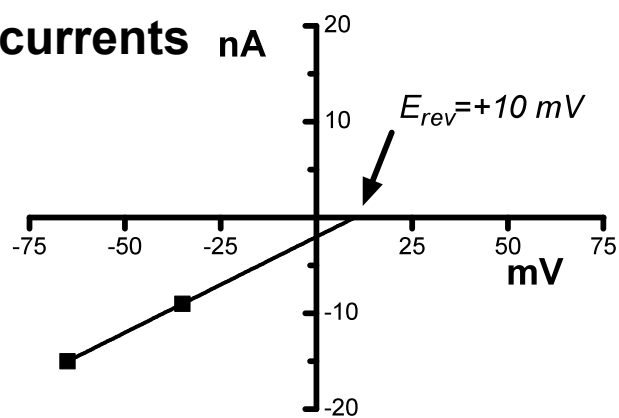


Fig. 6. Ramp-voltage study.

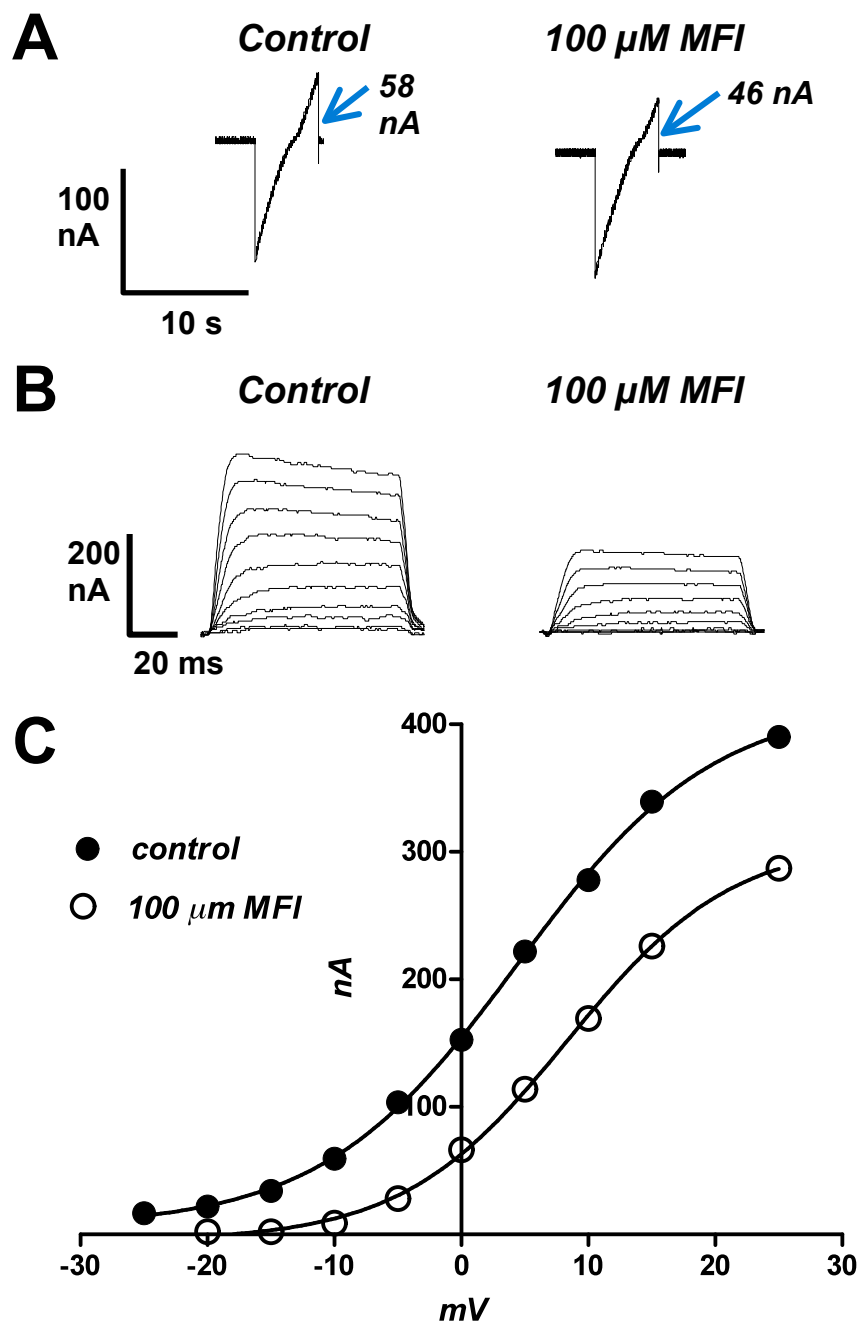


Fig. 7. Effect of MFI on depolarization-activated potassium currents in NMDG Ringer.

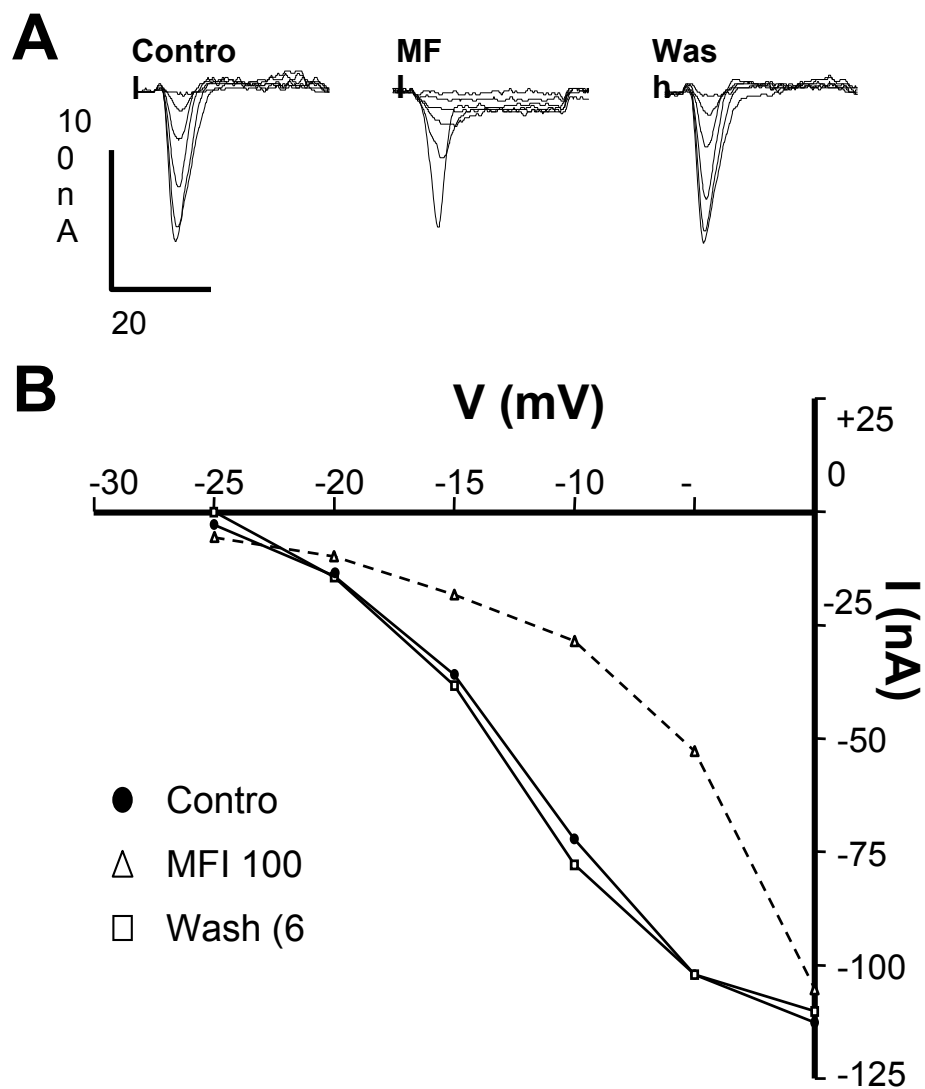


Fig 8. 100 μ M MFI increases the threshold for activation of the voltage-activated calcium currents.

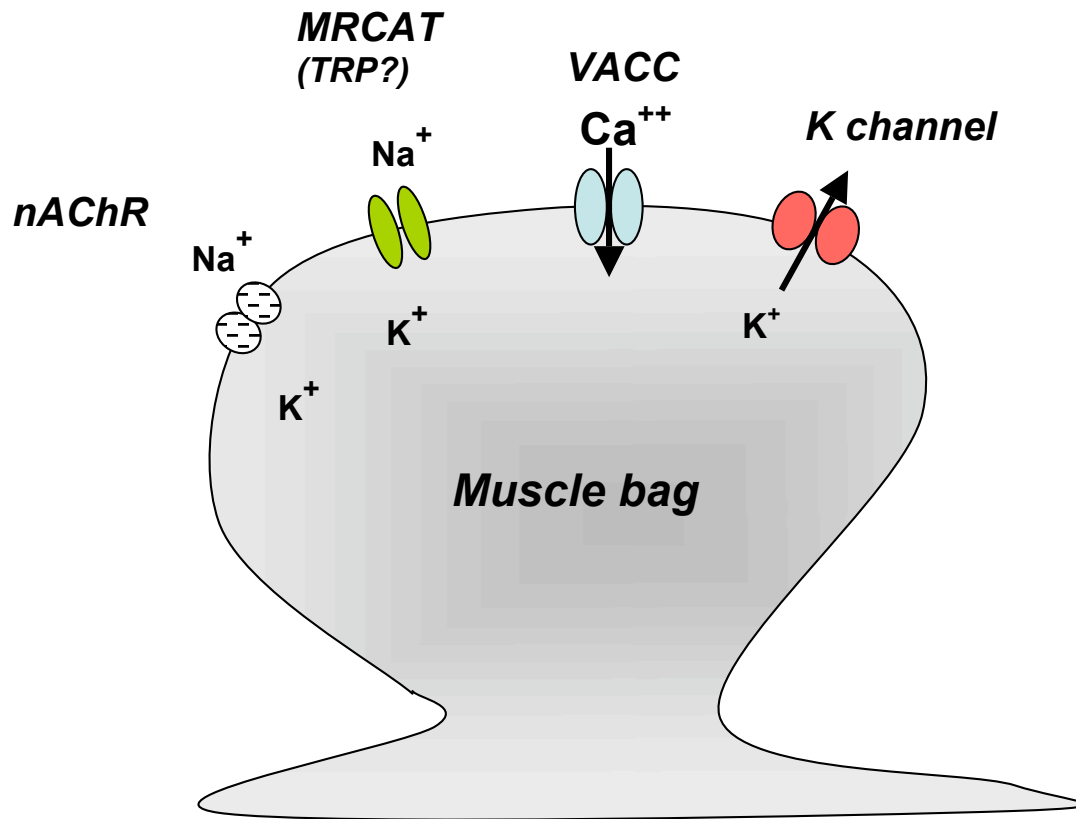


Fig 9. Summary diagram of the effects of MFI on the membrane ion-channel of the *A. suum* muscle. MFI is a weak agonist of the nicotinic acetylcholine channels on the bag (up arrow: nAChR).

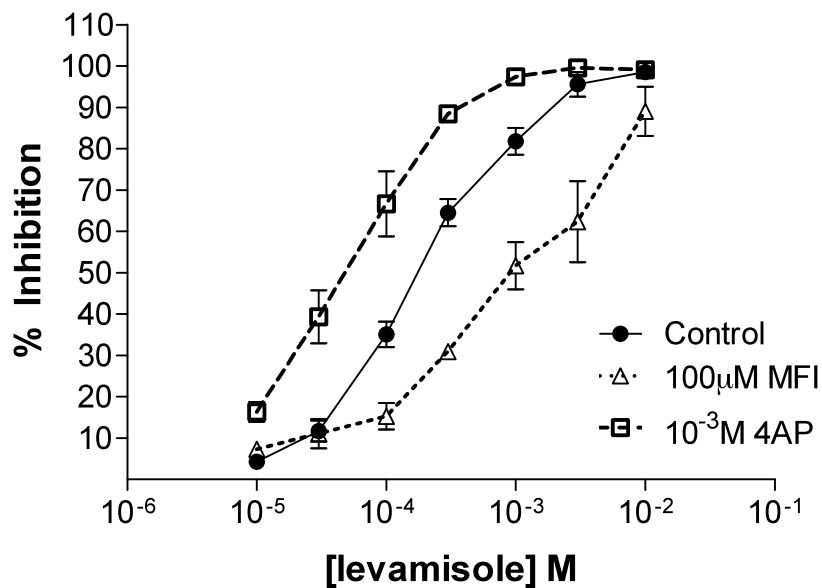


Fig 10. Potentiation effect of 100 μM 4-aminopyridine (4-AP) and antagonistic effect of 100 μM MFI on levamisole inhibition of larval migration. *O. dentatum* ex-sheathed L3 larval migration assay.

Chapter 6. General Discussion

As outlined previously in introduction I have investigated three hypotheses. Based on the results and observations I have come to certain conclusions for each hypothesis as mentioned below:

1. *Entry of calcium from extracellular sources is responsible for muscle contraction in A. suum somatic muscle cells. It is assumed that spikes and slow waves induced under current clamp in A. suum muscles are calcium dependent. These spikes are potentiated by the excitatory neuropeptide, AF2. Our first hypothesis was that spiking is due to the opening of voltage-activated calcium channels. AF2 increased the spiking and therefore AF2 will positively modulate the voltage-activated calcium currents.*

We were able to isolate the voltage-activated calcium currents from somatic muscle cells of *A. suum*. There were two distinct calcium currents isolated under voltage-clamp: transient peak currents (I_{peak}) and steady-state currents (I_{ss}). These currents were reduced in the absence of calcium demonstrating that majority of the current is carried by calcium. Also cobalt, a calcium channel blocker, abolished the inward calcium currents. These observations suggest that the calcium channels in nematodes are not exclusively permeable to calcium, but may also be permeable to other monovalent cations including sodium and potassium. The *A. suum* calcium current was most likely to be carried by calcium. A short duration application of AF2 produced long lasting potentiation of the I_{peak} currents. The increase in the inward current suggests that AF2 was responsible for the increase in spontaneous spiking

and depolarization. AF2 increased the frequency of large and small spikes under current-clamp.

2. *There are two distinct calcium currents in A. suum somatic muscle cells. The two currents are pharmacologically different. The second hypothesis was that the two currents can be modulated, negatively and positively, by FLPs. We investigated the effects of excitatory (AF3) and inhibitory (PF1) neuropeptide FLPs on the two calcium currents.*

The voltage-activated calcium currents were potentiated in the presence of AF3. The biggest effect of AF3 was on steady-state currents (I_{ss}) but as mentioned previously AF2 has its biggest effect on I_{peak} . The different actions by these two neuropeptides on the two currents imply that they can be modulated separately.

The inhibitory neuropeptide PF1 inhibited both, I_{peak} and I_{ss} , calcium currents. We also found that PF1 in the presence of calcium increased the potassium currents. The effect on potassium currents was abolished in absence of calcium and at higher concentrations of PF1. The effects of PF1 are important as a novel anthelmintic, emodepside, has been proposed to mimic the effect or induce the release of PF1. Emodepside has also been shown to produce its effect by modulation of a calcium-activated potassium channel (SLO-1). The effect of PF1 on calcium channels is also calcium dependent. It will be of interest to investigate the mechanism of action of emodepside on calcium channels to further elucidate the mechanism of action of emodepside (see Appendix).

3. *The third hypothesis was aimed at investigating the role of muscarinic receptors in muscle contraction. Our hypothesis was that muscarinic receptors play some role in somatic muscle contraction and muscarinic AChR's in nematodes modulate voltage-activated currents in the somatic muscle cells of A. suum. Colquhoun et al, (1991) tested effects of different mammalian cholinergic agonists including furtrethonium, muscarine, pilocarpine, arecoline, McN A343, bethanecol and oxtemorine, on A. suum somatic muscle cells. They found that furtrethonium was the most potent. We therefore selected 5-methylfurmethiodide (MFI), which is a potent muscarinic agonist for further study on muscle contraction in A. suum. We studied the effect of the muscarinic agonist, MFI along with levamisole and acetylcholine on contraction and electrophysiology of the somatic muscle cells in A. suum.*

MFI was a weak agonist producing muscle contraction. MFI did not produce a maximum contraction like ACh or levamisole but it acted as a weak nicotinic agonist in inducing muscle contraction. More importantly MFI lead to the opening of mecamlamine-resistant-non-selective cation channel and inhibition of voltage-activated potassium channels. MFI did not inhibit but raised the threshold of voltage-activated calcium channel currents. The properties of mecamlamine-resistant-non-selective currents (I_{bcat}) currents are similar to receptor operated channels of transient receptor potential channel (TRP) group. The similarities imply that the slow waves and I_{bcat} are conducted by MFI sensitive TRP-like channels. In mammalian preparations MFI has been shown to produce closure of an inwardly rectifying potassium channel current. MFI is known to activate M1 muscarinic receptors in rat

cervical ganglion (Caulfield *et al.*, 1994). We have demonstrated similar results where MFI induced depolarization and inhibition of voltage-activated potassium currents in *A. suum*.

The development of anthelmintic resistance against existing drugs is a cause for concern for human and animal health alike. Our approach was to investigate the actions of cholinergic anthelmintics (levamisole), to understand better mode of action of these drugs and to develop a pharmacological strategy for countering resistance to these compounds. The neuromuscular system is the target for some of the most effective classes of anthelmintics. Muscle cells are very closely associated with proper functioning of the parasitic worms as they are involved in feeding, locomotion and reproduction. The calcium channels in the nematode, *A. suum* are different from vertebrate as they are not blocked by vertebrate calcium channel blockers. These channels are modulated by nematode specific endogenous neuropeptides (FLPs). Some of the FLPs are cross species reactive but not in mammals. These qualities make the FLP receptors attractive targets for the development of anthelmintic drugs. Also the effects of cholinergic anthelmintics are potentiated by the excitatory FLP, AF2. These properties suggest that a synthetic FLP ligand could be used to potentiate the effects of cholinergic anthelmintics like levamisole. Modulation of the voltage-activated channels by muscarinic agonists also offers an alternative to increase the potency of cholinergic anthelmintics. Inhibition of voltage-sensitive potassium channels by the muscarinic agonist, MFI demonstrates a way to increase the efficacy of cholinergic anthelmintics.

For further investigation of these observations I suggest the study of the voltage-activated currents at single channel level. Also calcium imaging is another option to further characterize and locate these calcium channels in somatic muscle cells. Another future study which holds potential is to investigate these currents in *C. elegans*. A PCR-based cDNA approach has been widely successful in *C. elegans* similar methodologies can be applied to *A. suum* to characterize the voltage-activated channel currents. Once identified these channels could be expressed in *C. elegans* for further analysis as it offers the possibility of detailed electrophysiological studies. These results in future will contribute to a better understanding of the role and interaction of these peptides with different physiological systems in nematodes. Also, a better understanding of the mechanism of action of the existing anthelmintics will allow us to develop strategies to counter the development of resistant more effectively.

Appendix

In this portion of my dissertation I summarize the results and observations of experiments which are in preliminary stages and need further work. These experiments are a step towards the future line of work as I suggested in the general discussion.

Profender and emodepside

Profender, the brand name of a product from Bayer, is a topical solution for cats. Profender is a mixture of emodepside (15 mg) and praziquantel (60.1 mg) in each 0.7 ml tube. To check the effects of emodepside on voltage-activated currents we did preliminary studies with Profender for two reasons: i) unavailability of emodpeside and ii) to investigate the effects of other compounds in solution. The study so far is at a preliminary stage and we cannot conclude the results with absolute certainty. I am presneting the results and observations I have obtained so far.

Effects of Profender on voltage-activated potassium and calcium currents

Fig. 7.1A shows currents activated by steps from the holding potential of -35 mV to 0 mV and to +20 mV. The step potential of 0 mV (Fig. 7.1A, I_{peak}) shows activation of the calcium transient current (Verma *et al.*, 2007). The step potential to +20 mV (Fig. 3A, O) shows activation of the outward potassium current (Thorn *et al.*, 1987).

10 μ M Profender produced an effect on both the currents that increased slowly over a period of 10 minutes. In the representative recording, Fig. 7.1A,

Profender decreased the potassium current from 700 nA to 531 nA and the

I_{peak}

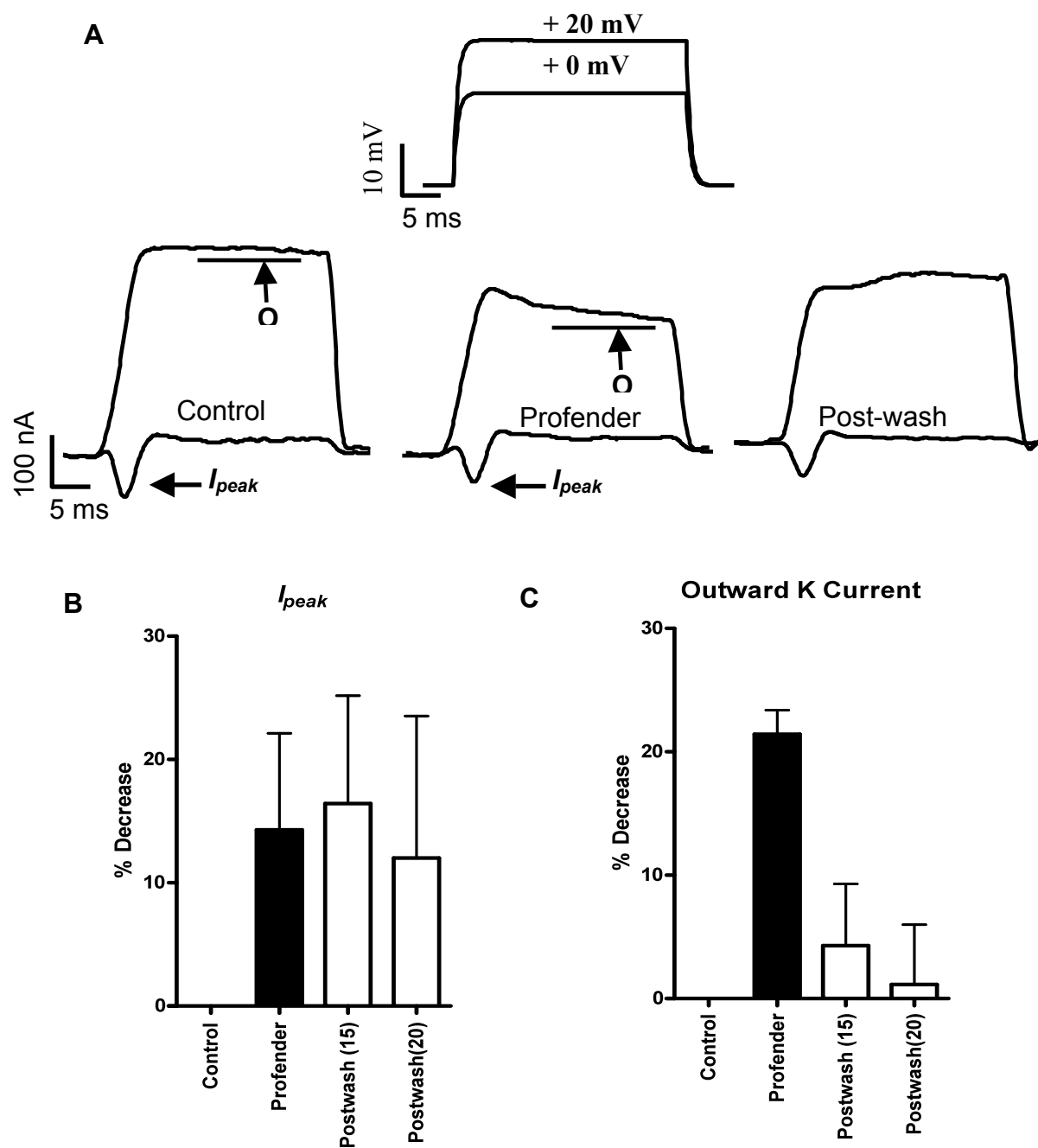


Figure 7.1 Effects of Profender on voltage-activated currents.

(A) Outward potassium currents (O) and calcium currents (I_{peak}) were suppressed in presence of Profender.

(B) Effects on calcium currents were irreversible.

(C) Outward potassium currents recovered post wash.

decreased from -173 nA to -112 nA. After 20 minutes of continuous wash, the potassium current increased to 680 nA but in contrast, the calcium transient current reduced to -103nA.

The effect on the potassium currents is reversed on washing but the effect on the calcium current is not reversed on washing. This difference in wash-out suggests that the two currents may be regulated differently. Fig. 7.1B & C summarizes the time dependent effects of Profender on the potassium and the calcium currents in 6 different preparations. It can be observed by comparing Fig. 7.1 B & C that the percentage decrease in the potassium currents, for the 6 recordings after 9 minutes application of Profender was $21 \pm 2 \%$ ($p=0.003$, $n=5$), which was bigger than the percentage decrease of the calcium currents, $14 \pm 8 \%$ ($p=0.04$, $n=5$). We can also see that during the wash period the potassium current returned to close to control levels; but the decrease in the calcium currents is maintained. Thus, we observed the effects of Profender on the two currents and that the effect on the potassium currents was proportionately bigger than on the calcium. The effect on calcium currents was not reversible.

Effects of Emodepside on voltage-activated potassium and calcium currents

Fig. 7.2A, shows a typical recording of the effects of emodepside on membrane potential; in this cell the resting membrane potential was -29 mV and input conductance was 3 μ S. Application of 1 μ M emodepside produced a hyperpolarization of 3 mV and conductance increase of 0.4 μ S. The effect was

not completely washed off even after 20 mins. Similar results were obtained in a total of 6 preparations. Fig. 7.2B summarizes the effects of emodepside on membrane potential. The effect of 1 μ M emodepside on membrane potential was statistically significant and the mean hyperpolarization was 2.6 ± 1 mV ($p = 0.04$).

Effect of emodepside on voltage-activated currents is different from the effects of profender. Fig. 7.2C shows currents activated by steps from the holding potential of -35 mV to 0 mV and to +20 mV. The step potential of 0 mV (Fig. 7.2C, I_{peak}) shows activation of the calcium transient current. The step potential to +20 mV (Fig. 7.2C, O) shows activation of the outward potassium current. 1 μ M Emodepside produced an effect on the currents that increased slowly over a period of 8 minutes. In the representative recording, Fig. 7.2C, unlike Profender, emodepside increased the potassium current from 577 nA to 726 nA and decreased the I_{peak} calcium currents from -101 nA to -75 nA. After 20 minutes of continuous wash, the potassium current decreased to 704 nA but in contrast, the calcium transient current reduced to -18 nA.

The effect on the potassium currents is reversed on washing but the effect on the calcium current is not reversed on washing these effects are similar to the effects seen previously with Profender. This difference in wash-out again demonstrates the possible different regulation of the two currents. Fig. 7.2B & C summarizes the time dependent effects on the potassium currents and the calcium currents in 6 different preparations. It can be seen by comparing Fig. 7.2 B & C that the percentage increase in the potassium

currents for the 6 recordings after 9 minutes application of emodepside was $4.2 \pm 4 \%$ ($p=0.5$, $n=6$) and was not significant. Whereas, percentage decrease of the calcium currents, $12 \pm 8 \%$ ($p=0.02$, $n=5$) and was significant. Interestingly potassium currents decreased to close to normal levels post-wash; but the decrease in the calcium currents is increased with time. Thus, we observed the effects of emodepside on the two currents and that the effect on the potassium currents was smaller than on the calcium but the effects on potassium currents was reversible.

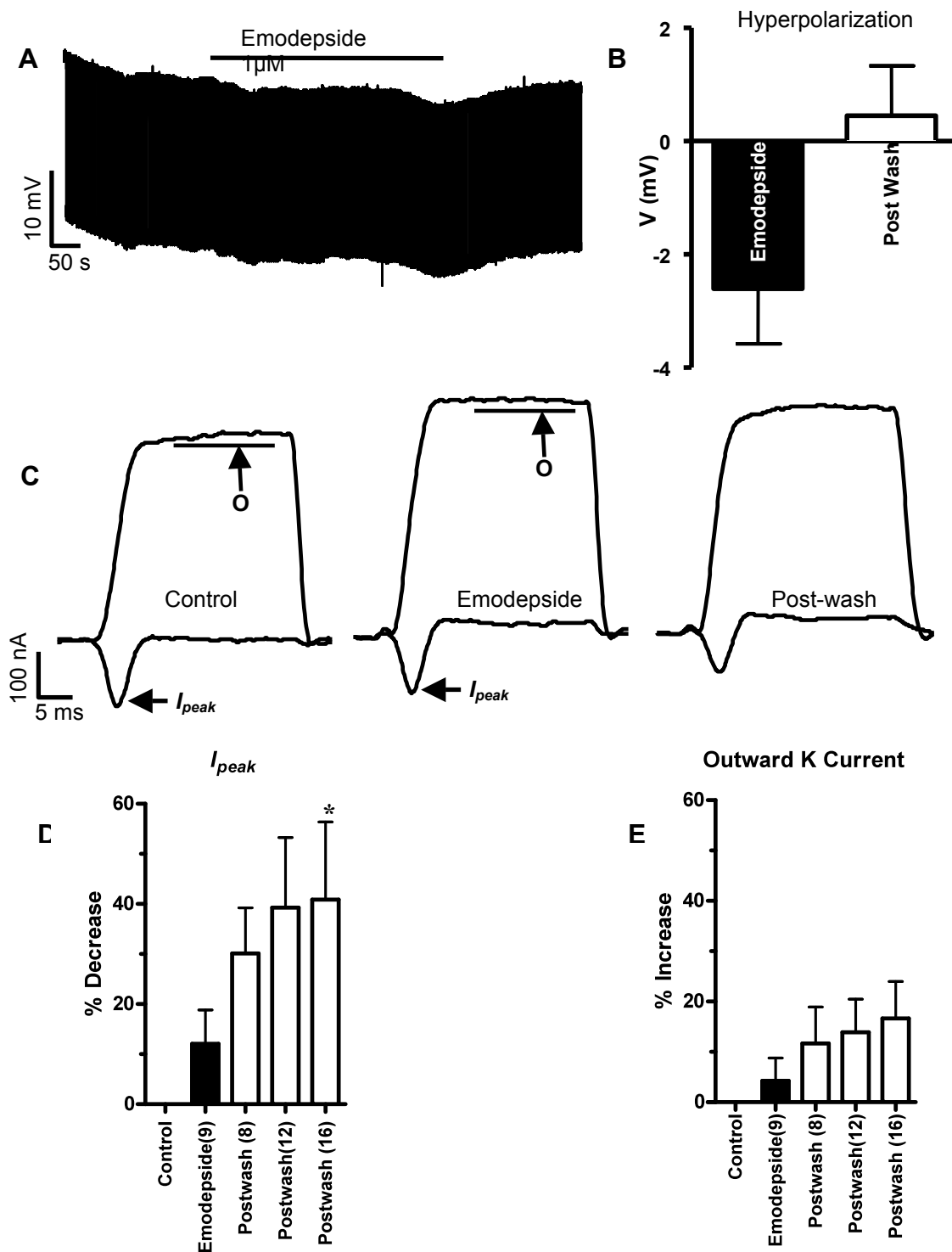


Figure 7.2 Emodepside (A) on membrane potential induced (B) hyperpolarization. Two effects of Emodepside on (C) Voltage-activated currents (paired t-test, $n=6$, $* P \leq 0.05$); (D) calcium currents were suppressed and (E) outward potassium currents potentiated.

AF1

AF1 is an excitatory FMRFamide peptide. I tested AF1 to compare the results of AF2 with other excitatory peptides. As mentioned effects of AF1 although encouraging were not consistent and weaker as compared to AF2.

Effect of AF1 on transient inward currents

Fig. 7.3 A demonstrates the effects of AF1 on membrane potential and conductance. AF1 produced depolarization of 1 mV with no change in conductance in 5 different recordings.

Fig 7.3 B shows a representative experiment of effects following a 2-minute application of 1 μ M AF1 on the peak transient inward current. We followed the same analytical approach as we did previously to prepare the activation curves and to test the effect of AF2. Fig. 7.3 B, C & D show that AF1 increased the current by shifting the activation curve to the left and increasing the maximum conductance change. The peak current at the 0 mV step increased from -141 nA in the control to -156 nA after AF1 application, Fig. 7.3 B. The control activation curve had a V_{50} of -12 ± 0.7 mV and a G_{max} of 3.2 ± 0.05 μ S. After AF1, V_{50} was -16 ± 2.8 mV and the G_{max} was 6.05 ± 0.2 μ S, Fig 7.3 D. Thus, there was an hyperpolarizing shift of 4 mV in V_{50} and a 53% increase in G_{max} in the representative experiment. The slope factor for the curve changed from the control 5.8 ± 0.7 mV to 6.4 ± 1.7 mV after application of AF1.

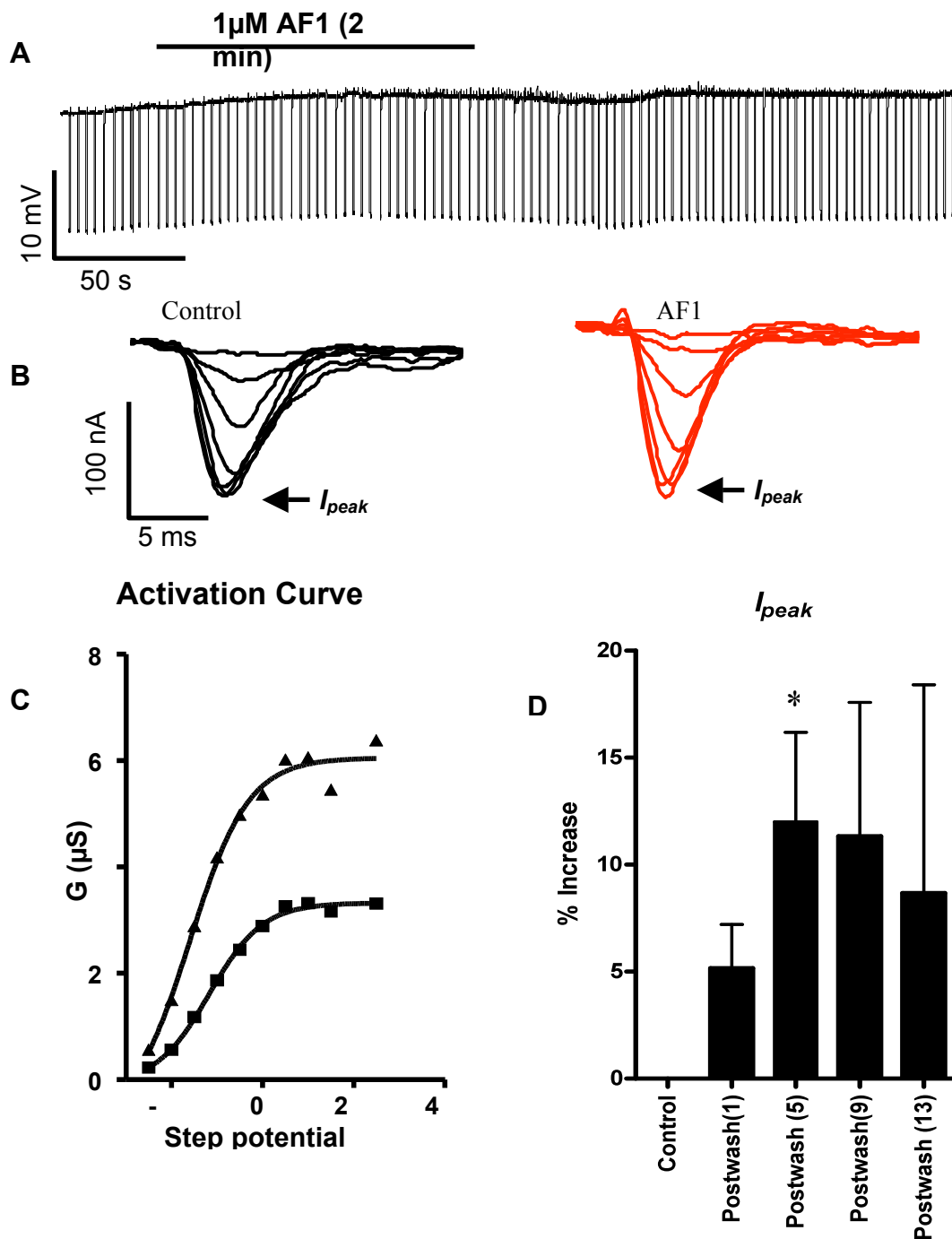


Figure 7.3 Effects of AF1 on voltage-activated currents. (A) Effect of AF1 on membrane potential. (B) AF1 potentiated calcium currents (I_{peak}). (C) Activation curve (I_{peak}). (D) AF1 significantly potentiated the inward current and the effect was reversible (paired t-test, $n=6$, * $P \leq 0.05$).

It was clear from the experiment described in Fig. 7.3 B-C and from similar observations in 10 other experiments that AF1 increased the transient inward current. We found that the potentiation took 4 minutes to reach a maximum and lasted for less than 15 minutes after washing the AF1. Fig.7C shows the mean \pm S.E. % increases from 5 experiments. The average potentiation for the 5 recordings after 5 minutes was 12 ± 4 % and was significant. The results from different preparations ranged from 21 % - 2%. In addition, we also examined the effect of continuous application of AF1 and the effects were not significantly different from control (5 preparations). The results demonstrate the possibility that the effects of AF1 were produced in a similar fashion as AF2. The effects of AF2 on calcium currents are much bigger and long lasting when compared with AF1.

C-terminal motif ^b	flp genes ^d																																		
	1	2	3	4	5	6	7	8	9	10	11	12	13	14	15	16	17	18	19	20	21	22	23	24	25	26	27	28	29	30	31	32			
AMRNSLVRFQ																																			
LYRPGPPRFQ																																			
QMREPLRFQ																																			
Ix ₀ MRFG																																			
VLMRFQ																																			
-GxRMRFQ																																			
EFNADDLTLRFQ																																			
-AF _i P _i X _i LL _i LRFG																																			
-YDFVRFQ																																			
-YDYIRFG																																			
VP _i X _i oXDM _i M _i K _i oRFQ																																			
-QDFLRFQ																																			
-KWMRFQ																																			
-GPRPLRFQ																																			
X ₀ MMRFQ																																			
-MxxOx ₀ RFQ																																			
-Pgx ₀ X ₀ RFQ																																			
KSAx ₀ VRFQ																																			
KSx _i Y ₀ RFQ																																			
-QTFVRFQ																																			
-Gp _i X _i Gp _i LRFG																																			
KHEYLRFQ																																			
-PLx ₀ RFQ																																			
-NKFEFIRFG																																			
-RNx ₀ LVRFQ																																			
-Yx ₀ RFQ																																			
KP _i SVRFQ																																			
KNEF ₀ RFQ																																			
-P _i x ₀ iRSx ₀ x ₀ RFQ																																			
KSAYMRFQ																																			
-K _i FIRFG																																			
-P _i FIRFG																																			
-SP ₀ oGTMRFQ																																			
-EPIRFQ																																			
-PNFLRFQ																																			
Species^e																																			
Clade I																																			
<i>Trichinella spiralis</i>														E																					
Clade III																																			
<i>Ascaris suum</i>						C		C				E	C		C		E		C						C								E		
<i>Brugia malayi</i>						E								E										E											
<i>Dirofilaria immitis</i>																																			
<i>Onchocerca volvulus</i>	E					E		E				E	E	E		E		E						E											
<i>Wuchereria bancrofti</i>	E										E																								
Clade IV																																			
<i>Globodera pallida</i>	C					C	E					C		C											C										
<i>Globodera rostochiensis</i>	E					E	E	E				E	E	E	E		E		E					E											
<i>Heterodera glycines</i>			E	E	C	C	C				E	C	E	C		E							E												
<i>Heterodera schachtii</i>	E																																		
<i>Meloidogyne arenaria</i>	E	E										E		E																					
<i>Meloidogyne chitwoodi</i>	E	E										E	E	E																					
<i>Meloidogyne hapla</i>	E	E										E	E	E																					
<i>Meloidogyne incognita</i>	C	E										E	C	E	C		E		C	E															
<i>Meloidogyne javanica</i>	E					E	E	E																											
<i>Meloidogyne paranaensis</i>	E																																		
<i>Panagrellus redivivus</i>																																			
<i>Parastrongyloides trichosuri</i>	E																																		
<i>Pratylenchus penetrans</i>																																			
<i>Pratylenchus vulnus</i>																																			
<i>Radopholus similis</i>																																			
<i>Strongyloides ratti</i>	E																																		
<i>Strongyloides stercoralis</i>	E																																		
<i>Xiphinema index</i>																																			
Clade V																																			
<i>Ancylostoma caninum</i>	E	E																																	
<i>Ancylostoma ceylanicum</i>	E																																		
<i>Caenorhabditis elegans^b</i>	C	C	C	C	C	C	C	C	C	C	C	C	C	C	C	C	C	C	C	C	C	C	C	C	C	C	C	C	C	C	C	C	C	C	
<i>Dictyocaulus filaria</i>																																			
<i>Dictyocaulus viviparus</i>																																			
<i>Haemonchus contortus</i>																																			
<i>Necator americanus</i>	E	E																																	
<i>Nippostrongylus brasiliensis</i>																																			
<i>Oesophagostomum dentatum</i>	C																																		
<i>Ostertagia ostertagi</i>	E																																		
<i>Pristionchus pacificus</i>																																			
<i>Teladorsagia circumcincta</i>																																			

Table 7.4 (McVeigh *et al.*, 2006) Distribution of *flp* genes across the phylum Nematoda.

^aFor further details see (5). ^bx, a variable hydrophilic residue; ^xg, a variable hydrophobic residue; cysteine has not been reported in any FLP. ^cNematodes are classified into five clades. Clade II is not shown because no genetic data are available for any Clade II species. ^dE, expressed sequence tag(s) (EST) is known; C, a complete propeptide open reading frame ^eDNA is available. All sequences are available on Genbank (<http://www.ncbi.nlm.nih.gov>), except ^e(C.L. Moffett, PhD Thesis, Queen's University Belfast, 2001) and ⁱ(I. Miskelly, PhD, Thesis, Queen's University, Belfast, 2006). ^gThe *flp-32* transcript is distinct from the *flp-11* cDNA in *Teladorsagia circumcincta*; *flp-32* is also present in the *C. elegans* genome. In *C. elegans*, *flp-11* and *flp-32* map to different chromosomes even though they encode some of the same peptides (C. Li, pers. commun. as reported in McVeigh *et al.*, 2006). We therefore deduce that these represent distinct genes rather than splice variants. ^hHomologs of *flp-1-20,24,26,27* have also been reported in the *C. elegans* genome.

Acknowledgements

I would never have been able to finish my dissertation without the guidance of my committee members, help from friends, and most importantly support from my family. It would not have been possible to write this doctoral thesis without the help and support of these kind people around me, to only some of whom it is possible to give particular mention here.

I would like to thank my major advisor Dr. Richard J. Martin, for his invaluable support, encouragement, supervision and useful suggestions throughout the duration of my research work. I would also like to express deepest gratitude to Dr. Alan P. Robertson. Alan provided refreshing insight, critical questions & an uncanny common sense that was exhilarating. It would have been a different lab without him. I am grateful to both of them for sharing their memories and experiences with me. I would like to thank Cheryl Clark our lab technician for keeping me organized and safe during my lab work (take my word for it). Cheryl was very helpful in research work, sometimes in most surprising ways. Thanks are owed to NIH for providing financial support (RO1 AI 047194) to RJM for the duration of my research.

I must acknowledge as well Dr. Sasa Trailovic who assisted, advised and supported me during the early phase of my graduate work. Special thanks to my colleague Dr. Hai Qian for sharing the lab space and thoughts with me. I would also like to thank my friends Mr. & Mrs. Sachan, Mr. & Mrs. Chug, Sreekanth, Samuel and Lucy who shared my sorrows and joys with me over the years. Also here I would

like to put a special note of thanks for Linda, Kim and Marilee for their continuous support.

I am as ever, especially indebted to my parents, Mr. Girish Verma and Mrs. Mani Verma for their love and support throughout my life. Here my brother Sameer Verma deserves a special mention for taking care of everything while I am away from home and my parents.

Finally I would like to thank my wife Parul, for unstinting reminder that there are other important things in life than a Ph.D. She was there cheering me up and stood by me through good times and bad. I have to say all that love did made the difference.